

**HANDHELD INFRARED CAMERA USE FOR SUICIDE
BOMB DETECTION:
FEASIBILITY OF USE FOR THERMAL MODEL
COMPARISON**

by

MATTHEW R DICKSON

B.S., Kansas State University, 2006

A THESIS

**Submitted in partial fulfillment of the
requirements for the degree**

MASTER OF SCIENCE

**Department of Mechanical and Nuclear Engineering
College of Engineering**

**Kansas State University
Manhattan, Kansas
2008**

Approved by:

**Major Professor
Dr. Akira Tokuhira**

ABSTRACT

One of the most deadly tactics used by today's terrorists is suicide bombing. Sensors have been developed and are being used in different situations to detect weapons and the people initiating suicide bombing attacks. The ideal detection technology would be fast, accurate, effective from long distances, and safe for the both detector and the object being detected.

One detector that has shown potential as a tool for detecting hidden weapons is an infrared detector. Infrared detectors are passive sensors that create infrared, or thermal, images without having to expose the subject to any radiation. These images show the heat signature that is given off by objects of interest.

Previous studies using infrared detectors for concealed weapon detection have tried to observe the image of the weapon. These have been largely unsuccessful, however, because infrared waves will not readily penetrate clothing. The research presented here determines the feasibility of modeling the heat signature produced by a suicide bomber using thermal models that predict the temperature of the exterior layers of clothing worn. The goal is to be able to compare the images acquired of the suspected bomber to the expected temperatures from the thermal models. If the presence of a hidden weapon affects the emitted heat signature to a point in which the clothing temperatures are not responding as predicted by a model, it is possible a detection system may be created using these models as a comparator and signal for detection.

This research also determines a temperature range for which an operator viewing infrared images for suicide bomb detection may be relatively certain of the presence of a foreign object. Testing was also completed to determine those variables that affect an infrared image in ways that help or hinder the use of the thermal models in predicting the temperatures that appear in the infrared images.

ACKNOWLEDGEMENTS

I would like to thank Dr. Akira Tokuhiko for his support of my research, my academic progress, and my future endeavors. I would also like to acknowledge and thank the students in my research group. I have learned as much from these people as I did through my research. I must thank my family for their unending support of my education. Lastly I would like to thank those persons at Insitu Inc. and Midwest Research Institute that encouraged my progress and contributed to my education while I was outside the walls of Kansas State University.

TABLE OF CONTENTS

TABLE OF CONTENTS	IV
LIST OF FIGURES	IX
LIST OF TABLES	XV
CHAPTER 1-CURRENT STATE OF SUICIDE BOMBINGS	1
SUICIDE BOMBER DEMOGRAPHICS	2
SUICIDE BOMBING TARGETS	3
SUICIDE BOMBING TACTICS	4
THWARTING OF ATTACKS	5
DETECTION TECHNOLOGY	7
<i>Current Technologies</i>	9
<i>IR Technology</i>	12
RESEARCH OBJECTIVES	19
CHAPTER 2-HUMAN THERMOGRAPHY	20
HUMAN THERMAL REGULATION	21
CHAPTER 3-SUICIDE BOMBER MODELING	23
HUMAN THERMAL MODEL PROGRAM	23
LCM MODEL	29
RESISTANCE MODEL	30
CHAPTER 4-EXPERIMENT SETUP	32
EQUIPMENT	32
<i>Camera</i>	32
<i>Manikin</i>	33

SETUP	34
<i>Camera</i>	34
<i>Manikin</i>	34
PROCEDURES	34
<i>Camera</i>	34
Procedure for Auto Focusing	35
Procedure for Manual Focus	35
Procedure for Auto/Manual Temperature Range	35
<i>Manikin</i>	36
CALIBRATION	36
<i>Camera</i>	36
<i>Manikin</i>	36
CHAPTER 5-TESTING PHASES	38
PHASE 1	38
<i>Focus</i>	39
<i>Camera Range</i>	39
<i>Material Emissivity</i>	39
<i>Shielding</i>	40
Transient Standing Best/Worst Case	40
PHASE 2	41
<i>Color Palettes</i>	41
<i>Bomb Package Material Characteristics</i>	42
<i>Transient-Standing-Best/Worst Case</i>	43
<i>Transient-Standing</i>	43
<i>Transient Changes While Walking</i>	43
<i>Transient Changes While Walking Best/Worst Case</i>	44

<i>Shielding</i>	44
Solar Simulations-Lights on	45
Solar Simulations-Lights out	45
PHASE 3	46
<i>Transient Walking</i>	46
<i>Comparison of Subject With and Without Bomb Vest</i>	47
<i>Effects of Sun</i>	47
<i>Clothing Design Features</i>	47
<i>Testing layering at distances</i>	47
CHAPTER 6- RESULTS	48
RESULTS-CALIBRATION	48
<i>Camera</i>	48
<i>Manikin</i>	49
RESULTS-TESTING PHASES	51
<i>Results of Camera Testing Phase 1</i>	51
Focus	51
Camera Range	52
Effects of Size on Range	53
Effects of Emissivity on Range	54
Material Emissivity/Reflectivity	55
Shielding	56
Transient Standing Best/Worst Case	60
<i>Results of Camera Testing Phase 2</i>	66
Color Palettes	66
Bomb Package Material Characteristics	68
Transient-Standing-Best/Worst Case	72
Transient-Standing-	78

Transient Changes While Walking	82
Transient Changes While Walking Best/Worst Case	90
Test Comparison	90
Pre-cooled Bomb Package Under Solar Simulation with Fan	91
Pre-cooled Bomb Package Under Solar Simulation without Fan	92
Pre-warmed Bomb Package Under Solar Simulation with Fan	93
Pre-warmed Bomb Package Under Solar Simulation without Fan	94
Shielding	105
<i>Results of Camera Testing Phase 3</i>	111
Transient Changes While Walking	111
Comparison of vest vs. no vest	124
Effects of Solar Irradiation	129
Clothing Characteristics	139
Imaging at Various Distances	141
1.3 Meters (6 Feet)	141
3.66 Meters (12 ft)	142
7.62 Meters (25 Feet)	144
CHAPTER 7- DISCUSSION OF RESULTS	145
MODEL COMPARISON	145
ENVIRONMENTAL EFFECTS ON IMAGES	146
MANUAL VS. AUTOMATIC TEMPERATURE RANGE	148
SYSTEM OPERATION	150
CHAPTER 8- CONCLUSIONS	152
PROPOSED SOLUTIONS	156
<i>Distances</i>	156
<i>Fusion</i>	156
<i>Controlling Checkpoints</i>	157

<i>Confidence intervals</i>	157
FINAL CONCLUSIONS	161

LIST OF FIGURES

FIGURE 1—INFRARED RADIATION MEASUREMENT OFF HUMAN	12
FIGURE 2—FLIR THERMACAM MODEL S65 USED IN RESEARCH	33
FIGURE 3—GRAYSCALE COLOR PALETTE	42
FIGURE 4—INVERSE GRAYSCALE COLOR PALETTE	42
FIGURE 5—INFRARED IMAGE OF ICECUBES	48
FIGURE 6—INFRARED IMAGE OF BOILING WATER	49
FIGURE 7—EFFECTS OF COUPON AREA ON VISIBLE DISTANCE	53
FIGURE 8—EFFECTS OF EMISSIVITY ON VISIBLE DISTANCE	54
FIGURE 9—MATERIAL COUPONS	55
FIGURE 10—EXTERNAL CLOTHING TEMPERATURE WITH APPLICATION OF CLOTHING LAYERS	57
FIGURE 11—CLAY MATERIAL HIDDEN IN VEST POCKET	58
FIGURE 12—CLAY MATERIAL HIDDEN IN VEST POCKET AND SHIELDED BY 1 T-SHIRT	58
FIGURE 13—CLAY MATERIAL HIDDEN IN VEST POCKET AND SHIELDED BY 2 T-SHIRTS	59
FIGURE 14—CLAY MATERIAL HIDDEN IN VEST POCKET AND SHIELDED BY 3 T-SHIRTS	59
FIGURE 15—BOMB TEMPERATURES ON MANIKIN WITH COLD PACK	62
FIGURE 16—BOMB WITH COLD PACK ATTACHED TO MANIKIN AT 0 MINUTES	63
FIGURE 17—BOMB WITH COLD PACK ATTACHED TO MANIKIN AT 140 MINUTES	63
FIGURE 18—BOMB WITH COLD PACK ATTACHED TO MANIKIN AT 180 MINUTES	64
FIGURE 19—BOMB TEMPERATURES ON MANIKIN WITH HOT PACK	64
FIGURE 20—BOMB WITH HOT PACK ATTACHED TO MANIKIN AT 0 MINUTES	65
FIGURE 21—BOMB WITH HOT PACK ATTACHED TO MANIKIN AT 90 MINUTES	65
FIGURE 22—BOMB WITH HOT PACK ATTACHED TO MANIKIN AT 150 MINUTES	66
FIGURE 23—BLUE-RED COLOR PALETTE	67
FIGURE 24—INVERTED BLUE-RED COLOR PALETTE	67
FIGURE 25—GRAYSCALE COLOR PALETTE	67

FIGURE 26—INVERTED GRAYSCALE COLOR PALETTE	67
FIGURE 27—IRON COLOR PALETTE	67
FIGURE 28—INVERTED IRON COLOR PALETTE	67
FIGURE 29—RAINBOW COLOR PALETTE	68
FIGURE 30—INVERTED RAINBOW COLOR PALETTE	68
FIGURE 31—HIGH CONTRAST RAINBOW COLOR PALETTE	68
FIGURE 32—INVERTED HIGH CONTRAST RAINBOW COLOR PALETTE	68
FIGURE 33—METAL PACKAGE HIDDEN IN VEST SHIELDED BY 1 TIGHT T-SHIRT	71
FIGURE 34—PLASTIC PACKAGE HIDDEN IN VEST SHIELDED BY 1 TIGHT T-SHIRT	71
FIGURE 35—BOMB TEMPERATURES ON HUMAN WITH HOT PACK	73
FIGURE 36—BOMB TEMPERATURES ON HUMAN WITH COLD PACK	74
FIGURE 37—DIFFERENCE BETWEEN THE BOMB AREA TEMPERATURE AND THE TORSO TEMPERATURE	74
FIGURE 38—BOMB WITH HOT PACK ATTACHED TO HUMAN AT 0 MINUTES	75
FIGURE 39—BOMB WITH HOT PACK ATTACHED TO HUMAN AT 27 MINUTES	75
FIGURE 40—BOMB WITH HOT PACK ATTACHED TO HUMAN AT 1 HOUR 40 MINUTES	76
FIGURE 41—BOMB WITH COLD PACK ATTACHED TO HUMAN AT 0 MINUTES	76
FIGURE 42—BOMB WITH COLD PACK ATTACHED TO HUMAN AT 1 HOUR 30 MINUTES	77
FIGURE 43—BOMB WITH COLD PACK ATTACHED TO HUMAN AT 3 HOURS	77
FIGURE 44—STANDING IN HEATED CHAMBER WITHOUT BOMB PACKAGE AT 1 MINUTE	78
FIGURE 45—STANDING IN HEATED CHAMBER WITHOUT BOMB PACKAGE AT 5 MINUTES	79
FIGURE 46—STANDING IN HEATED CHAMBER WITHOUT BOMB PACKAGE AT 51 MINUTES	79
FIGURE 47—METAL BOMB WHILE STANDING STILL AT 0 MINUTES	80
FIGURE 48—METAL BOMB WHILE STANDING STILL AT 11 MINUTES	81
FIGURE 49—METAL BOMB WHILE STANDING AT 15 MINUTES	81
FIGURE 50—METAL BOMB WHILE STANDING AT 19 MINUTES	82
FIGURE 51—TORSO TEMPERATURE COMPARISON WITH MODELS	83
FIGURE 52—TORSO TEMPERATURE COMPARISON WITH MODELS	84

FIGURE 53—IMAGE TEMPERATURE OF BOMB AREA COMPARISON WITH THERMOCOUPLE	85
FIGURE 54—TORSO TEMPERATURE AND BOMB TEMPERATURE COMPARISON	85
FIGURE 55—WALKING ON TREADMILL WITH METAL BOMB AT 0 MILES	86
FIGURE 56—WALKING ON TREADMILL WITH METAL BOMB AT 1.5 MILES	86
FIGURE 57—TORSO TEMPERATURE COMPARISON WITH MODELS	88
FIGURE 58—COMPARISON OF IMAGE TEMPERATURE WITH THERMOCOUPLE	88
FIGURE 59—TORSO TEMPERATURE AND BOMB TEMPERATURE COMPARISON	89
FIGURE 60—WALKING ON TREADMILL WITH PLASTIC BOMB AT 0 MILES	89
FIGURE 61—WALKING ON TREADMILL WITH PLASTIC BOMB AT 1.5 MILES	90
FIGURE 62—TORSO TEMPERATURE COMPARISON WITH MODELS OF HUMAN ON TREADMILL WITH BOMB	95
FIGURE 63—COMPARISON OF IMAGE TEMPERATURE WITH THERMOCOUPLE	96
FIGURE 64—TORSO TEMPERATURE AND BOMB TEMPERATURE COMPARISON	96
FIGURE 65—TORSO TEMPERATURE COMPARISON WITH MODELS OF HUMAN ON TREADMILL WITH BOMB	97
FIGURE 66—COMPARISON OF IMAGE TEMPERATURE WITH THERMOCOUPLE	97
FIGURE 67—TORSO TEMPERATURE AND BOMB TEMPERATURE COMPARISON	98
FIGURE 68—TORSO TEMPERATURE COMPARISON WITH MODELS OF HUMAN ON TREADMILL WITH BOMB	98
FIGURE 69—COMPARISON OF IMAGE TEMPERATURE WITH THERMOCOUPLE	99
FIGURE 70—TORSO TEMPERATURE AND BOMB TEMPERATURE COMPARISON	99
FIGURE 71—TORSO TEMPERATURE COMPARISON WITH MODELS OF HUMAN ON TREADMILL WITH BOMB	100
FIGURE 72—COMPARISON OF IMAGE TEMPERATURE WITH THERMOCOUPLE	100
FIGURE 73—TORSO TEMPERATURE AND BOMB TEMPERATURE COMPARISON	101
FIGURE 74—WALKING ON TREADMILL WITH COOLED BOMB- LIGHTS ON- FAN ON- 0 MILES	101
FIGURE 75—WALKING ON TREADMILL WITH COOLED BOMB- LIGHTS ON- FAN ON- 1.5 MILES	102
FIGURE 76—WALKING ON TREADMILL WITH ICED BOMB-LIGHTS ON- FAN OFF- 0 MILES	102
FIGURE 77-- WALKING ON TREADMILL WITH ICED BOMB-LIGHTS ON- FAN OFF- 1.5 MILES	103
FIGURE 78-- WALKING ON TREADMILL WITH WARMED BOMB-LIGHTS ON- FAN ON- 0 MILES	103
FIGURE 79-- WALKING ON TREADMILL WITH WARMED BOMB-LIGHTS ON- FAN ON - 1.5 MILES	104

FIGURE 80-- WALKING ON TREADMILL WITH WARMED BOMB-LIGHTS ON- FAN OFF - 0 MILES	104
FIGURE 81-- WALKING ON TREADMILL WITH WARMED BOMB-LIGHTS ON- FAN OFF- 1.5 MILES	105
FIGURE 82—METAL PACKAGE HIDDEN IN VEST SHIELDED BY 1 TIGHT T-SHIRT	107
FIGURE 83—PLASTIC PACKAGE HIDDEN IN VEST SHIELDED BY 1 TIGHT T-SHIRT	108
FIGURE 84—METAL PACKAGE HIDDEN IN VEST SHIELDED BY 2 LOOSE T-SHIRT	108
FIGURE 85—PLASTIC PACKAGE HIDDEN IN VEST SHIELDED BY 2 LOOSE T-SHIRTS	109
FIGURE 86—METAL PACKAGE HIDDEN IN VEST SHIELDED BY 1 TIGHT T-SHIRT	109
FIGURE 87—PLASTIC PACKAGE HIDDEN IN VEST SHIELDED BY 1 TIGHT T-SHIRT	110
FIGURE 88—METAL PACKAGE HIDDEN IN VEST SHIELDED BY 2 LOOSE T-SHIRTS	110
FIGURE 89—PLASTIC PACKAGE HIDDEN IN VEST SHIELDED BY 2 LOOSE T-SHIRTS	111
FIGURE 90—TORSO TEMPERATURE COMPARISON WITH MODELS OF HUMAN WALKING OUTDOORS	113
FIGURE 91—COMPARISON OF IMAGE TEMPERATURE USING AUTOMATIC TEMPERATURE	114
FIGURE 92—TORSO TEMPERATURE AND BOMB TEMPERATURE COMPARISON	114
FIGURE 93—WALKING OUTSIDE WITH METAL BOMB AT 0 MILES	115
FIGURE 94—WALKING OUTSIDE WITH METAL BOMB AT 0.5 MILES	115
FIGURE 95—WALKING OUTSIDE WITH METAL BOMB AT 1 MILE	116
FIGURE 96—WALKING OUTSIDE WITH METAL BOMB AT 1.5 MILES	116
FIGURE 97—TORSO TEMPERATURE COMPARISON WITH MODELS OF HUMAN WALKING OUTDOORS	117
FIGURE 98—COMPARISON OF IMAGE TEMPERATURE USING MANUAL TEMPERATURE	117
FIGURE 99—TORSO TEMPERATURE AND BOMB TEMPERATURE COMPARISON	118
FIGURE 100—WALKING OUTSIDE WITH METAL BOMB AT 0 MILES	118
FIGURE 101—WALKING OUTSIDE WITH METAL BOMB AT 0.5 MILES	119
FIGURE 102—WALKING OUTSIDE WITH METAL BOMB AT 1.0 MILE	119
FIGURE 103—WALKING OUTSIDE WITH METAL BOMB AT 1.5 MILES	120
FIGURE 104—TORSO TEMPERATURE COMPARISON WITH MODELS OF HUMAN WALKING OUTDOORS WITH PLASTIC BOMB HIDDEN IN VEST-AUTOMATIC TEMPERATURE RANGE SETTING	120
FIGURE 105—COMPARISON OF IMAGE TEMPERATURE USING AUTOMATIC TEMPERATURE	121

FIGURE 106—TORSO TEMPERATURE AND BOMB TEMPERATURE COMPARISON	121
FIGURE 107—WALKING OUTSIDE WITH PLASTIC BOMB AT 0 MILES	122
FIGURE 108—WALKING OUTSIDE WITH PLASTIC BOMB AT 0.5 MILES	122
FIGURE 109—WALKING OUTSIDE WITH PLASTIC BOMB AT 1 MILE	123
FIGURE 110—WALKING OUTSIDE WITH PLASTIC BOMB AT 1.5 MILES	123
FIGURE 111—TORSO TEMPERATURE COMPARISON WITH	125
FIGURE 112—TORSO TEMPERATURE COMPARISON WITH	125
FIGURE 113—COMPARISON OF IMAGE TEMPERATURE WITH THERMOCOUPLE	126
FIGURE 114—TORSO TEMPERATURE AND BOMB TEMPERATURE COMPARISON	126
FIGURE 115—WALKING OUTSIDE WITHOUT BOMB OR VEST 0 MILES	127
FIGURE 116—WALKING OUTSIDE WITHOUT BOMB OR VEST 0.5 MILES	127
FIGURE 117—WALKING OUTSIDE WITHOUT BOMB OR VEST 1 MILE	128
FIGURE 118—WALKING OUTSIDE WITHOUT BOMB OR VEST 1.5 MILES	128
FIGURE 119—SUN BEHIND SUBJECT WITH METAL BOMB PACKAGE-	131
FIGURE 120—SUN BEHIND SUBJECT WITH ONLY T-SHIRT-	131
FIGURE 121—SUN BEHIND CAMERA WITH METAL BOMB PACKAGE-	132
FIGURE 122—SUN BEHIND CAMERA WITH ONLY T-SHIRT-	132
FIGURE 123—SUN BEHIND SUBJECT WITH METAL BOMB PACKAGE -	133
FIGURE 124—SUN BEHIND SUBJECT WITH ONLY T-SHIRT-	133
FIGURE 125—SUN BEHIND CAMERA WITH METAL BOMB PACKAGE-	134
FIGURE 126—SUN BEHIND CAMERA WITH ONLY T-SHIRT-	134
FIGURE 127—SUN BEHIND SUBJECT WITH METAL BOMB PACKAGE —	135
FIGURE 128—SUN BEHIND SUBJECT WITH ONLY T-SHIRT-	135
FIGURE 129—SUN BEHIND CAMERA WITH METAL BOMB PACKAGE-	136
FIGURE 130—SUN BEHIND CAMERA WITH ONLY T-SHIRT-	136
FIGURE 131—SUN BEHIND SUBJECT WITH METAL BOMB PACKAGE —	137
FIGURE 132—SUN BEHIND SUBJECT WITH ONLY T-SHIRT-	137

FIGURE 133—SUN BEHIND CAMERA WITH METAL BOMB PACKAGE-	138
FIGURE 134—SUN BEHIND CAMERA WITH ONLY T-SHIRT-	138
FIGURE 135—SCREENPRINTED T-SHIRT WITH GRAYSCALE COLOR PALETTE	139
FIGURE 136—SCREENPRINTED T-SHIRT WITH HIGH CONTRAST	140
FIGURE 137—SCREENPRINTED T-SHIRT WITH HIGH CONTRAST	140
FIGURE 138—METAL BOMB PACKAGE SHIELDED BY 1 T-SHIRT AT 6FT-	141
FIGURE 139—METAL BOMB PACKAGE SHIELDED BY 1 T-SHIRT AT 6FT-	142
FIGURE 140—METAL BOMB PACKAGE SHIELDED BY 1 T-SHIRT AT 12FT-	143
FIGURE 141—METAL BOMB PACKAGE SHIELDED BY 1 T-SHIRT AT 12FT-	143
FIGURE 142—METAL BOMB PACKAGE SHIELDED BY 1 T-SHIRT AT 25FT-	144
FIGURE 143—GUIDE TO FIND BOMB WITH INFRARED CAMERA	150
FIGURE 144—POSSIBLE INFRARED CAMERA SYSTEM OPERATION	158

LIST OF TABLES

TABLE 1—CURRENT TECHNOLOGY DEVELOPMENT FOR CONCEALED WEAPON DETECTION	11
TABLE 2--VOLTAGES USED BY FLIR IR CAMERA	15
TABLE 3-- TABLE 6 ON PAGE 8.8 IN 2005 ASHRAE FUNDAMENTALS	25
TABLE 4—TYPICAL METABOLIC HEAT GENERATION FOR VARIOUS ACTIVITIES	27
TABLE 5—OVERVIEW OF TESTING PHASES IN RESEARCH	38
TABLE 6—TEMPERATURE READINGS OF THERMAL OBSERVATION MANIKIN	50
TABLE 7—FOCUS TIMES AT VARIOUS DISTANCES	51
TABLE 8—FOCUS TIMES AT VARIOUS DISTANCES AFTER CAMERA VIEWING ANGLE CHANGE	52
TABLE 9—MAXIMUM VISIBLE DISTANCES OF VARIOUS COUPONS	53
TABLE 10—EXTERIOR CLOTHING TEMPERATURES FOR TORSO AND BOMB PACKAGE AREAS	70
TABLE 11—TEMPERATURES MEASURED IN VARIOUS CHAMBER CONDITIONS WHILE WALKING ON A TREADMILL	91
TABLE 12—EXTERIOR CLOTHING TEMPERATURES FOR TORSO AND BOMB PACKAGE AREAS WITH VARIOUS LAYERING AND PACKAGE MATERIAL COMBINATIONS	107
TABLE 13—AVERAGE TORSO TEMPERATURES WITH EXPOSURE TO SUN	130
TABLE 14—AVERAGE BOMB PACKAGE TEMPERATURES WITH EXPOSURE TO SUN	130
TABLE 15—TORSO AND BOMB PACKAGE TEMPERATURE DIFFERENCE WITH EXPOSURE TO SUN	130
TABLE 16—GENERAL CONCLUSIONS FROM PHASE 1 TESTING	153
TABLE 17—GENERAL CONCLUSIONS FROM PHASE 2 TESTING	154
TABLE 18—GENERAL CONCLUSIONS FROM PHASE 3 TESTING	155

CHAPTER 1-CURRENT STATE OF SUICIDE BOMBINGS

The main tactics used by terrorists have consistently been: bombings, attacks on installations by tactics other than bombing, hijacking, assassinations, and kidnapping. Between 1968 and 1994 bombing accounted for 40% to 50% of all terrorist activity. Since then, armed attack has taken over as the most common terrorist tactic, but bombings are still a major concern (Smith, 2001). One of the most deadly tactics used is suicide bombing. Suicide bombing has only been used in ten of the 69 countries that have seen violent uprisings in the last half century, but the effects of suicide attacks are much more lethal than most armed attacks (Berman, 2005). Between 2000 and 2002 only 1% of attacks in Israel were attributed to suicide attacks, but 44% of the Israeli casualties were a result of these attacks (Nunn, 2004). The tactic's lethality has been noticed by certain organizations and its use continues to be adopted.

Most organizations using suicide attacks are in conflict with an established state. Many times suicide attacks are used in conflicts where opposing sides belong to different racial, ethnic, religious, or national groups. It is the hope of the organization that these attacks will shock the opposing force and help the organization raise awareness of their cause. In monetary terms, suicide attacks are relatively inexpensive. The price of the materials used in a suicide attack in Israel can be obtained for about \$150 (Cronin, Audrey K., 2003). From an economic point of view, this is a small price to pay for the destruction that is caused in the attack. On the other hand, losing dedicated organization members is extremely wasteful if it is unnecessary to do so, so organizations only resort to these tactics when it is absolutely necessary (Berman, 2005).

Suicide attacks are rarely used by organizations trying to win over members of the population to their ideologies. This being the case, suicide attacks are rarely used in ideological

wars that revolve around party membership and ideological affiliation. In cases where the tactics are accepted, they are usually only supported if the organization has exhausted all other options in their fight (Bloom, 2004).

Public outcry and support for suicide attacks vary greatly on the target of a suicide attack. Not only are citizens targets, but so are military personnel, military bases, infrastructure, international organizations, and non-governmental organizations. In cases where hatred for opposing sides is unrelenting and violence is commonplace, suicide attacks will be less discerning between military and civilian targets (Bloom, 2004).

Attackers will usually choose targets that will have the largest impact to the conflict's opposing side. Because military installations are usually heavily guarded, many times the easiest targets are civilian ones. If attacks on civilians are frowned upon by the supporting population, then the groups will usually refocus their attacks on military targets despite the increased possibility of failure.

SUICIDE BOMBER DEMOGRAPHICS

Terrorist organizations are very dynamic and adaptable. This is evident in the membership of organizations that carries out these suicide attacks. There is no single description of the typical suicide attacker, so profiling suspects is very difficult. What formally seemed to be the typical traits of a suicide bomber are no longer the same. There is less of a connection between the social and economic status of the people that fill the suicide bomber role and the reasons for why they participate. In the past it seemed that the attackers were youths that came from lower class backgrounds. These people had little or no education, few skills, and very few opportunities in life. These trends are becoming less noticeable as the profile of a typical suicide bomber changes. In the past, suicide attacks were mostly carried out by males, but females have

been increasingly filling the role of the attacker. More suicide bombers are coming from a background in which they are well educated and able to obtain employment unrelated to the militant organization. It is believed that this increase is due to their knowledge and understanding of the ideological message that is promoted by the organization's leadership (Berman, 2005). In very diverse countries like the United States, it is likely that an attacker could be from many different backgrounds (Nunn, 2004).

Many organizations that use suicide techniques are secular in nature, but a growing number of religious groups seem to be adopting these strategies. It appears as if some of these religious groups have an easier time recruiting persons to carry out these attacks.

There seem to be two different types of people that carry out suicide attacks. The first type is people raised within the organization and taught to believe in the ideologies for which the organization stands. These attackers are persuaded to sacrifice their life for the greater good of the organization (Berman, 2005). The second type is people educated outside of the organization but are drawn to the organization because of personal reasons. An example of this would be people taking vengeance for a loved one that was killed in opposing attacks (Bloom, 2004). Other people may be willing to commit to suicide attacks because of rewards they are promised. These rewards may be spiritual in nature such as promises of riches in the afterlife or that the attacker's families will join them in the afterlife. Rewards may also be in the form of cash and security for the attackers remaining family members.

SUICIDE BOMBING TARGETS

Prime targets for suicide bombing attacks include military bases, airports, large public gathering places, public buildings, subways, schools, banks, and malls (Toet, 2003). These are all places where there are dense populations of people or the infrastructures are important to

society's operation. Soldiers in foreign countries are facing terrorism tactics from opposing forces. All of these areas would benefit greatly from technologies that enabled the detection of suicide attackers and their weapons (McMakin, 1996).

Most targets can be categorized into four main situations. They are: a marketplace, an entry point, a one-on-one situation, and a passageway. The typical marketplace is an open area that is filled with many people moving in different directions. This situation has a high probability for having large numbers of casualties and injuries due to the large number of people. The second situation is a checkpoint. This may be military or otherwise. Many times the bomber must travel through an entry point or check point in order to arrive at their desired destination. Many times there are current technologies installed at these points to reveal concealed weapons. The third situation that may be encountered is a one-on-one situation in which the suicide bomber may approach from an open area without people present. The last main situation that may be encountered is that of meeting a suicide bomber in a passageway. This is close to the entry point scenario, but there may be other people around.

Each of these situations allow for the use of differing technologies for weapon detection. Some detection technologies are more applicable in certain situations and areas. For instance, the entry point or passageway may allow the use of technologies that work at short distances. In a typical marketplace scenario a detection system would have to differentiate between people and accurately locate the threat at much greater distances.

SUICIDE BOMBING TACTICS

Explosives are not the only threat in a suicide attack. Bombers also pack shrapnel with the explosives in order to increase the effectiveness of the blast. This shrapnel causes injury to people at distances further from the initial blast site. Many times there are more injuries due to

this shrapnel than there are from the actual blast. Most shrapnel consists of small metallic projectiles such as ball bearings, nails, and bolts.

THWARTING OF ATTACKS

There are four main area of focus when trying to interdict a suicide attack: prevention, detection, neutralization, and response. Ideally all attacks would be stopped in the first step. Much work goes on to stop attacks at this point. Intelligence is constantly being gathered by intelligence agencies and local law enforcement. These agencies may pay off members of the organization to obtain information, or they may even imbed agents inside the organization to gather intelligence. If not directly observing an organization the agencies may watch for specific behaviors in suspects that may be clues that they are involved with an attack.

Suicide attacks are routinely stopped before they are initiated. For example, the Israel Defense Force stopped 25 attacks in June 2003. Many of these potential attacks were discovered by checkpoints, security guards, and aerial surveillance technologies. Information may also be given to the authorities by informants within the organization.

It is desirable to decrease the ability of attackers to obtain the required materials for the weapons, but this is difficult since many of the weapons are made with everyday household items. Explosives remain the main concern though. Between 1993 and 1997 over ten tons of explosives were stolen in the US (Nunn, 2004).

Preventing an individual from acting on their own accord is by far the most difficult event to prevent. There is little communication to intercept in order to figure out what will happen, and many times the reasons for their action are unclear and unpredictable. It is extremely difficult to gather intelligence for such a situation.

If we fail to prevent the beginning of a suicide attack we then must be able to detect the

attacker or weapon while the attack is in progress. One aspect that makes suicide attacks very hard to detect is that a planned attack can change once it is in progress. This flexibility remains to be the greatest advantage for a suicide attacker.

The desired result will usually dictate what type of detection is needed. The counterforce to the attacker must reflect the accuracy of the device. If the goal is to kill the suicide attacker before they begin their attack, then the detection method must not produce any type of false alarm. If the intention is to pull them aside and search them further, a less certain method may be used. In addition to determining who the attacker is, we must also determine the type and size of the threat. This information is important in preparing emergency personnel.

How we deal with an identified attacker is the fourth major area of interdiction. It must be determined how to respond to situations once the threat is identified. In an ideal case the threat can be diverted from its target and disarmed with no injuries. The US ATF has guidelines on how to deal with “homicide bombers”. Because the bombers have already decided to end their life for the cause, these guidelines emphasize not closing distances with the bomber because “close and negotiate” tactics will not work. This makes it very hard to disarm a threat.

While there are many attempts at thwarting these attacks by addressing the root cause issues for this destructive behavior, we must try to stop any attack that may be in planning or in progress. Technology use is a key factor in stopping these attacks.

DETECTION TECHNOLOGY

People that do not want to be caught with a weapon will go to great lengths to conceal the object. Small weapons may be carried on the body in areas that make it unobservable to the casual eye or even a thorough visual search. Many times these people will attempt to hide these weapons inside the orifices of their body. Technologies that are able to detect these hidden objects are desirable (Costianes, 2006).

The ideal detection technology would have many different characteristics. It would be fast, accurate, work from long distances, and safe for the detector and the subject of observation. Being able to detect at a distance allows the detector to take more control of the situation. It allows for more time to make decisions about how to respond to the threat. Detection from a distance also provides more protection for those who are operating the detection device (McMakin, 1996). This ability to detect threats from a distance becomes very critical when the flow of people is not in an organized and controlled manner because it is much harder to plan responses in such a situation (Chen, 2005).

Because many different materials are used in making weapons we need detectors that are capable of detecting all types of materials. The current systems used in portal detection situations are usually for detecting metal objects. These systems will not necessarily detect weapons made of plastics or other non-metal materials.

In order to detect suicide bombers the technologies would need to be able to detect through clothing and other masking techniques. The technologies need to be safe for use on humans. The technology needs to be comfortable for general public use as many innocent people will be subjected to the detection procedures. In the case of a suicide bomber it is also necessary that the detection systems works in real time or close to real time as the bomber may

activate the weapon as soon as they know they have been discovered. The quicker the threat is detected, the more time there is to disable the threat (Slamani, 1999).

Currently the most common use for detectors is in controlled situations. These may be in terminal gates at transportation hubs, entrances to public buildings, or entrances to large public gatherings. All of these situations control the flow of people and cargo through specific areas. This allows detectors to be set up with optimum conditions for detection of threats. It also allows for a planned response in the case that a threat is detected. It is common to see metal detector portal systems, hand wand systems, and even physical searches, these systems are usually not capable of detecting threats from long distances (McMakin, 1996), but these technologies speed up the necessary inspections of people and cargo.

With the increase in suicide bombings we are seeing a need for threat detection in uncontrolled environments. For example, the military is constantly encountering situations in which they are unfamiliar with and have no control over their surroundings. It is impossible to implement many of the technologies that are used in controlled access situations. Having detection techniques and technologies that worked in these situations would be a major advantage.

There has been an increased interest in mobile detection systems that can be used in these uncontrolled environments. These may be some type of handheld device or a system mounted in a vehicle. Because of the mobile nature of the detectors suicide bombers would not be able to plan for, or even be aware of, the detection system. Because these devices can be used without the consent of the public, many people are uncomfortable with the use of these technologies. Many people consider this an invasion of privacy (Jain, 2004).

Threats are continuously changing and will take advantage of the deficiencies of current

detection systems. Because of this we need to continuously improve the current technologies as well as add new technologies that address the weakness of the technologies currently in use.

CURRENT TECHNOLOGIES

A desirable concealed weapon detection system detects threats in real time, at long distances, and through clothing or other masking devices. To date there is not a single sensor that satisfies these characteristics well enough to be used as a stand-alone system. Sensors usually have some of the ideal capabilities but fail to adequately perform all of them (Slamani, 1999).

The most common sensors currently used will sense certain wavelengths in the electromagnetic spectrum. These sensors are either active or passive. Active sensors must send out low-power radiation waves in order to illuminate the scene. The sensor is then able to measure reflected waves that reach the sensor. Passive systems require no amount of illumination or applied radiation to operate. These passive systems only detect electromagnetic waves that are already present. Active sensing technologies face much more criticism than passive systems because of the radiation exposure they inflict on subjects. In many cases warnings must be posted with these active detectors. If warnings are posted the effectiveness of a covert detection scheme is decreased (Chen, 2005). There have been many advances with concealed weapon detection sensors, both active and passive, that aid in detecting threats carried on a person. Many of these sensors will detect objects concealed by clothing or within a bag or suitcase, but most of these technologies work at distances of 0.5 meters or less. These sensors are usually used in portal entryways, or hand-held devices (Costianes, 2006).

Most current methods used for detection of explosive materials at distances are not suitable for use on people as they require active methods of sensing. These methods would

expose people to an unacceptable amount of radiation. There is work currently being done to use these technologies with much lower amount of radiation, but a passive method which does not subject the person to radiation would be more likely to be accepted by the public.

Two of the most successful methods used to detect threats use millimeter waves or microwaves. These areas of the electromagnetic spectrum have been found to easily penetrate clothing layers to detect hidden objects. The downside to these sensors is that they work only over short distances and take a relatively long time to detect a threat (Toet, 2003) (McMillan, 2000). Millimeter Wave also have much poorer resolution than other available sensors. Many times MMW sensors are paired with higher resolution sensors in fusion systems (Chen, 2001).

Because not all weapons are made from metallic materials, sensors are needed in order to detect other materials fashioned into weapons. Terahertz Spectroscopy has been used to detect plastic explosives such as C-4. Like many other sensor technologies this method is an active system. It uses gamma rays from neutron beams to detect the presence of the substance in question. An overview of current detection technologies adapted from (Paulter, 2001) is given in Table 1.

One detector that has shown potential as a tool for detecting hidden weapons is an infrared detector. Infrared detectors are passive sensors that create infrared, or thermal, images without having to expose the subject to any amount of radiation. These images show the heat signature that is given off by objects of interest. One advantage of infrared detectors is they work at long ranges. These systems can also work in near real time. These two requirements of the ideal detector are fulfilled, but IR detectors tend to lack the ability to penetrate clothing and other masking systems such as briefcases or duffle bags (Slamani, 1999).

*Table 1—Current Technology Development for Concealed Weapon Detection
Adapted from (Paulter, 2001)*

Description	Illumination	Proximity	Portability	Energy
Hard object detector	Active	Far	Portable	acoustic
Imaging Portal	Active	Near	Transportable	Magnetic
Body Cavity Imager	Active	Near	Fixed Site	Magnetic
Microwave Holographic Imager	Active	Near	Transportable	EM Wave
Microwave Dielectrometer Imager	Active	Near	Transportable	EM Wave
X-Ray Imager	Active	Near	Transportable	EM Wave
Microwave Radar Imager	Active	Far	Transportable	EM Wave
Millimeter-Wave/Terahertz-Wave Imager	Active	Far	Transportable	EM Wave
Millimeter-Wave Radar Detector	Active	Far	Handheld	EM Wave
Infrared Imager	Passive	Far	Handheld	EM Wave
Passive Millimeter-Wave System	Passive	Far	Transportable	EM Wave
Active Millimeter Wave System	Active	Far	Transportable	EM Wave

IR TECHNOLOGY

IR detectors measure the natural thermal radiation given off by objects that are above temperatures of absolute zero. They use these properties of absorption, reflectance, and transmittance along with other information in order to calculate and display temperature of objects giving off the radiation.

Infrared detectors will detect radiation that is omitted by the object of interest as well as scattered radiation from the atmosphere. The radiation that originates from the object of interest has two components. One is the radiation that is omitted by the object itself, and the other is the infrared radiation that is omitted by other objects and is bounced off the object of interest towards the detector (Kribus, 2003). Figure 1 depicts the radiation sources detected by the infrared camera.

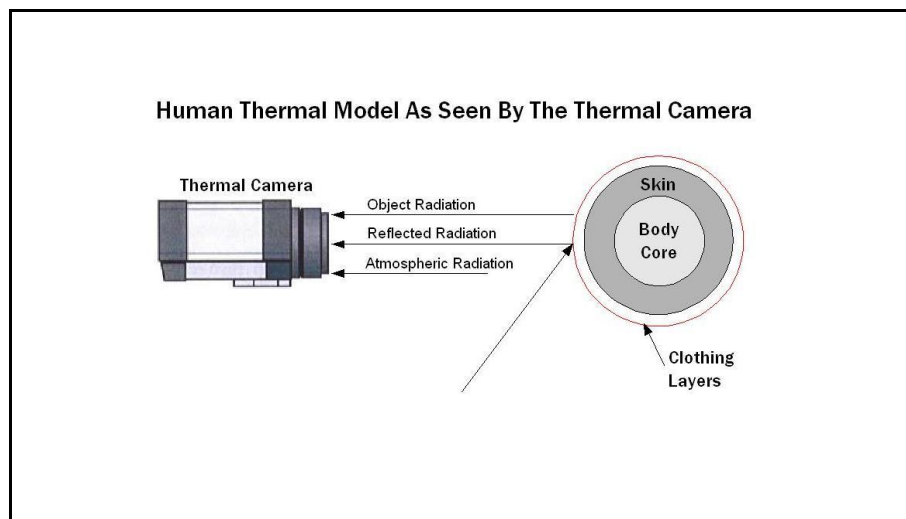


Figure 1—Infrared Radiation Measurement Off Human

A blackbody is an object that absorbs all radiation that encounters it. No radiation passes through it or is reflected from it. Real objects are rarely ever considered true blackbodies. Non-

blackbodies, or graybodies, differ from the ideal case due to their properties of absorption, reflectance, and transmittance.

According to (FLIR, 2004) the spectral absorption α_λ is defined as the ratio of the spectral radiant power absorbed by an object to that incident upon it. The spectral reflectance ρ_λ is the ratio of the spectral radiant power reflected by an object to that incident upon it, and the spectral transmittance τ_λ is the ratio of the spectral radiant power transmitted through an object to that incident. At any wavelength λ the sum of these three ratios must add up to 1.

$$\alpha_\lambda + \rho_\lambda + \tau_\lambda = 1$$

In the case of an opaque material, no radiation is transmitted through the object, so the τ_λ term is 0 and the summation simplifies to:

$$\alpha_\lambda + \rho_\lambda = 1$$

The emissivity ε_λ of an object plays a large role in determining the radiation given off by an object. Emissivity is the ratio of the radiation emitted from an object to that of a perfect blackbody at the same wavelength. A true blackbody has an emissivity of 1 while a graybody will have a emissivity value less than 1. The emissivity of a material is expressed mathematically as:

$$\varepsilon_\lambda = \frac{W_{\lambda o}}{W_{\lambda b}}$$

A property derived from Kirchhoff's Law states that for any specific temperature and wavelength the spectral emissivity and spectral absorption of a body are equal. Hence:

$$\varepsilon_\lambda = \alpha_\lambda$$

For opaque materials we can replace the emissivity term for the absorption term of the

summation $\alpha_\lambda + \rho_\lambda = 1$ and get:

$$\varepsilon_\lambda + \rho_\lambda = 1$$

A general form for calculating the object temperature can be formulated from the calibrated camera output. The radiation power from a blackbody source is W . For a graybody source with emissivity ε this power is considered εW_{source} . This power generates an output signal from the camera of U_{source} that is proportional to the power input

$$U_{source} = C\varepsilon W_{source}$$

where C is a constant.

A power term for each of the three types of radiation is then formulated:

- 1) The emission from the object is $\varepsilon\tau W_{obj}$ where ε is the emittance of the object, τ is the transmittance of the atmosphere, and the temperature of the object is T_{obj} .
- 2) The emission reflected from ambient sources is $(1-\varepsilon)\tau W_{refl}$. The emissivity and reflectivity property for opaque materials, $\varepsilon_\lambda + \rho_\lambda = 1$, is rearranged to be $\rho_\lambda = 1 - \varepsilon_\lambda$ and is used as the term representing the reflectance of the object. τ is the transmittance of the atmosphere and the ambient sources have the temperature T_{refl} .
- 3) The emission from the atmosphere is $(1-\tau)\tau W_{atm}$. $(1-\tau)$ is the emittance of the atmosphere, and the temperature of the atmosphere is T_{atm} .

These three terms can now be collected and summed to get a total received radiation power of:

$$W_{tot} = \varepsilon\tau W_{obj} + (1-\varepsilon)\tau W_{refl} + (1-\tau)W_{atm}$$

Each term is then multiplied by the constant C , and the CW products are replaced by the corresponding U to get:

$$U_{tot} = \varepsilon\tau U_{obj} + (1-\varepsilon)\tau U_{refl} + (1-\tau)U_{atm}$$

Solving this equation for U_{obj} we get:

$$U_{obj} = \frac{1}{\varepsilon\tau}U_{tot} - \frac{(1-\varepsilon)}{\varepsilon}U_{refl} - \frac{(1-\tau)}{\varepsilon\tau}U_{atm}$$

This is the general measurement formula that all FLIR infrared products use. The voltages of the formula are shown in Table 2.

*Table 2--Voltages used by FLIR IR Camera
Reproduced from Camera Documentation*

U_{obj}	Calculated camera output voltage for a blackbody of temperature T_{obj} . This voltage can be directly converted into true requested object temperature.
U_{tot}	Measured camera output voltage for the actual case.
U_{refl}	Theoretical camera output voltage for a blackbody of temperature T_{refl} according to the calibration.
U_{atm}	Theoretical camera output voltage for a blackbody of temperature T_{atm} according to the calibration.

The resulting voltage from the camera's calculation is then compared to a calibration curve for the camera. The FLIR algorithm that creates this calibration curve is based on radiation physics. Parameters required by the algorithm for calculating the calibration curve and temperature are the object's emittance ε and the effective temperature of the object's surrounding. Other parameters must be supplied in order to calculate to what extent the waves are scattered by the atmosphere between the object and the detector. These are the temperature of the atmosphere T_{atm} , the distance between the detector and the object, and the relative humidity, which is defined as the ratio of the partial pressure of water vapor in the air to the saturated vapor pressure of water at a certain temperature (FLIR, 2004). The temperature distribution found by the sensor is then used to create an image than can be perceived by the

human eye (Jones, B.F. 2002) (Chen, 2005).

One difficulty with using infrared imaging is the effect of background radiation. The background radiation can have a significant effect in the situation when the emitted radiation from the object of interest is of the same order of magnitude as the reflected background radiation at the wavelength of interest. This occurs in measurements of objects at moderate temperatures in a terrestrial environment when the 8-14 μ m infrared band is used (Kribus, 2003).

Each sensor type has its disadvantages, and infrared detectors are no exception. These sensors distinguish a threat from its surroundings based on temperature differentials. The larger these temperature differences are the more obvious the threat appears. Problems begin to occur when these temperature differentials are small. For example, when a weapon is being carried on a body, over time it comes into thermal equilibrium with its surrounding. This makes it hard for the sensor to differentiate between the weapon and the rest of the body (McMillan, 2000).

Problems also arise when the weapon is hidden under multiple layers of clothing. This, and other masking techniques, cause the threat to appear with less contrast and diffused into the background (Slamani, 1999). It has been found that radiation with wavelengths longer than 20 microns will penetrate clothing layers for detection better than shorter wavelengths (McMillan, 2000) (Liu, 2006).

Infrared detectors have been used to detect weapons under thin layers of clothing. Because of the nature of clothing's insulating properties when radiation is emitted by the body, it is absorbed by the clothing. It is then re-emitted by the clothing. Some travels towards the detector and some back towards the body. Couple this weaker re-emittance with thick and loose clothing, the weapon's infrared image becomes weaker and spread over a larger clothing area. This makes the weapons image hard to discern (McMillan, 2000) (Chen, 2005). Most

research about using infrared detectors for concealed weapon detection has concentrated on creating an image of the weapon that is hidden under the clothing of a suspect.

Wrinkles in clothing also mask a threat in an infrared image. The temperature variation due to clothing wrinkles over a small area can be significant. This makes it hard to detect the presence of the image of a hidden weapon (Varshney, 1999).

Electro-optical sensors are dependent on ambient illumination. Visible light is required in order to produce an image. This renders EO cameras useless at night or when trying to produce an image of a scene without illumination. IR sensors are not dependant on visual illumination in order to produce an image. Therefore they can produce an image in the absence of visible light (Socolinsky, 2002). The image appears the same in an IR image at night just as it would during the day given the same conditions (Xue, 2003).

Even so, when heat in the form of radiation accompanies the light source, it can change what is seen with the IR sensor. This is obvious in an outdoor setting when a shadow falls across an object. The object will appear much cooler in the areas covered by the shadow. This causes problems when observing humans in an outdoor situation. The direction of the sun and obstructions that cause shadows can greatly change the temperature of an object. When these areas are shaded, they are not absorbing the radiation from the surrounding environment the same as the unshaded areas. This will cause large temperature gradients in the image.

The shading issue is only one factor that makes IR sensing difficult in an outdoor environment. Various conditions may cause a sudden in temperature of an object. These may include environment temperature, wind, rain, and humidity to name a few. All these uncontrollable conditions make IR sensing in an outdoor environment extremely difficult (Socolinsky, 2004)(Kribus, 2003).

A concealed weapon may appear as a certain temperature in an image, but this is not to say it will be the only object in the scene that appears in that particular color. Because of this, there must be other mechanisms that contribute to determining what part of an image is a weapon (Slamani, 1999). Image fusion may be the answer to this problem (Xue, 2002).

Although there are many shortcomings for infrared detectors, one must take a serious look at the technology for use in concealed weapon detection systems due to the advantages of infrared detectors being passive systems, working at long distances, and being non-invasive to the subject under scrutiny (Prokoski, 1992).

RESEARCH OBJECTIVES

Previous studies using infrared detectors for concealed weapon detection have focused on trying to observe the image of the weapon. The shortcomings of the infrared detectors led to a search for alternate ways in which to use infrared technology to aid in suicide bomb detection.

It is the objective of this research to determine the feasibility of comparing the infrared images acquired of a suspected suicide bomber to thermal models predicting the temperature of the exterior layers of clothing worn by the subject in order to create a standoff bomb detection system. If the presence of a hidden weapon affects the emitted thermal signature such that the clothing temperatures do not correspond to that predicted by the model, a detection system may be developed in which the model and raw image may facilitate the detection of hidden objects.

This research also attempts to determine those variables that influence the image produced by infrared detectors in ways that help or hinder the use of the thermal models in predicting the temperatures of a subject's clothing.

Lastly, the final objective of this research is to determine a temperature range over which an operator viewing infrared images may be relatively certain of the presence of a foreign object being carried on a subject's body as compared to a thermal model.

CHAPTER 2-HUMAN THERMOGRAPHY

The medical community has been using IR technologies to study the body and its ailments. In order to get consistent results with an IR camera in a clinical setting, most studies control as many variables as possible. This includes environmental conditions, human activity, and human habits. The human body has mechanisms that react to all of these variables and will change the thermal condition of the body and the resulting IR image.

One major factor that affects the human body's temperature is the environment. In a clinical setting the environmental conditions are tightly controlled. Temperature, humidity, lighting, air flow, and temperature gradients are all critical to consistent measurements (Kakuta, 2002) (Shoji, 1997). The body will adjust to whatever surroundings it is subjected to, but this does not happen instantaneously. In order to have the body in an equilibrium state for imaging in clinical studies, the subject is usually brought into a controlled environment for a period of time in order for them to acclimate to their surroundings. The time required for this process will depend on the previous environment to which the body was subjected (Kakuta, 2002).

It has been discovered that the human body has a temperature cycle that changes throughout the day. If consistent measurements are wanted then researchers must take the temperature measurements at the same time during the day. Studies have shown that a two hour period before noon each day seems to be the most stable temperature of the body for the day. Human habits can also affect body temperature results. Smoking, alcohol consumption, drug use, and eating have all have been found to affect body temperatures. Because of these effects, in a clinical situation where IR images are taken, these actions are usually controlled for a certain time period before the images are taken in order for their thermal effect to wear off (Ring, 1990).

Other factors that may affect the thermal appearance of the human are the persons'

metabolism, activity level, stress, or anxiety. These, like other habits, are individual to the person being tested (Wang, 2004). Many of these conditions increase the blood flow in the body which changes the heat signature. This increase in blood flow is a natural human response to its surroundings and cannot be controlled.

Human activity can have an impact on the image in different ways. An active body will produce a higher temperature average, but some area of the body may react differently. In the case of leisurely walking, a gradual cooling of the nasal passage can be detected due to a more active breathing pattern (Pavlidis, 2000).

HUMAN THERMAL REGULATION

Much research has been done on the body's reaction to environmental conditions. The human body operates in a variety of extreme temperature conditions. In order to maintain proper function, the human body must regulate its core body temperature to within very specific limits in order for its vital organs to operate correctly. There are many mechanisms that the body uses to regulate these temperatures. The body's metabolism as well as contracting muscles generates heat that is distributed throughout the body through circulating blood. Parts of the Hypothalamus, the region of the brain responsible for controlling certain metabolic processes, detect the temperature of the blood and send out signals to the body on how to regulate the temperature in order to keep the core temperature within specific limits. If there is a decrease in blood temperature is detected then the body will begin vasoconstriction. The blood vessels near the surface of the body will constrict which in turns allows less blood to flow through. This keeps the heat transferred in the blood closer to the core of the body in order to keep the body's vital organs within their temperature limits. The body will also raise the hair on the skin in order to trap a layer of air that will help insulate the body. It may also generate heat from shivering

and other muscle activities.

When the Hypothalamus detects an increase in blood temperature it will send signals to the body to initiate heat loss. Blood vessels near the skin surface will dilate in order to bring more blood to the skin surface. This vasodilatation helps the body lose heat to the environment. Regulating mechanisms such as perspiration and exhalation are initiated. The metabolic rate may also be lowered in order to maintain this critical core temperature (Jones, B.F. 2002). When vasoconstriction and vasodilatation occur in the body there is a noticeable difference in the temperature changes across the body. Because the body's extremities have smaller volumes and thermal capacitance, they show the effects of blood flow changes quicker than the torso and head (Kakuta, 2002).

The regulation mechanisms are not instantaneous. When moving from one environment to another, there is a lag in the temperature control. A person imaged just after changing environment conditions will appear different than a person that has been acclimated to the imaging environment.

Research on the human body has been done in order to simulate how the body will react to different environmental conditions, clothing, and activity. For the purpose of studying how a suicide bomb package will affect the human body's thermal reaction to its environment one of these simulation models was used. The Tranmod model used was developed at Kansas State University for studying the human body reaction to transient environmental conditions with different clothing ensembles. Professor Byron Jones, one of the developers, was consulted for help using the Tranmod model for this research.

CHAPTER 3-SUICIDE BOMBER MODELING

Modeling the suicide bomber scenario is not a trivial task. There are many uncontrollable variables that the modeler has no control over. In almost all suicide bombing scenarios the model used should be of transient nature due to the changing thermal conditions encountered.

HUMAN THERMAL MODEL PROGRAM

There are common characteristics to most human thermal models. Input data usually includes temperature of the surrounding air, humidity, the radiant field around the person, type and amount of clothing worn, sweat rate, and the person's activity. Many of these characteristics not only vary due to location, but they also vary over time. Human thermal models can take these transient conditions into account when predicting a model response. Computer models are useful since they can simulate the human response to changing conditions without having to take experimental measurements under all possible conditions (Kakuta, 2002).

In order to satisfy the laws of conservation of energy and mass, a basic model will show the heat and moisture exchange with the environment. The models will either show steady-state or transient responses to the heat generated within the body and the heat released to the environment.

Simple human models such as the Fanger Model and the Gagge Two-node model use only a one-dimensional approximation of the body and of the heat and mass exchange with the environment. The two-node model treats the skin temperature, sweating, clothing, and heat loss as being the same over the entire surface of the body (Jones, 1992).

The Tranmod model is focused on providing a transient 1-D model of heat and moisture transport through the clothing. The system is modeled as transient because people are constantly

changing their activity, their clothing, and their environment. It uses a relatively simple thermal model of the actual body (Jones B.W., 1992). The Tranmod model is a modified version of the two-node model that incorporates a transient clothing model. This two-node model was used for its relative simplicity as well as its transient nature. The two-node model treats the human body as two separate nodes, hence the name. The first node is the inner core of the body and the second node is the outer skin. The two-node model simulates the heat and mass transfer between these two nodes and the environment.

An important aspect of the Tranmod model is how it transforms the simple two-node model into a more useful model by breaking the skin node up into segments. The core continues to be a single node, but the skin is divided into the following 12 segments: head front, head back, chest, back, abdomen, buttocks, upper arms, lower arms, hands, thighs, calves, and feet. Each of these segments represents a user specified fraction of the total body surface area. In the Tranmod model each of these individual segments has their own clothing coverage. This gives a more realistic model than the two-node model's uniform covering of the entire body. Each one of these twelve segments can also be further divided into subsegments for greater clothing coverage accuracy (Jones & McCullough, 1985). These subsegments make the Tranmod model quasi-three dimensional since each subsection of each section has clothing coverage that actually corresponds to a human clothing ensemble (Jones B.W., 1992).

The Tranmod model was created to simulate the entire person-clothing system in transient situations and account for changes in environments, clothing, and activity. The Tranmod model has been validated using both human calorimetric data and thermal manikin heat flow data (Jones B.W., 1992). Because these same transient factors are being studied in this research, this model serves as a reliable way to calculate human skin temperatures when a bomb package is

added to the clothing worn by the subject.

In order to run a simulation with the human thermal model (HTM) program the data about the test environment must be input into the program. The program allows the environment to change a maximum of twenty times over the course of the simulation. The interval over which the environmental conditions are applied is input along with the environmental variables. The environmental variables required for the Tranmod program are: air temperature ($^{\circ}\text{C}$), mean radiant temperature ($^{\circ}\text{C}$), convection coefficient ($\text{W}/(\text{m}^2\cdot^{\circ}\text{C})$), linearized radiation coefficient ($\text{W}/(\text{m}^2\cdot^{\circ}\text{C})$), and the relative humidity (fraction). The convection coefficient needed by the program can be found in Table 6 on page 8.8 of the 2005 ASHRAE Fundamentals Handbook and has been reproduced in Table 3.

Table 3-- Table 6 on Page 8.8 in 2005 ASHRAE Fundamentals

Equations for Convection Heat Transfer Coefficients			
Equation	Limits	Condition	Remarks/Sources
$h_c = 8.3V^{0.6}$	$0.2 < V < 4.0$	Seated with moving air	Mitchell(1974)
$h_c = 3.1$	$0 < V < 0.2$		
$h_c = 2.7 + 8.7V^{0.67}$	$0.15 < V < 1.5$	Reclining with moving air	Colin and Houdas (1967)
$h_c = 5.1$	$0 < V < 0.15$		
$h_c = 8.6V^{0.53}$	$0.5 < V < 2.0$	Walking in still air	V is walking speed (Nishi and Gagge 1970)
$h_c = 5.7(M-0.8)^{0.39}$	$1.1 < M < 3.0$	Active in still air	Gagge et al. (1976)
$h_c = 6.5V^{0.39}$	$0.5 < V < 2.0$	Walking on treadmill in still air	V is treadmill speed (Nishi and Gagge 1970)
$h_c = 14.8V^{0.69}$	$0.15 < V < 1.5$	Standing person in moving air	Developed for data presented by Seppanen et al. (1972)
$h_c = 4.0$	$0 < V < 0.15$		
Note: h_c in $\text{W}/(\text{m}^2\cdot\text{K})$, V in m/s , and M in mets, where 1 met = $58.1 \text{ W}/\text{m}^2$.			

In order to solve for the sensible heat loss from the human skin the linearized radiation coefficient (h_r) is needed. The equation to find this value is found in the ASHRAE Fundamentals Book and has been reproduced here:

$$h_r = 4\varepsilon\sigma \frac{A_r}{A_D} \left[273.2 + \frac{t_{cl} + \bar{t}_r}{2} \right]^3$$

In order to solve this equation one must know both the mean radiation temperature \bar{t}_r and the mean temperature of the outer surface of the clothed body t_{cl} . A_r is the effective radiation area of the body in m^2 . A_D is the DuBois surface area in m^2 and can be calculated by:

$$A_D = 0.202m^{0.425}l^{0.725}$$

where m is the mass of the person in kg and l is the height in meters. The ratio A_r/A_D for a sitting person is 0.70 while it is 0.73 for a standing person. The last value needed to define the environment is the relative humidity. This is used in the calculation of evaporative heat loss from the skin.

After the environment for the simulation has been defined the conditions of the human being simulated must be input into the program. Like the environment, the conditions of the human over the total simulation time can be split into at most twenty intervals. The only variable that must be defined over each of these intervals is the metabolic heat generation rate. This is in units of $W/(m^2 \cdot ^\circ C)$. These metabolic rates were obtained from Table 4 on page 8.6 in the 2005 ASHRAE Fundamentals Handbook. This chart has been reproduced in part in Table 4.

Table 4—Typical Metabolic Heat Generation for Various Activities

Typical Metabolic Heat Generation for Various Activities		
	W/m ²	met
Resting		
Sleeping	40	0.7
Reclining	45	0.8
Seated, quiet	60	1
Standing, relaxed	70	1.2
Walking (on level surface)		
3.2 km/h (0.9 m/s)	115	2
4.3 km/h (1.2 m/s)	150	2.6
6.4 km/s (1.8 m/s)	220	3.8
Sources: Compiled from various sources. For additional information, see Buskirk (1960), Passmore and Durnin(1967), and Webb (1964)		

The HTM program simulates the bomb as a layer of clothing covering the chest area. This is an area of 0.184 square meters. This area matches the area of the package used in the experimental testing. The bomb is assumed to be made of steel like the simulated bomb package used in our testing. The bomb is 25mm thick. A person was modeled as standing still in 40°C (104°F) environment in order to simulate the climate in current warzones in which suicide bombing is being used as a tactic. Because the suicide bombers attempt to conceal their weapon as much as possible, it is assumed that that bomb is attached directly to the human's skin in order to make the hidden package as small as possible. If this assumption is used, the skin is in thermal equilibrium with the interior of the bomb package. This would not be the case if there were an air gap between the bomb and the skin or another type of insulating surface.

The heat transfer from each individual segment is calculated by:

$$\dot{Q}_i = A_i \frac{T_{si} - T_e}{R_i}$$

\dot{Q}_i is the heat loss, T is temperature, R is the thermal resistance, and A is the area. The subscripts e, s, and i represent ambient environment, skin, and the subsegment number respectively. The thermal resistance R_i is the sum of the fabrics and air layers covering the subsegment represented in subscript i and is calculated by:

$$R_i = A_o \left[\sum_{j=1}^n \left(\frac{R_{aj}}{A_{j-1}} + \frac{R_{cj}}{A_j} \right) \right] + \frac{R_e}{A_n}$$

Again, R is the thermal resistance and A is area. Subscripts a, c, and j represent air layer, clothing type, and clothing layer respectively. A_o is the skin area and R_e is the thermal resistance between the outside surface of the clothing and the environment. This includes thermal resistances for both radiation and convection from the outer surface of clothing. This model assumes still air so the value is set at $0.11 \text{ m}^2 \text{ K/W}$. The resistance of the air layer is:

$$R_{aj} = \frac{1}{h + \frac{k}{t_{aj}}}$$

Where h is the linearized radiation heat transfer coefficient, t is the thickness of the air layer j , and k is the thermal conductivity of air. In this model the values of h is set to $4.9 \text{ W/m}^2 \text{ K}$ and k is set to $0.025 \text{ W/m}^2 \text{ K}$.

The resistance of each clothing layer is calculated from its thickness:

$$R_{cj} = B \cdot t_{cj}$$

where B is a proportionality constant with a value of $0.025 \text{ m}^2 \text{ K/W mm}$.

The total heat loss from the body \dot{Q}_T is calculated by summing the heat loss from all individual subsegments. Using the total heat loss and the heat generated by the human, the model is able to calculate the skin temperature.

LCM MODEL

One of the simplest ways to model a transient conduction problem is with the lumped capacitance method. This method closely approximates the actual transient thermal scenario if the resistance to conduction within the solid is small compared with the resistance to heat transfer between the solid and its surroundings. This method is used under the assumption that the temperature of the solid is spatially uniform at any instant during the transient process.

The Biot Number is used to verify that the scenario in question is capable of being modeled with the lumped capacitance method. If the Biot Number (Bi) $\ll 1$ then the condition requiring the resistance to conduction within the solid be less than the resistance to convection across the fluid boundary layer is met. If this condition is satisfied using the following criteria

$$Bi = (h \cdot L_c) / k < 0.1$$

then the error in using the lumped capacitance method is small. In this formulation of the condition, $L_c = V/A_s$ where V is the object's volume and A_s is the object's surface area (Incropera & DeWitt, 2002). It was determined that Biot Number condition was satisfied for case of modeling the outer layer of clothing, thus allowing the use of the lumped capacitance model.

The lumped capacitance method is implemented by performing an energy balance on the solid. This energy balance relates the rate of change of the internal energy to the heat loss at the surface of the solid.

For the purpose of this research the program Interactive Heat Transfer v2.0 was used in order to help solve these energy balances. This program helped set up the energy balance equations and was used as an equation solver. The computer code and equations used for the energy balance are included in Appendix C.

The solid body that was of interest for this study was the outermost layer of material on

the subject's body covering the area of the simulated bomb package. In these models the area of the material located outside the bomb package was assumed to be 0.25 meters (10 inches) by 0.36 meters (14 inches). Accounting for the two sides of the material this fabric layer had 0.18 square meters of surface area. To stay as consistent with other models as possible, the material properties of the fabric layer were from the database used by the Tranmod program that is discussed in the Human Thermal Model Program section. The convection coefficient and applied heat flux used in the model were also used in the Tranmod program. These values were obtained from the ASHRAE Fundamentals Handbook and are discussed in the Human Thermal Model section as well.

The lumped capacitance model used in this research accounted for the convection due to the movement of the person, the internal heat generated by the human, the irradiation from the sun, and the initial shirt temperature. One must take into consideration the limitations of this model for the suicide bomber scenario. The LCM model does not account for the human body's temperature control mechanisms. For example, the production of sweat from the body will lower the temperature as the sweat is evaporated from the body and clothing. This thermal regulation mechanism will keep the temperature of the clothing from continuing to rise even with the addition of heat emitted from the body and the irradiation from the sun. These human physiological variables that will affect the temperature of the material layer are not accounted for in the lumped capacitance model; however this model serves as a useful reference under limited conditions and assumptions.

RESISTANCE MODEL

The HTM model provides a good prediction of what the average skin temperature should be under certain test conditions. In order to have a good comparison with the infrared imaging

camera it is desirable to have a predicted temperature of the exterior layer of clothing. This is the temperature that the camera will most likely acquire in an operational scenario. In this research the exterior temperature was predicted by combining the HTM model with a thermal resistance model.

This combined resistance model uses the HTM model to predict the average skin temperature. Other data needed by the model include environmental temperatures, size of the predicted bomb and torso area, and material characteristics of the bomb material and clothing such as thickness, heat transfer coefficients, thermal conductivities, and emissivity.

Resistance models are used for steady state analysis of thermal systems. In the case of the suicide bomber scenario most plausible situations will be transient. It is expected that the thermal resistance model will respond faster to temperature changes than experimental results, due to the assumption in the resistance model that the input temperature is steady state. General assumptions for the resistance model assume that the modeling of resistances in series is solved precisely while solutions of parallel resistances are approximated because of an assumed one-dimensional temperature distribution.

An air gap is assumed to exist between the body and clothing and between the bomb and the innermost layer of clothing. This assumption is made because the person is most likely moving and a slight gap will most likely be formed from this movement. Assuming the bomber attempts to contain the bomb as close to the body as possible the resistance model has no assumed air gap between the bomb vest and the bomb. If more than one layer of exterior clothing is modeled it was assumed that no air gap existed between these exterior layers.

The following resistance equation used for the model:

$$\begin{aligned}
& \left[\frac{1}{\frac{L_{gap}}{k_{gap} \cdot A_{tot}} + \frac{1}{h_{r_gap} \cdot A_{tot}}} \right]^{-1} + \frac{L_{vest}}{k_{vest} \cdot A_{tot}} \\
& + \left[\frac{1}{\frac{L_{bomb}}{k_{bomb} \cdot A_{bomb}} + \frac{1}{h_{r_ait_bomb_gap} \cdot A_{air_bomb_gap}} + \frac{1}{h_{c_ait_bomb_gap} \cdot A_{air_bomb_gap}}} \right]^{-1} \\
& + \left[\frac{1}{\frac{L_{gap}}{k_{gap} \cdot A_{tot}} + \frac{1}{h_{r_gap} \cdot A_{tot}}} \right]^{-1} + \frac{L_{cotton}}{k_{cotton} \cdot A_{tot}} + \left[\frac{1}{\frac{1}{h_{r_ext} \cdot A_{tot}} + \frac{1}{h_{c_ext} \cdot A_{tot}}} \right]^{-1}
\end{aligned}$$

In cases where no bomb or vest was worn the second, third, and fourth terms were removed from the equation. When more than one layer of clothing was worn, terms for the corresponding layer of clothing were added using the form of the fifth term.

While the HTM model accounts for body movement in its calculations of the skin temperature, the resistance model does not account for any of these effects when calculating the external fabric temps. This discounting of movement-induced convective effects and the lag in the temperature calculation due to the scenario's transient nature are the two main sources of error in this resistance model.

CHAPTER 4-EXPERIMENT SETUP

EQUIPMENT

CAMERA

The infrared sensor used in these experiments was a standard commercial grade infrared

camera. The infrared camera model used was a FLIR ThermaCAM S65. The camera specifications are found in Appendix A. This is a long wave infrared camera that operates between 7.5 and 13 μ m.



Figure 2—FLIR ThermaCam Model S65 used in Research

MANIKIN

A Thermal Observation Manikin (TOM) from The Cord Group was used in this testing. This manikin has the ability to regulate its body temperature to mimic that of a human. This provided a consistent way to measure the camera's abilities. The different body parts can be specifically set to desired temperatures for testing. The manikin also responds to outside temperature influences and regulates its own temperature like the human body. Not only does this manikin regulate its temperature like a human, it is also the same size and weight of a human.

This makes it a very good way to produce a simulation of the human body and its effects on the environment around it.

SETUP

CAMERA

In each test the infrared camera was mounted to a tripod. This provided a steady platform to take images from. The camera was using a battery for its power, so it is a very mobile system. When each image was taken it was stored to the cameras internal memory. When that memory was full, the images were transferred to a computer by a Flash Memory card.

MANIKIN

The manikin was set up in two different positions. In some instances it was mounted to a stand that held the manikin in a vertical “standing” position. When in this position, the camera could image the whole body. In other cases the manikin was set on a table in a sitting position with the legs straight out in front of its body. This position was used for images of the upper body only. The manikin was clothed with the desired clothing for each test. After it was clothed it would be turned on for the test.

PROCEDURES

CAMERA

The camera has autofocus and manual focus capabilities. Skilled operators of the camera may find themselves just as quick as the camera's auto-focusing feature. With experience this time may be decreased as the operator knows the full focusing capabilities at certain distances.

PROCEDURE FOR AUTO FOCUSING

When taking pictures the autofocus function was used as much as possible. In cases when camera could not select the correct object for focusing, the camera was manually focused. Even though this greatly increased the amount of time to take a picture, it produced a focused picture.

PROCEDURE FOR MANUAL FOCUS

Many times the autofocus will not focus on the desired object. This is especially true when the subject is far away from the camera lens. When this happens, the camera must be manually focused. When manually focusing the camera, the operator focuses on a small detailed object that will bring the subject's body into focus. In the case of humans, focusing on the subject's hair and facial features was the most accurate way to accomplish this. These objects work well for focusing as they are small relative to the human body and usually contrast well against the body temperature.

PROCEDURE FOR AUTO/MANUAL TEMPERATURE RANGE

After the camera is focused on the desired object the temperature scale must be adjusted. This procedure found the minimum and maximum temperatures within the field of view and set the minimum and maximum of the temperature scale to the corresponding values.

The temperature range that appears in each image may be set in two different manners. In order to set the temperature scale to the maximum and minimum temperatures of the current image the range may be set automatically. For this the auto-adjust function of the camera was used. This would scale the visible temperatures to match the temperature scale that is displayed with each image.

The other option which was also used in this research is to manually adjust the

temperature scale. This allows the operator to control the temperature scale displayed on the image. This required the operator to switch the camera over to the manual mode and then select a minimum and maximum temperature. The image then just displayed temperatures in a scene that fell between these two controlling temperatures. The operator can make the scale as small or as large as they would like in order to focus on certain temperatures or areas in a photograph.

MANIKIN

Basic operation of the Thermal Observation Manikin followed the following guidelines. The manikin was first clothed with the desired amount of clothing. The power and data cords were then connected from the manikin to the power interface. The controlling computer was connected to the power interface. The power interface was turned on and the TOM program was started on the computer. A new file was started and the desired skin temperatures for the manikin were set. After the temperatures were set and the simulation was started, the manikin will heat up and maintain the set temperature for the duration of testing. At the end of testing the TOM computer program was stopped and power and control cables were unattached in reverse order.

CALIBRATION

CAMERA

In order to learn about the capabilities of the camera we began by taking pictures of where the temperature of the subject was known. This tested the accuracy of the camera. We began with taking pictures of boiling water and ice.

MANIKIN

In order to test the accuracy of the measuring devices a test was set up using the thermal

test manikin. The default manikin temperature that was used for testing was set to have a skin temperature of 32°C (89.6°F). 32°C is a good average of the skin across the entire human body in a neutral state. Then the thermal camera was used to acquire the temperatures. The temperatures were also measured with thermocouples. Each part of the manikin was tested and the data was recorded. In general the thermocouples read temperatures slightly lower than the thermal camera. In all but two cases the infrared sensor was within 0.56°C (1°F) of the temperature the TOM was set to.

CHAPTER 5-TESTING PHASES

Testing was divided into three phases. Phase 1 focused on the abilities of the camera in an indoor situation, Phase 2 studied the use of the camera on humans in indoor situations, and Phase 3 studied the use of the camera on humans in outdoor situations. These phases are outlined in Table 5 and described further in the section.

Table 5—Overview of Testing Phases in Research

Overview of Testing Phases			
	Phase 1	Phase 2	Phase 3
Subject	Manikin	Human	Human
Environment	Indoors	Indoors	Outdoors
Temperature	Room Temperature	Warm/Hot	Warm/Hot
Phase Focus	Camera Settings/ Capabilities	Controlled Environment Capabilities	Uncontrolled Environment Capabilities

PHASE 1

The first phase of experiments focused on the application of the technology to an indoor situation. These tests used controlled environmental settings. Lighting, heat sources, materials, airspeed, etc were all known and controllable. The thermal test manikin was used for these tests so that the body temperature measurements could be controlled. The controlled nature of these tests provided a demonstration platform for the concept. These tests would determine the

following: camera accuracy, camera resolution, useful camera settings, focus abilities, emissivity effects, and effects of layered shielding. This provided a gauge on how the camera would respond when the environment was controlled.

FOCUS

Testing of the autofocus features were completed in this step. Outside it is nearly impossible to precisely focus on a subject. The shaded viewfinder image is extremely small and the external 4 inch LCD is difficult to view when outdoors. Focusing on the subject's face produces the best results since the face has small features the camera can detect. For best results the camera was linked to a computer using the supplied IEEE 1394 cable and used MATLAB®'s video acquisition techniques to display the live image on the computer screen. This displays the image at full size and allows for the most precise focusing.

The camera can also be manually focused. In most instances manual focusing takes longer than using the autofocus, but this technique insures the image is focused on the correct object in a scene and with maximum clarity. With experience the time required for manual focusing may be decreased as the operator learns the focusing capabilities at certain distances.

CAMERA RANGE

Experiments were done to find the effective operating range of the camera. Coupons of various sizes were placed in front of a warm background in order to simulate a package between the camera and the human body.

MATERIAL EMISSIVITY

A test board was built that held 5cm x 5cm square coupons of different materials so that material with different emissivities could be compared in a single picture. Coupons of copper,

aluminum foil, clay, wax, and two cotton materials were used. The board was allowed to come into thermal equilibrium with the room temperature before it was imaged. The board was placed in front of a blank background that had also come to thermal equilibrium.

SHIELDING

Since most suicide bombs are concealed underneath a person's clothing it was desired to use the Thermal Observation Manikin to simulate the effects of different amounts of clothing shielding the simulated bomb package. Temperatures of the manikin were taken with no shielding, one t-shirt, two t-shirts, and three t-shirts. These measurements were taken at four different distances. These same tests were completed with a simulated bomb package in a vest worn by the manikin underneath the shielding t-shirts.

TRANSIENT STANDING BEST/WORST CASE

It is assumed that not all bomb packages are in thermal equilibrium when worn by a suicide bomber. It was desired to know the amount of time that it takes these bomb packages to come into equilibrium with the human body. In order to find the difference between the longest and shortest amount of time for these packages to reach an equilibrium external heat sources were used to speed up and slow down the equilibrium times. A medical hot pack was attached to the simulated bomb package to make it increase from room temperature to its equilibrium temperature faster than normal. A cold pack was used to slow the process down. These packages were placed on the Thermal Observation Manikin for imaging in order to simulate the effects of these hot and cold packs combined with the heat from the thermal observation manikin.

PHASE 2

The second phase used an actual human in the indoor setting. These tests were a continuation of the phase one tests, but they had the added human element. The tests in this phase were conducted with real human subjects instead of the Thermal Observation Manikin.

Some experiments in this phase were conducted in an environmental chamber at the Institute for Environmental Research at Kansas State University. The environmental chamber is capable of measuring human physiological responses to various thermal environments. It is computer controlled and can simulate variables such as radiant heating, temperature variation, air flow over a subject, and other extreme thermal environments. Testing in the chamber allowed for controlled environmental conditions. This consistent background led to smaller temperature gradients between the test subject and its surroundings. This allowed for easier viewing of the simulated bomb package. Because it was desirable to know how this infrared technology would work in current warzones, the chamber was used in order to simulate a hotter thermal environment than was possible than with the current outdoor conditions. This hot climate would better simulate the warzones in which suicide bombing tactics are used.

COLOR PALETTES

The camera has many different image color palettes to choose from. According to Jim Haney, a Technical Support Representative for the camera's manufacturer FLIR, different industries seem to favor different color palettes. The military and surveillance industries almost exclusively used the grayscale color palette for their applications. The medical industry tends to like the low definition palettes. In our correspondence he mentioned that picking a color palette for an application is "all trial and error, experimenting, and experience".

The following color palettes were tested inside the IER environmental chamber: Blue-

Red, Gray, Iron, Rainbow, and Rainbow HC (high contrast). The inverse color palette for each of these 5 palettes was tested as well. An example of inverse color palettes is given in Figure 3 and Figure 4.



Figure 3—Grayscale Color Palette



Figure 4—Inverse Grayscale Color Palette

BOMB PACKAGE MATERIAL CHARACTERISTICS

Two different types of simulation bomb packages were used. One package used steel pipes as the exterior material. This was chosen because most suicide bombers use metallic packaging materials that will become shrapnel in the blast and cause injury to people that are further removed from the initial bomb site. Tests were also completed with plastic pipes in order to have a comparison with the metallic material. The plastic and metal pipes were chosen for the simulated bomb packages due to their common use by suicide bombers. These materials are used often because of they are inexpensive and common materials that are difficult to track and little care is taken in controlling their use.

The packages were put on the body and imaged at regular intervals until the packages appeared to be in equilibrium in the infrared image by visual inspection. Images of both types of simulated bomb packages were then taken using varying amounts of clothing as shielding.

TRANSIENT-STANDING-BEST/WORST CASE

The use of hot and cold packs was again used to simulated bomb package equilibrium times. In order to find the difference between the longest and shortest amount of time for these packages to reach an equilibrium external heat sources were used to speed up and slow down the equilibrium times on a human in the controlled indoor conditions. A medical hot pack was attached to the simulated bomb package and placed on the human body's torso and images were taken at intervals of 10 minutes over the course of three hours. A medical hot pack was attached to the simulated bomb package to make it increase from room temperature to its equilibrium temperature faster than normal. A cold pack was used to slow the process down. These packages were placed on the human for imaging in order to simulate the effects of these hot and cold packs combined with the heat from the body.

TRANSIENT-STANDING

Images were taken of a human standing still in an environmental chamber with a simulated bomb package. The package was held in a vest underneath one t-shirt. The test would show how long the image of the package stayed visible if the subject carrying the simulated bomb package were to stand still for an extended period of time. The simulated bomb package used was a metal package that began at room temperature. The environmental chamber was held at 40°C for these tests to simulate a hot environment. As mentioned by the FLIR company technical representative experimenting was done with all available color palettes on the camera to discover if a certain color palette tended to work better than the others in the given conditions.

TRANSIENT CHANGES WHILE WALKING

Tests were completed in the environmental chamber to study the effect of human activity

on the IR image. This was done by having the subject walk on a treadmill while pictures were taken at predefined walking distances. By completing these tests in the environmental chamber we were able to control some of the external conditions that will be experienced in an outdoors setting. The temperature was set at 33.33°C (92°F) with a humidity of 0.3. The bomb packages were allowed to sit out in the environment until they had reached equilibrium before being put on the person. In these tests the bomb was worn in a vest underneath a t-shirt.

TRANSIENT CHANGES WHILE WALKING BEST/WORST CASE

Tests were done to look at the best and worst cases for the package to come to thermal equilibrium. A simulated bomb package, initially in a bath of ice water, was immediately attached to a person's body and the subject began to walk on a treadmill. This was conducted in an environmental chamber at 40°C (104°F). This was run with and without a fan blowing towards the person at approximately 20mph. These same tests were also performed with simulated metal bombs that had come to thermal equilibrium inside the 40°C chamber before being attached to the body. The subject walking was told to pick a comfortable walking speed for the tests. In all of these instances the bomb was worn in a vest and covered with one t-shirt.

SHIELDING

The subjects being tested wore shirts of three different sizes. The tight shirts clung tightly to the person making approximately 85% of full contact with the chest and bomb vest. The semi-tight shirt made approximately 50% of full contact with the chest and bomb vest while the loose t-shirt hung over the bomb vest making approximately 30% of full contact.

The shielding of both metal and plastic simulated bomb packages was tested with different amounts of clothing shielding the hidden package.. The test subject was wearing the

shielding clothing over a vest which contained the bomb packages. These images were taken in the environmental chamber that had been set at 40°C (104°F). To further test the settings of the camera, an image was taken with each of the camera's color palettes in both the automatic mode and manual mode. This gave provides a full combination of camera setting results to analyze on three different clothing scenarios. Comparisons for each settings combination could be made to discover it different combinations seemed to work better in certain situations.

When in manual mode the temperature range was manually adjusted to show the bomb package. The camera was set to show a range of three to four degrees in temperature difference. Then the temperature range was scanned to find where the image of the bomb package was most easily detected.

SOLAR SIMULATIONS-LIGHTS ON

Testing in the chamber was helpful because we had hot conditions with a relatively consistent background. When the solar lights were turned on there was a temperature gradient on the wall that was visible to the camera, but there were no "hot spots" on the wall to change the temperature scale dramatically. The chamber was set at 40°C (104°F). In the chamber we completed a variety of different tests. With the solar lights on we looked at both metal and plastic simulation bomb packages. With each package we tested the effects of the shielding of different clothing ensembles. The test subject was wearing the vest which contained the bomb packages directly on his bare skin for all the tests.

SOLAR SIMULATIONS-LIGHTS OUT

We also did testing with the solar lights turned off. The chamber was set at 40°C (104°F). Having the solar lights turn off produced a very consistent temperature background. Both simulation bomb packages were set out on a table in the room to reach a stable temperature.

The metal bomb package was placed in the vest which was shielded by one semi-tight T-shirt. Then the first shirt was replaced by a loose t-shirt and the same pictures were taken. Then pictures were taken of the subject wearing both t-shirts as shielding. In this test the semi-tight shirt was worn over the vest and bomb package and that was covered by the loose cotton t-shirt. Each clothing combination was imaged with each color palette and its inverse color palette. These pictures were manually focused,

For each clothing and color palette combination, both an auto-adjusted temperature range image and a manually adjusted temperature range image are taken. When the manual temperature range was used, the color range was manually adjusted to show the bomb package. The camera was set to show a range of three to four degrees in temperature difference. The plastic bomb package was also put through the same tests as the metal bomb package.

PHASE 3

The third phase moved the testing into an uncontrolled outdoor environment. These tests were completed with a human subject. This phase really showed the applicability of this technology for use in the field where the operator has no control of environment of human condition.

TRANSIENT WALKING

In order to investigate the effects on the bomb package image due to walking in an outdoor setting the camera was set up in an outdoor location where the subject could be imaged at particular distances. The camera was set up in the shade while the subject was walking in an area exposed to sun. The subject walked a certain distance and returned to the camera at specified intervals in order to be imaged. The interval used for these experiments was 0.1 miles.

In addition to taking the image of the person, measurements of the temperature on the inside and the outside of the bomb package were also recorded. These outdoor walking tests were run with and without the bomb package. In both cases the vest was worn underneath 1 t-shirt. The outdoor temperature during this test was 21.11°C (70°F) with a relative humidity of 60%.

COMPARISON OF SUBJECT WITH AND WITHOUT BOMB VEST

In addition to testing the autoscaling color mode the manual color scaling capability of the camera was tested. These same tests were completed with the camera in a manual mode in which the temperature scale was set manually so that the torso region had the largest possible temperature contrast.

EFFECTS OF SUN

The sun is an important source of heat in the outdoor environment and will change how a subject is imaged. Various combinations of images were taken outside with the subject and camera positioned differently with respect to the sun under shade and no shade.

CLOTHING DESIGN FEATURES

Shirts with different clothing designs were tested in uncontrolled outdoor conditions in order to determine how clothing features may mask the heat signature of the simulated bomb package. The shirts had combinations of screen-printing and embroidery on the side being imaged.

TESTING LAYERING AT DISTANCES

We began by looking at a simulated metallic bomb packages. At each distance an image was taken of the subject with each color palette.

CHAPTER 6- RESULTS

RESULTS-CALIBRATION

CAMERA

As shown in Figure 6Figure 5 the camera displayed the expected value of 0°C (32°F) for ice. The expected value of 100°C (212°F) for boiling water was also obtained and is shown in Figure 6. While the thermal sensitivity of the camera is 0.08°C at 30°C, the camera displays the temperature scale in units of whole degrees. According to the camera specifications, the camera's accuracy is $\pm 2^{\circ}\text{C}$ or $\pm 2\%$. These results show the camera well within that accuracy.

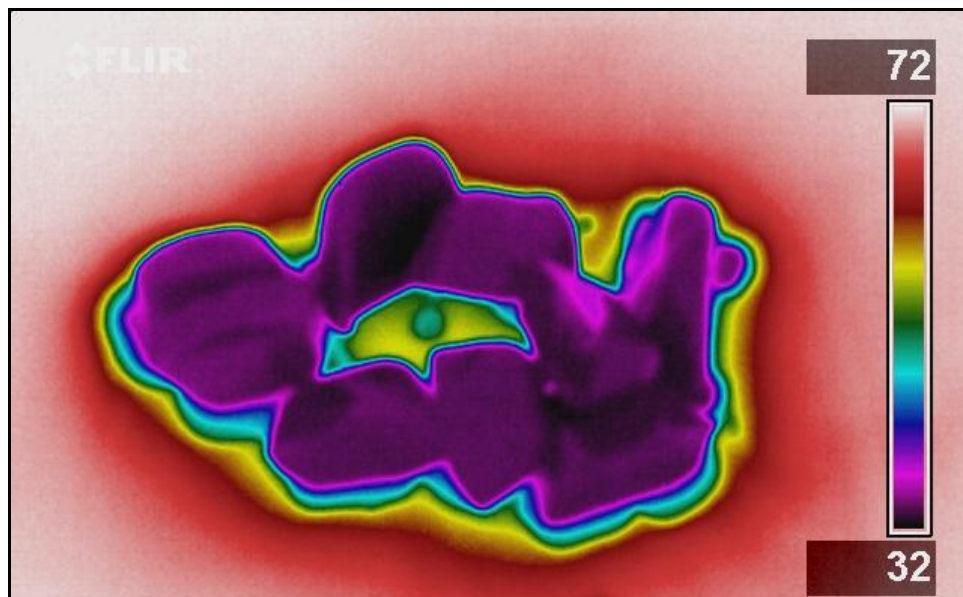


Figure 5—Infrared Image of Icecubes

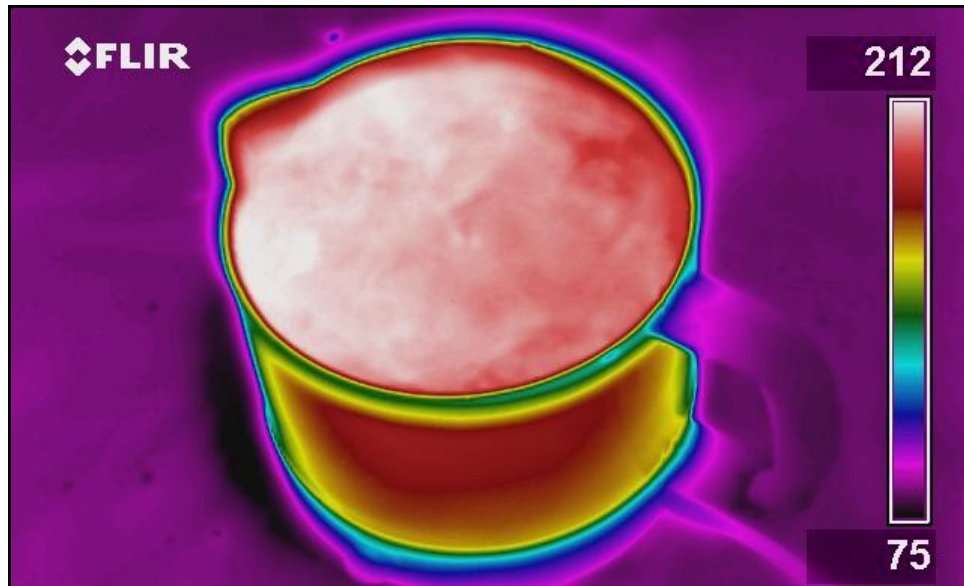


Figure 6—Infrared Image of Boiling Water

MANIKIN

A comparison of results between the thermal observation manikin settings, the thermocouple measurements and the infrared camera images are shown in Table 6. In almost all cases other than when imaging the right leg, the thermocouple camera measured within 0.5°C of the manikin set temperature. When imaging the left foot the camera measurement was different from the manikin setting by 1.6°C. Of the 26 measurements taken, all but 7 were within 1°C of the manikin settings. Further, the largest difference between the manikin settings and the thermocouple readings was 1.7°C. This appears to be consistent with the camera's accuracy specifications of $\pm 2^\circ\text{C}$.

Table 6—Temperature Readings of Thermal Observation Manikin

Manikin Segment	Manikin Temperature Reading		
	TOM	Camera	Thermocouple
Head-Front	32.0	31.7	31.0
Head-Back	32.0	31.6	30.7
Chest	32.0	31.6	30.7
Back	32.0	31.5	30.6
Abdomen	32.0	31.5	30.9
Buttocks	32.0	31.9	30.8
Right Upper Arm-Front	32.0	32.4	30.8
Right Upper Arm-Back	32.1	32.2	30.7
Right Lower Arm-Front	32.0	32.4	30.8
Right Lower Arm-Back	32.0	32.3	30.8
Right Hand	32.1	32.4	31.0
Left Upper Arm-Front	32.1	32.1	30.4
Left Upper Arm-Back	32.0	32.3	30.7
Left Lower Arm-Front	32.0	32.7	30.5
Left Lower Arm-Back	32.0	32.6	31.1
Left Hand	32.0	32.9	31.0
Right Upper Leg-Front	32.0	33.0	31.0
Right Upper Leg-Back	32.0	33.0	30.9
Right Lower Leg-Front	32.1	32.8	30.8
Right Lower Leg-Back	32.0	32.9	30.8
Right Foot	32.0	33.0	30.6
Left Upper Leg-Front	32.0	33.4	31.3
Left Upper Leg-Back	32.1	31.2	31.4
Left Lower Leg-Front	32.0	30.8	30.9
Left Lower Leg-Back	32.1	31.0	30.8
Left Foot	32.9	31.3	31.1

RESULTS-TESTING PHASES

RESULTS OF CAMERA TESTING PHASE 1

FOCUS

In order to test the focusing ability of the camera two tests were run. The first test measured its ability to focus while in a static position. In the second test the camera was moving before focusing. For the static test the camera lens was covered so there was no line of sight between the camera and the focusing target. The obstruction was then removed and the time for the camera to focus on an object at a given distance was recorded. Initially, coupons of differing materials were used in this test to see if the target material affected the focus time, but this was found to not be a factor. This procedure was repeated for objects at distances of 6, 12, 25, 50, and 100 feet. The results from this testing are shown in Table 7. The times for each distance are an average of 10 trials.

Table 7—Focus Times at Various Distances

Distance (ft)	Average Focus Time (sec)	Standard Deviation
6	1.60	0.05
12	1.59	0.39
25	1.27	0.13
50	1.12	0.06
100	1.03	0.17

For the second test the camera was focused on a wall at a right angle to the object. The camera was rapidly turned from the wall to focus on the object. The time recorded began at the start of the turn and ended after the camera had focused on the object. The results for this rotation testing have slight inconsistencies in the rotation speed of the camera, but, this testing

may be a better representation of the real world applications of this camera. These results are shown in Table 8.

Table 8—Focus Times at Various Distances after Camera Viewing Angle Change

	6 ft	12 ft	25 ft	50 ft	100 ft
Trial	Time				
1	1.91	1.59	1.62	1.69	1.94
2	1.96	1.5	1.35	1.69	1.87
3	2	1.59	1.78	1.71	2.32
4	1.54	1.69	1.53	1.78	1.75
5	1.62	1.59	1.79	1.85	1.9
6	1.84	1.65	1.59	2.03	1.81
7	1.85	1.57	1.53	2.13	1.59
8	1.6	1.28	1.38	1.85	1.68
9	1.79	1.79	1.82	1.94	1.63
10	1.91	1.53	1.69	2.32	1.78
Average	1.802	1.578	1.608	1.899	1.827
St Dev	0.1529575	0.1266333	0.1567035	0.1978611	0.1969797

It was noticed during testing that when the battery charge dropped past a specific point the focusing times increased significantly. To avoid inconsistent data the camera must be plugged in or kept charged. This is possible in a laboratory setting, but would be a major inconvenience in a mobile operational scenario.

CAMERA RANGE

There are multiple factors that affect the ability of the camera to view an object. Two of them are the size of the object and distance from the camera. Another is the difference in the levels of radiated energy between the object and its surroundings. In order to study the effects of size and emissivity on the range of the camera, coupons of different materials were made. Coupons of copper, aluminum, and paper were constructed into various sized squares. These squares measured 3 cm, 6 cm, and 15 cm, on a side. By finding the maximum range that the camera could distinguish these coupons, the effect of size and emissivity were studied.

Table 9—Maximum Visible Distances of Various Coupons

Maximum Distance Visible (Feet)			
Material	Size (cm ²)		
	3x3	6x6	15x15
Copper	84	95	167
Aluminum	68	118	175
Paper	10	77	136

EFFECTS OF SIZE ON RANGE

As expected it was easier to discern the larger coupons at greater distances than the small coupons. It was found the maximum effective distance for detection of smaller objects was 25 feet. The distance from the camera to the object appears to have minimal effect on the temperature readings. Figure 7 shows how the size of the object affects the distance at which the object can be seen.

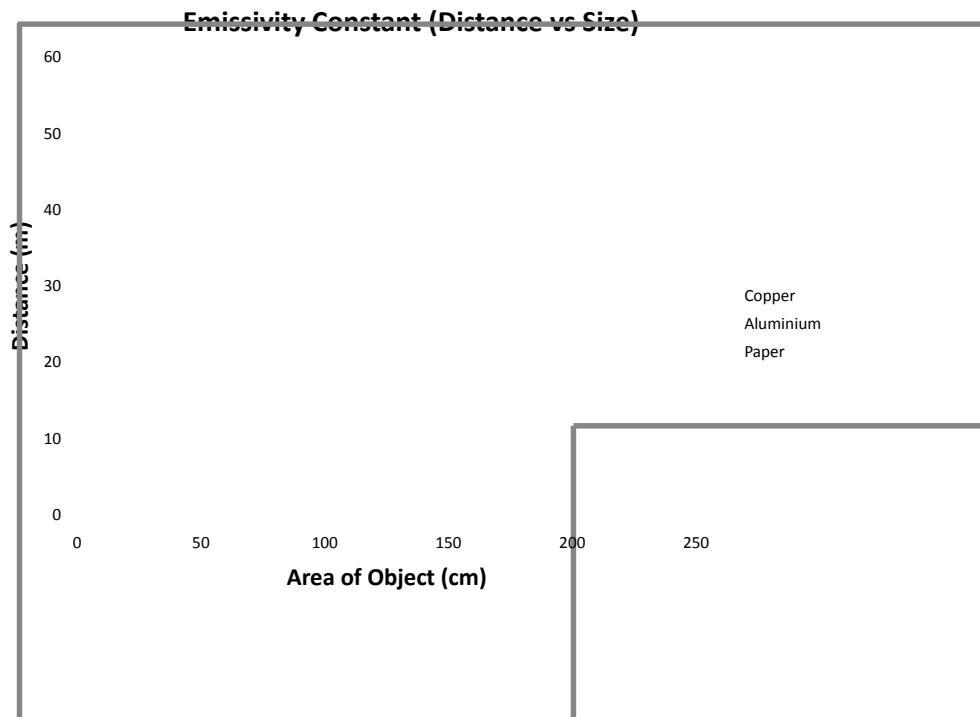


Figure 7—Effects of Coupon Area on Visible Distance

EFFECTS OF EMISSIVITY ON RANGE

It was determined that the objects with higher emissivity cannot be seen from as far away as objects with lower emissivity. In these tests the human body was the hottest object in the image, so the coupons show up as cold spots. In the camera's automatic temperature scaling mode the lower emissivity objects appear colder than the objects with higher emissivity at the same temperature. This creates a larger thermal differential in the picture, which makes the object show up more easily on the human body. The lower emissivity of the copper and aluminum coupons made them easier to see at longer distances. Figure 8 shows how the emissivity affects the distance at which the object can be seen.

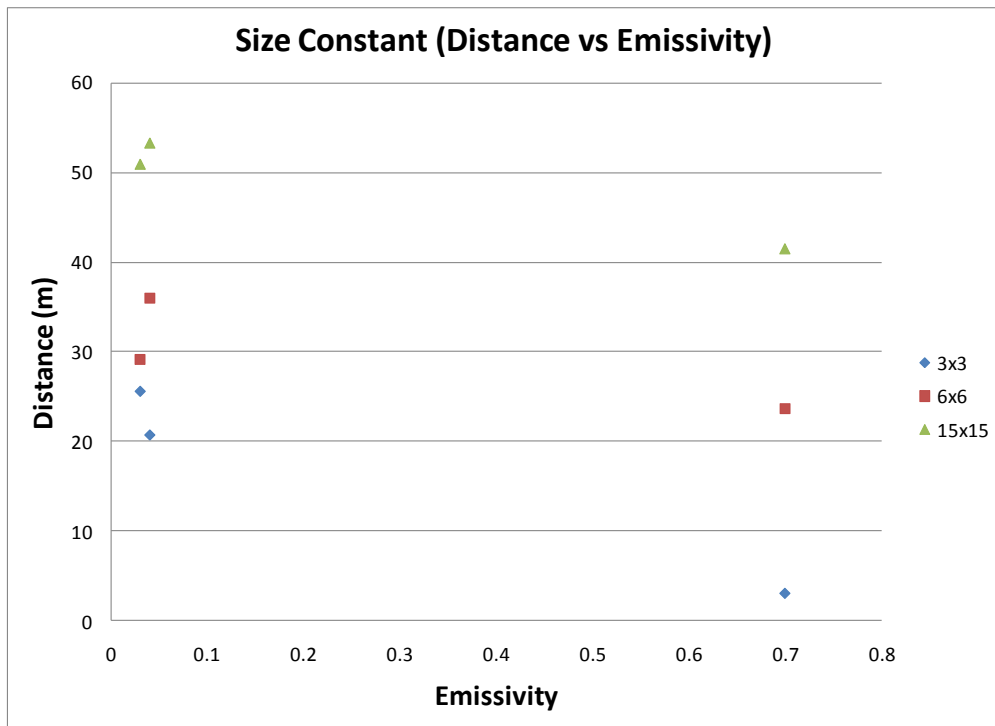


Figure 8—Effects of Emissivity on Visible Distance

MATERIAL EMISSIVITY/REFLECTIVITY

Effects of the emissivity of an object were studied by creating a board with an array of six coupons of varying materials. The coupons were all square and 6cm on a side. The first test was conducted with all of the materials at room temperature. The board with the coupon array was placed in front of a background with no temperature gradient. This is shown in Figure 9.



*Figure 9—Material Coupons
Top Row—Copper, Aluminum Foil, Blue Cotton Material
Bottom Row—Paraffin Wax, Clay, Yellow Cotton Material*

For opaque materials $\varepsilon_{\lambda} = \alpha_{\lambda}$ and $\tau_{\lambda} = 0$, so with substitutions the summation $\alpha_{\lambda} + \rho_{\lambda} + \tau_{\lambda} = 1$ becomes $\varepsilon_{\lambda} + \rho_{\lambda} = 1$. Under these conditions the reflectivity will increase as the emissivity decreases, so a metallic material with low a low emissivity will have a high reflectivity. With all coupons at the same temperature, the difference in the infrared image

caused by emissivity and reflectivity was obvious. Whereas the nonmetals appeared very close in color to the board and background at the same temperature, the metal coupons appeared very differently due to their higher reflectivity.

This effect was also influenced by the surface texture of the metal coupons. The copper coupon was relatively smooth with only a few distortions. The aluminum foil coupon had a more crinkled surface. These surface differences were visible with the camera as temperature gradients over a very small surface. The distortions in the surface change the reflection angles of the reflected radiation. This will direct more or less radiation towards the camera making the coupon appear to have areas of different temperatures even though the temperature was the same across the coupon. The wax, clay, and cotton coupons had a much more consistent surface texture and so did not have these distortions.

The infrared sensor assumes an emissivity in calculating the temperature. Under this assumption, when two objects at the same temperature but with differing emissivities are shown in the same scene with the camera the object with the lower emissivity appears cooler than the object with the high emissivity. When these objects are placed in front of a warm background like the human body, the larger temperature gradient produced by the lower emissivity object is much easier for the camera to detect.

SHIELDING

The effects of shielding were tested by imaging the manikin with varying layers of clothing. The manikin would begin bare and then three white cotton t-shirts would be added one at a time. As each shirt was added the temperature of the manikin would be measured with the camera and the thermocouple. This process was repeated at four distances and with both blue and yellow cotton t-shirts. The effects of distance and t-shirt color were both negligible.

Because the effects of distance were negligible the temperatures were averaged for each configuration and displayed in Figure 10. The difference between the thermocouple measurement and the camera measurement was less than 0.25°C. It can be seen with these results that the exterior shirt temperature dropped as layers were added. This is due to the increased thermal resistance between the outer clothing layer and the manikin. As the resistance between the body surface increases, one would expect the outer layer of clothing to approach the temperature of the ambient environment.

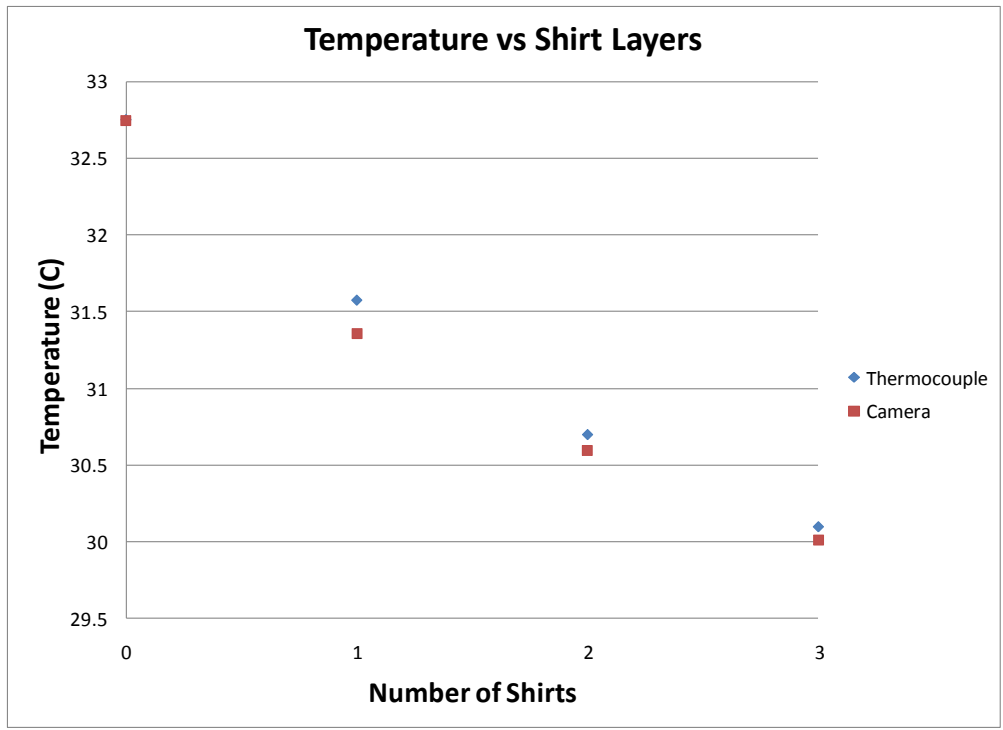


Figure 10—External Clothing Temperature with Application of Clothing Layers



Figure 11—Clay Material Hidden in Vest Pocket

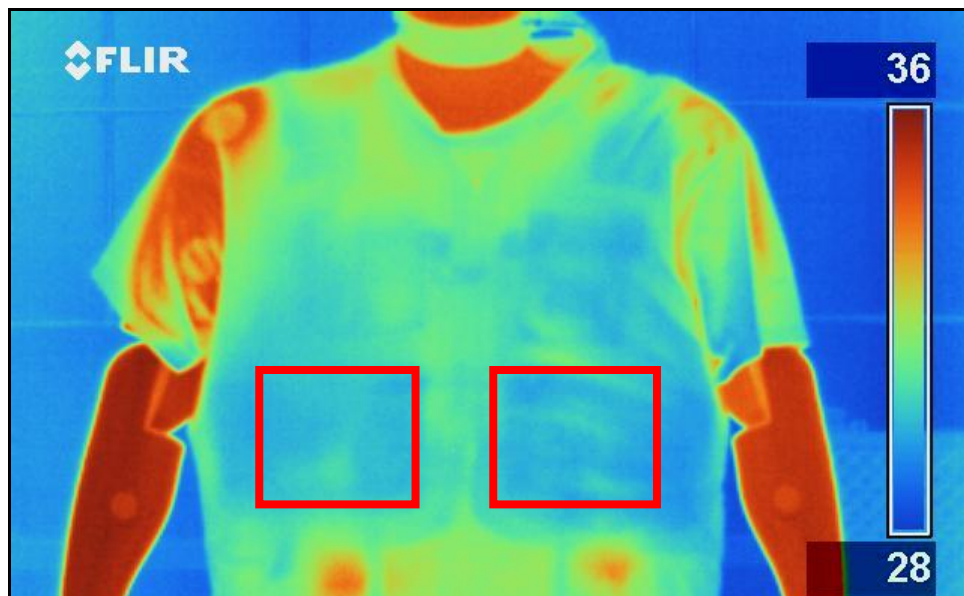


Figure 12—Clay Material Hidden in Vest Pocket and Shielded by 1 T-shirt

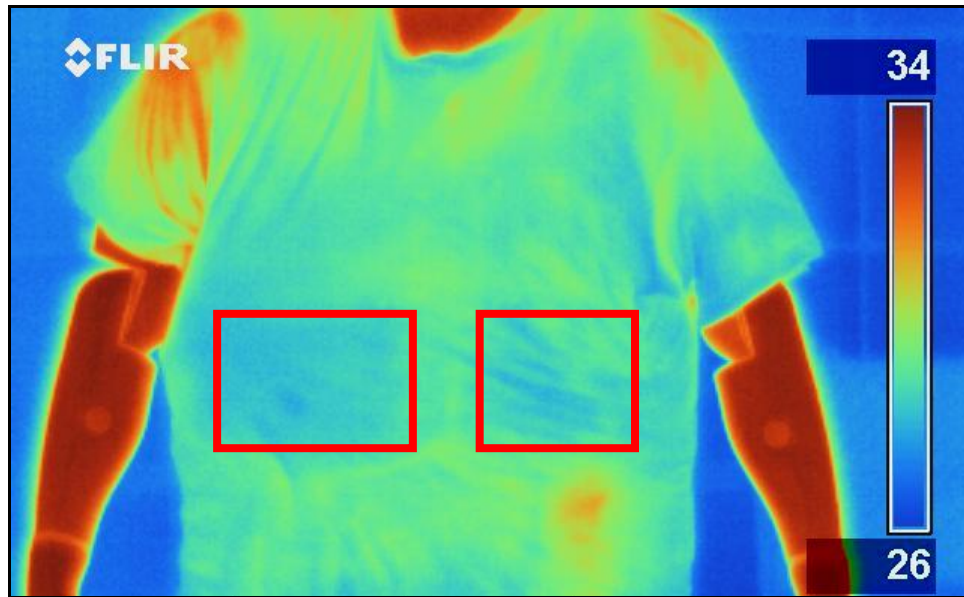


Figure 13—Clay Material Hidden in Vest Pocket and Shielded by 2 T-shirts

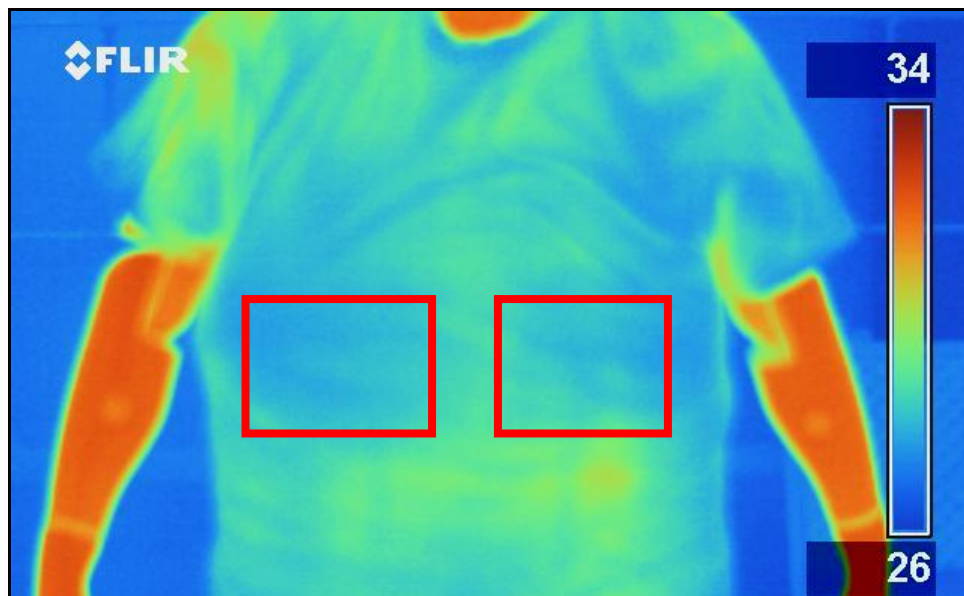


Figure 14—Clay Material Hidden in Vest Pocket and Shielded by 3 T-shirts

TRANSIENT STANDING BEST/WORST CASE

When a weapon is hidden under clothing against the human body the temperature of the weapon will come into equilibrium with the body after a certain time period under stable environmental conditions. It was desired to know the upper and lower bounds of how long this process may take. In order to simulate these cases a test was developed to both speed up and slow down the normal equilibrium process. By adding heat to the simulated bomb package using a medical heating pad it was possible to speed up the equilibrium process. In order to slow the process down a medical cold pack was attached to the package during the imaging process. This allowed measurements to be made for upper and lower bounds on the time required for the temperature equilibrium process.

There was a noticeable difference between the two tests. While being tested on the manikin the hot pack made the bomb package reach a visible equilibrium within 20 minutes. The simulated bomb package with the cold pack attached was still easily visible after 3 hours. This shows that external heat sources can have significant effects on how long it takes a bomb package to reach a thermal equilibrium with the body.

For the cold pack test the surface of the thermal observational manikin was held at 32°C (89.6°F) for this test. At the beginning of the test, there is a visible dip in the temperature. This was attributed to the chemical reaction in the cold pack having not reached a stable point before the cold pack was applied to the bomb package. As the reaction progresses, the temperature reading from the camera begins to rise. Both the overall average temperature of the torso was found as well as the temperature of the layers directly between the bomb and the camera. As shown in Figure 15 the bomb area temperature was generally between 3 and 5 degrees lower than the average temperature of the entire torso. The bomb area average temperature is compared

to the overall torso temperature to give a quantitative measure of how distinct the bomb appears in the image to the human eye. The larger the difference in this temperature, the easier it is for the person to distinguish the bomb from the torso.

The bomb area temperature levels out at approximately 22.22°C (72°F). Figure 16 thru Figure 18 show the changes in the IR image over the course of three hours. Figure 18 shows the manikin at three hours and the bomb with the cold pack attached is still easily seen in the image. The difference between the bomb area average temperature and the torso average in this case is approximately 1.67°C (3°F).

In this case it is very easy for a human to distinguish the bomb in the image. The images in this experiment displayed an overall temperature scale of 20°F . The 3°F difference between the average torso temperature and the bomb area is a 15% of this overall temperature scale.

The surface of the thermal observational manikin was held at 32°C (89.6°F) while testing the simulated bomb package with a hot pack attached. Just like in the cold pack experiment, the overall average of the torso was found as well as the temperature of the layers directly between the bomb and the camera. For approximately the first hour, the bomb package area was slightly cooler than the average torso temperature calculated by the camera. This is shown in Figure 19. After the first hour the average external layer temperature around the bomb was within 0.3°F of the average torso temperature.

The bomb area temperature levels out at approximately 25° (77°F). Figure 20 thru Figure 22 show the changes in the IR image over the course of three hours. Figure 20 shows the manikin with the bomb package easily visible, but Figure 21 and Figure 22 show how it becomes much harder to distinguish the bomb package from the rest of the torso as time passes. This equilibrium process is quickened by the hot pack that is attached. After an hour there is virtually

no difference between the bomb area average temperature and the torso average temperature. In this case it is much harder for a person to distinguish the bomb in the image. There are still features of the bomb that are recognizable, but they have a tendency to blend into the rest of the clothing in the image.

In this case it becomes very difficult for a human to distinguish the bomb in the image. The overall temperature scale used in these images is 18°F. For most of the hot pack experiment there was a 0.3°F difference between the average torso temperature and the bomb area. In this case the difference is less than 2% of this overall temperature scale.

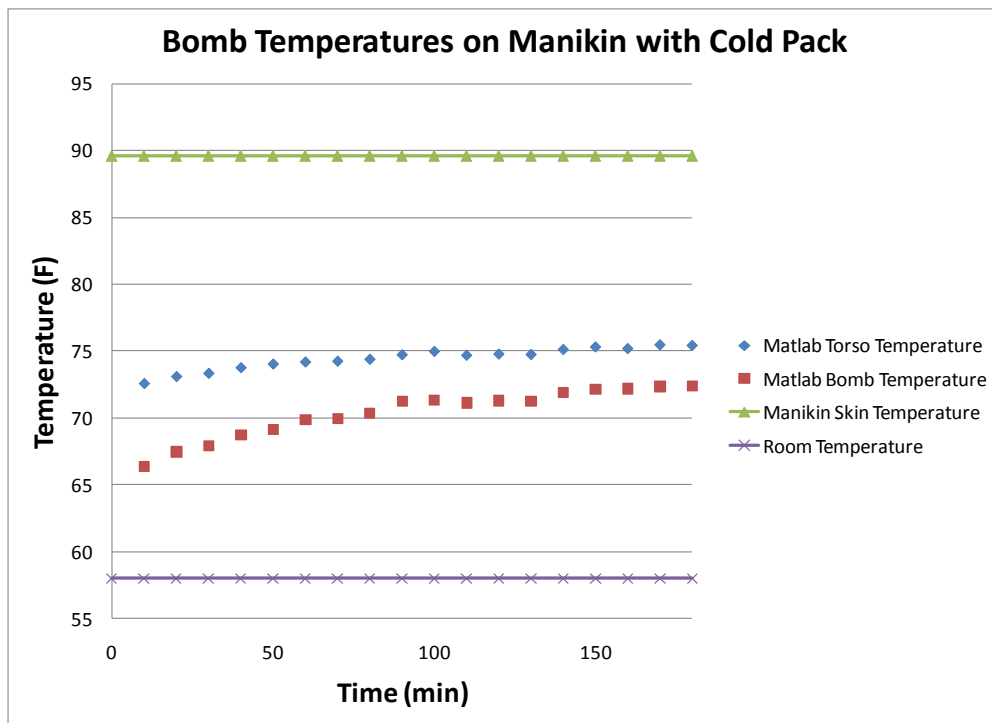


Figure 15—Bomb Temperatures on Manikin with Cold Pack



Figure 16—Bomb with Cold Pack Attached to Manikin at 0 Minutes

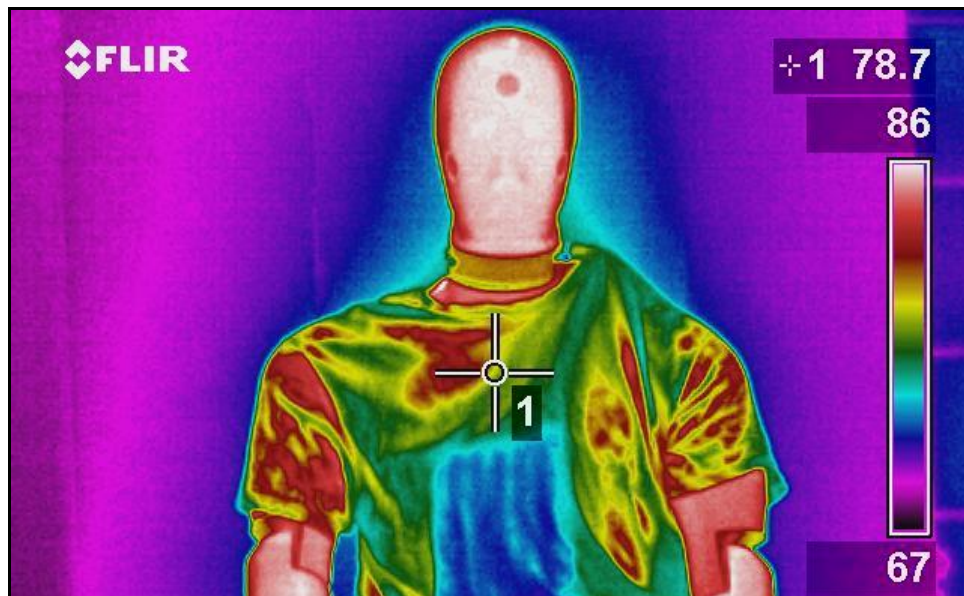


Figure 17—Bomb with Cold Pack Attached to Manikin at 140 Minutes

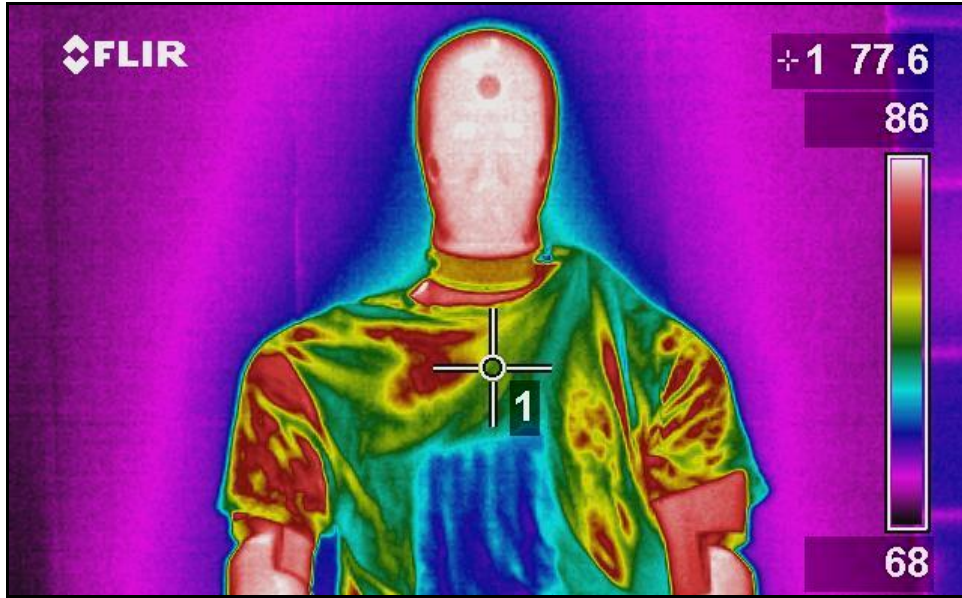


Figure 18—Bomb with Cold Pack Attached to Manikin at 180 Minutes

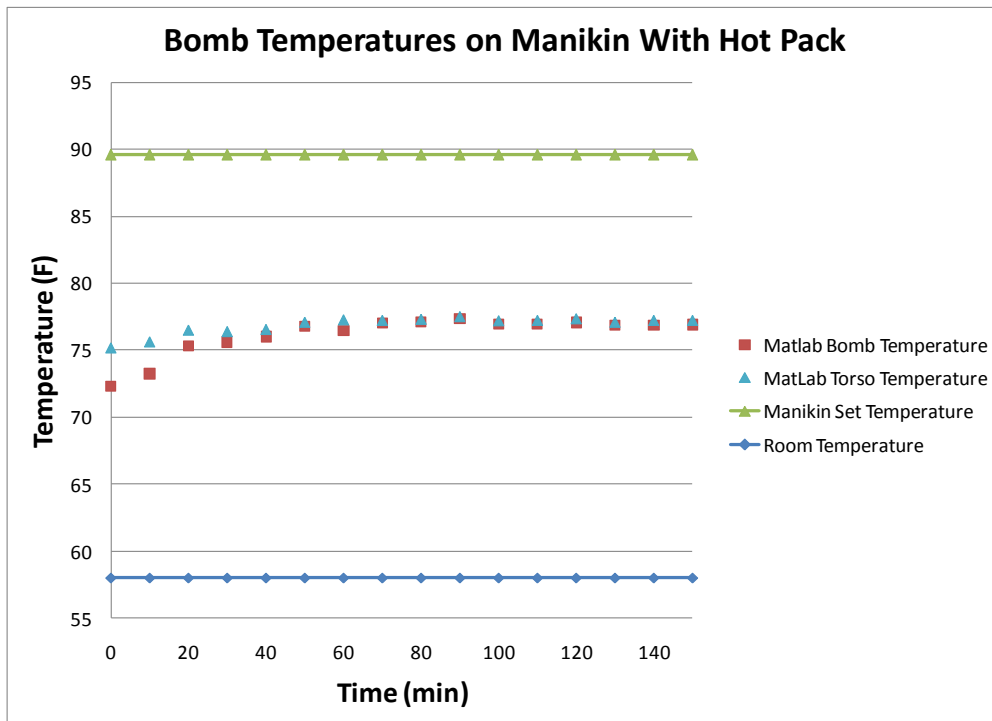


Figure 19—Bomb Temperatures On Manikin With Hot Pack



Figure 20—Bomb with Hot Pack Attached to Manikin at 0 Minutes

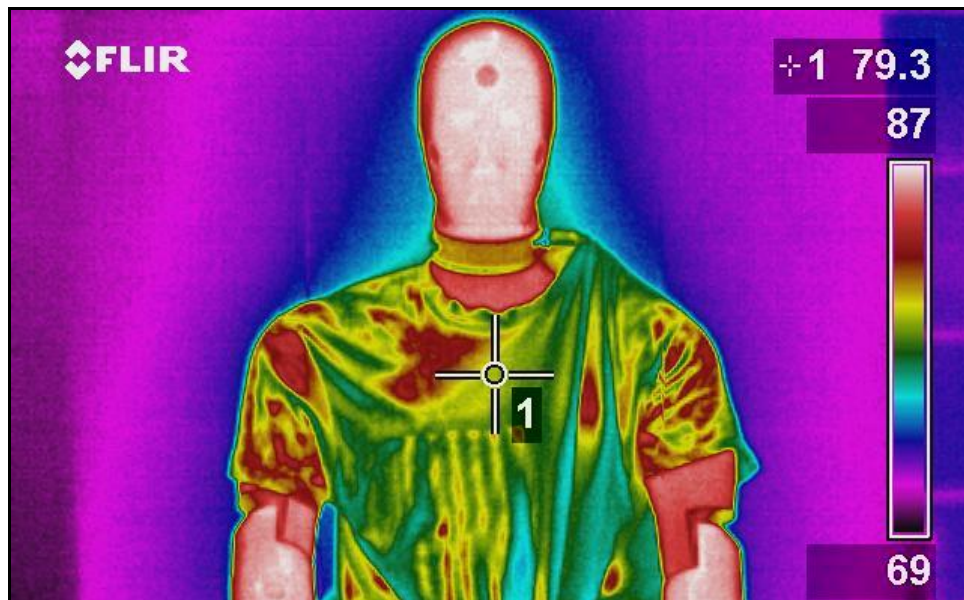


Figure 21—Bomb with Hot Pack Attached to Manikin at 90 Minutes

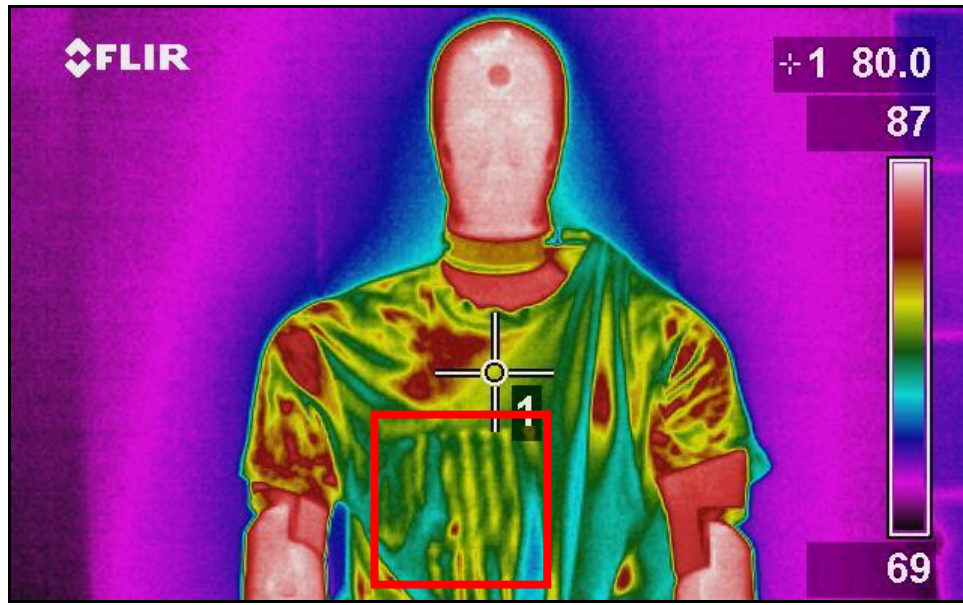


Figure 22—Bomb with Hot Pack Attached to Manikin at 150 Minutes

RESULTS OF CAMERA TESTING PHASE 2

COLOR PALETTES

Figure 23 thru Figure 32 show the five color palettes tested on the camera as well as their inverse color palette. These images are successive images of the same scene after an equilibrium period. The Blue-Red color palette is shown in Figure 23 and Figure 24. In its non-inverted state the Blue-Red color palette is very intuitive in its representation of heat. The grayscale color palette is advantageous to the viewer in that it smoothes the temperatures out and makes an image that has few distracting elements that draw attention away from the body. In contrast, the color palettes do a better job of accentuating the small temperature differences in an area. Because the color palette has a wider range of contrasting color to choose from, many times a package is more apparent in a color image. The High Contrast Rainbow color palette seemed to accentuate the differences in the areas of a simulated bomb package more than the other color palettes. Because of this, most of the images used in this paper use the High Contrast Rainbow color palette.



Figure 23—Blue-Red Color Palette



Figure 26—Inverted Grayscale Color Palette



Figure 24—Inverted Blue-Red Color Palette



Figure 27—Iron Color Palette



Figure 25—Grayscale Color Palette



Figure 28—Inverted Iron Color palette



Figure 29—Rainbow Color Palette

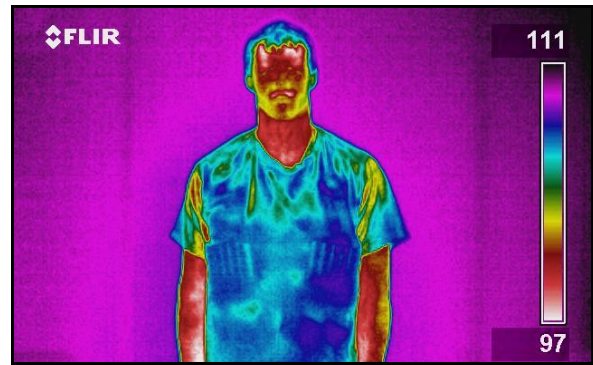


Figure 31—High Contrast Rainbow Color Palette

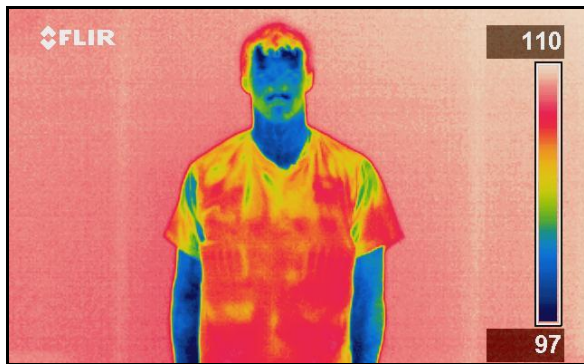


Figure 30—Inverted Rainbow Color Palette

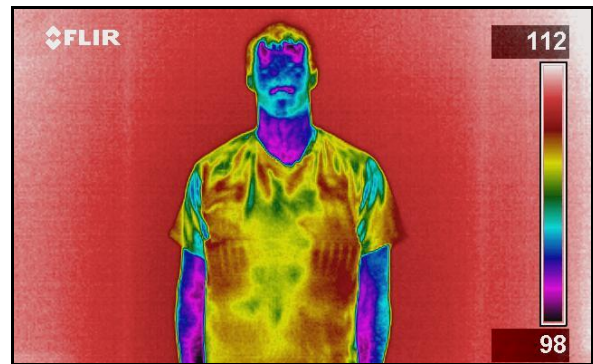


Figure 32—Inverted High Contrast Rainbow Color Palette

BOMB PACKAGE MATERIAL CHARACTERISTICS

As detection technologies change, suicide bombers continually change their tactics and technologies in order to avoid capture. Currently, the majority of the bomb packages used are made with metallic materials, but it is very possible that this may change in the future. Considering this possibility, it was desired to have additional results with a material other than metal as the basis for the simulated bomb package.

Metal and plastic simulated bomb packages were compared to see how the different material properties of the materials would affect the infrared image. Images were taken of both package types using both the automatic and manual modes on the camera. These tests were

completed with various amounts of shielding.

The thermal resistivity of the materials used in the bomb package did have an effect on the temperature of the external layers of clothing. When the ambient environmental temperature was higher than the skin temperature, the plastic bomb package transferred less of the heat away from the clothing towards the body. The metal package, with the lower thermal resistance, more readily transferred the heat away from the external layers of clothing.

The plastic packages were barely discernable with only one t-shirt covering the package. They became almost impossible to see when more than one shirt was worn over the package. When imaging the plastic package under 1 tight t-shirt using the automatic mode on the camera produced an average temperature of the bomb area of 41.83°C (107.29°F) and an average temperature for the entire torso at 41.49°C (106.68°F). This is only a difference of 0.34°C (0.61°F). The manual mode produced similar results. Manual adjustment showed an average temperature of the bomb area of 41.71°C (107.08°F) and an average temperature for the entire torso at 41.89°C (107.40°F). This is only a difference of 0.25°C (0.45°F).

When these same tests were completed wearing a loose t-shirt the camera showed a difference of 0.23°C (0.41°F) for the auto-adjustment and 0.31°C (0.55°F) for the manual adjustment. For the case of having two t-shirts covering the package, the differences were 0.07°C (0.13°F) for the auto-adjust images and 0.13°C (0.24°F) for the manual-adjust images. These results are compiled in Table 10.

When imaging the metal package under 1 tight t-shirt using the automatic mode on the camera produced an average temperature of the bomb area of 41.33°C (106.39°F) and an average temperature for the entire torso at 41.19°C (106.15°F). This is only a difference of 0.13°C (0.24°F). The manual mode produced similar results when imaging a metal package as the

plastic package case. Manual adjustment showed an average temperature of the bomb area of 41.58°C (106.85°F) and an average temperature for the entire torso at 41.37°C (106.47°F). This is only a difference of 0.21°C (0.38°F).

When these same tests were completed with the subject wearing a loose t-shirt, the camera measured a difference of 0.27°C (0.48°F) for the auto-adjustment and 0.09°C (0.16°F) for the manual adjustment. For the case of having two t-shirts covering the package, the differences were 0.14°C (0.25°F) for the auto-adjust images and 0.03°C (0.05°F) for the manual-adjust images.

The metal packages were seen in the images with one shirt covering the package and still had distinctive features visible with two shirts covering the package. Glimpses of the package could be seen in the images where the package was covered by three shirts. By viewing each color palette it could be seen the how well the package showed up sometimes depended on what color palette was used. Again, this shows that there is no one optimum color palette for human viewing.

Table 10—Exterior Clothing Temperatures for Torso and Bomb Package Areas with Various Layering and Package Material Combinations

		Metal Package			Plastic Package		
		1 Tight T-Shirt	1 Loose T-Shirt	2 T-Shirts	1 Tight T-Shirt	1 Loose T-Shirt	2 T-Shirts
MATLAB® Average Torso Temperature	Automatic Temperature Range	106.15	105.45	106.06	106.68	106.74	106.44
	Manual Temperature Range	106.47	107.08	107.86	107.08	107.12	107.17
MATLAB® Average Bomb Temperature	Automatic Temperature Range	106.39	105.93	105.81	107.29	107.15	106.57
	Manual Temperature Range	106.85	107.24	107.81	107.53	107.67	107.41

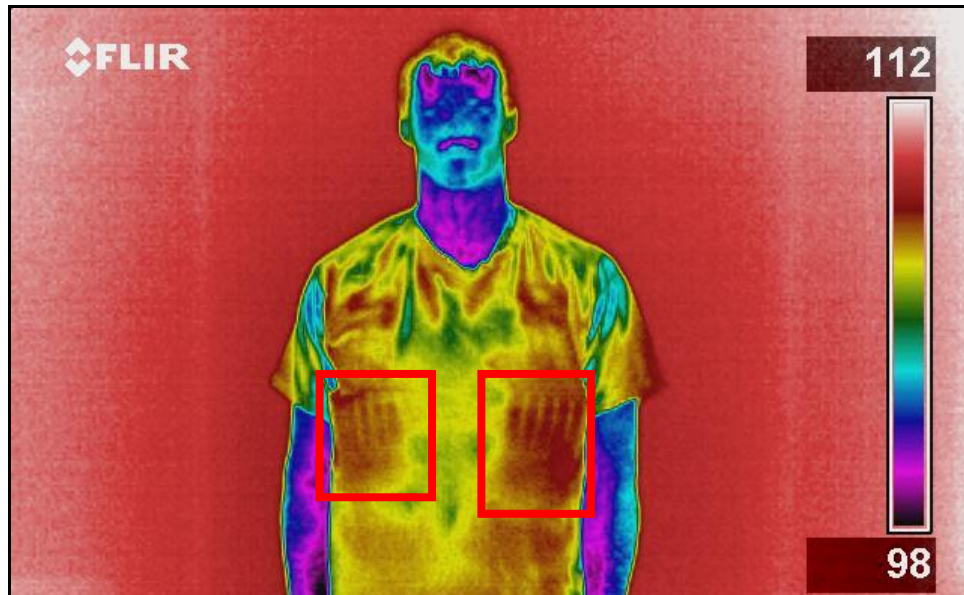


Figure 33—Metal Package Hidden in Vest Shielded by 1 Tight T-Shirt

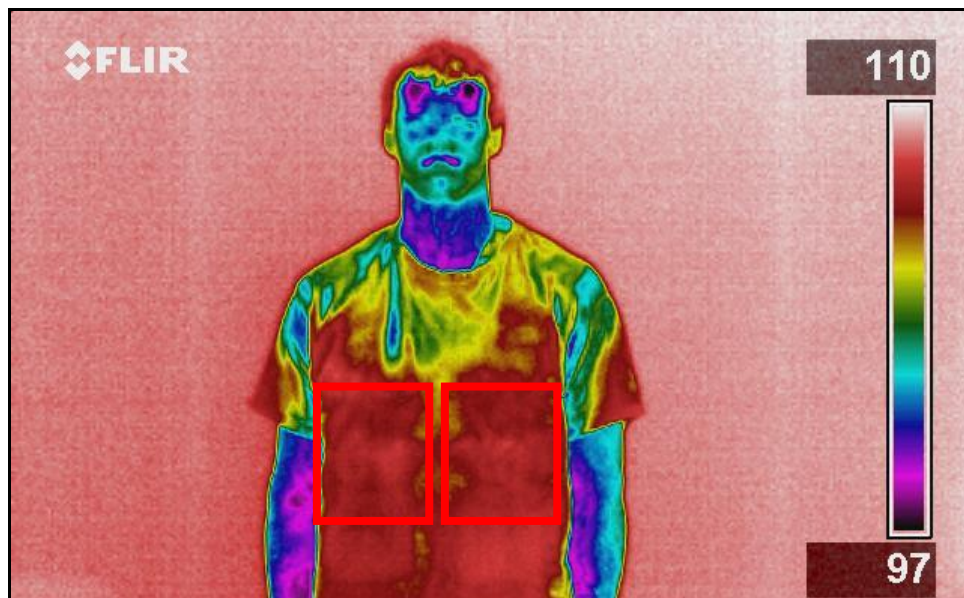


Figure 34—Plastic Package Hidden in Vest Shielded by 1 Tight T-Shirt

TRANSIENT-STANDING-BEST/WORST CASE

When tested on the human the simulated package with the hot pack reached a visible equilibrium within 20 minutes. At initial reading there was a 2.61°C (4.7°F) difference between the bomb area temperature and the torso temperature. After ten minutes there was only a 1.22°C (2.2°F) difference between the bomb area and the torso. At twenty-seven minutes there was 0.41°C (0.73°F) difference between the bomb area and the torso area. These results are presented in Figure 35. Representative images from the series are shown in Figure 38 thru Figure 40. This appears to agree with the test conducted on the Thermal Observation Manikin. Although the package was in visible equilibrium after 20 minutes, it was still visible in the image. In environmental temperatures at or below the skin temperature the human and bomb package seems to have a much greater effect on the external clothing temperature than the environment. Due to the lower external temperature, the heat transferred through the bomb package to the outside of the clothing is not masked by the temperature increase to the clothing by the external temperature. This would indicate that a human would have a better chance to visually see the bomb in a infrared image when the environmental temperature is lower than the body temperature.

In order to slow the bomb package equilibrium this procedure was repeated with a cold pack attached to the package instead of the hot pack. The results are plotted in Figure 36. Just as with the Thermal Observation Manikin, the package was still easily visible after 3 hours with very little change. This is shown in Figure 43. After three hours there was still a temperature difference of more than 0.56°C (1°F) between the average temperature of the bomb area on the clothing and the average temperature of the torso. These results are presented in Figure 41 thru Figure 43.

These results match those using the Thermal Observation Manikin in Phase 1 of the testing very well. In both cases there was a noticeable difference between having a hot pack attached to the bomb package compared to having a cold pack attached to the bomb package. In the case of the hot pack, the temperatures measured by the camera were slightly higher for the clothing than it was on an actual person, but the amount of time it took for the bomb area temperature and the torso temperature to come into a visible equilibrium was approximately the same. In the case of the cold pack, the temperatures measured were very similar as was the amount of time necessary for the package to come into a visible equilibrium.

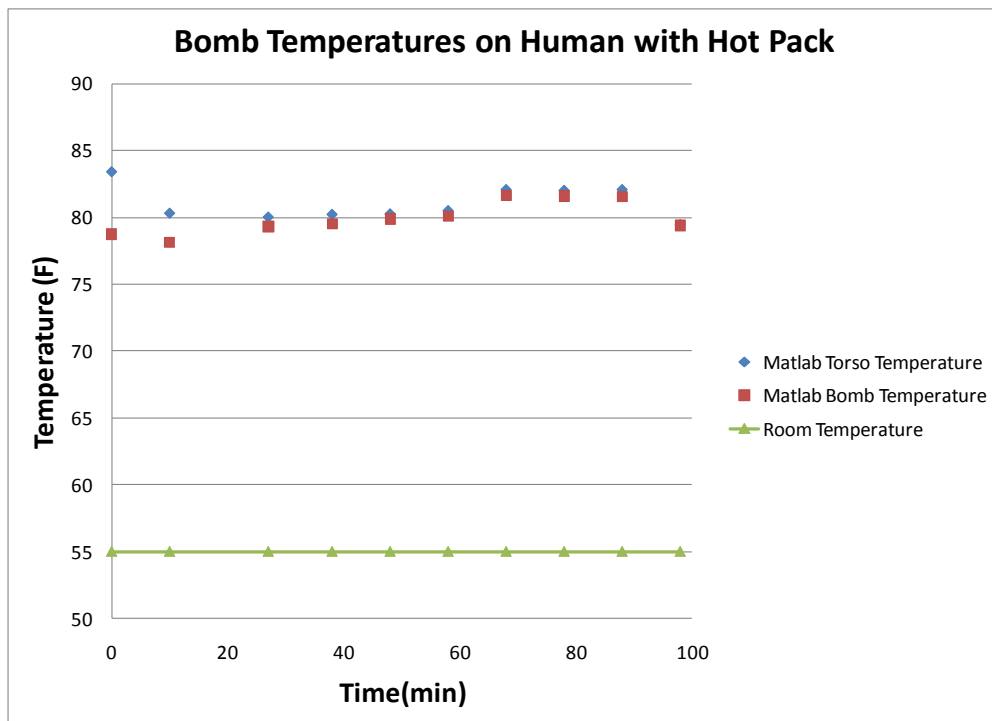


Figure 35—Bomb Temperatures on Human with Hot Pack

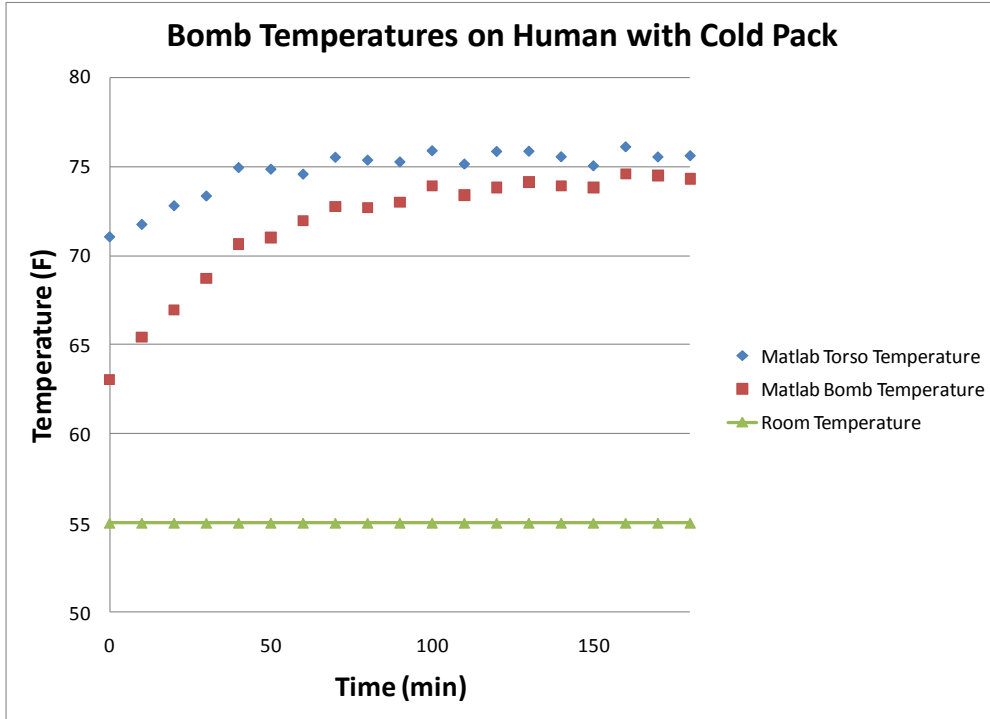


Figure 36—Bomb Temperatures on Human with Cold Pack

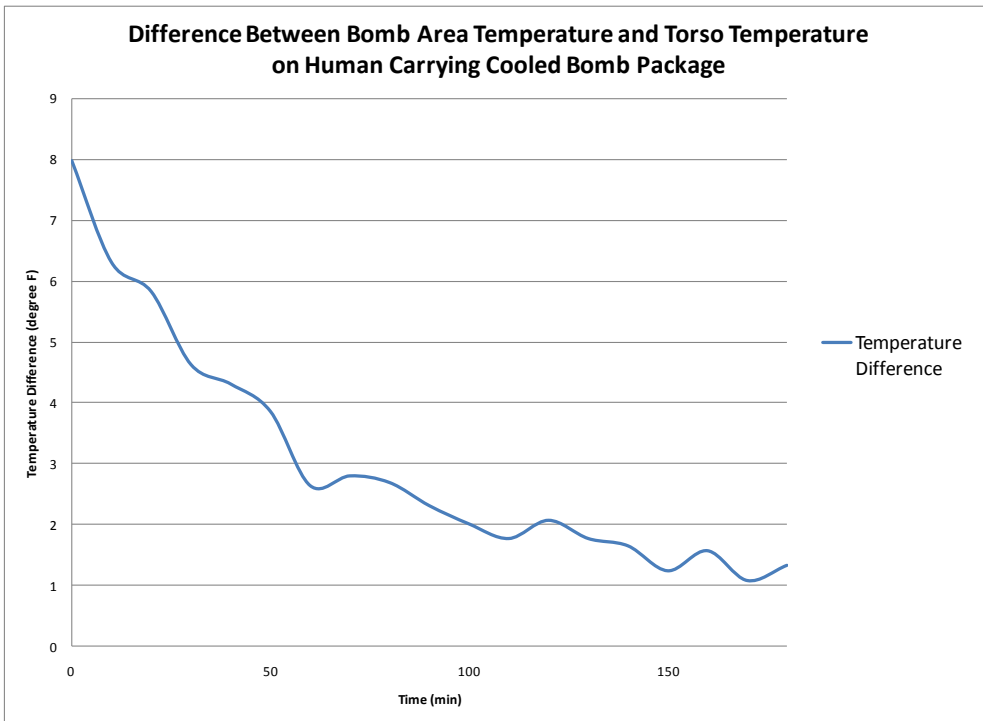


Figure 37—Difference Between the Bomb Area Temperature and the Torso Temperature on Human Carrying Cooled Bomb Package



Figure 38—Bomb with Hot Pack Attached to Human at 0 Minutes



Figure 39—Bomb with Hot Pack Attached to Human at 27 Minutes



Figure 40—Bomb with Hot Pack Attached to Human at 1 Hour 40 Minutes

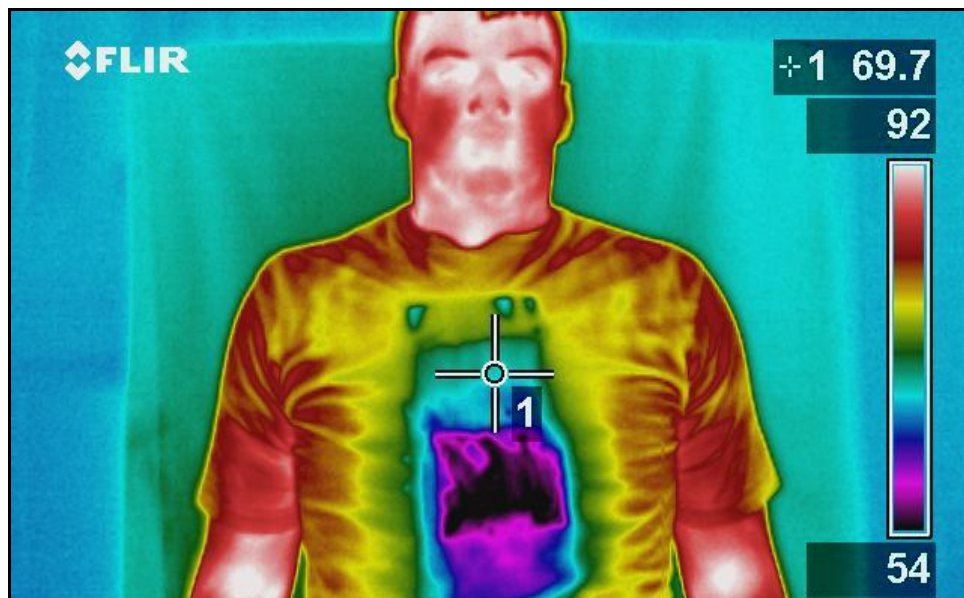


Figure 41—Bomb with Cold Pack Attached to Human at 0 Minutes



Figure 42—Bomb with Cold Pack Attached to Human at 1 Hour 30 Minutes



Figure 43—Bomb with Cold Pack Attached to Human at 3 Hours

TRANSIENT-STANDING-

The t-shirts temperatures were brought to equilibrium inside the environmental chamber, which was set at 40°C (104°F). After putting on the shirt, with no simulated bomb package, and standing still in the environmental chamber the exterior t-shirt temperature drops to 39.44°C (103°F) within a minute as seen in Figure 44. Within 5 minutes it drops to 38.33°C (101°F) as seen in Figure 45. The temperature of the t-shirt then fluctuated around this temperature for the remainder of the test period. This drop in temperature was due to the initial temperature of the t-shirt being higher than the body temperature. After it was applied to the body the shirt temperature lowered to an equilibrium point between the environmental temperature and the body temperature.

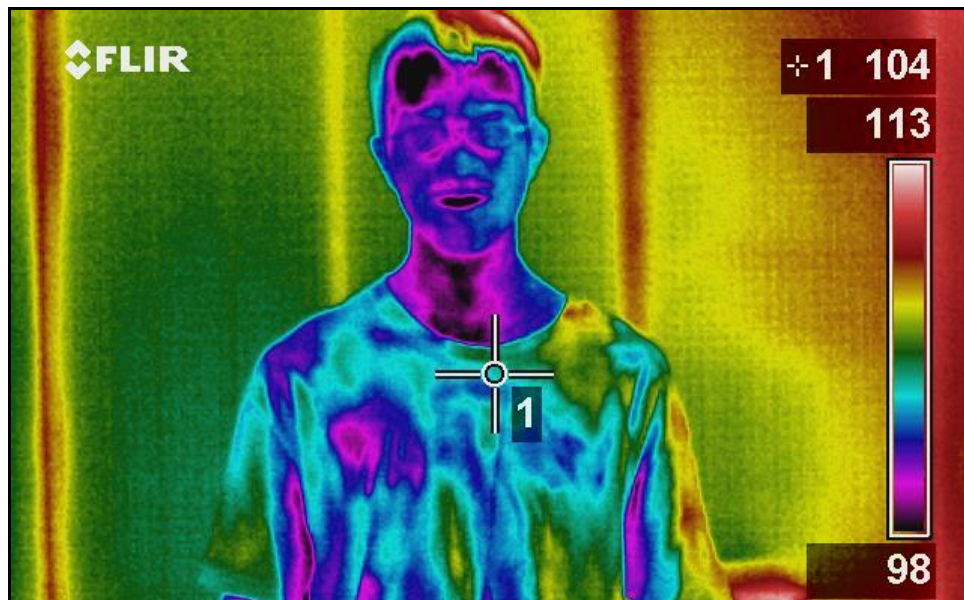


Figure 44—Standing in Heated Chamber without Bomb Package at 1 Minute

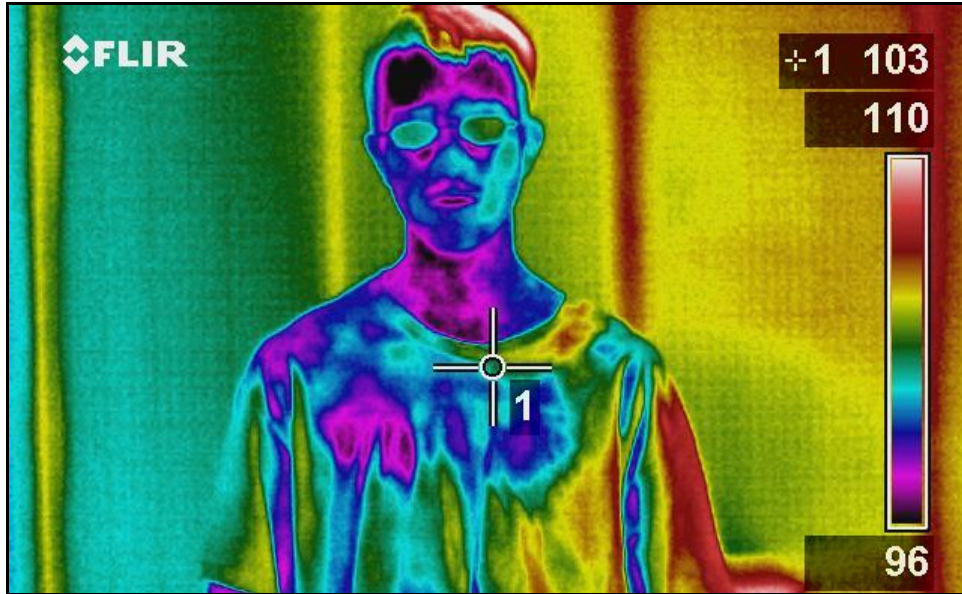


Figure 45—Standing in Heated Chamber without Bomb Package at 5 Minutes

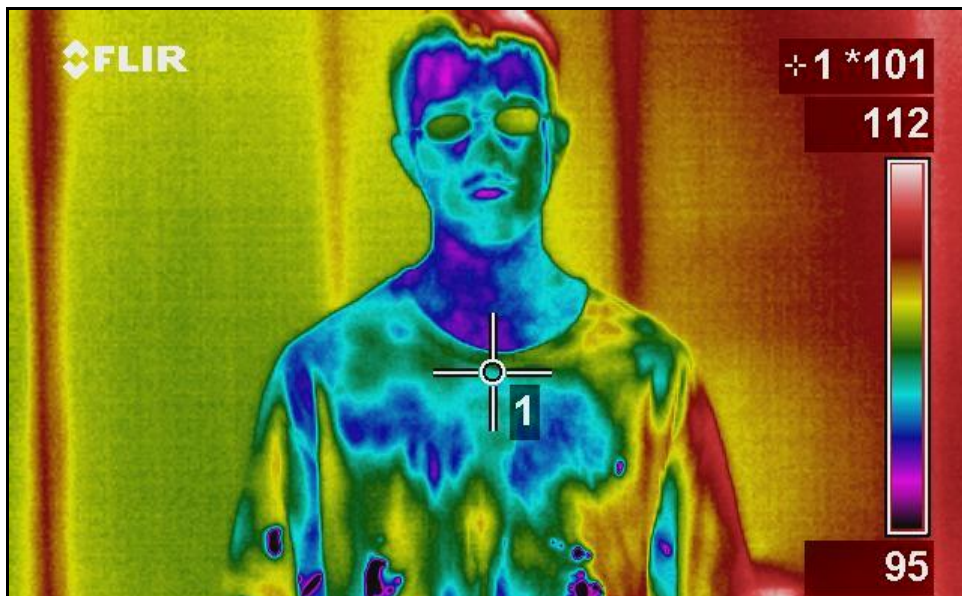


Figure 46—Standing in Heated Chamber without Bomb Package at 51 Minutes

When a metal bomb package was tested, it was easily discernible in the image for the first 15 minutes after the bomb/vest package was put on. This is shown in Figure 47 thru Figure 50. By minute 19 the package is mostly indiscernible from the rest of the torso as shown in Figure 50.

This testing indicates that it takes approximately 15 minutes for the bomb package to reach a point of thermal equilibrium with the body while standing and the clothing in conditions near 40°C.



Figure 47—Metal Bomb While Standing Still at 0 Minutes



Figure 48—Metal Bomb While Standing Still at 11 Minutes

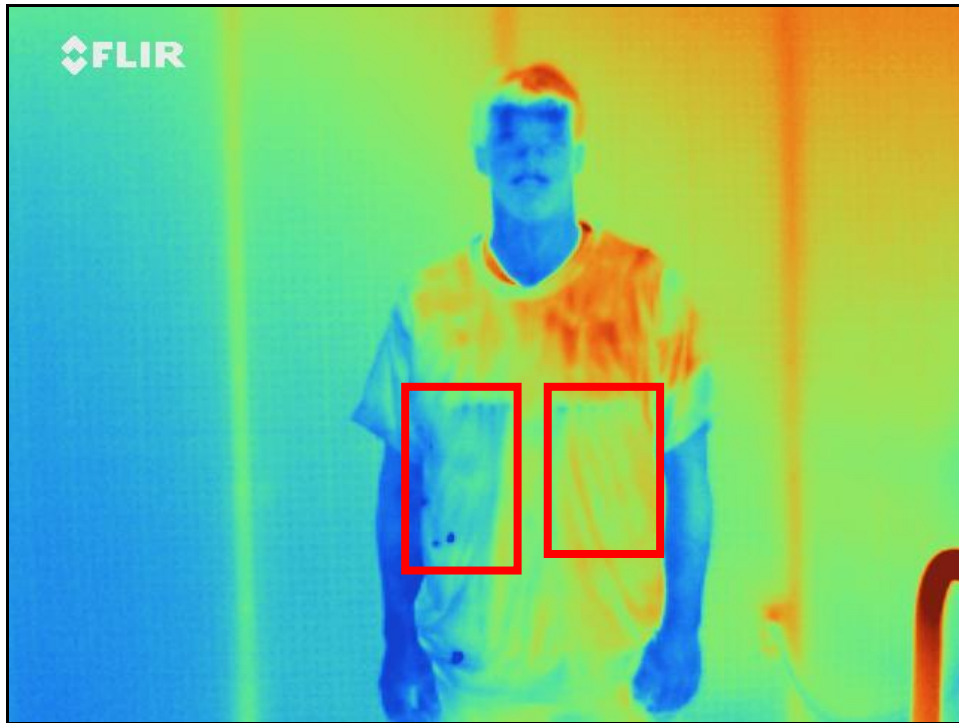


Figure 49—Metal Bomb While Standing at 15 Minutes



Figure 50—Metal Bomb While Standing at 19 Minutes

TRANSIENT CHANGES WHILE WALKING

When walking on a treadmill without a bomb vest the MATLAB® temperature averaging program gave an average torso temperature at 0 miles of 33.89°C (93°F). After walking 1.5 miles the torso was still an average temperature of 33.89°C (93°F). These results are presented in Figure 51. The chamber temperature during this test was 31.67°C (89°F).

After walking 1.5 miles the resistance model approaches the temperature of the clothing measured by the camera. The LCM model predicts higher temperatures than that measured by the camera. This is most likely a higher temperature because the irradiation to and from the environment was not model in this case due to lack of data on the environmental conditions.

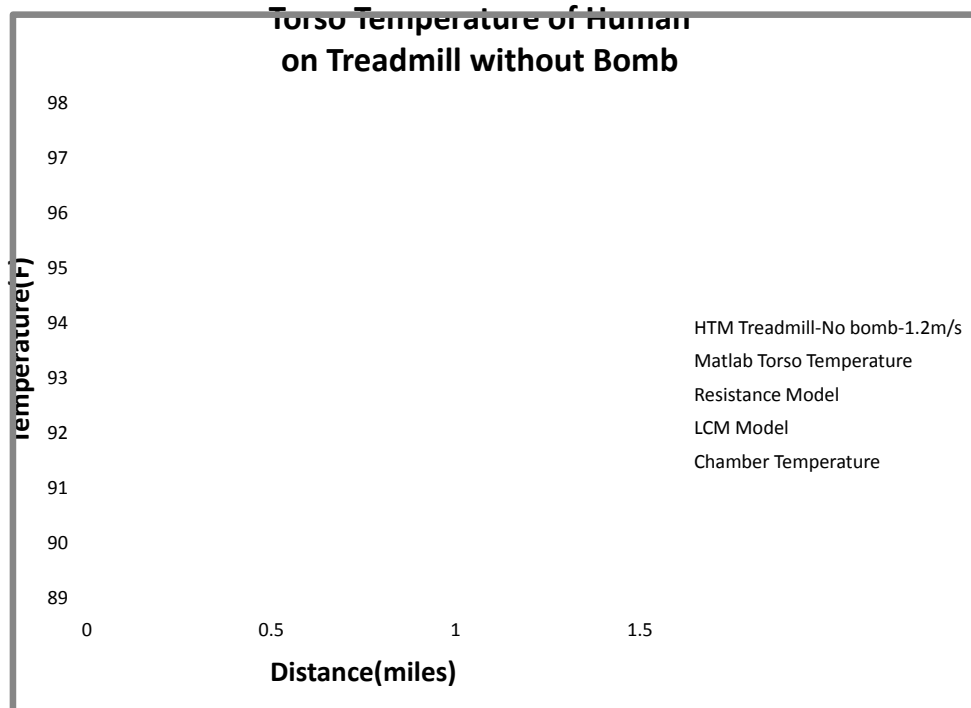


Figure 51—Torso Temperature Comparison with Models Of Human on Treadmill without Bomb

In the case of concealing a metal package while walking on the treadmill, the bomb area average temperature over the distance of 1.5 miles does not rise above the ambient temperature of 35°C (95°F). Results are presented in Figure 52. The MATLAB® temperature averaging program gave an average torso temperature for the metal package at 0 miles of 32.38°C (90.29°F). After walking 1.5 miles the torso was an average temperature of 35.08°C (95.14°F). At 0 miles the bomb area temperature was 31.43°C (88.57°F) and at 1.5 miles it was 34.14°C (93.46°F). The difference between the temperature of the bomb area and the torso was approximately 1.5°F to 2°F.

The overall rise in temperature is consistent with the rise of the LCM model, although the experimental data shows fluctuations in the temperature during the rise. The resistance model again shows higher results because it does not consider convective cooling due to the movement

of the person. The thermocouple measurements of the inside and outside of the bomb package fluctuated around temperatures of 35°C and 35.56°C (95 and 96°F) respectively. In this test the outside of the bomb is always at a higher temperature than the inside of the bomb.

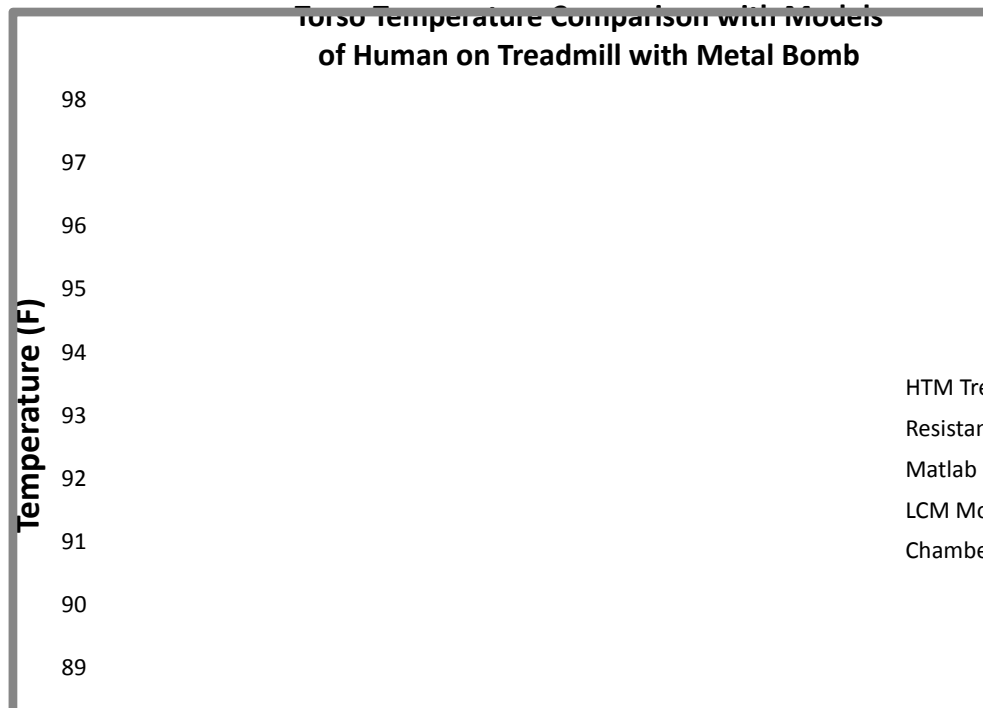


Figure 52—Torso Temperature Comparison with Models Of Human on Treadmill with Metal Bomb

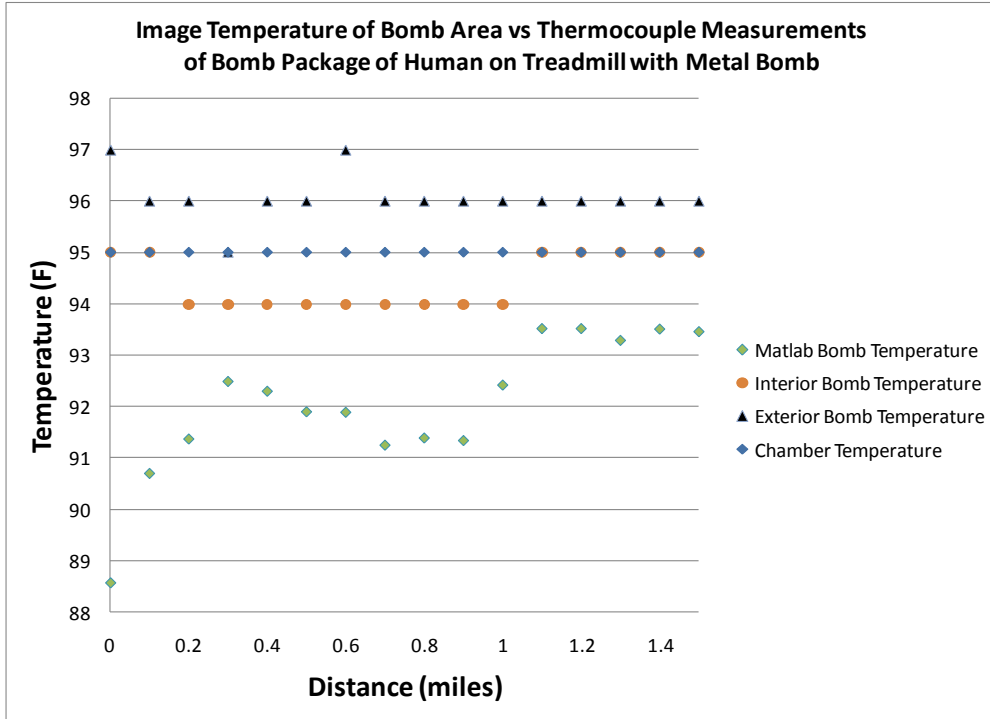


Figure 53—Image Temperature of Bomb Area Comparison with Thermocouple Measurements of Bomb Package of Human on Treadmill with Metal Bomb

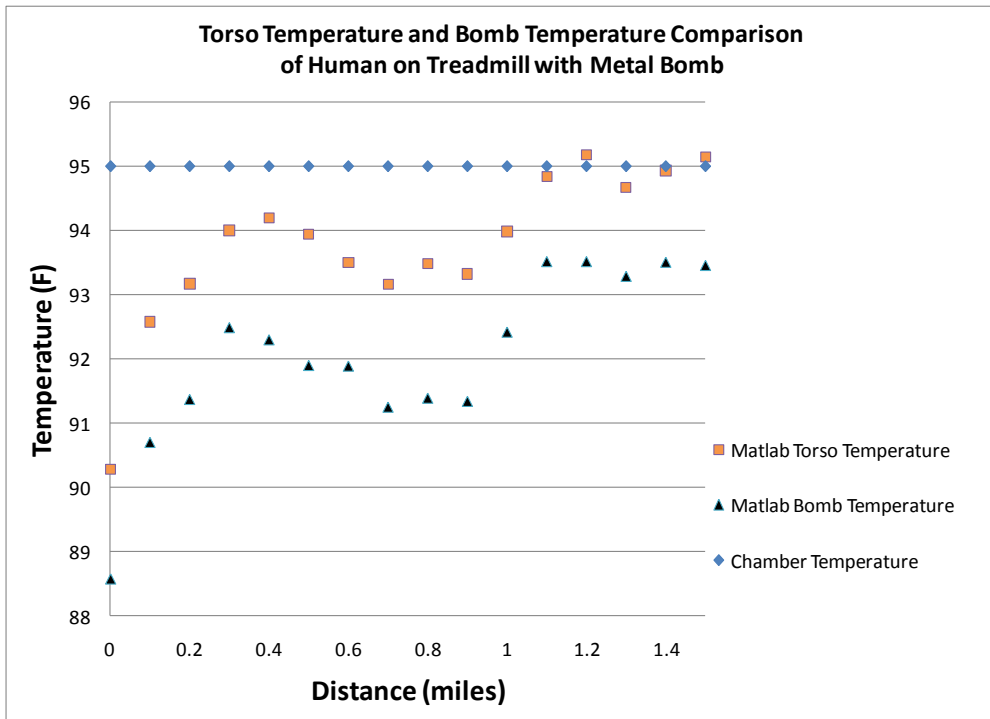


Figure 54—Torso Temperature and Bomb Temperature Comparison of Human on Treadmill with Metal Bomb

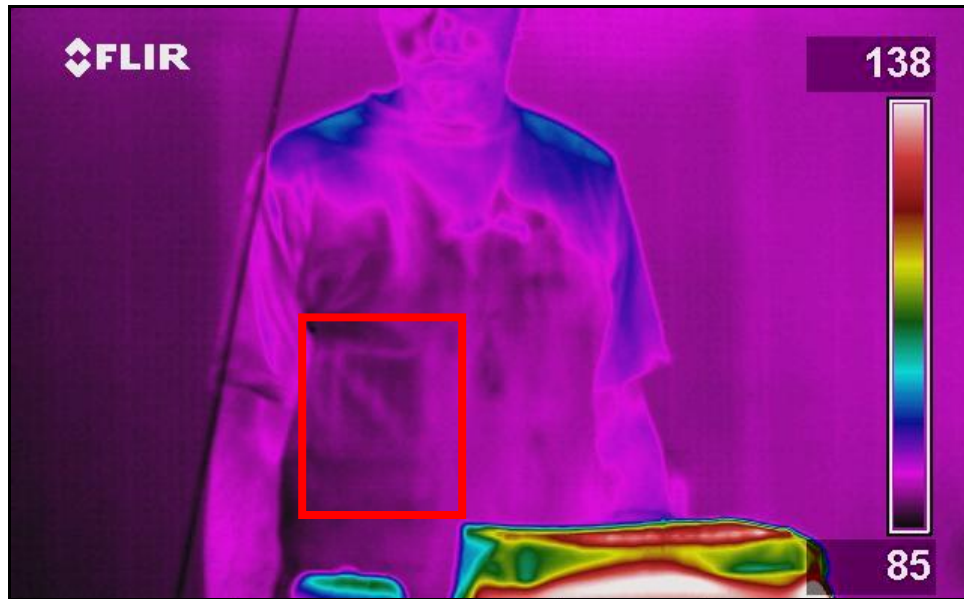


Figure 55—Walking on Treadmill with Metal Bomb at 0 Miles



Figure 56—Walking on Treadmill with Metal Bomb at 1.5 Miles

For the plastic packages the initial torso temperature at 0 miles was 31.49°C (88.69°F), and after 1.5 miles of walking it was 34.35°C (93.83°F). For the plastic packages the initial bomb area temperature at 0 miles was 30.12°C (86.22°F), and after 1.5 miles of walking it was 32.62°C (90.72°F). The temperature was still climbing after 1.5 miles. These results are shown in Figure 57 thru Figure 59.

In this experiment the bomb area tended to be 2-4°F less than the average torso temperature as shown in Figure 59. As can be seen in Figure 60 thru Figure 61, a 2-4°F difference is hard to distinguish when the scale covers a range of 50°F. In this case the temperature difference between the bomb area and the rest of the torso it is less than 6% of the overall temperature scale. At the beginning of the experiment the inside temperature of the bomb was higher than the outside until about 0.5 miles. From about 0.5 miles to 0.75 miles the inside and outside temperatures were even. This is shown in Figure 58. After about 0.75 miles the outside temperature was higher than the inside temperature. When one compares this case to that of the metal bomb, one can see that it takes longer for the ambient air temperature to affect the temperature of the bomb. This would make sense due to the plastic bomb's lower thermal conductivity.

This case illustrates one of the difficulties of the infrared technologies. The treadmill the subject is walking on appears in the image. The plastic material is at a much higher temperature than the torso temperature and causes the large increase in the temperature scale range in the image. This external object causes what may be a visible temperature difference in another setting to be unperceivable in this image.

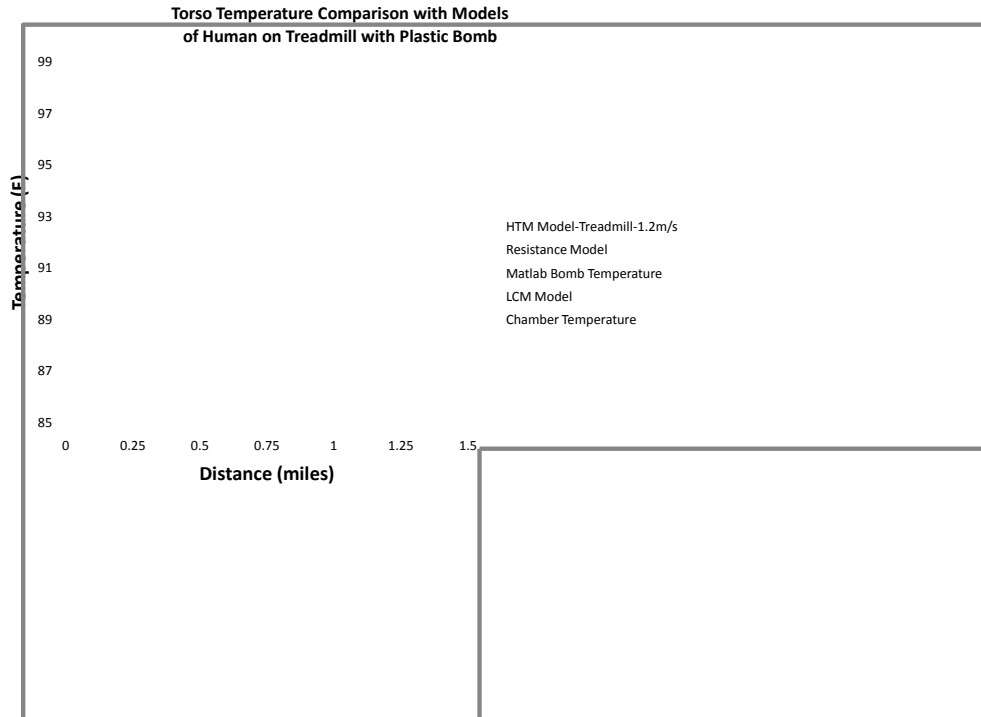


Figure 57—Torso Temperature Comparison with Models Of Human on Treadmill with Plastic Bomb

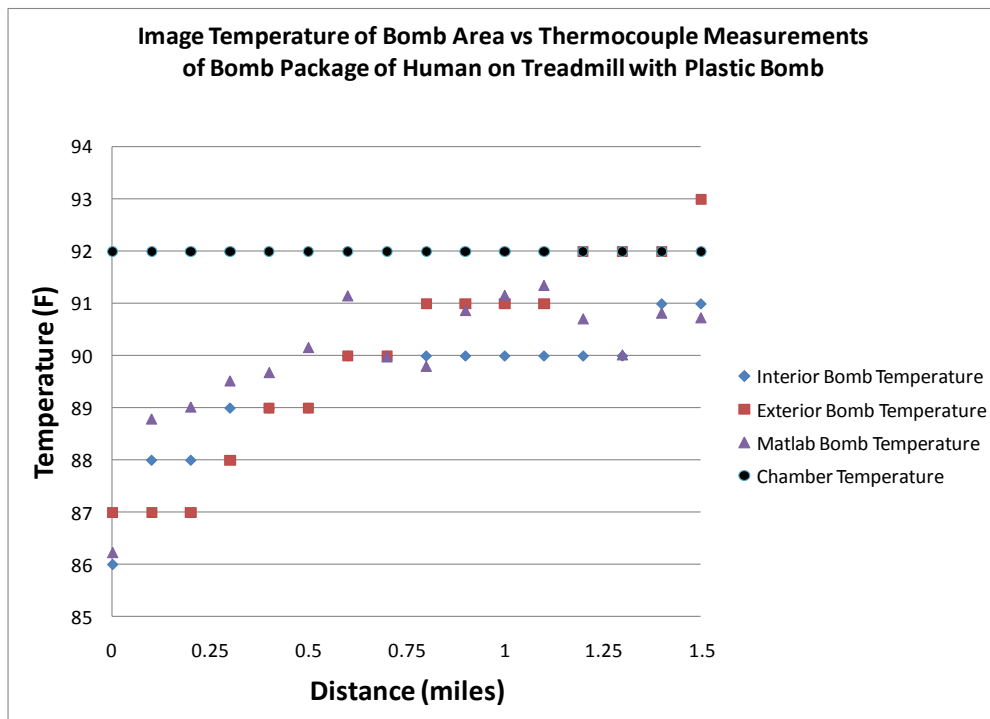


Figure 58—Comparison of Image Temperature with Thermocouple Measurements of Plastic Bomb Package on Human on Treadmill

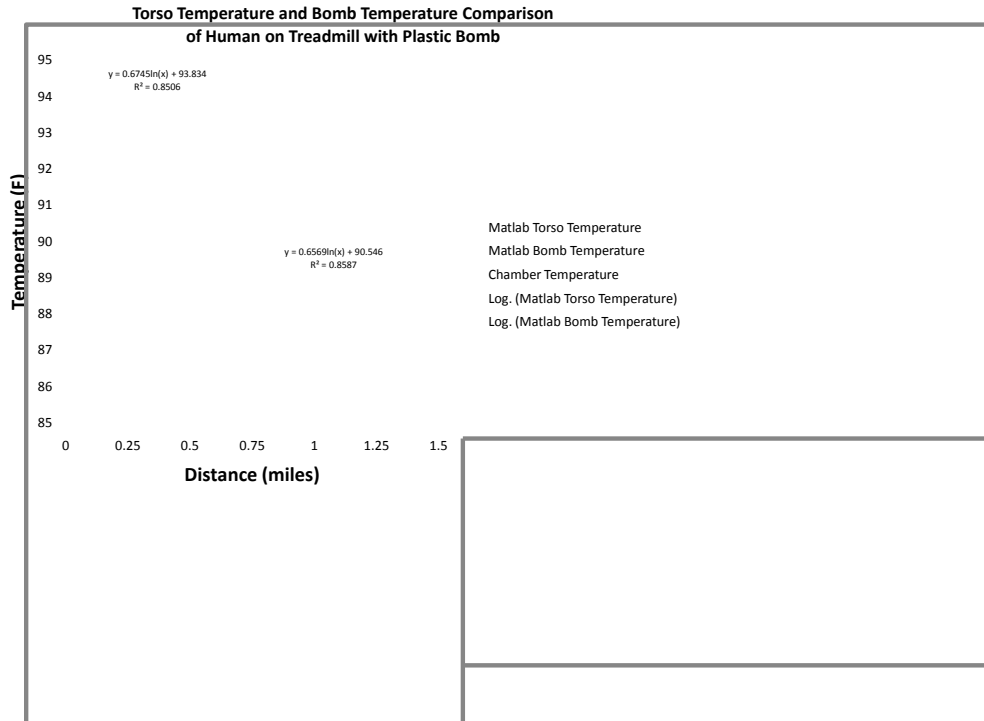


Figure 59—Torso Temperature and Bomb Temperature Comparison Of Human on Treadmill with Plastic Bomb



Figure 60—Walking on Treadmill with Plastic Bomb at 0 Miles



Figure 61—Walking on Treadmill with Plastic Bomb at 1.5 Miles

TRANSIENT CHANGES WHILE WALKING BEST/WORST CASE

TEST COMPARISON

The use of the fans had a major impact on how fast the bomb temperature increased in temperature. When the iced package is tested without the fan running it starts at 7.22°C (45°F) and rises to 32.22°C (90°F) by the end of 1.5 miles. This is 2.78°C (5°F) higher than with the fan running.

It is assumed that the temperature of the clothing is very dependent on the environment due to the wide fluctuations in temperature while the bomb temperature stayed steady.

Fluctuations in the measurements of the clothing may also have been affected because of the differing temperature scales. When the fan was running the treadmill measures 30°F cooler than when the fan is not running. This changes the temperature scale and how precisely the MATLAB® algorithm can calculate the temperature.

Samples of the data have been combined in Table 11. It appears that the amount of time a

subject is exposed to the environmental condition is more dominant in determining the final temperature on the clothing than the distance they covered in that period of time. Due to restriction on human research for this study we were not able to complete tests extending past distances of 1.5 miles.

Table 11—Temperatures Measured in Various Chamber Conditions While Walking on a Treadmill

Description	Speed	Time	Distance (miles)	inside	outside	Matlab Torso Temperature	Matlab Bomb Temperature
Ice-Lights-Fan	3.17mph	0 min	0	48	51	100.09	98.68
		9min 37 sec	0.5	81	82	105.35	102.71
		18min 56sec	1	86	89	105.84	102.83
		28min 20sec	1.5	91	94	105.68	104.76
Ice-Lights-No Fan	1.98mph	0 min	0	45	48	99.83	95.37
		15min 48sec	0.5	89	90	110.65	108.08
		30min 42sec	1	95	98	109.64	107.71
		45min 32sec	1.5	99	100	115.41	115.07
Warm-Lights-Fan	3.38mph	0min	0	104	106	100.12	101.1
		8min 53sec	0.5	101	104	107.04	106.84
		17min 46sec	1	101	104	107.9	109
		28min 37sec	1.5	102	105	106.88	106.98
Warm-Lights-No Fan	2.66mph	0min	0	103	105	102	101.92
		13min 43sec	0.5	103	106	108.14	109.01
		23min 47 sec	1	104	107	109.3	110.9
		33min 50sec	1.5	105	107	108.42	107.96

PRE-COOLED BOMB PACKAGE UNDER SOLAR SIMULATION WITH FAN

The MATLAB® acquired temperature of the bomb area followed the LCM model closely. The measured temperature was within 1°F for almost the entire period. This is shown in Figure 62. The LCM model accounts for both the simulated solar irradiation and the convection due to the fan.

The bomb package did not have sufficient to come to a complete equilibrium. This is not unexpected as it was pre-cooled and began the test at 50°F. This is seen in Figure 63. This effect

on the bomb area of the shirt in seen in Figure 62 as the measured temperature is still increasing at the end of the test.

As can be seen in Figure 63, at the beginning of the test there was a difference between the clothing material and the bomb package of 50°F but only a 10°F difference between the bomb package and the environment. After 1.5 miles there was still a 15°F difference between the bomb package and the clothing layer while the difference between the environmental temperature and the bomb package was only 5°F.

The thermocouple temperatures of the bomb package are shown in Figure 63. Throughout the test the interior of the bomb package was 2°F to 3°F lower than the exterior of the bomb package.

When comparing the bomb area temperature on the shirt to the torso area temperature of the shirt it can be seen in Figure 55 that the bomb area is consistently 2°F to 3°F cooler than the entire torso area. The overall temp range varies between 28°F and 30°F. Over this range of temperatures the 2°F to 3°F difference is between 8% and 11% of the overall temperature scale. In this case the bomb package is relatively easy to see.

PRE-COOLED BOMB PACKAGE UNDER SOLAR SIMULATION WITHOUT FAN

Similar to the test in which the fan was running, the bomb package did not have sufficient time to come to equilibrium. Again, this is not unexpected as the bomb package was pre-cooled and began the test at 50°F. This is seen in Figure 66. As a result, Figure 65 shows the bomb area temperature on the shirt still increasing at the end of the test period.

As can be seen in Figure 66, at the beginning of the test there was a difference between the clothing material and the bomb package of 50°F but only a 13°F difference between the bomb package and the environment. After 1.5 miles there was still a 10°F difference between

the bomb package and the clothing layer while the difference between the environmental temperature and the bomb package was only 5°F.

The thermocouple temperatures of the bomb package are shown in Figure 66. Throughout the test the interior of the bomb package was 2°F to 3°F lower than the exterior of the bomb package.

It can be observed from Figure 66 that while the temperature of the bomb may be consistent there may still be spikes in the temperature measured on the external clothing layers.

When comparing the bomb area temperature on the shirt to the torso area temperature of the shirt it can be seen in Figure 67 that the bomb area begins about 4.5°F lower than the torso temperature and decreases to a difference of 0.5°F. As shown in Figure 76 the bomb package is relatively easy to see in the image. At the end of the 1.5 miles it is hard to distinguish from the rest of the torso. This is shown in Figure 77.

The overall temperature range is 68F in the first image and drops to 62F in the last image. With these temperature ranges, the temperature difference between the bomb area temperature and the torso temperature begins at 7% of the temperature ranges and drops to 2% of the temperature range.

PRE-WARMED BOMB PACKAGE UNDER SOLAR SIMULATION WITH FAN

When using a pre-warmed package the temperature of the bomb area on the clothing quickly jumps to near the resistance model predicted temperature. After the initial reading, the temperature was never more than 3°F away from the resistance model temperature. This is shown in Figure 68.

While the bomb are temperature on the shirt with a pre-cooled bomb package did not reach equilibrium it can be seen in Figure 68 and Figure 69 that the temperature of both the

bomb package and the bomb area temperature on the clothing is consistent within 2°F or 3°F throughout the test.

As can be seen from the thermocouple reading in Figure 69, except for one spike in the temperature reading, the temperature of the bomb area on the shirt remained midway between the bomb temperature and the environmental temperature throughout the test. Throughout the test, the interior of the bomb package was 3°F lower than the exterior of the bomb package. It can also be seen that there was an initial drop from its pre-heated temperature to its equilibrium temperature with the body and environment. Again, it can be seen that large spikes in the bomb area temperature on the clothing are possible even when the bomb temperatures are consistent.

In Figure 70 one can see that for the pre-warmed case the bomb area on the clothing is not always cooler than the average temperature over the entire torso. This was not observed for the pre-cooled case. This made it very difficult to distinguish the bomb package area from the rest of the torso.

PRE-WARMED BOMB PACKAGE UNDER SOLAR SIMULATION WITHOUT FAN

In the case of a pre-warmed bomb without using the fan, the temperature of the bomb area on the clothing tends to fluctuate around the resistance model temperature but with larger variations than seen in the other tests. While it was usually within 3°F to 5°F, at one point it jumped to 10°F above the resistance model temperature.

In comparison to the temperature of the bomb, the temperature of the bomb area on the shirt varied widely. It can be seen in Figure 72 that large spikes in the bomb area temperature on the clothing are possible even when the bomb temperatures are consistent. Like in the case of having the fan running, the interior of the bomb package was 3°F lower than the exterior of the bomb package.

In Figure 73 one can see that for the pre-warmed case the bomb area on the clothing is not always cooler than the average temperature over the entire torso, but these temperatures were usually within 1°F of each other. This made it very difficult to distinguish the bomb package area from the rest of the torso.

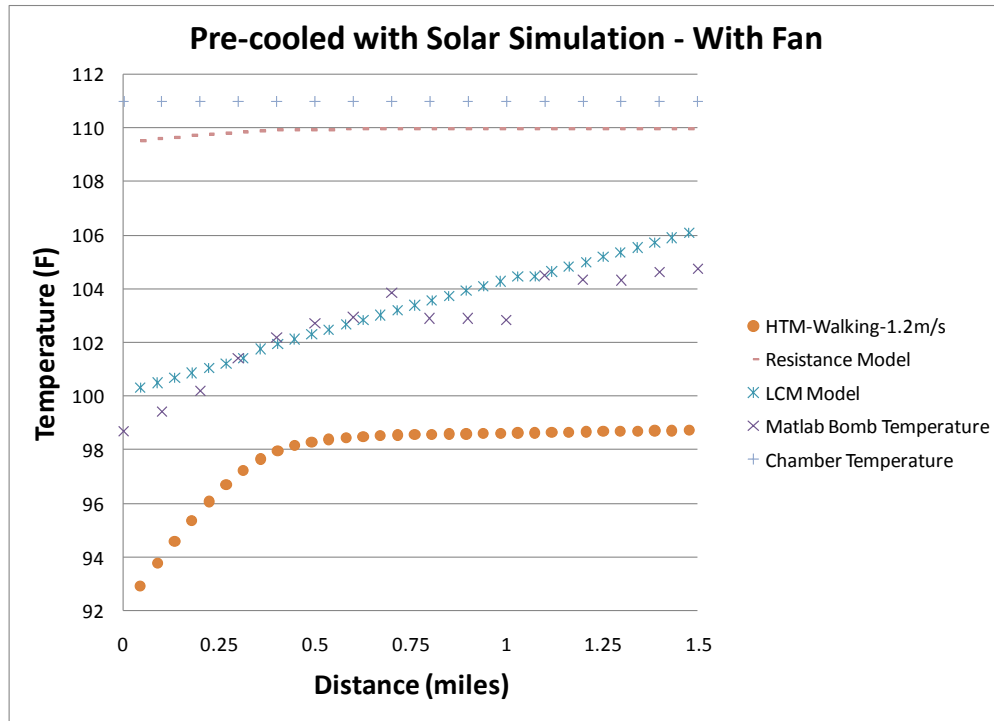


Figure 62—Torso Temperature Comparison with Models of Human on Treadmill with Bomb Chamber Conditions: Lights On- Fan On- Bomb Package: Cooled

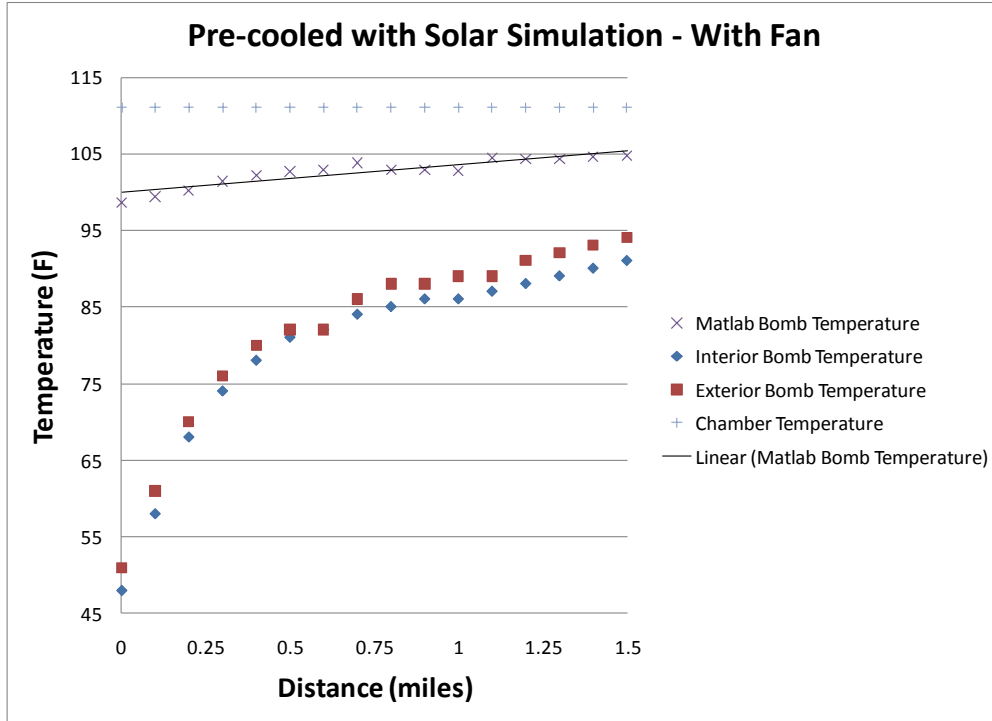


Figure 63—Comparison of Image Temperature with Thermocouple Measurements of Pre-cooled Bomb under Simulated Solar and Fan

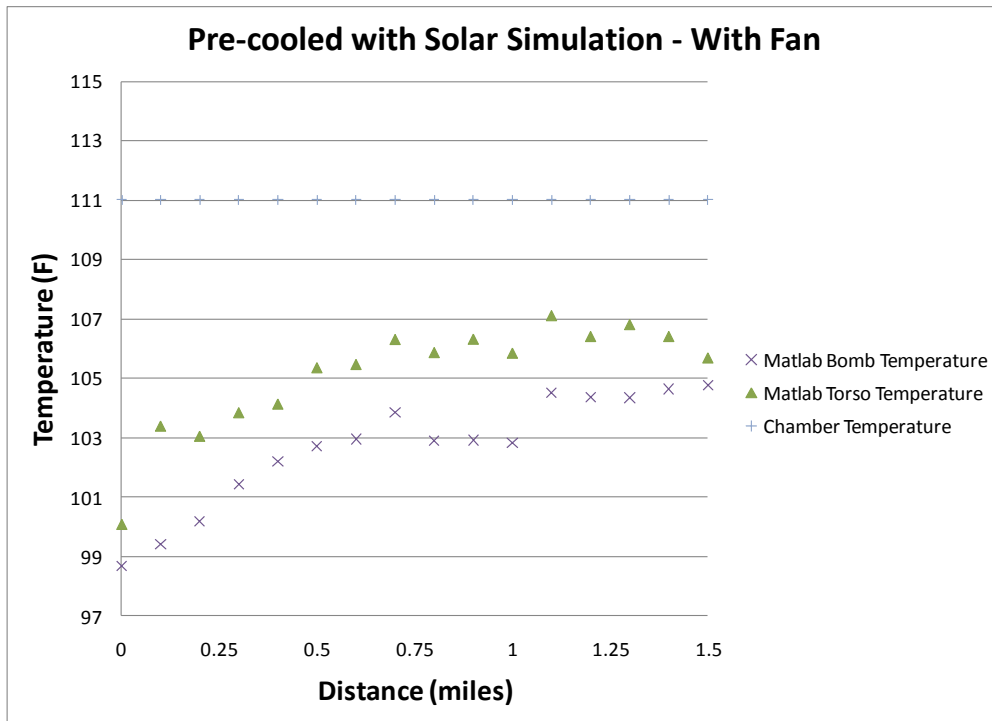


Figure 64—Torso Temperature and Bomb Temperature Comparison

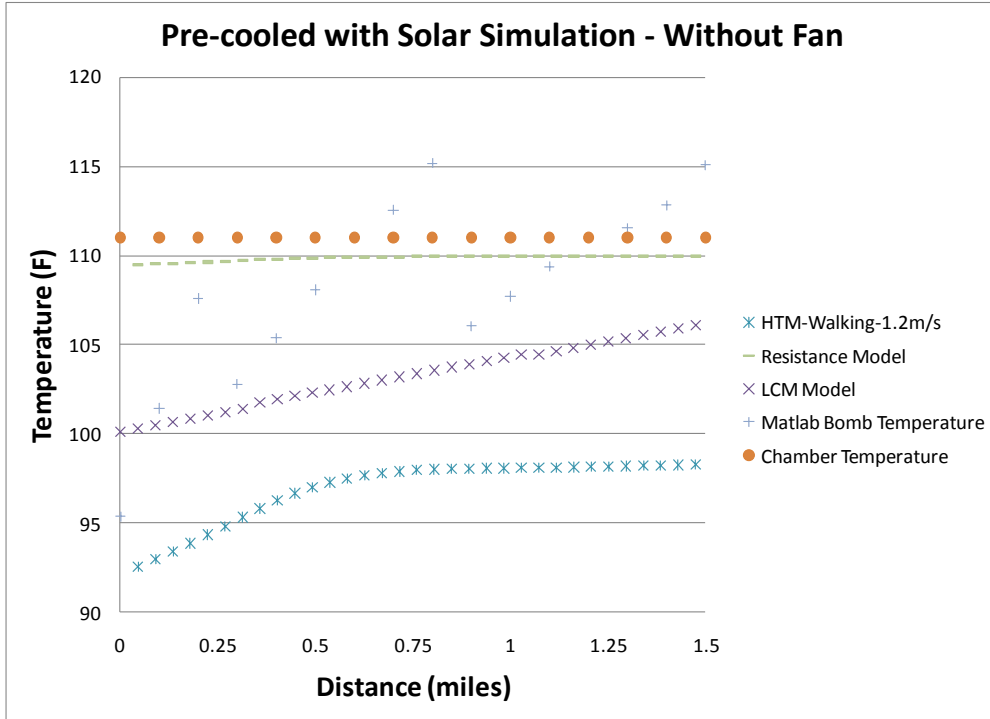


Figure 65—Torso Temperature Comparison with Models of Human on Treadmill with Bomb Chamber Conditions: Lights On- Fan Off- Bomb Package: Cooled

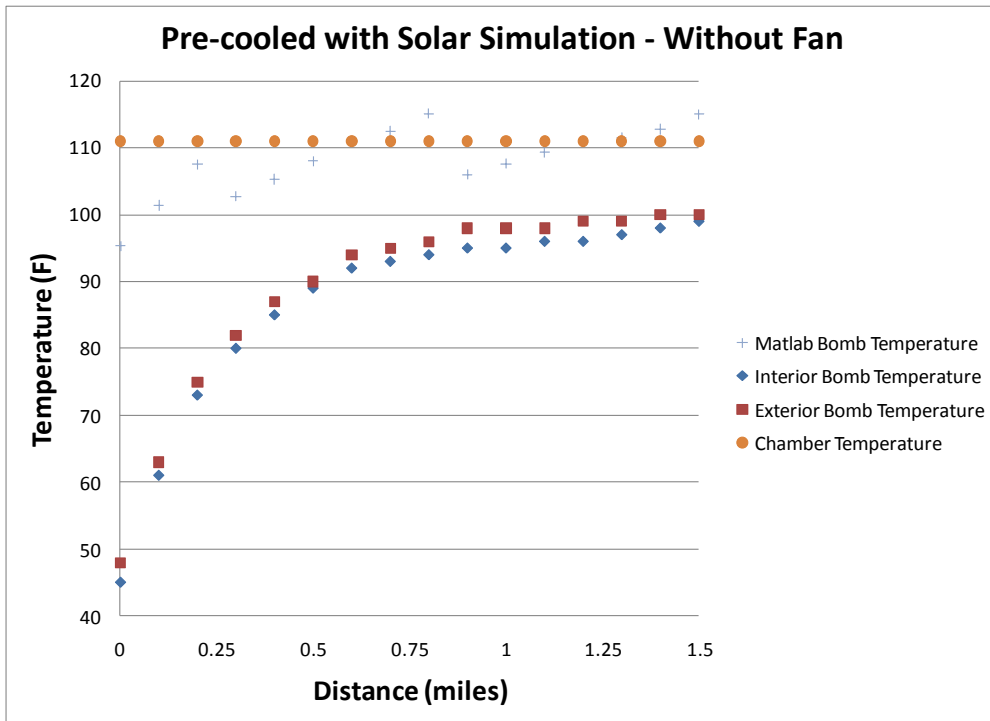


Figure 66—Comparison of Image Temperature with Thermocouple Measurements of Pre-cooled Bomb under Simulated Solar and Without Fan

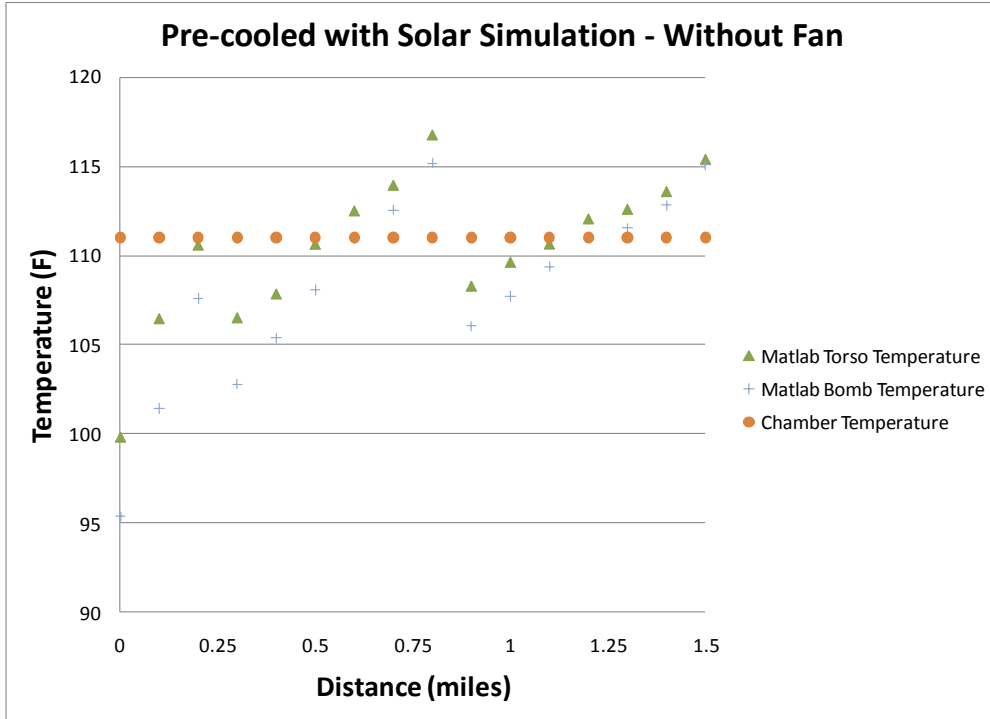


Figure 67—Torso Temperature and Bomb Temperature Comparison

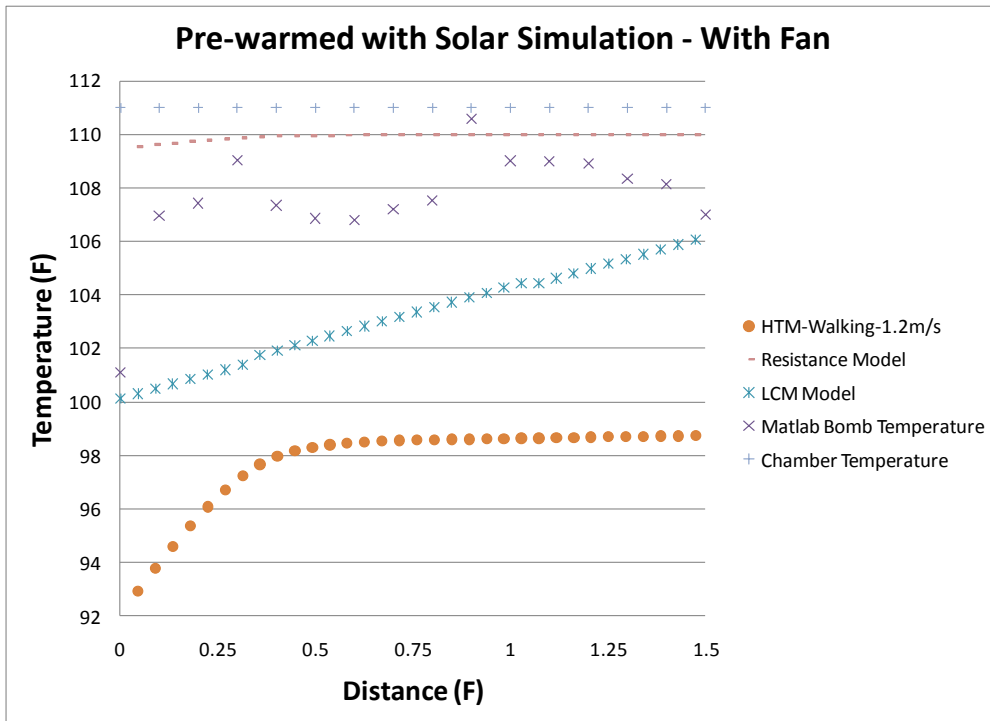


Figure 68—Torso Temperature Comparison with Models of Human on Treadmill with Bomb Chamber Conditions: Lights On- Fan On-Bomb Package: Warmed

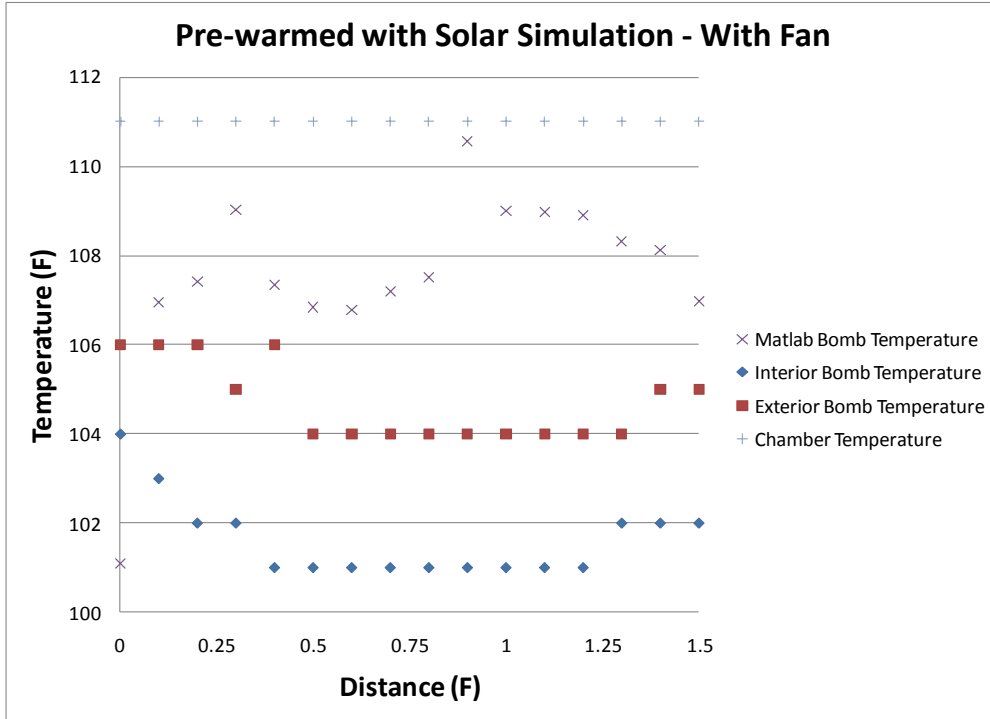


Figure 69—Comparison of Image Temperature with Thermocouple Measurements of Pre-warmed Bomb under Simulated Solar and Fan

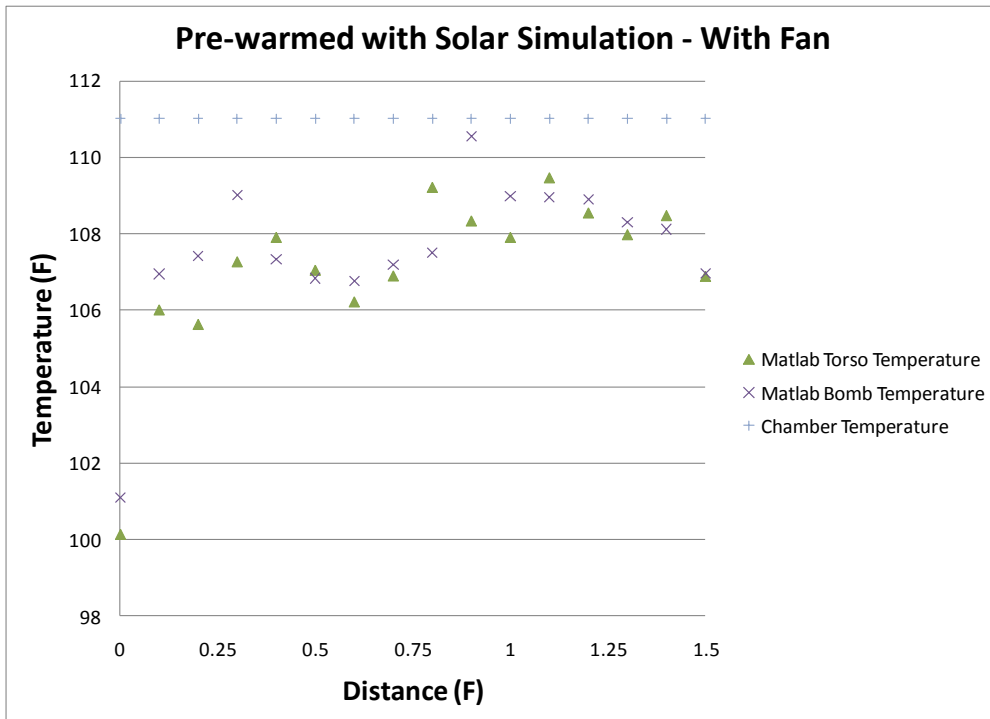


Figure 70—Torso Temperature and Bomb Temperature Comparison

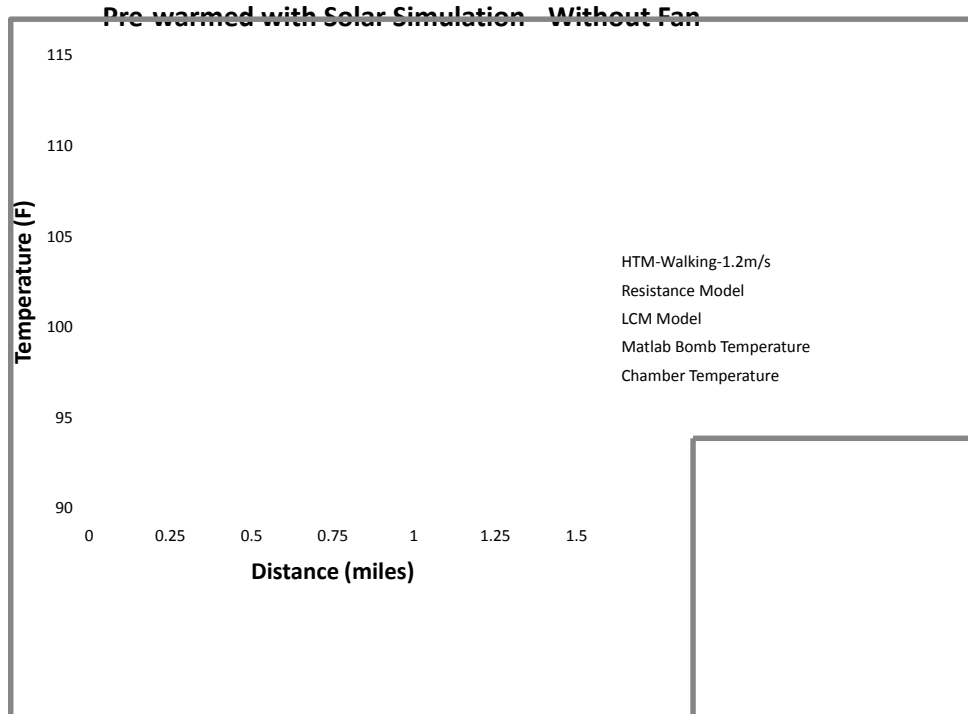


Figure 71—Torso Temperature Comparison with Models of Human on Treadmill with Bomb Chamber Conditions: Lights On- Fan Off- Bomb Package: Warmed

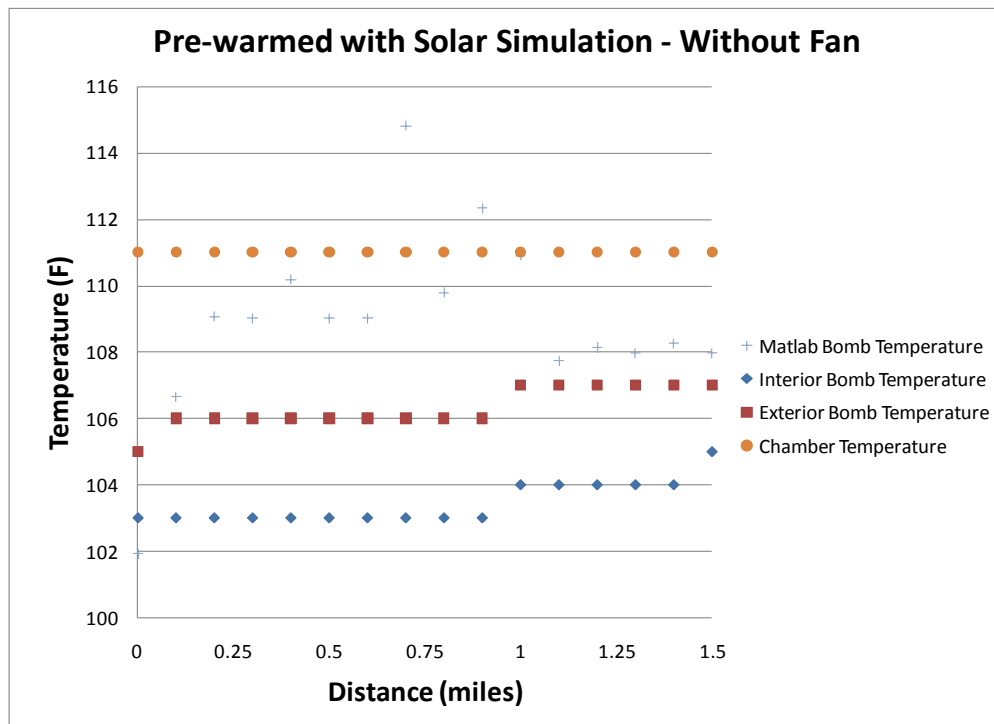


Figure 72—Comparison of Image Temperature with Thermocouple Measurements of Pre-warmed Bomb under Simulated Solar and Without Fan

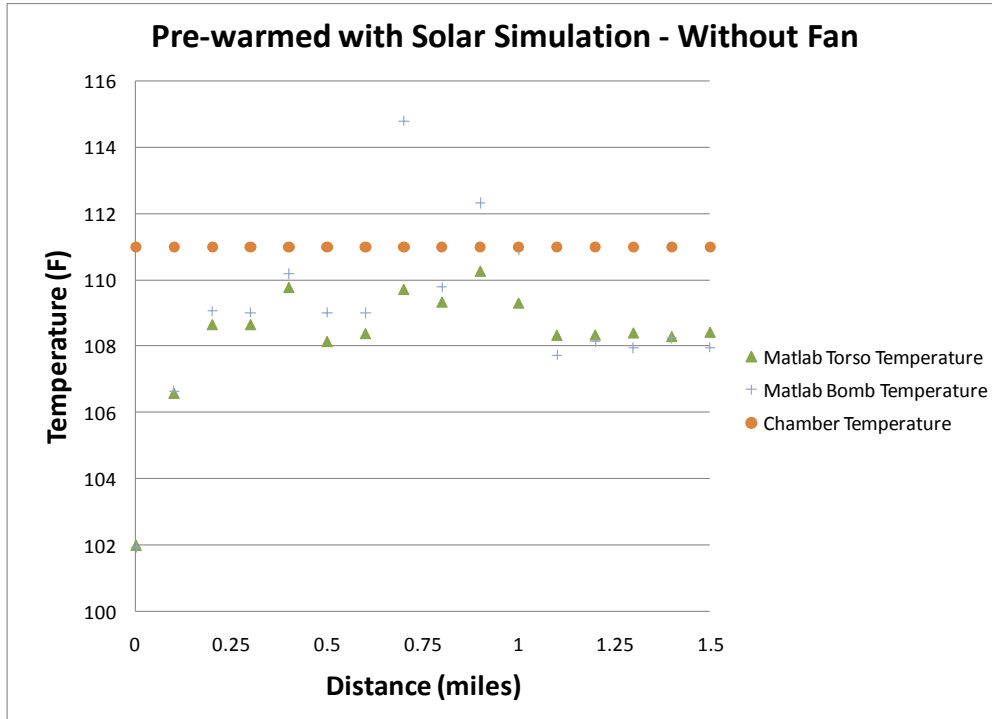


Figure 73—Torso Temperature and Bomb Temperature Comparison

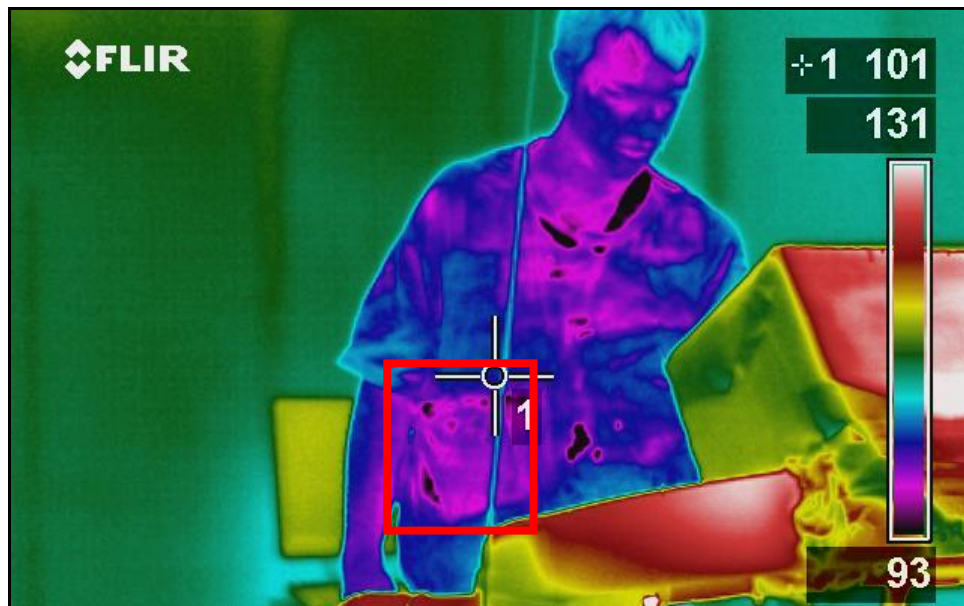


Figure 74—Walking on Treadmill with Cooled Bomb- Lights On- Fan On- 0 miles



Figure 75—Walking on Treadmill with Cooled Bomb- Lights On- Fan On- 1.5 miles

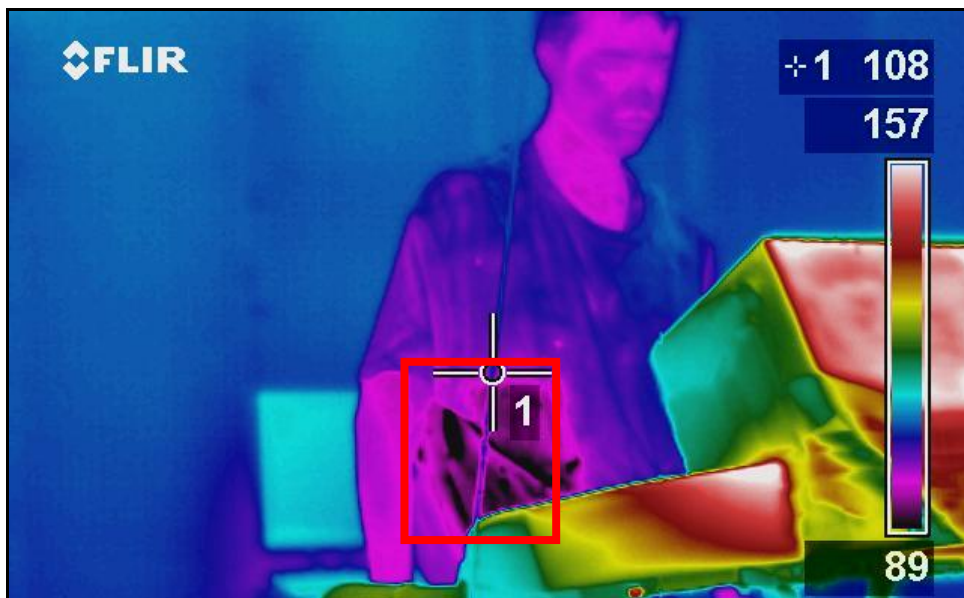


Figure 76—Walking on Treadmill with Iced Bomb- Lights On- Fan Off- 0 miles

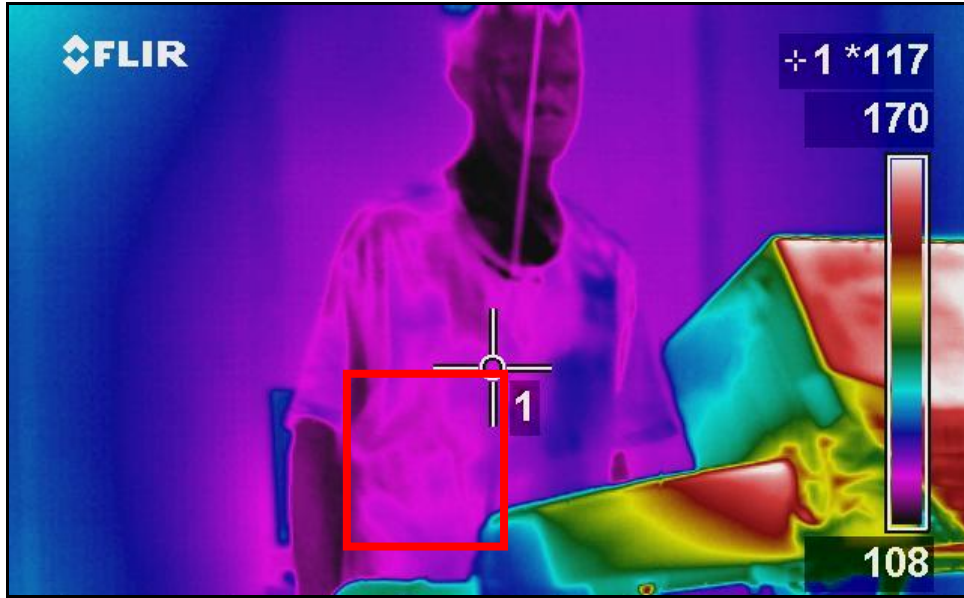


Figure 77-- Walking on Treadmill with Iced Bomb-Lights On- Fan Off- 1.5 miles

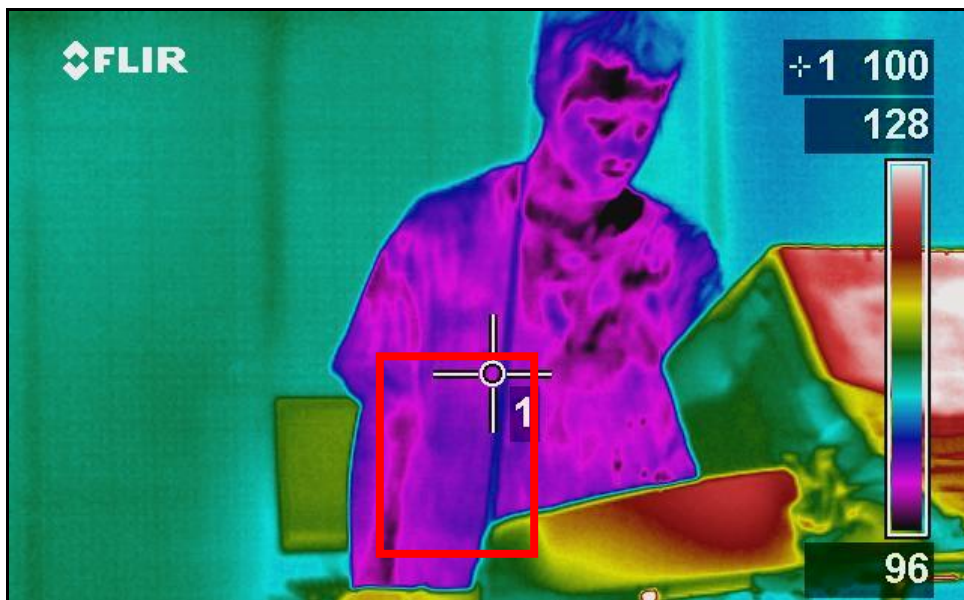


Figure 78-- Walking on Treadmill with Warmed Bomb-Lights On- Fan On- 0 Miles

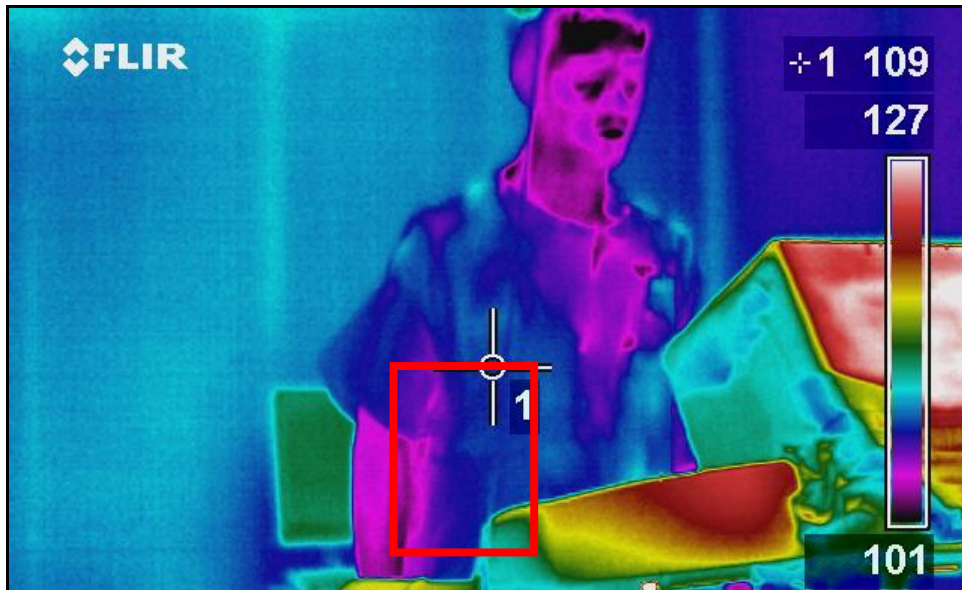


Figure 79-- Walking on Treadmill with Warmed Bomb-Lights On- Fan On - 1.5 Miles

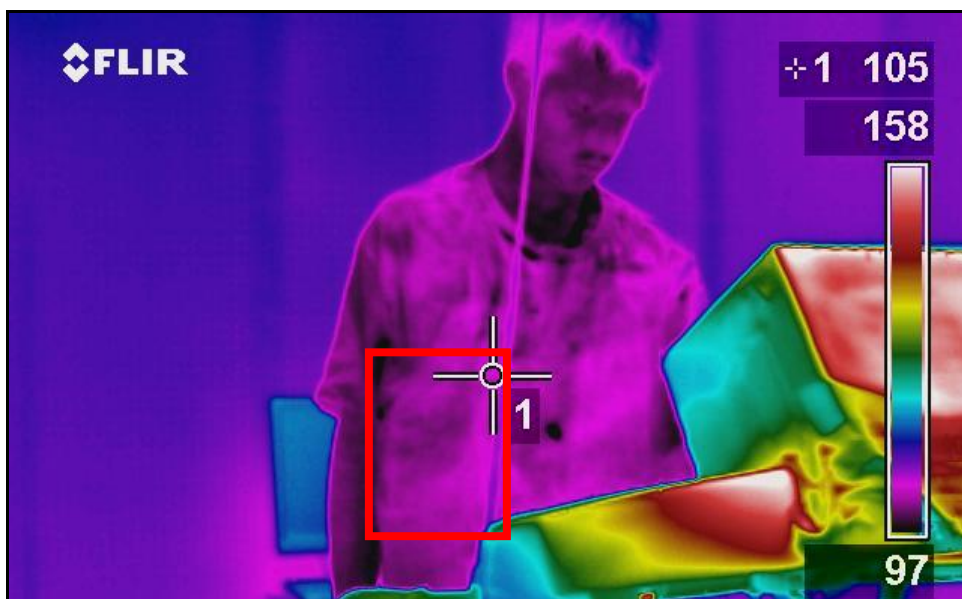


Figure 80-- Walking on Treadmill with Warmed Bomb-Lights On- Fan Off - 0 Miles

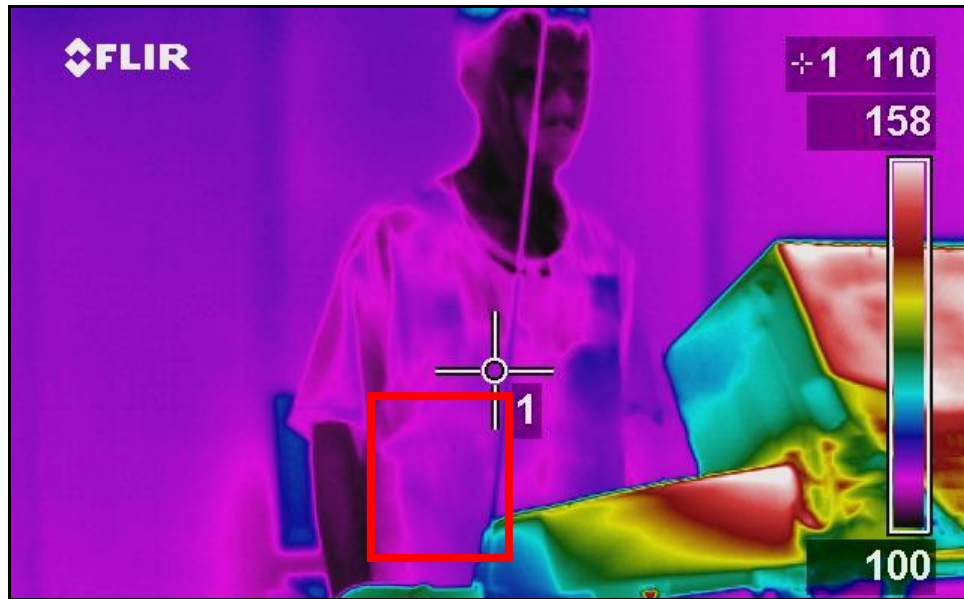


Figure 81-- Walking on Treadmill with Warmed Bomb-Lights On- Fan Off- 1.5 Miles

SHIELDING

Using the auto-adjust temperature scale mode we first looked at the effects of a single semi-tight fitting solid color cotton shirt. The automatic setting displayed the image with a temperature scale of 12° to 13°F. The metal package was completely visible when one semi-tight t-shirt was worn. This is shown in Figure 82. The temperatures measured for the bomb area and torso are presented in Table 12Table 12. We then tested a single solid color loose fitting cotton shirt. The metal bomb package was still visible but less so than during the tests with the semi-tight fitting shirt. The shirts were then layered. The semi-tight shirt was worn directly over the vest and bomb package and then covered with the loose shirt. The packages were not nearly as obvious, but one could still make out the shape of the package as well as the vertical lines produced by the pipes. This is shown in Figure 84. In all three cases there is little difference between the bomb area temperature and the torso temperature measured by the infrared camera. There is also little difference in average torso temperature between the different layering

configurations. The three different tests all had average temperatures within 0.7°F of each other. When two clothing layers were worn as shielding the bomb package temperature was indiscernible from the rest of the torso.

The plastic simulation bomb package was put through the same tests as the simulated metal bomb package. When wearing the semi-tight shirt the package was only visible where it was directly touching the shirt. This is shown in Figure 83. The same was true when looking at the loose cotton shirt. This is shown in Figure 85. The results are presented in Table 12 with the results of the metal bomb package tests. There is little difference between the torso temperature and the bomb temperature and there is very little difference between the different layering combinations. Like the metal package, the plastic package was indiscernible in the image when they are covered by two t-shirts.

The metal and plastic package testing was then repeated using the manual temperature range mode on the camera. In these tests the manual setting displayed the image with a temperature scale of 3°F to 4°F. Using these smaller temperature scales the slight difference between the simulated bomb package and the subject's body becomes more distinguished. When the temperature range is set to manual the difference between the bomb and the torso is much more apparent. Any area of the image that is above or below the range of displayed temperatures appears as the color on the corresponding end of the scale. This usually makes the background of the photo a consistent color and makes the subject stand out much better as compared to auto-adjusted photos. Average temperatures for each combination of automatic and manual temperature range, metal and plastic bomb packages, and amount of clothing are compiled in Table 12. When in manual mode, both the plastic and the metal bomb packages are distinct from the rest of the torso when covered by two t-shirts.

In all tests the bomb package was easiest to detect with tighter shielding clothing. As the amount of clothing covering the package increased the bomb packages became much more difficult to see in the image. This addition of clothing layers makes human visual detection very unlikely using this infrared technology.

Table 12—Exterior Clothing Temperatures for Torso and Bomb Package Areas with Various Layering and Package Material Combinations

		Metal Package			Plastic Package		
		1 Tight T-Shirt	1 Loose T-Shirt	2 T-Shirts	1 Tight T-Shirt	1 Loose T-Shirt	2 T-Shirts
MATLAB® Average Torso Temperature	Automatic Temperature Range	106.15	105.45	106.06	106.68	106.74	106.44
	Manual Temperature Range	106.47	107.08	107.86	107.08	107.12	107.17
MATLAB® Average Bomb Temperature	Automatic Temperature Range	106.39	105.93	105.81	107.29	107.15	106.57
	Manual Temperature Range	106.85	107.24	107.81	107.53	107.67	107.41

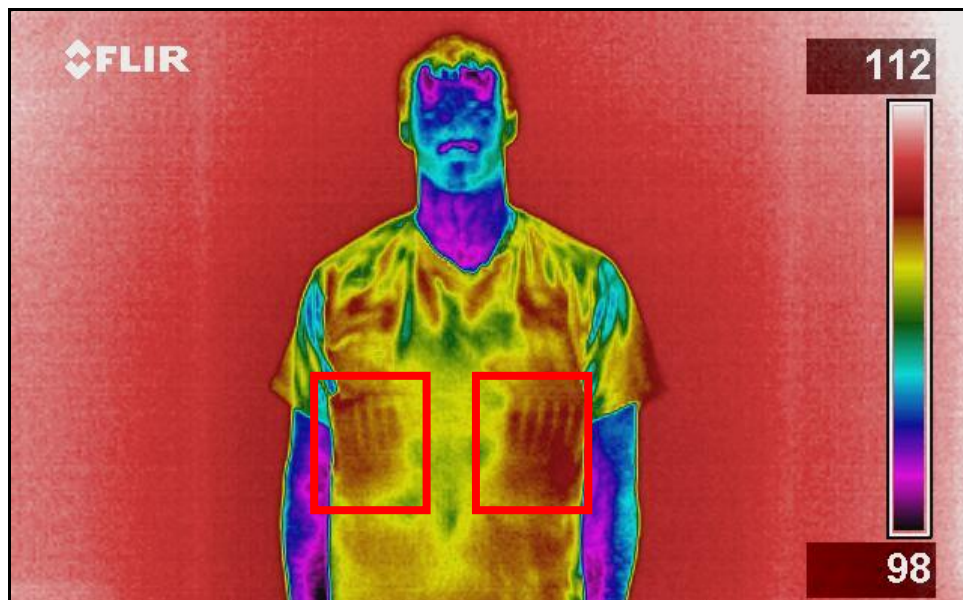
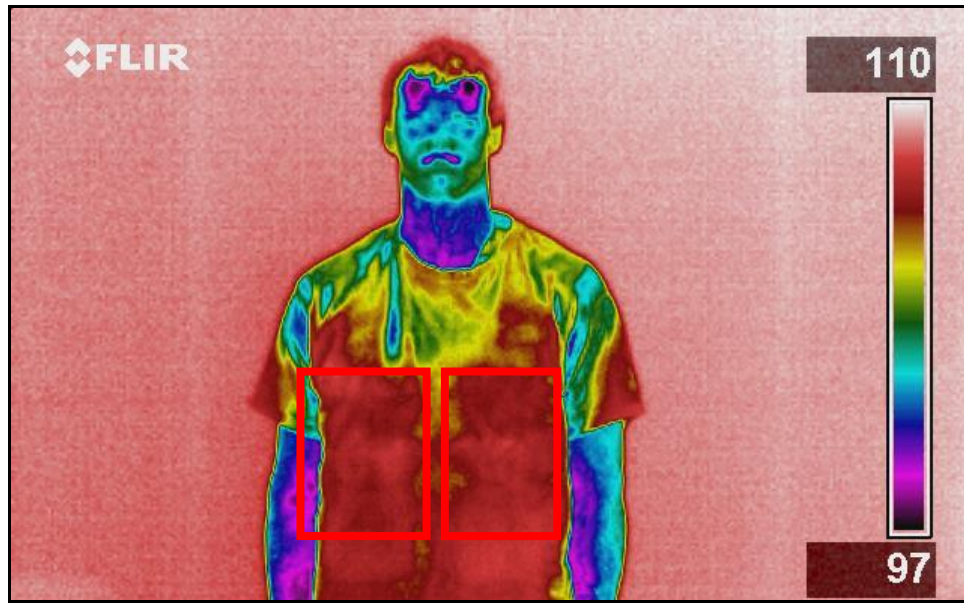
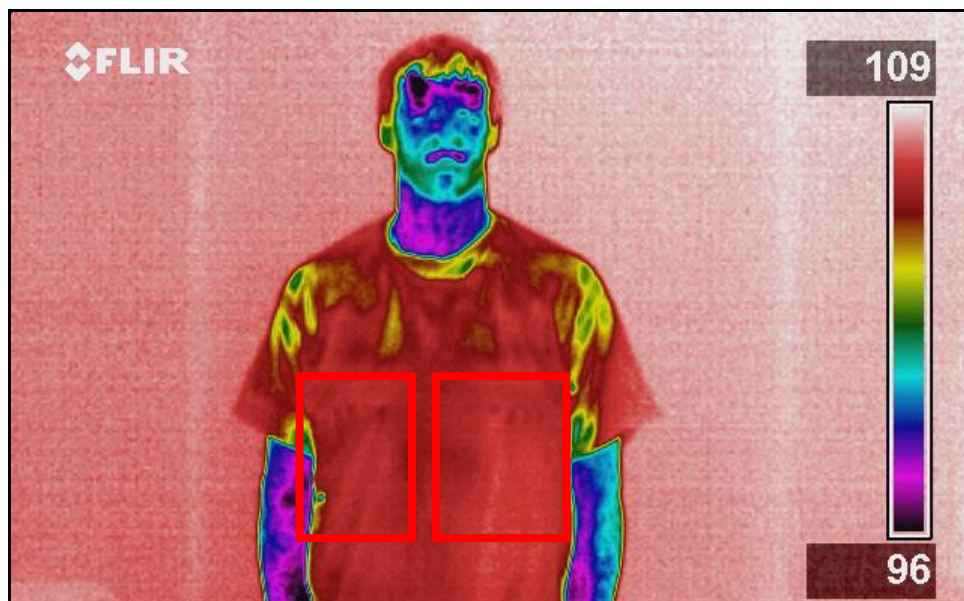


Figure 82—Metal Package Hidden in Vest Shielded by 1 Tight T-Shirt -Automatic Temperature Range Setting



*Figure 83—Plastic Package Hidden in Vest Shielded by 1 Tight T-Shirt
-Automatic Temperature Range Setting*



*Figure 84—Metal Package Hidden in Vest Shielded by 2 Loose T-Shirt
-Automatic Temperature Range Setting*

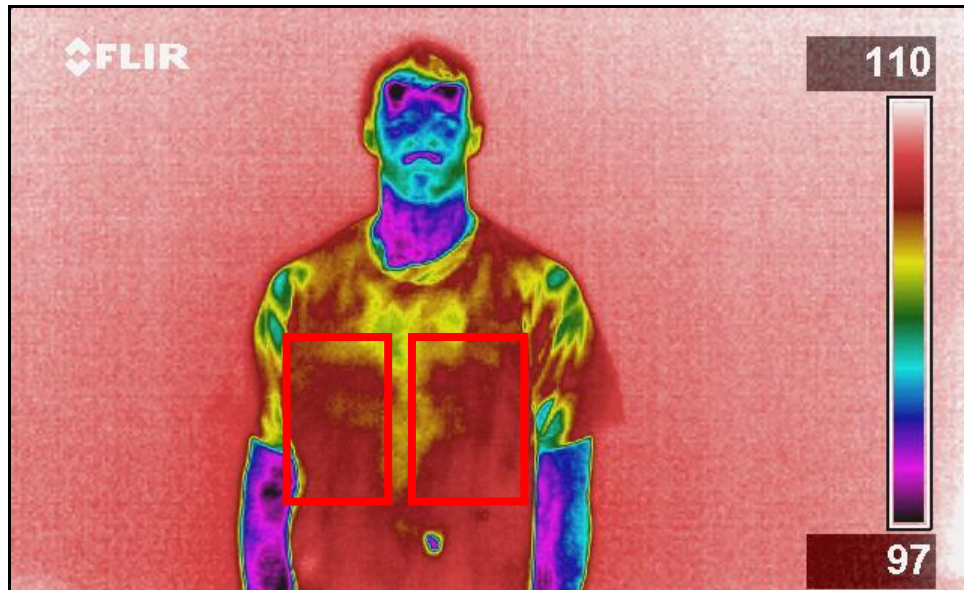


*Figure 85—Plastic Package Hidden in Vest Shielded by 2 Loose T-Shirts
-Automatic Temperature Range Setting*

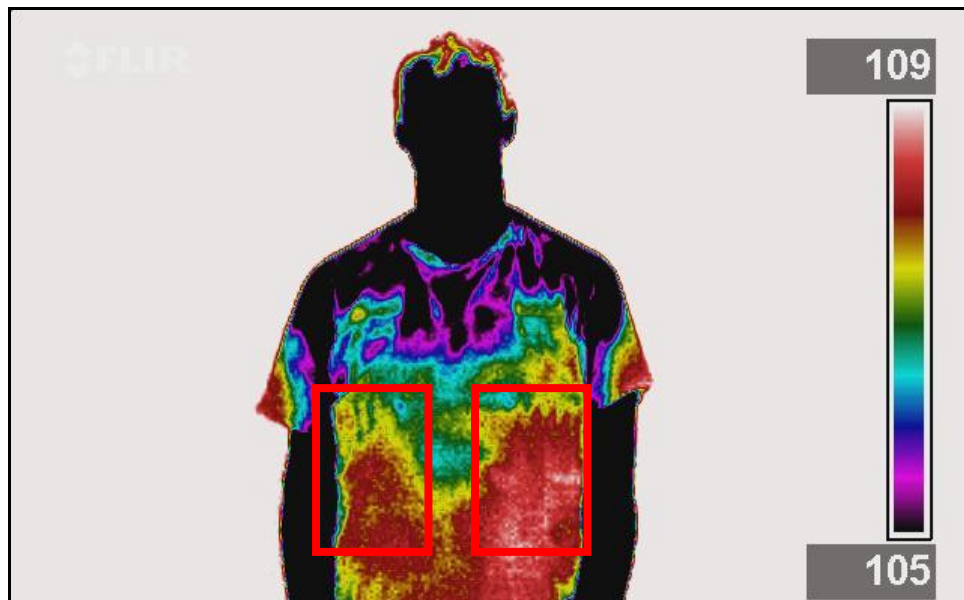


*Figure 86—Metal Package Hidden in Vest Shielded by 1 Tight T-Shirt
-Manual Temperature Range Setting*

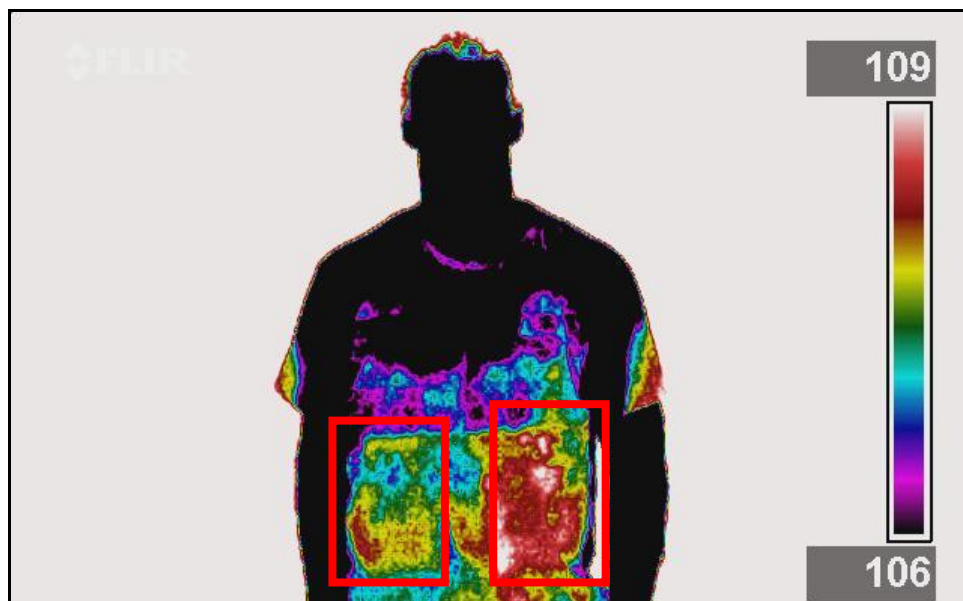


*Figure 87—Plastic Package Hidden in Vest Shielded by 1 Tight T-Shirt
-Manual Temperature Range Setting*



*Figure 88—Metal Package Hidden in Vest Shielded by 2 Loose T-Shirts
-Manual Temperature Range Setting*

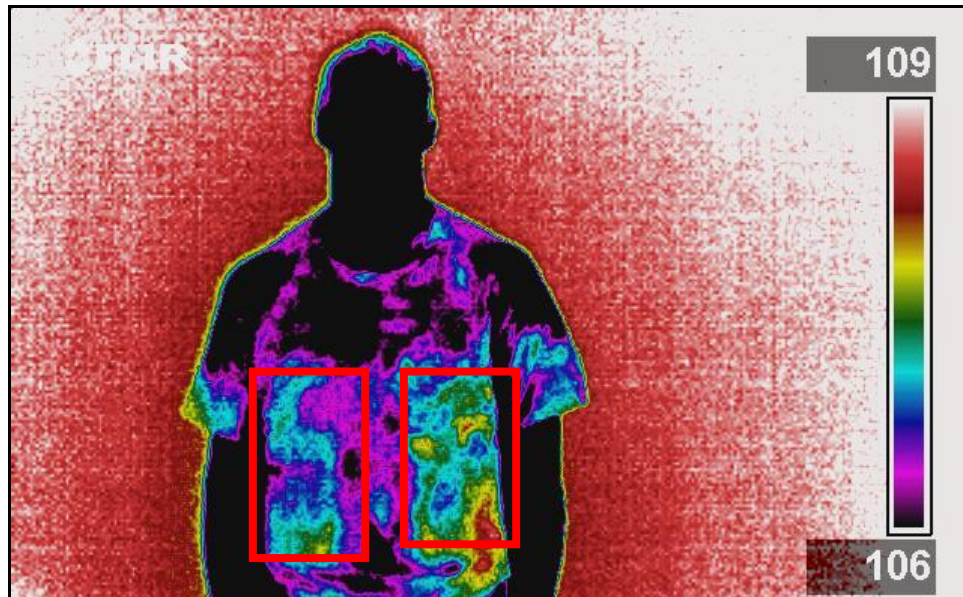


*Figure 89—Plastic Package Hidden in Vest Shielded by 2 Loose T-Shirts
-Manual Temperature Range Setting*

RESULTS OF CAMERA TESTING PHASE 3

TRANSIENT CHANGES WHILE WALKING

When imaging the metal bomb package while walking outside the temperature increase of the bomb and torso follow the rise of the LCM model closely. The resistance model predicts a much higher temperature due to the fact it does not account for the extra convective cooling caused by the movement of the body. The thermocouple measurements of the inside and outside of the bomb package measured the same throughout this test so they are overlaid in Figure 91. They began at 24.44°C (76°F) and rose to 35.56°C (96°F). In this test the HTM program results, the RTD measurements of the bomb, and the temperatures acquired by the IR images all seem to converge at a walking distance of 1.5 miles. At the beginning of the test there is almost a 2.22°C (4°F) difference between the average torso temperature and average bomb area temperature. After walking one-half mile there is less than 2°F (1.11 °C) difference between these

temperatures, and after walking one mile there is less than 1°F (0.56 °C) difference in temperatures. The overall temperature scale in these images is 45°F to 46°F, (25°C) so the temperature differences seen in these images represent 9% of the scale at the beginning of the distance and 3% at the end. When the difference represents around 9% of the temperature scale the bomb package is relatively easy to distinguish from the torso, but become quite difficult to distinguish when it only represents around 3% of the scale.

The plastic bomb package temperatures acquired by the IR camera were usually two to three degrees higher than the RTD measurements of the bomb package, but they increased at the same rate. This is shown in Figure 105. In this test the HTM program results, the RTD measurements of the bomb, and the temperatures acquired by the IR images all rose at a semi-consistent rate until the walking distance of 0.8 miles. After that the HTM levels out while the other measurements continue to climb. At the beginning of the test there is a 0.72°C (1.3°F) difference between the average torso temperature and average bomb area temperature. Over the first 0.7 mile this difference drops to 0.56°C (1°F) and then drops quickly to a difference of approximately 0.28°C (0.5°F) by 1 mile. After 1 mile it settles to a difference of 0.22°C (0.4°F). The overall temperature range begins at 46F for the first image and expands to 52F for the last image. These small temperature differences between the bomb area and the torso temperature represent only 1% to 3% of the temperature scale used in the images. This makes the packages very difficult to distinguish in the images.

The thermocouple measurements showed the inside temperature of the bomb package consistently one degree above the temperature of the outside of the bomb. This result is different than what was seen in most of our other testing. It stands to reason that the increased heat from the body walking in the hot outdoor environment had a larger influence on the temperature of the

bomb than in other tests, while at the same time there is a larger convective cooling effect on the exterior of the bomb package due to the movement while walking.

Due to IRB restrictions on this research limiting the time that the subject could be submitted to the environment and physical conditions, the results from this experiment did not reach a steady state during the test.

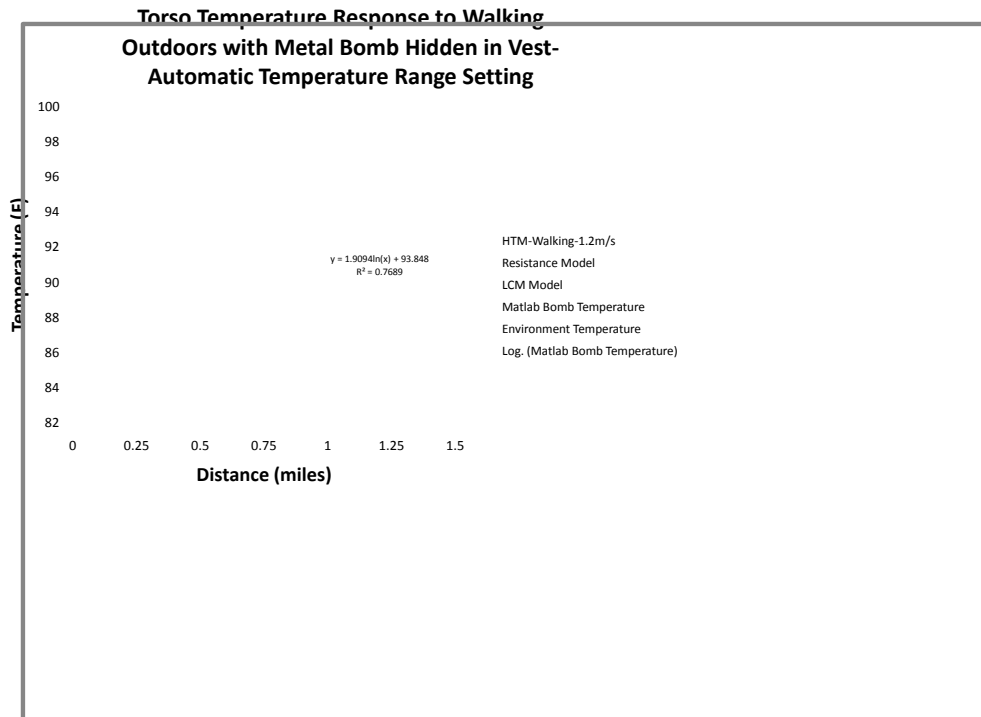


Figure 90—Torso Temperature Comparison with Models of Human Walking Outdoors With Metal Bomb Hidden in Vest-Automatic Temperature Range Setting

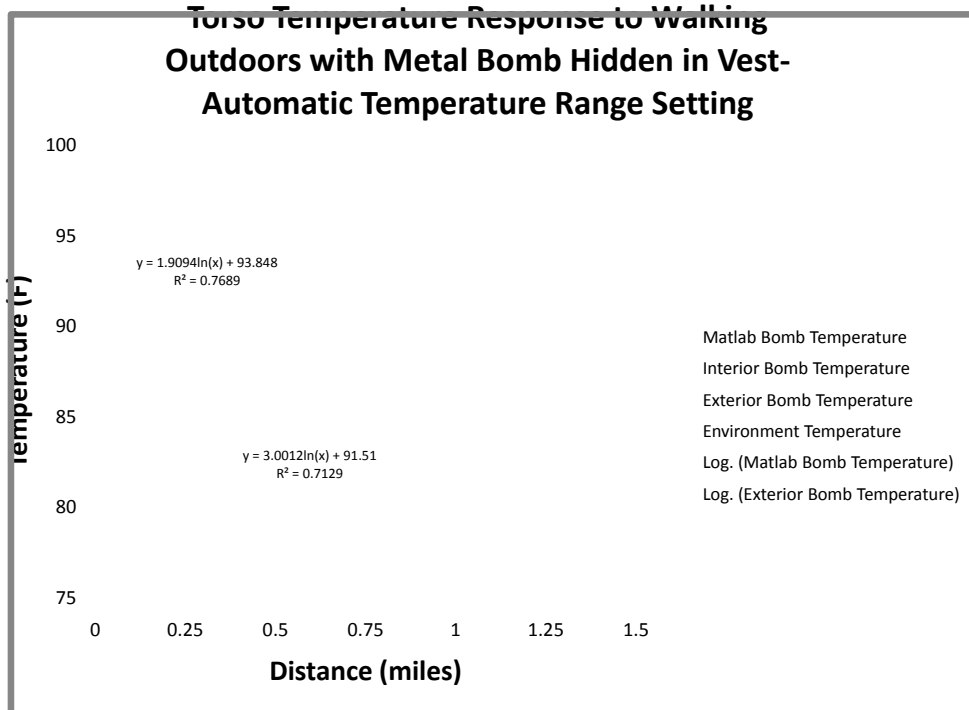


Figure 91—Comparison of Image Temperature Using Automatic Temperature Range with Thermocouple Measurements of Metal Bomb

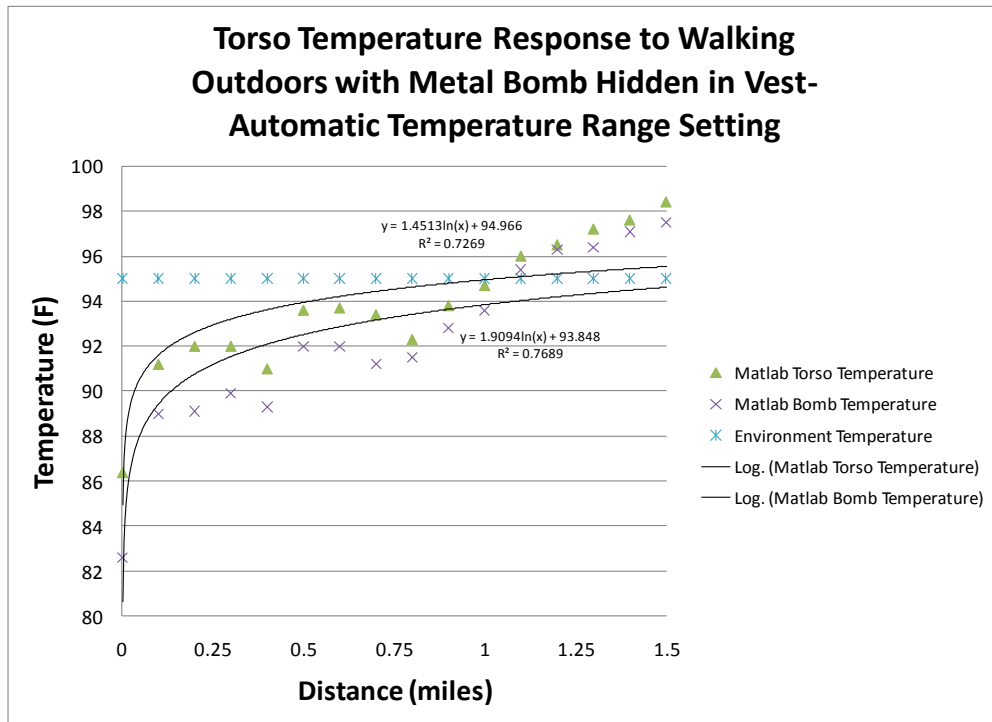


Figure 92—Torso Temperature and Bomb Temperature Comparison of Human Walking Outside with Metal Bomb

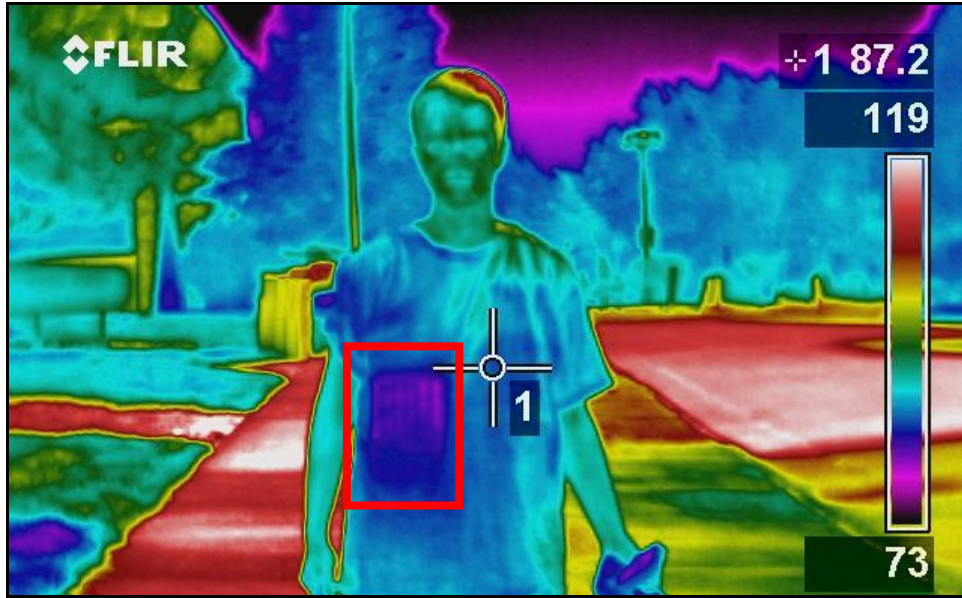


Figure 93—Walking Outside with Metal Bomb at 0 Miles
- Automatic Temperature Scale Setting

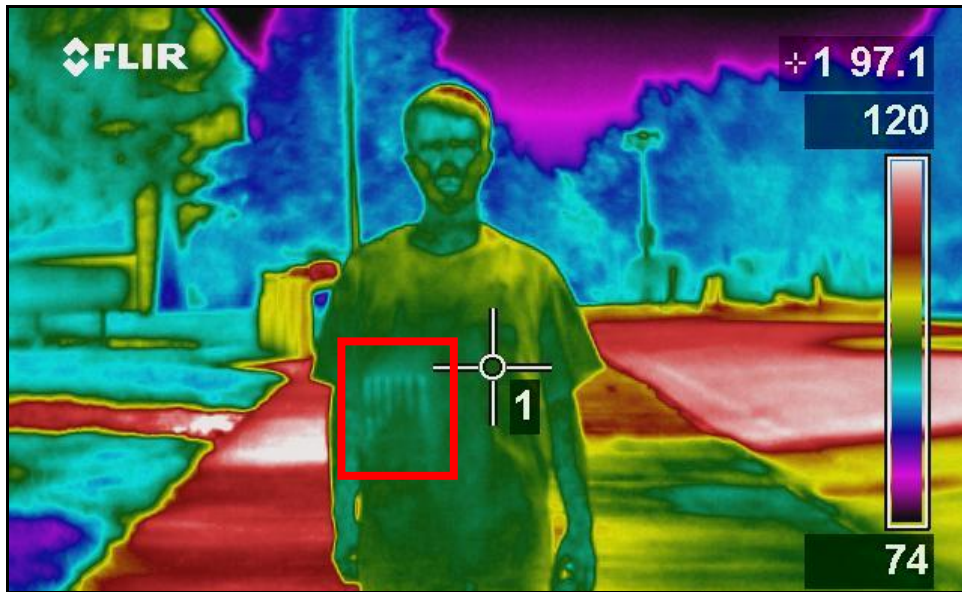


Figure 94—Walking Outside with Metal Bomb at 0.5 Miles
- Automatic Temperature Scale Setting

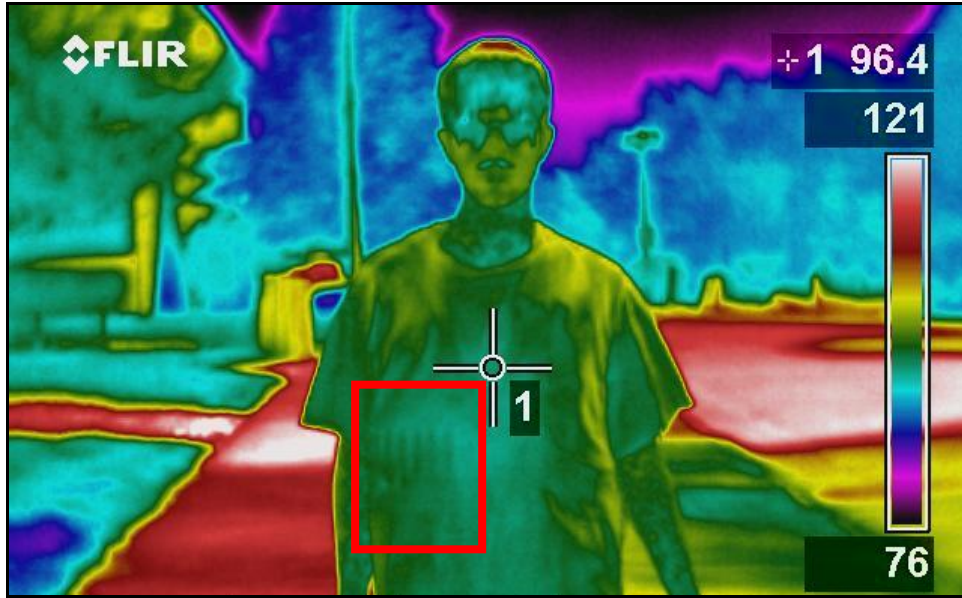


Figure 95—Walking Outside with Metal Bomb at 1 Mile
- Automatic Temperature Scale Setting

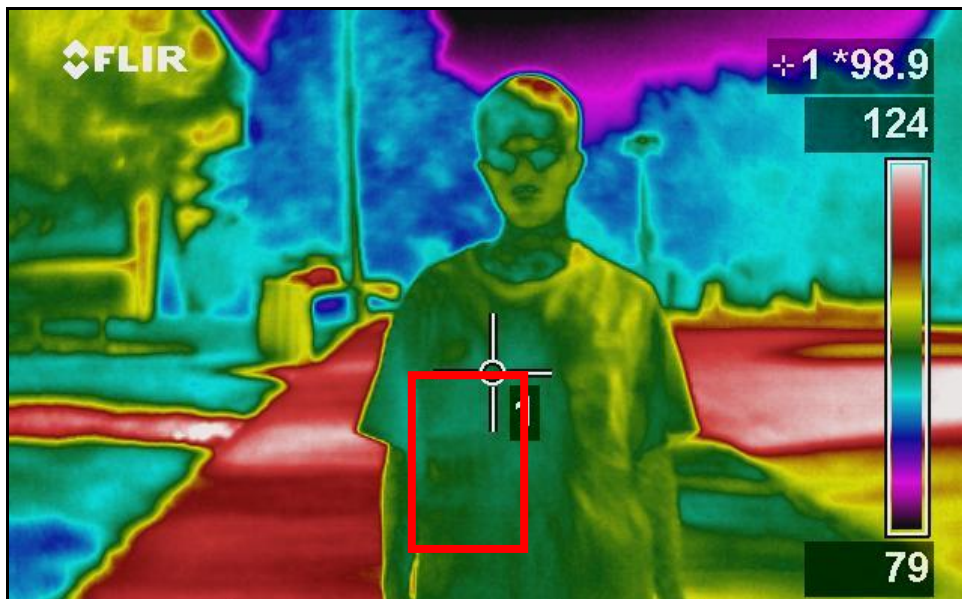


Figure 96—Walking Outside with Metal Bomb at 1.5 Miles
- Automatic Temperature Scale Setting

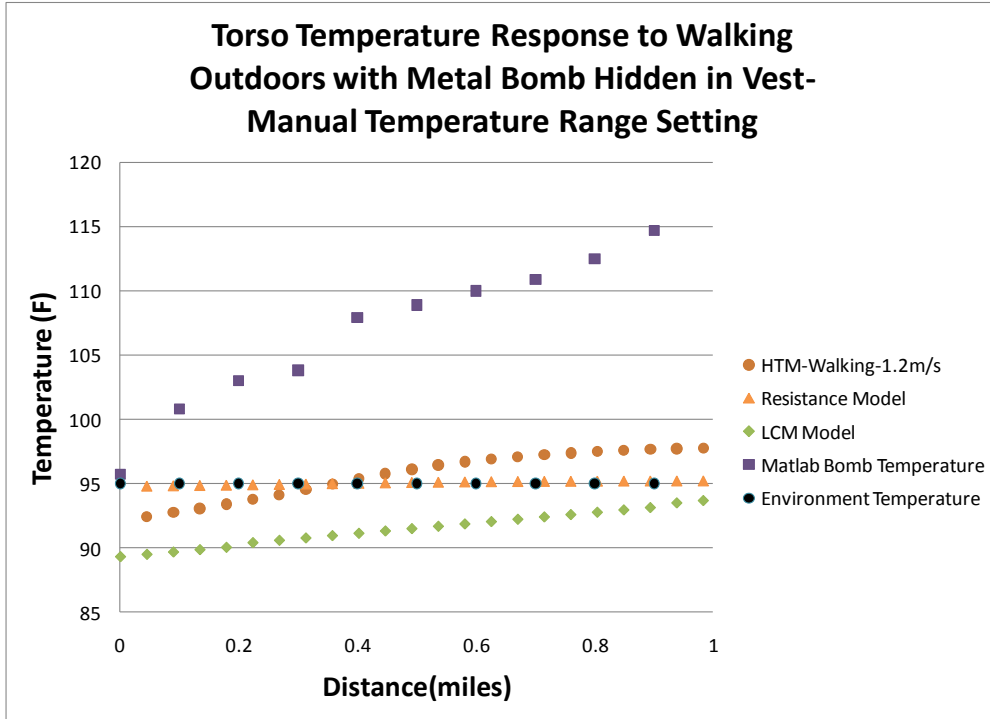


Figure 97—Torso Temperature Comparison with Models of Human Walking Outdoors With Metal Bomb Hidden in Vest-Manual Temperature Range Setting

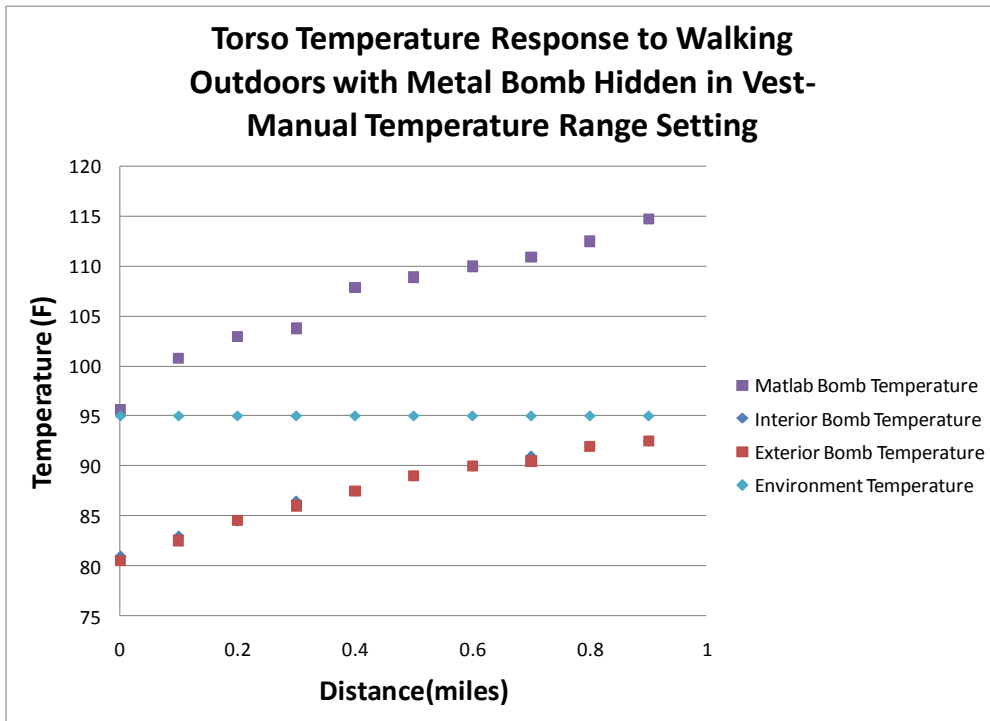


Figure 98—Comparison of Image Temperature Using Manual Temperature Range with Thermocouple Measurements of Metal Bomb

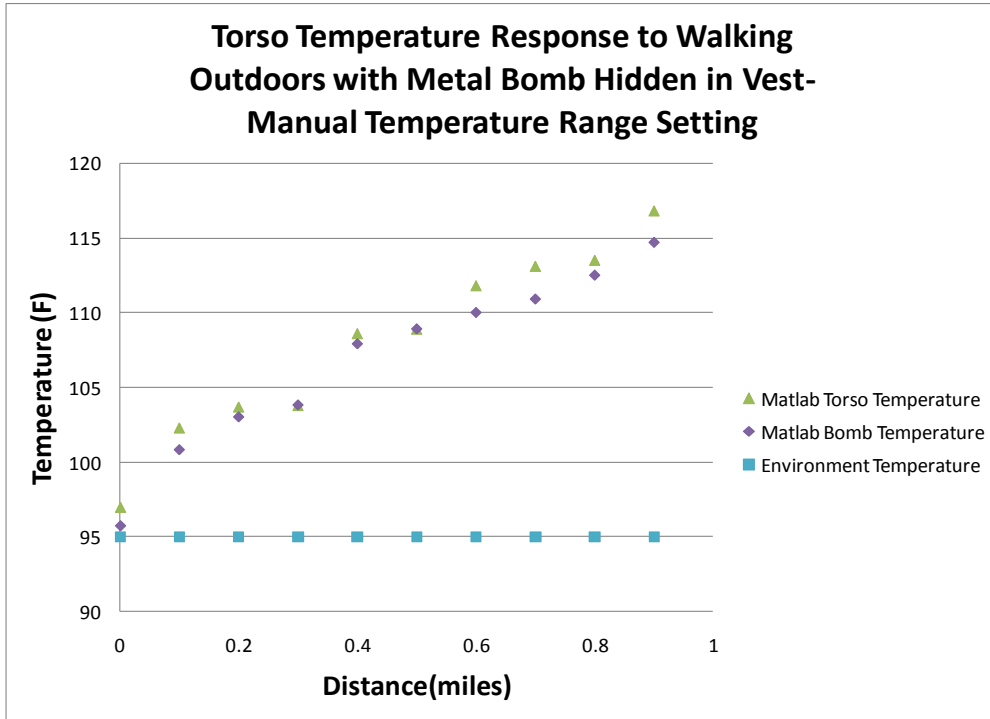


Figure 99—Torso Temperature and Bomb Temperature Comparison of Human Walking Outside with Metal Bomb

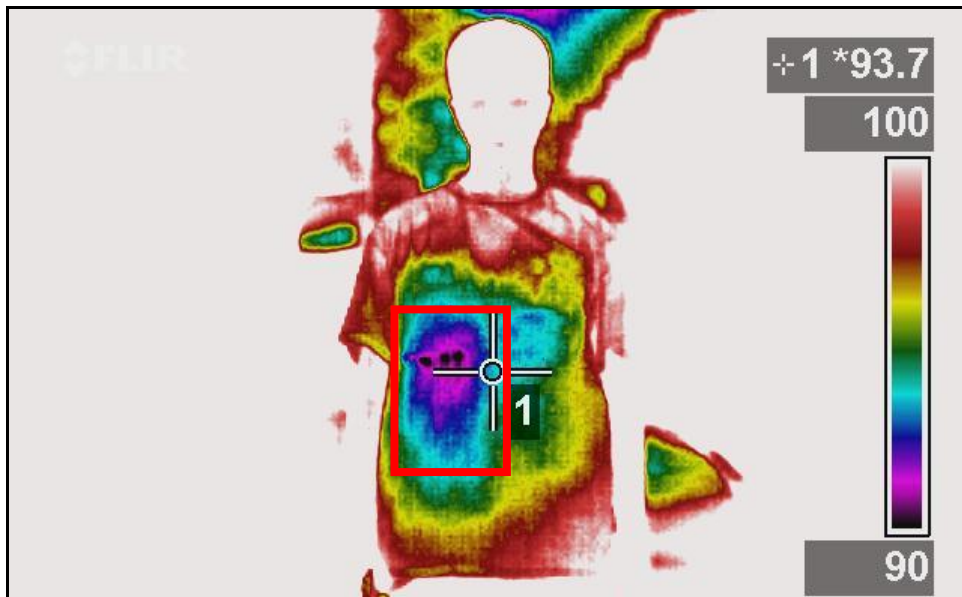
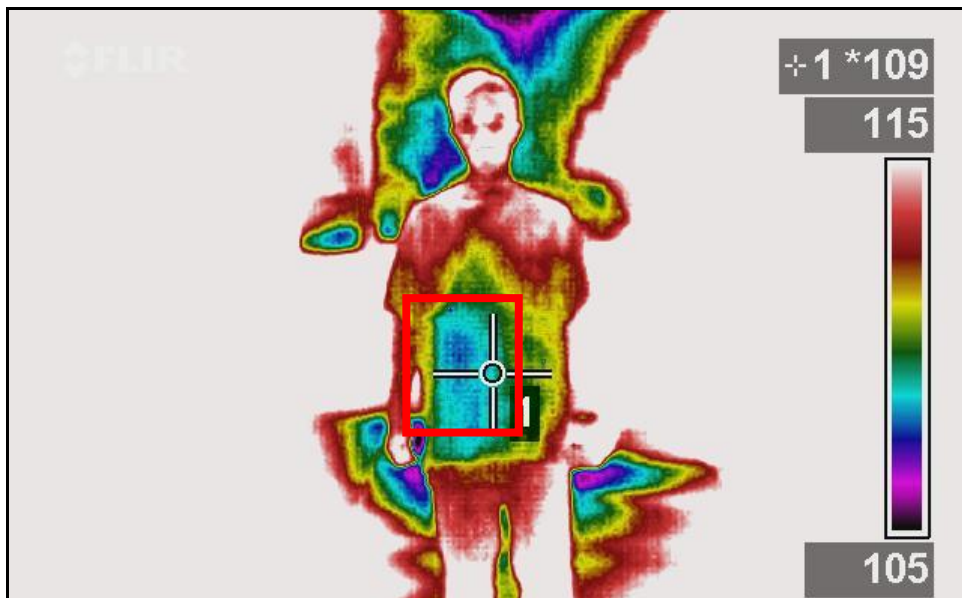


Figure 100—Walking Outside with Metal Bomb at 0 Miles - Manual Temperature Scale Setting



*Figure 101—Walking Outside with Metal Bomb at 0.5 Miles
- Manual Temperature Scale Setting*



*Figure 102—Walking Outside with Metal Bomb at 1.0 Mile
- Manual Temperature Scale Setting*

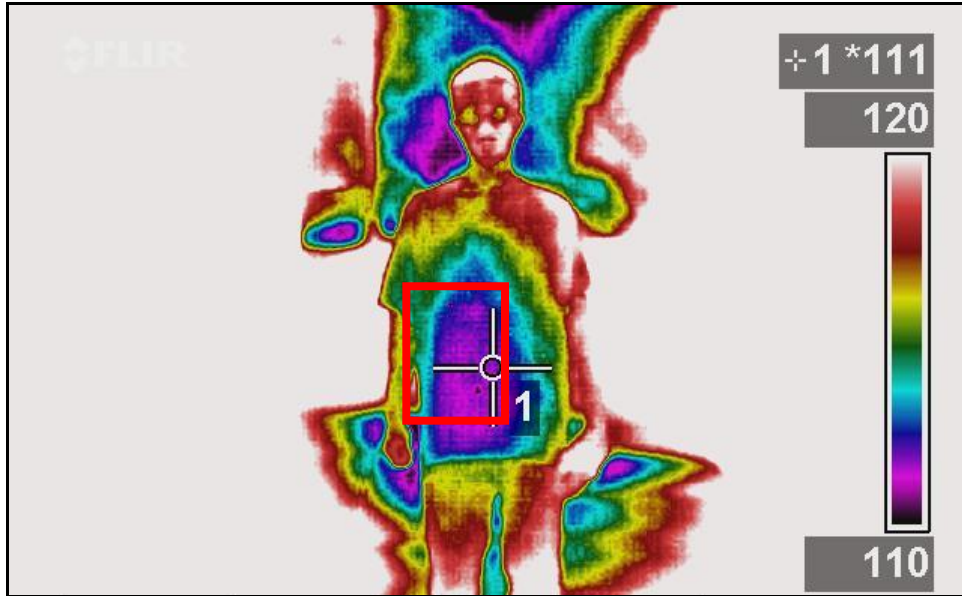


Figure 103—Walking Outside with Metal Bomb at 1.5 Miles
- Manual Temperature Scale Setting

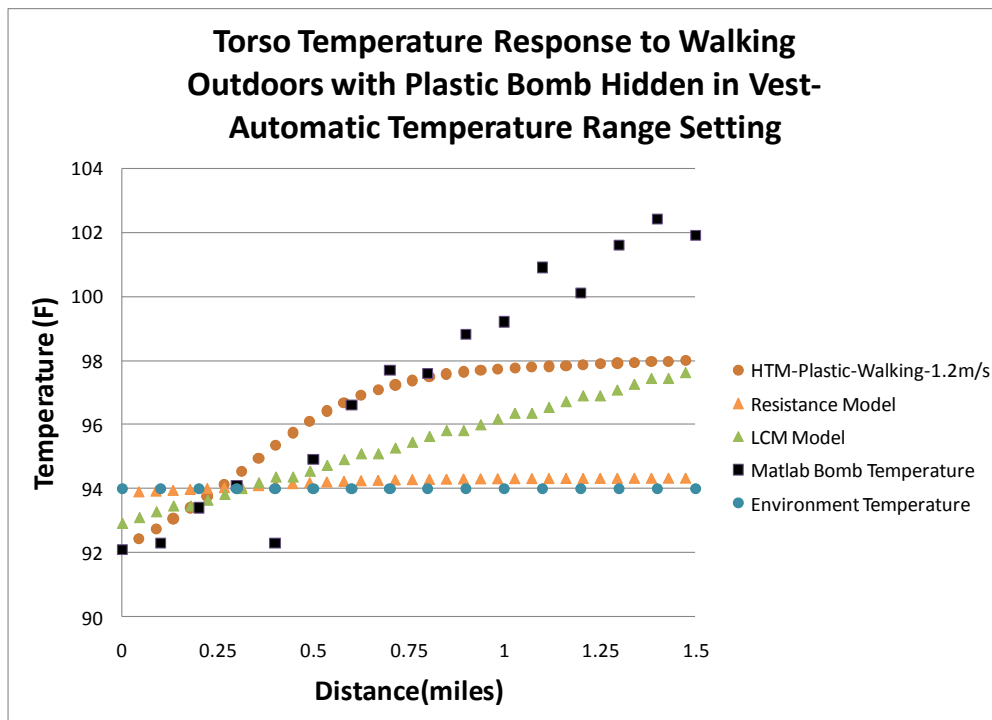


Figure 104—Torso Temperature Comparison with Models of Human Walking Outdoors With Plastic Bomb Hidden in Vest-Automatic Temperature Range Setting

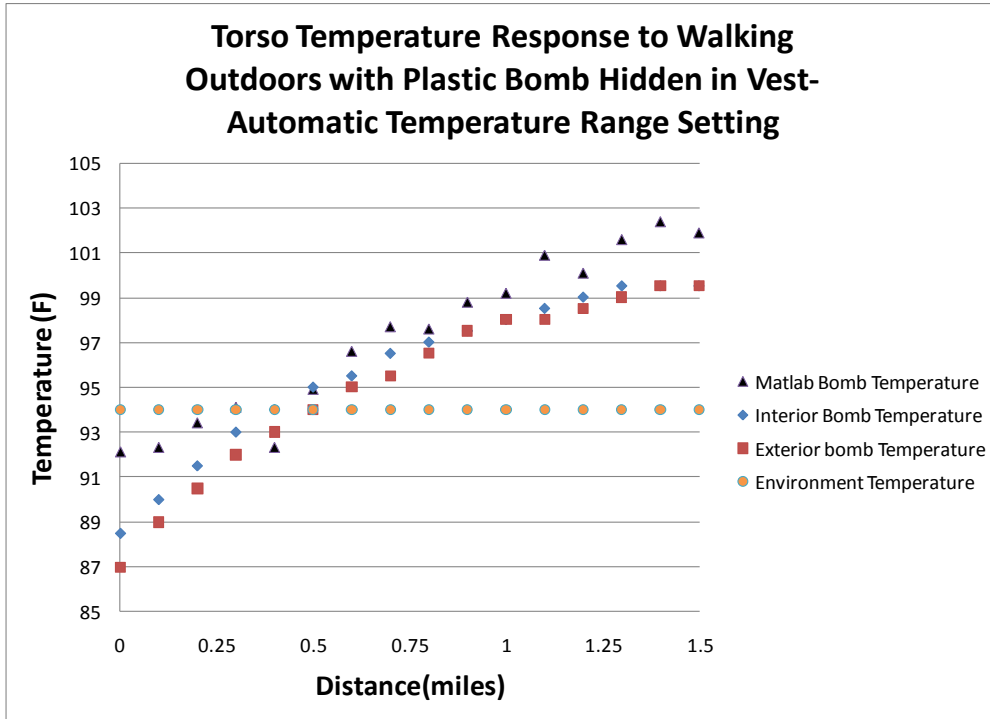


Figure 105—Comparison of Image Temperature Using Automatic Temperature Range with Thermocouple Measurements of Plastic Bomb

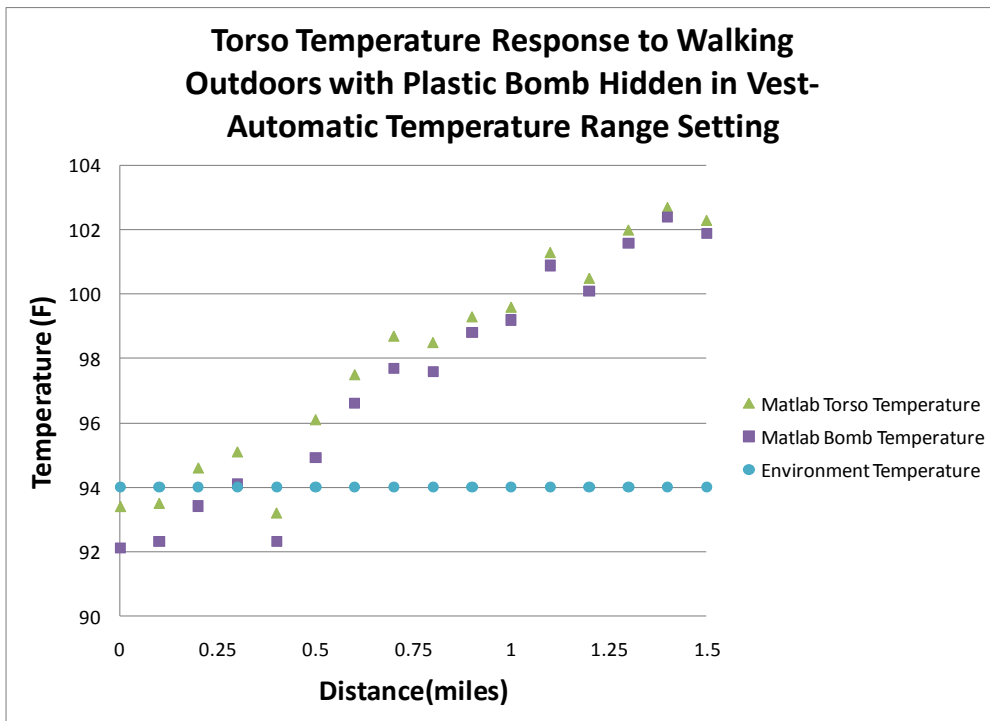


Figure 106—Torso Temperature and Bomb Temperature Comparison Of Human Walking Outside with Metal Bomb

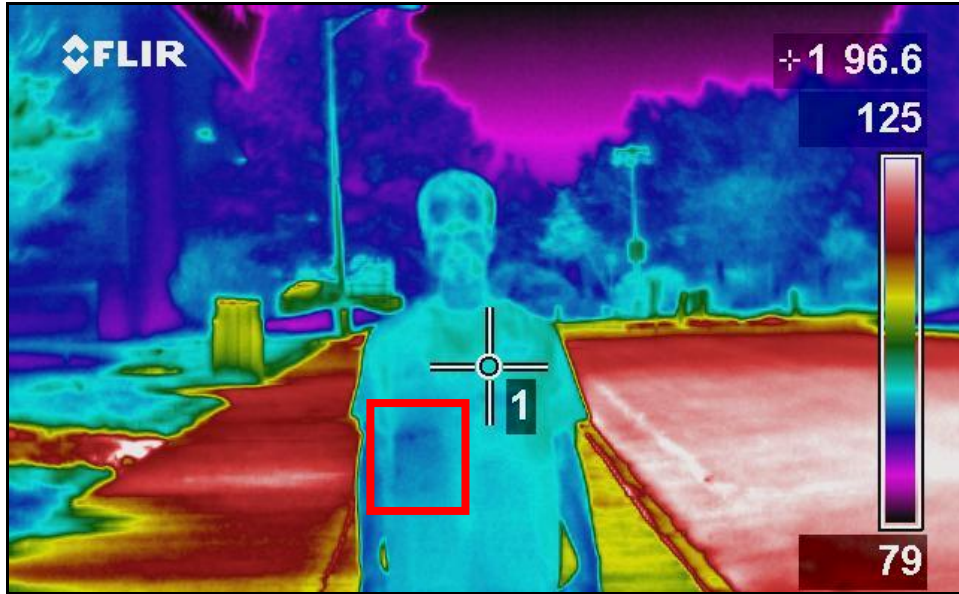


Figure 107—Walking Outside with Plastic Bomb at 0 Miles
- Automatic Temperature Scale Setting

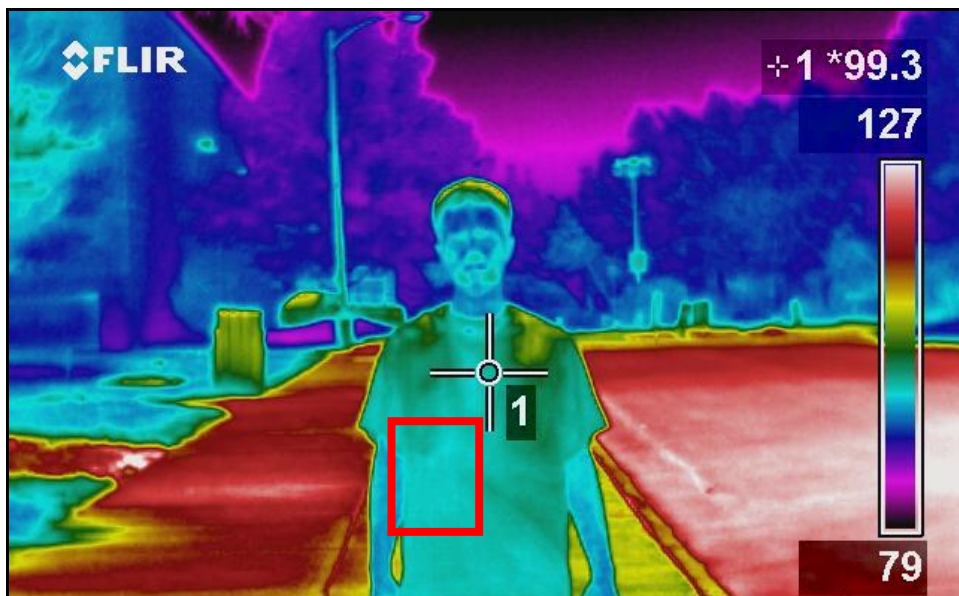


Figure 108—Walking Outside with Plastic Bomb at 0.5 Miles
- Automatic Temperature Scale Setting



Figure 109—Walking Outside with Plastic Bomb at 1 Mile
- Automatic Temperature Scale Setting

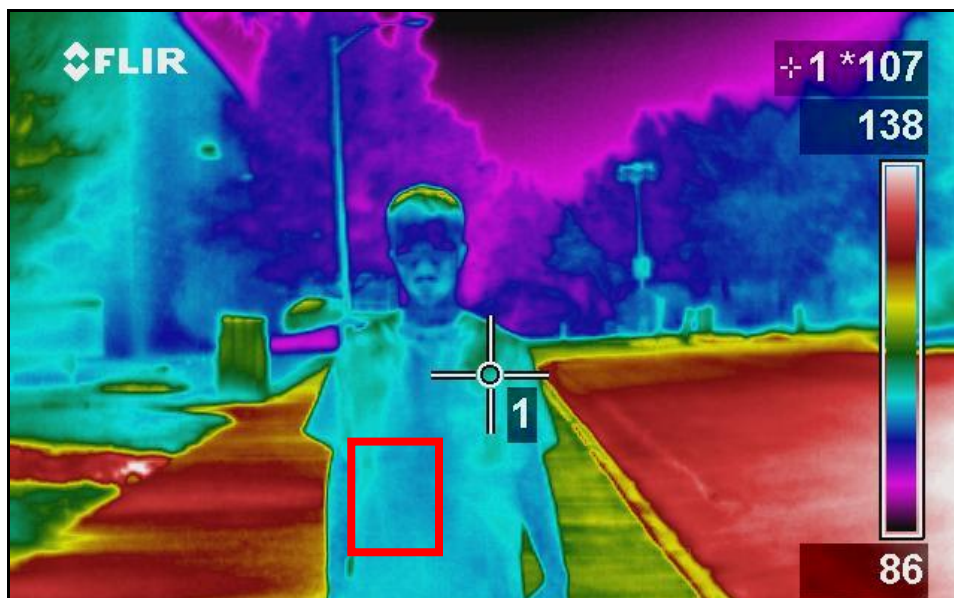


Figure 110—Walking Outside with Plastic Bomb at 1.5 Miles
- Automatic Temperature Scale Setting

COMPARISON OF VEST VS. NO VEST

When the test was run without the bomb package, the average external torso temperature as calculated by the MATLAB® averaging program was 31.44°C (88.6°F) at 0 miles and 37.89°C (100.2°F) after 1.5 miles. During this test the outdoors temperature was 32.22°C (90°F). These results can be seen in Figure 112. As shown in this figure the temperatures acquired from the image tend to follow the HTM model for the first mile.

When the subject was wearing the bomb package in the vest, the average torso temperature was 35.11°C (95.2°F) at 0 miles and 45.5°C (113.9°F) at 1.5 miles. The difference between the average torso temperature and the bomb area fluctuated around 1.11°C (2°F) for the length of the test. The average torso temperature for the human with the bomb vest began the test 3.61°C (6.5°F) higher than human without the bomb vest and ended the test higher by 7.61°C (13.7°F). These results are seen in Figure 114. It is believed that the temperature is higher for the clothing with the bomb package underneath because the thermal resistance of the package slowed the transfer of heat from the solar irradiation from the shirt to the body.

The results from this experiment did not have a chance to reach a steady state during the test due to time restrictions for the amount of time the subject could be submitted to the environment and physical conditions.

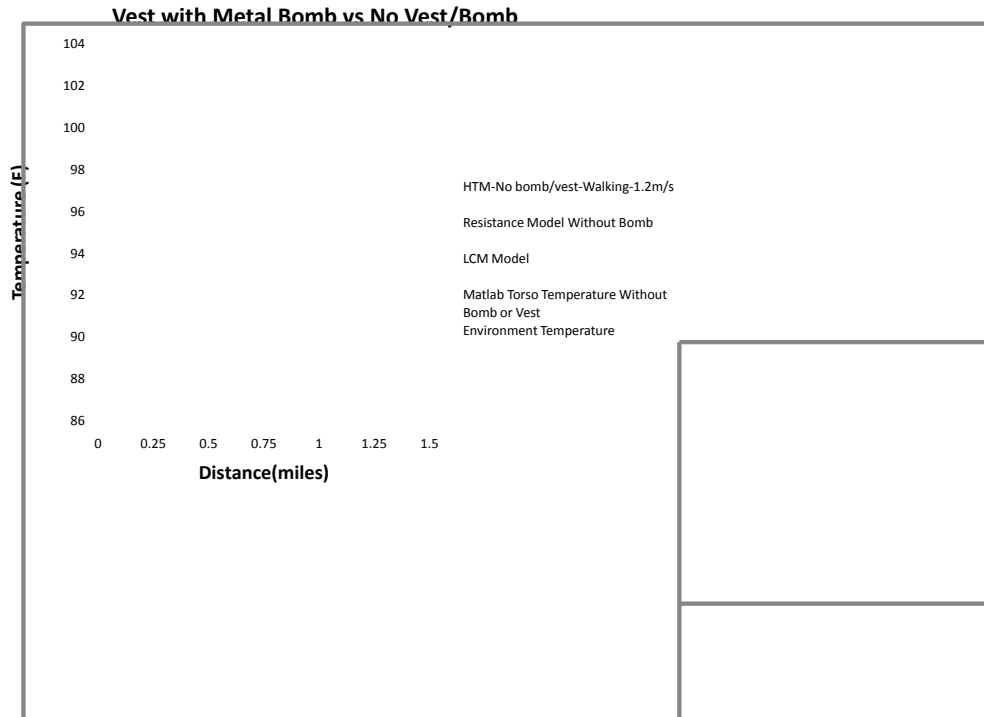


Figure 111—Torso Temperature Comparison with Models of Human without Vest/Bomb

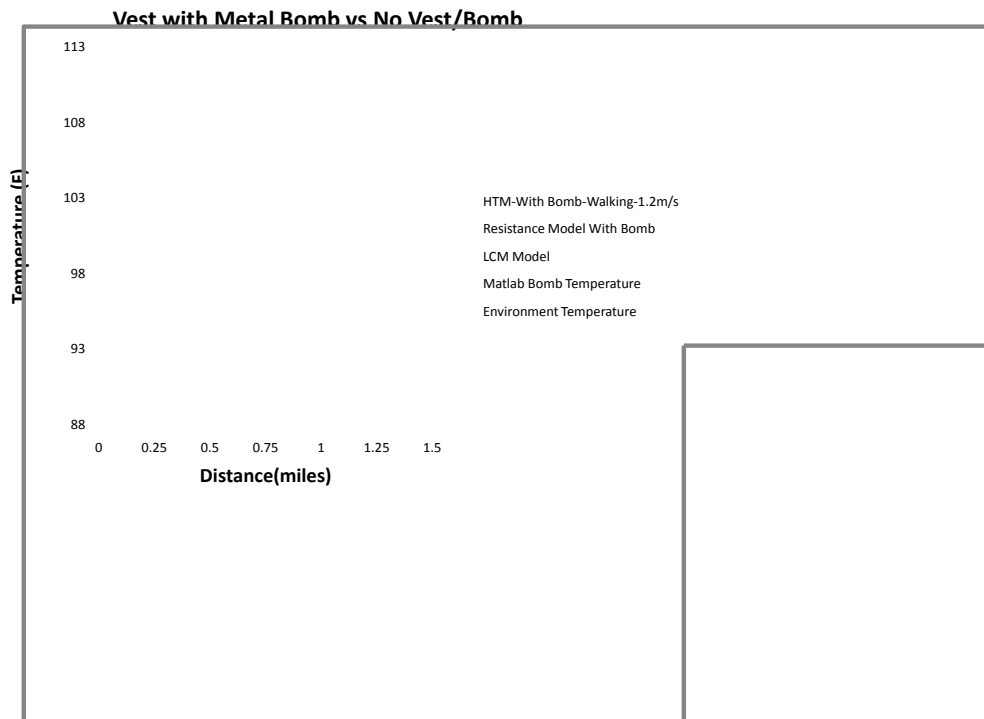


Figure 112—Torso Temperature Comparison with Models of Human with Vest/Bomb

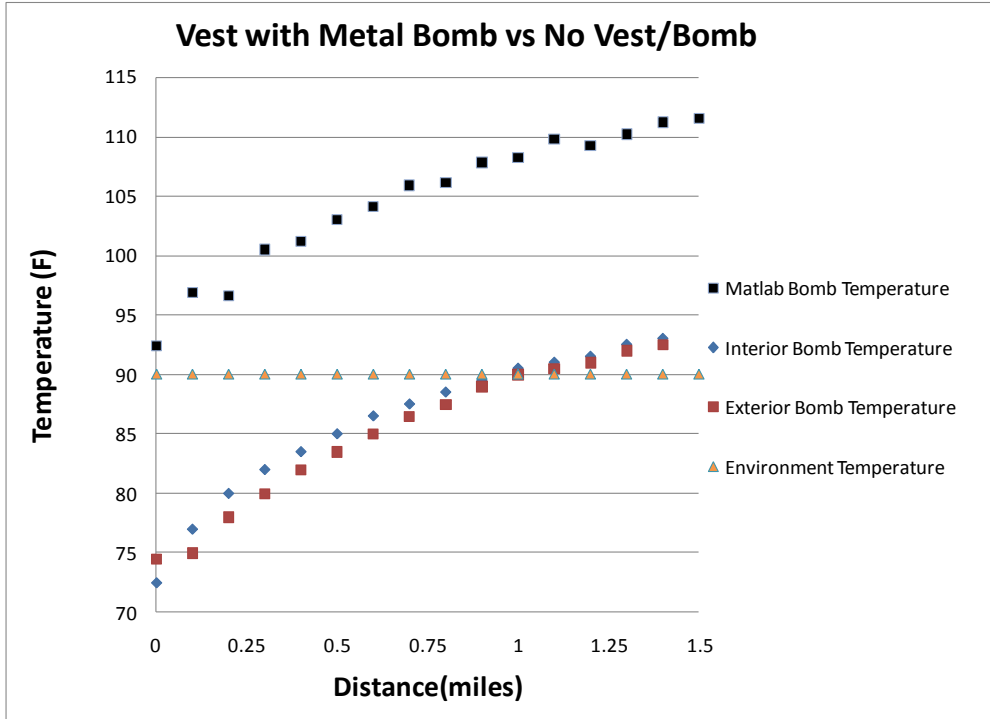


Figure 113—Comparison of Image Temperature with Thermocouple Measurements of Walking with Vest/Bomb versus Without Vest/Bomb

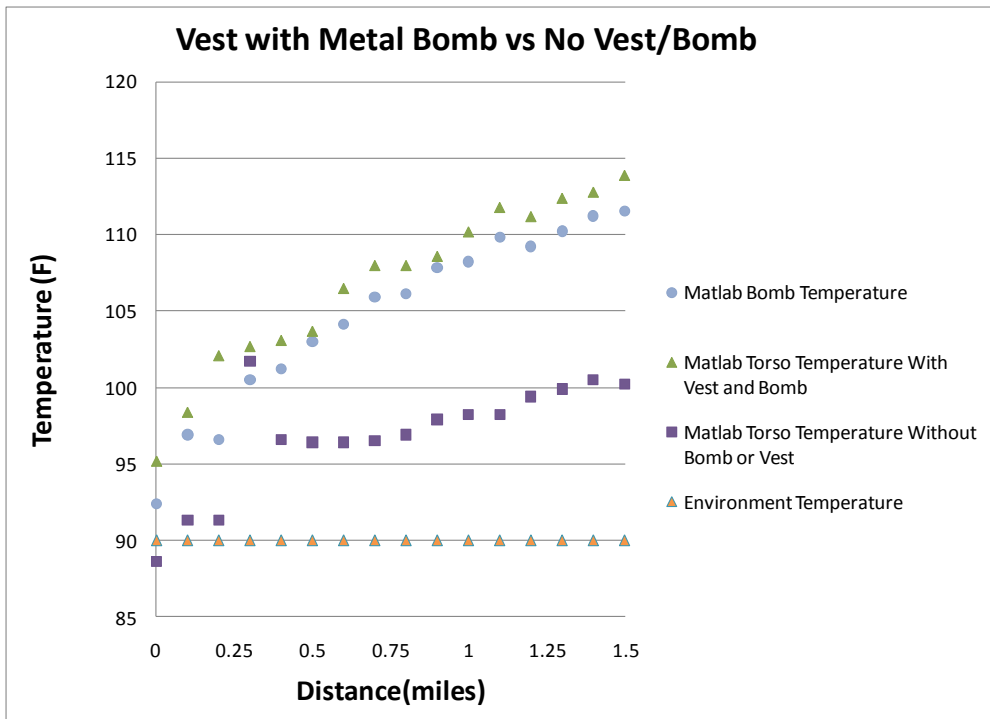
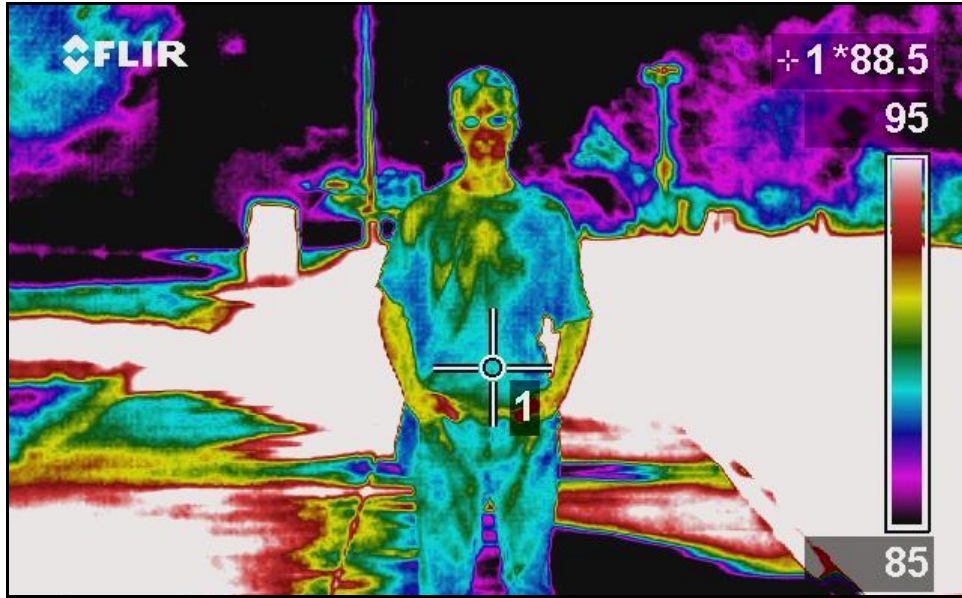
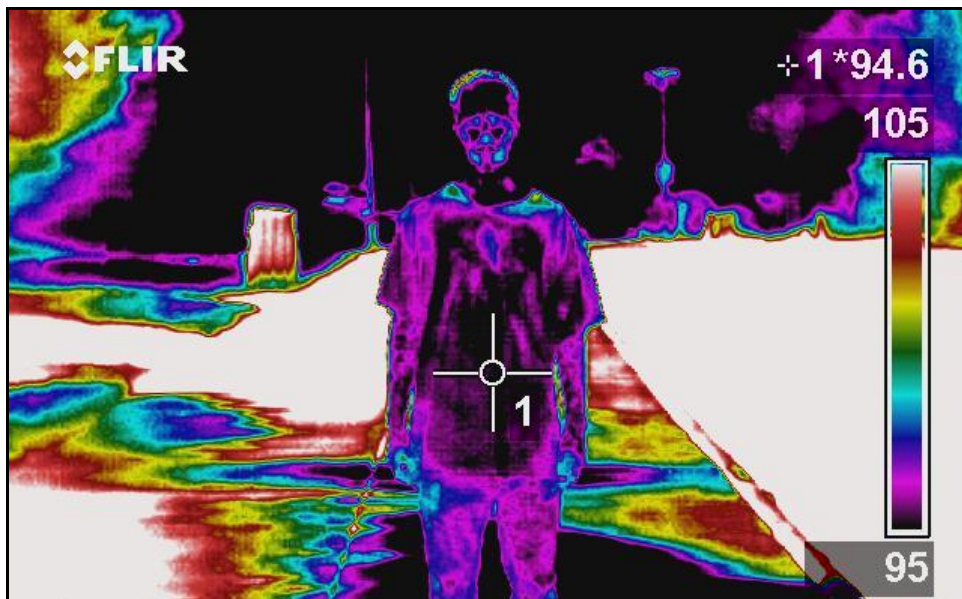


Figure 114—Torso Temperature and Bomb Temperature Comparison of Human With and Without Bomb Vest



*Figure 115—Walking Outside Without Bomb or Vest 0 Miles
- Manual Temperature Range Setting*



*Figure 116—Walking Outside Without Bomb or Vest 0.5 Miles
- Manual Temperature Range Setting*

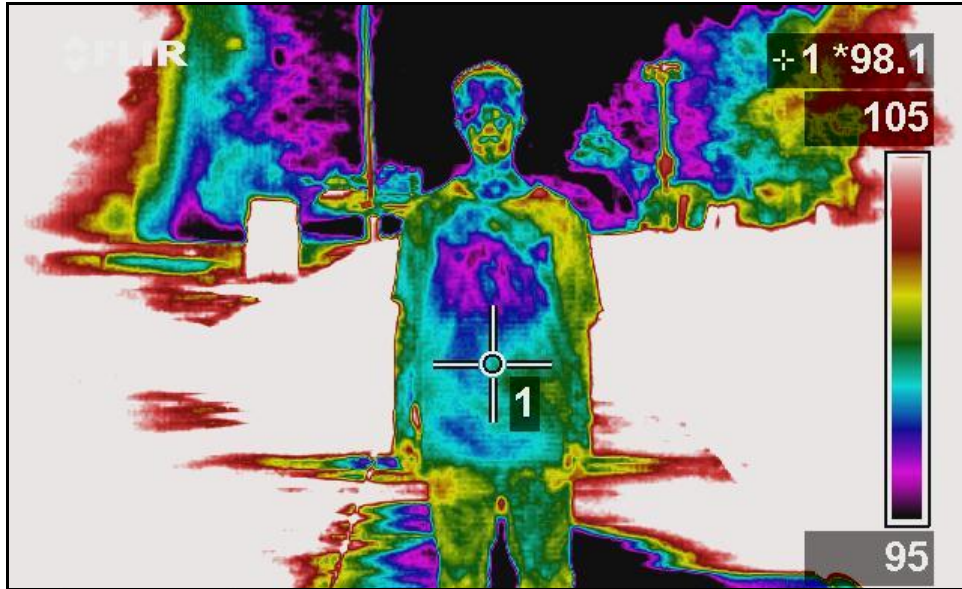


*Figure 117—Walking Outside Without Bomb or Vest 1 Mile
- Manual Temperature Range Setting*

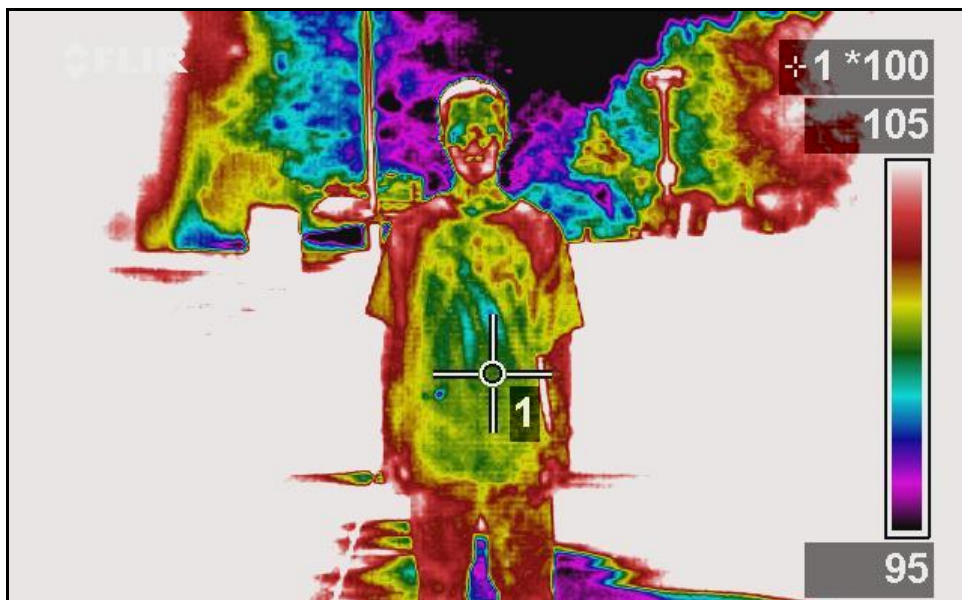


*Figure 118—Walking Outside Without Bomb or Vest 1.5 Miles
- Manual Temperature Range Setting*

EFFECTS OF SOLAR IRRADIATION

When studying the effects of the sun on the infrared images it was found that the direction the subject is facing and whether or not they were shaded had a major impact on the temperature measured and the ability to detect concealed weapons.

The highest temperatures were observed when the sun was behind the camera and the subject was unshaded. This can be seen in Figure 121, Figure 122, Figure 129, and Figure 130. The lowest temperatures were observed when the subject being imaged was in the shade and the sun was behind the camera. This can be seen in Figure 123, Figure 124, Figure 131, and Figure 132. In all of the images where the subject is shaded the clothing temperature is significantly lower than in the images where the subject is exposed to direct sunlight. Having the camera in the shade and the subject in the sun has average external torso temperatures almost 5°C (9°F) higher than having both camera and subject in the shade.

The temperature results have been compiled in Table 13, Table 14, and Table 15. Examples of sun position combinations are given in Figure 119 thru Figure 134. The data shows larger temperature differences when the subject is in the sun. Larger temperature differences were also measured when the sun was positioned behind the camera.

The wide range in temperatures measured due to the differing solar irradiation exposures shows that modeling of the sun's irradiation on the subject is very important when trying to predict clothing temperature.

Table 13—Average Torso Temperatures with Exposure to Sun

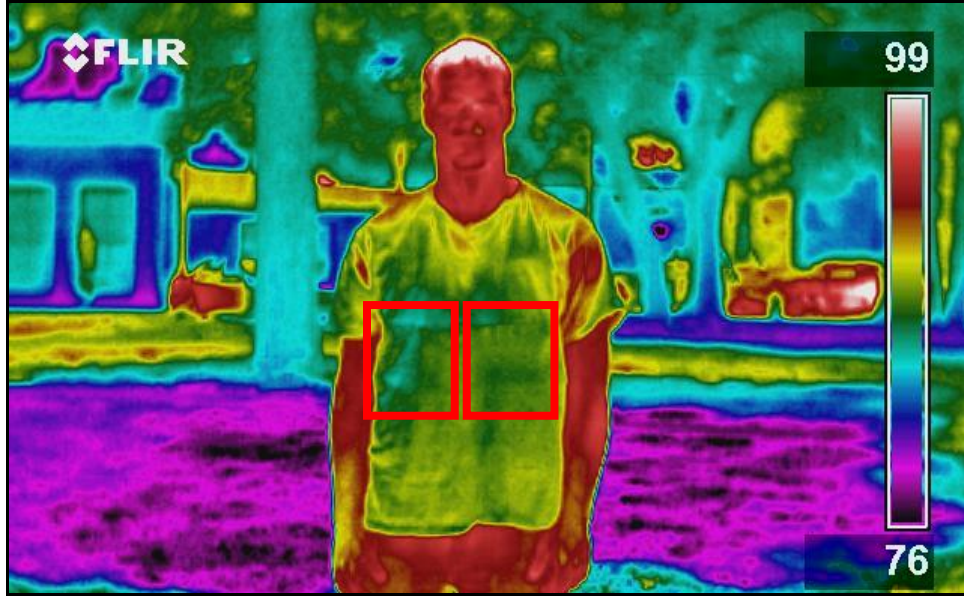
	Sun behind subject w/ Bomb Package	Sun behind camera w/ Bomb Package
both in sun	89.3	94.5
camera-sun subject-shade	86.4	87.3
camera-shade subject-sun	89.9	95.6
both in shade	87.2	86.0

Table 14—Average Bomb Package Temperatures with Exposure to Sun

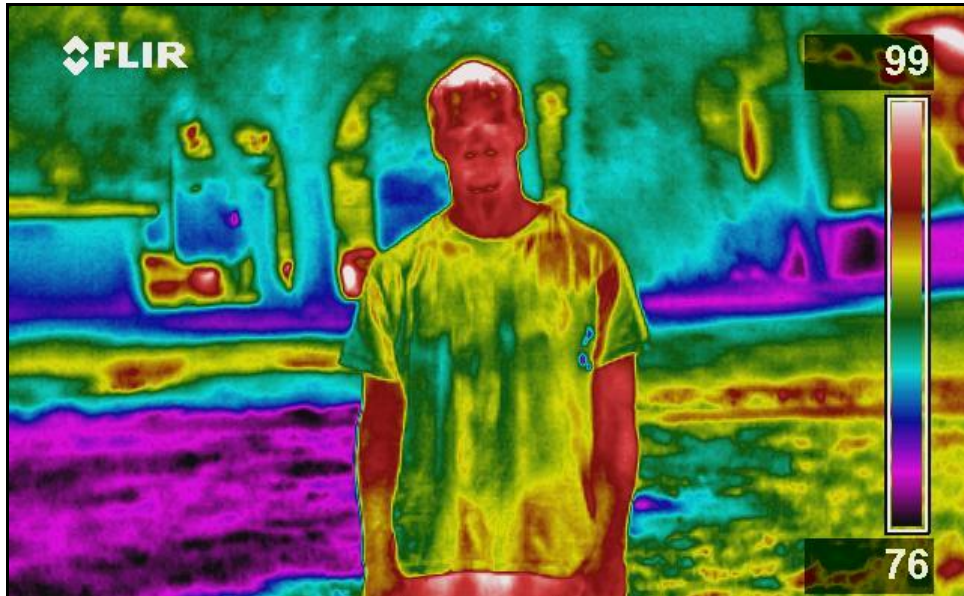
	Sun behind subject w/ Bomb Package	Sun behind camera w/ Bomb Package
both in sun	88.8	93.6
camera-sun subject-shade	86.6	87.5
camera-shade subject-sun	89.6	95.0
both in shade	87.2	86.1

Table 15—Torso and Bomb Package Temperature Difference with Exposure to Sun

	Sun behind subject w/ Bomb Package	Sun behind camera w/ Bomb Package
both in sun	0.5	0.9
camera-sun subject-shade	-0.2	-0.2
camera-shade subject-sun	0.3	0.6
both in shade	0	-0.1



*Figure 119—Sun Behind Subject with Metal Bomb Package-
Both Subject and Camera in Sun*



*Figure 120—Sun Behind Subject with Only T-shirt-
Both Subject and Camera in Sun*

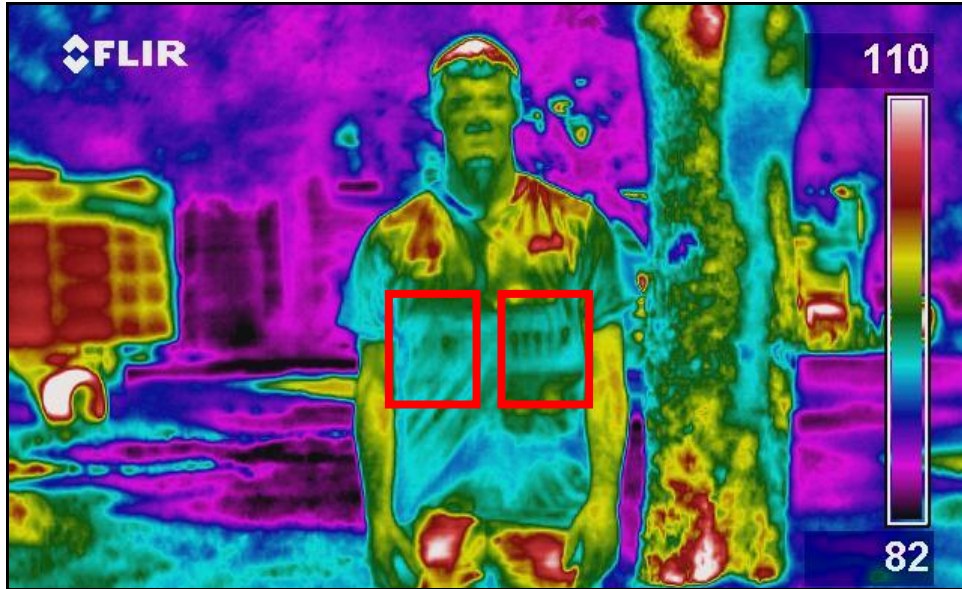


*Figure 121—Sun Behind Camera with Metal Bomb Package-
Both Subject and Camera in Sun*

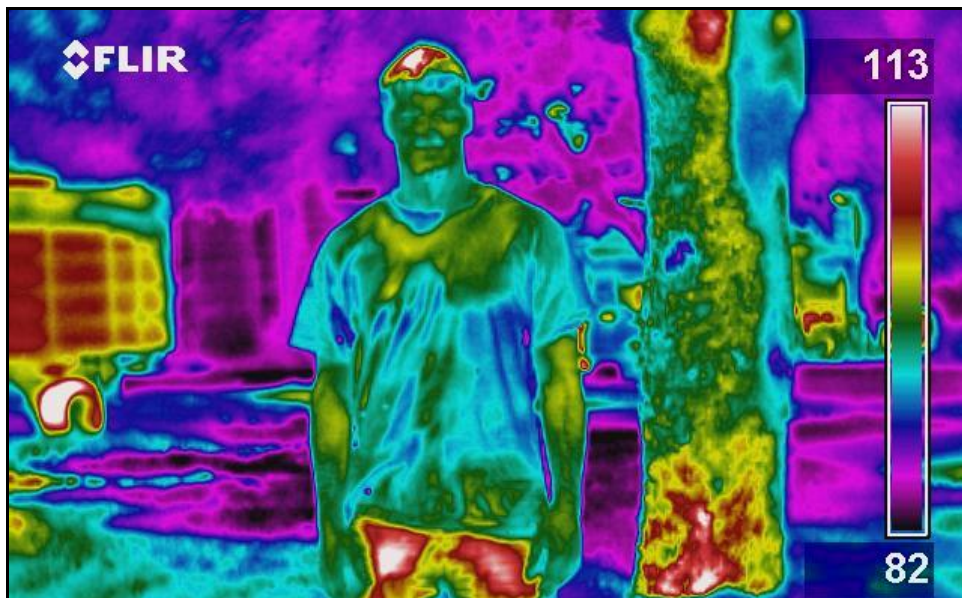


*Figure 122—Sun Behind Camera with Only T-shirt-
Both Subject and Camera in Sun*

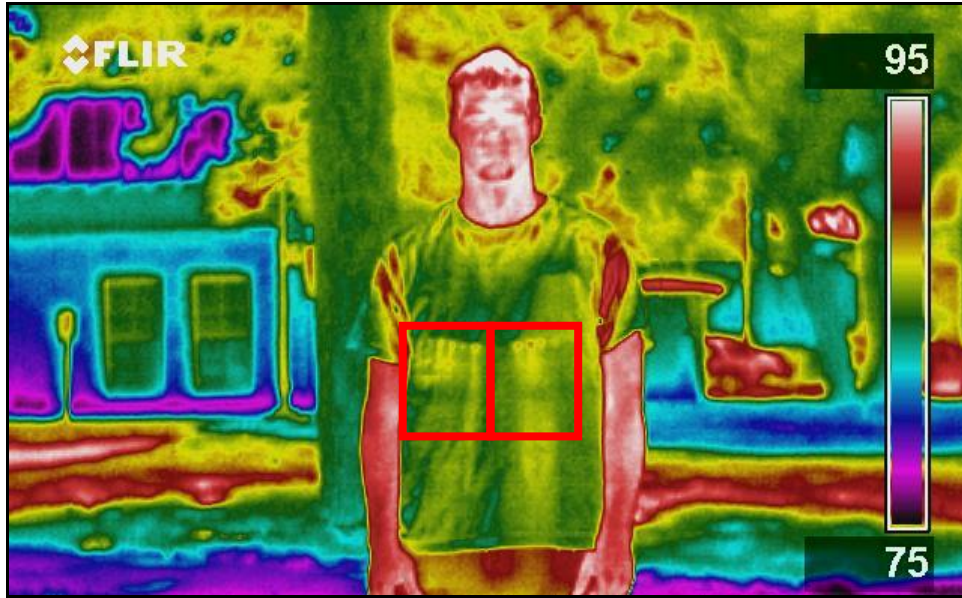


Figure 123—Sun Behind Subject with Metal Bomb Package - Camera in Sun-Subject in Shade

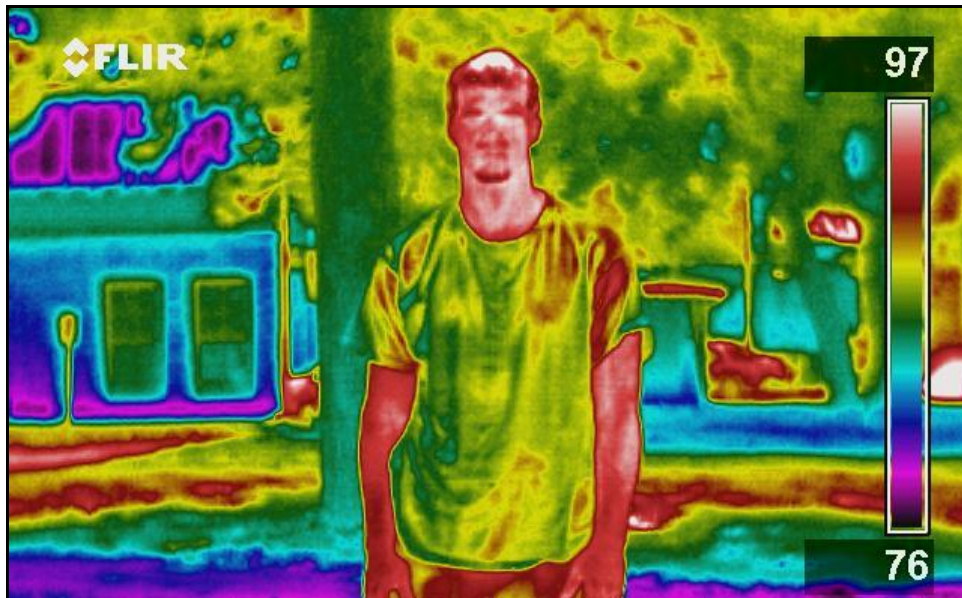
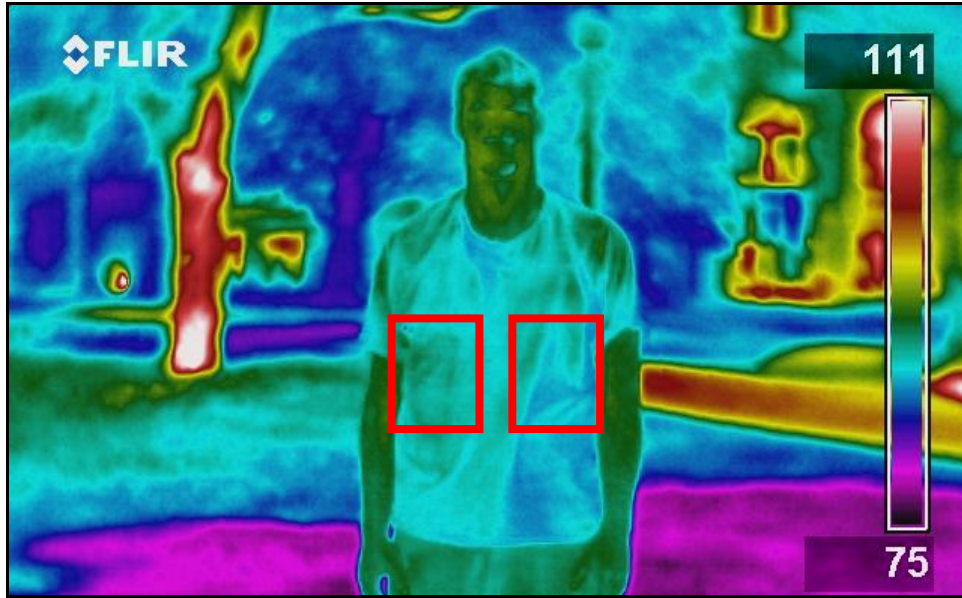
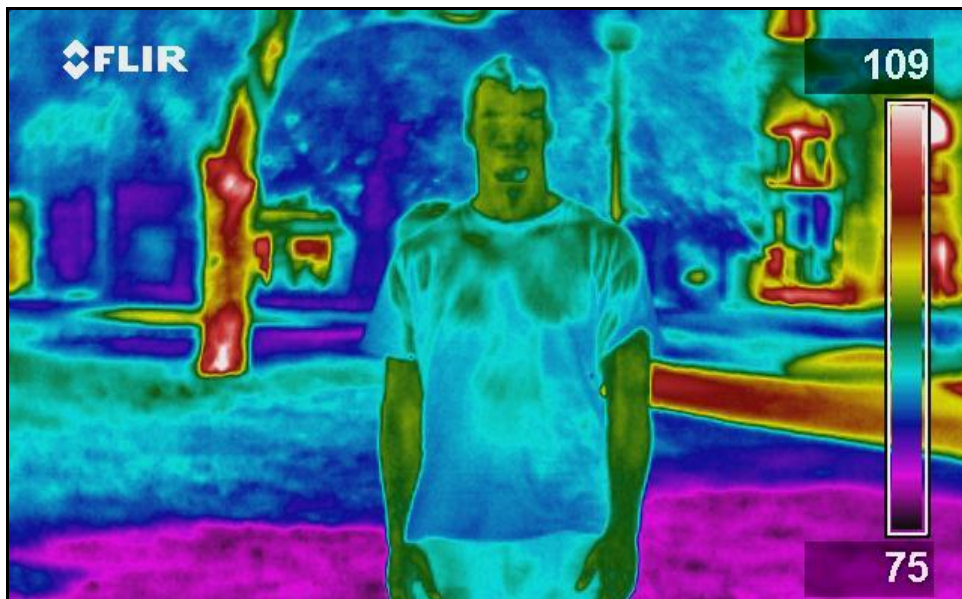


Figure 124—Sun Behind Subject with Only T-shirt- Camera in Sun-Subject in Shade



*Figure 125—Sun Behind Camera with Metal Bomb Package-
Camera in Sun-Subject in Shade*



*Figure 126—Sun Behind Camera with Only T-shirt-
Camera in Sun-Subject in Shade*

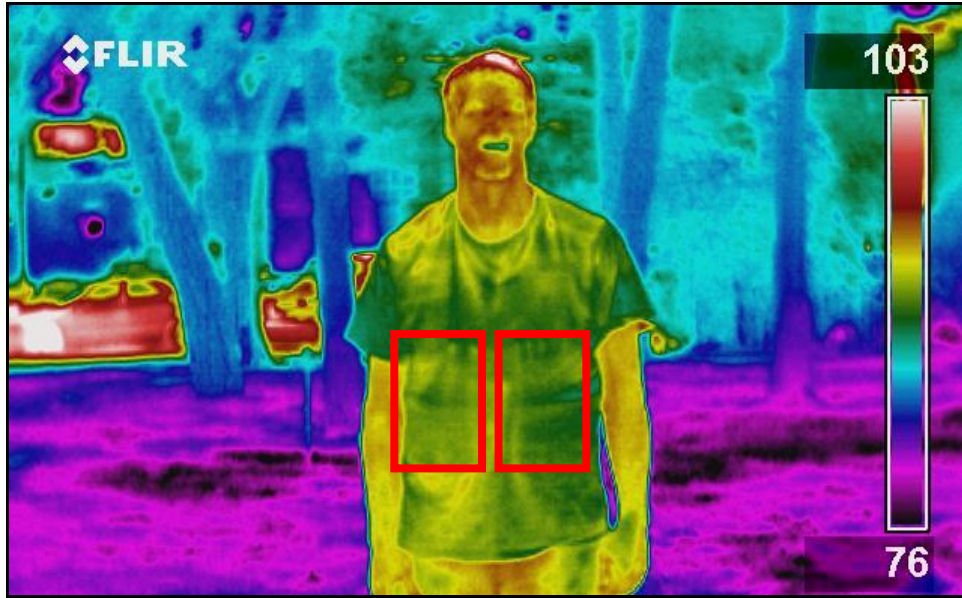


Figure 127—Sun Behind Subject with Metal Bomb Package – Camera in Shade-Subject in Sun

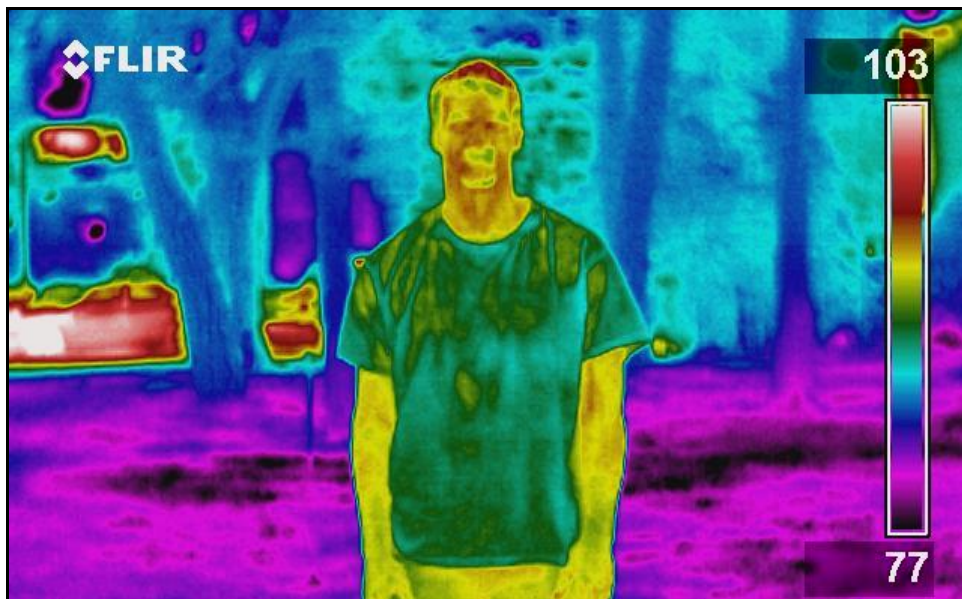
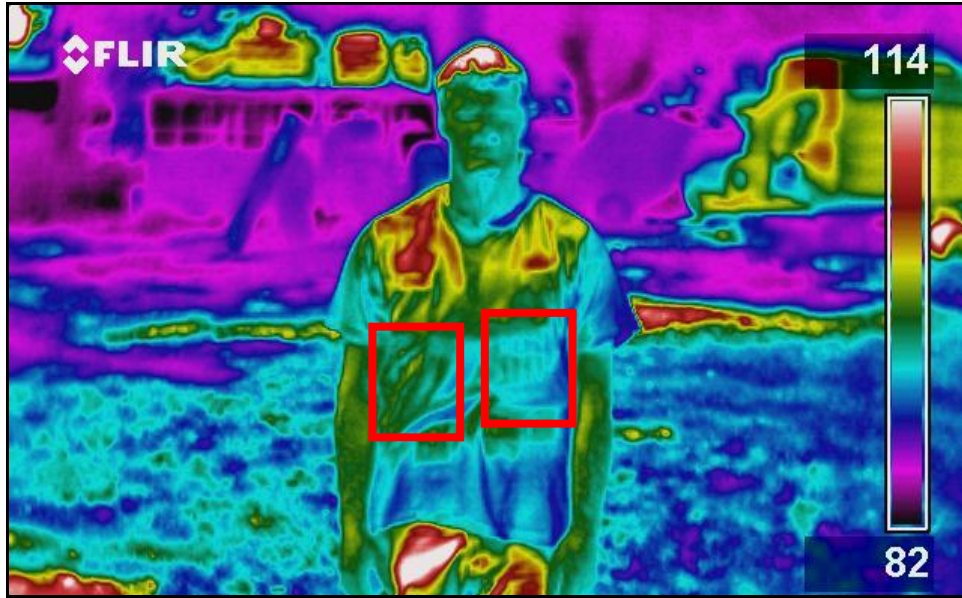


Figure 128—Sun Behind Subject with Only T-shirt- Camera in Shade-Subject in Sun



*Figure 129—Sun Behind Camera with Metal Bomb Package-
Camera in Shade-Subject in Sun*



*Figure 130—Sun Behind Camera with Only T-shirt-
Camera in Shade-Subject in Sun*



Figure 131—Sun Behind Subject with Metal Bomb Package – Both Camera and Subject in the Shade

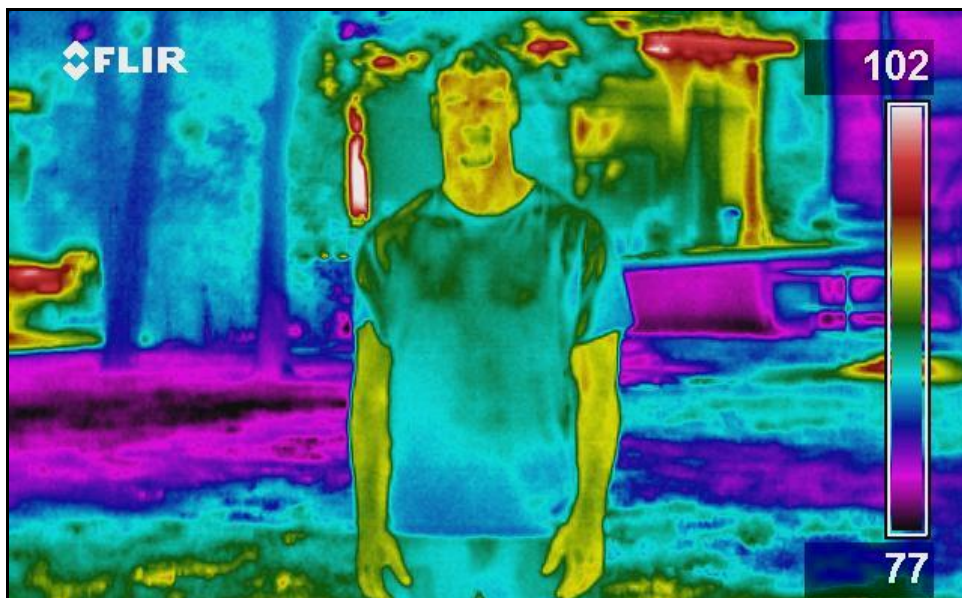
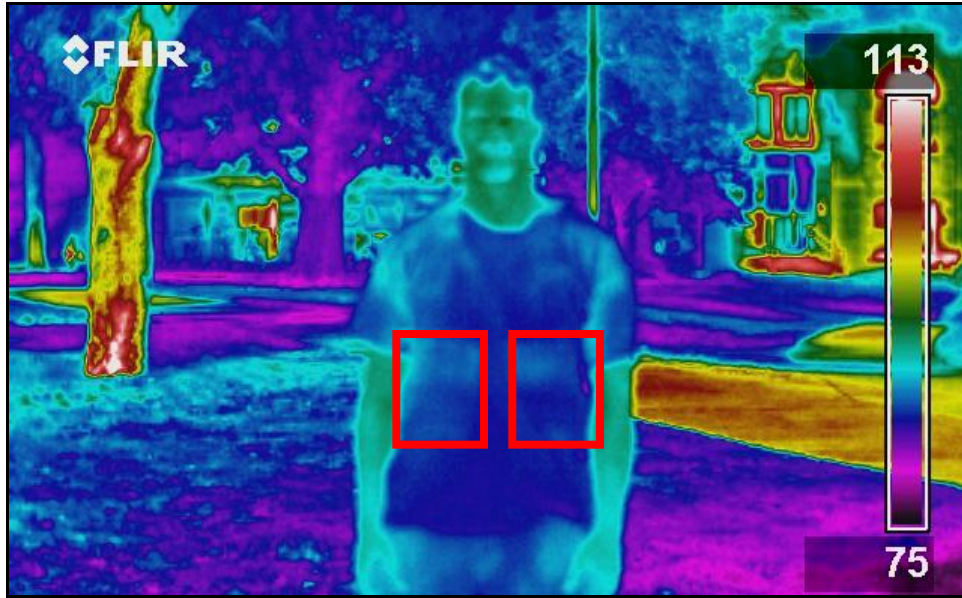
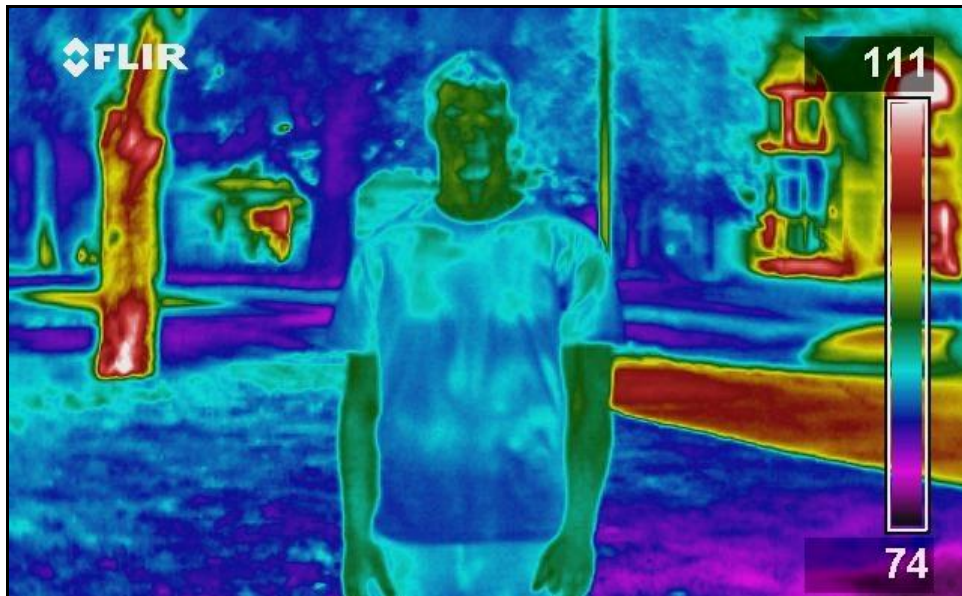


Figure 132—Sun Behind Subject with Only T-shirt- Both Camera and Subject in the Shade



*Figure 133—Sun Behind Camera with Metal Bomb Package-
Both Camera and Subject in the Shade*



*Figure 134—Sun Behind Camera with Only T-shirt-
Both Camera and Subject in the Shade*

CLOTHING CHARACTERISTICS

Testing of clothing with aesthetic details and logos found that these features can affect the appearance in the infrared image. Figure 135 shows a grayscale infrared image that clearly shows a shirt with a rabbit screen-printed on the front. Figure 136 and Figure 137 use the Rainbow HC color palette to demonstrate how this printing can affect the image in other color palettes. There is nothing hidden underneath the clothing in these images. This situation illustrates that even though most of the images used in this paper appear in the Rainbow HC Color Palette; it may not always be the best choice and that using multiple different images may aid in the detection of threats.



Figure 135—Screenprinted T-Shirt with Grayscale Color Palette



Figure 136—Screenprinted T-shirt with High Contrast Rainbow Color Palate Background #1

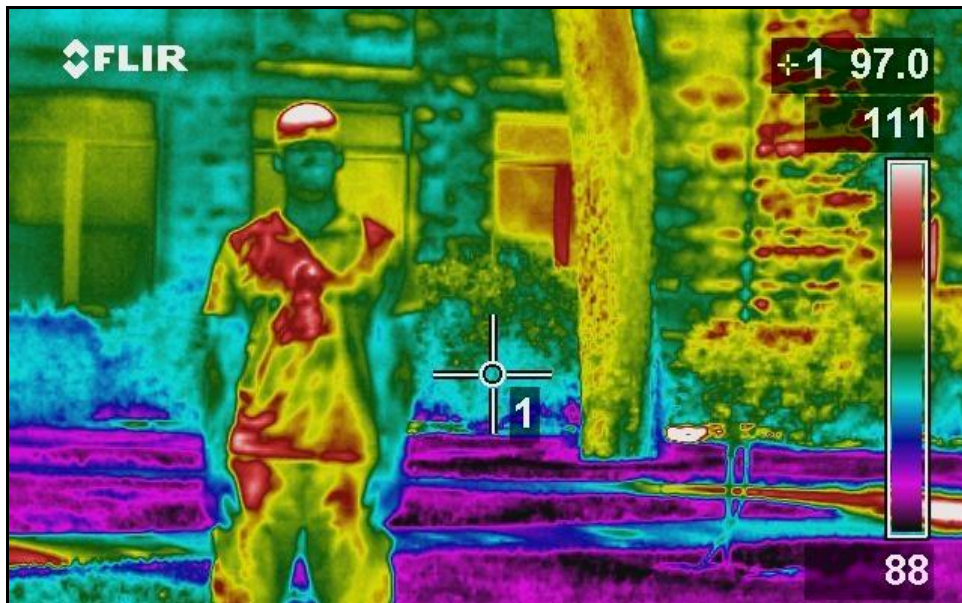


Figure 137—Screenprinted T-shirt with High Contrast Rainbow Color Palate-Background #2

IMAGING AT VARIOUS DISTANCES

When the camera is used outdoors it is capable of picking up the defined image of the bomb package if it is within 6-10 feet of the target. Past that distance, it is very hard to distinguish the bomb package's features from the rest of the torso, but it was possible to see a change in temperature on the shirt due to the vest and bomb at distances up to 25 feet.

1.3 METERS (6 FEET)

At six feet it is possible to make out the top of the bomb package. Pictures were taken with the automatic settings of the camera as well as having the camera set on manual. With these tests there was not a huge difference between the two settings. Images of automatic and manual settings at 6ft are given in Figure 138 and Figure 139. The package was noticeable in the area where the bomb package was directly touching the shirt. The package is also much more noticeable on the side of the shirt away from the direct sunlight.

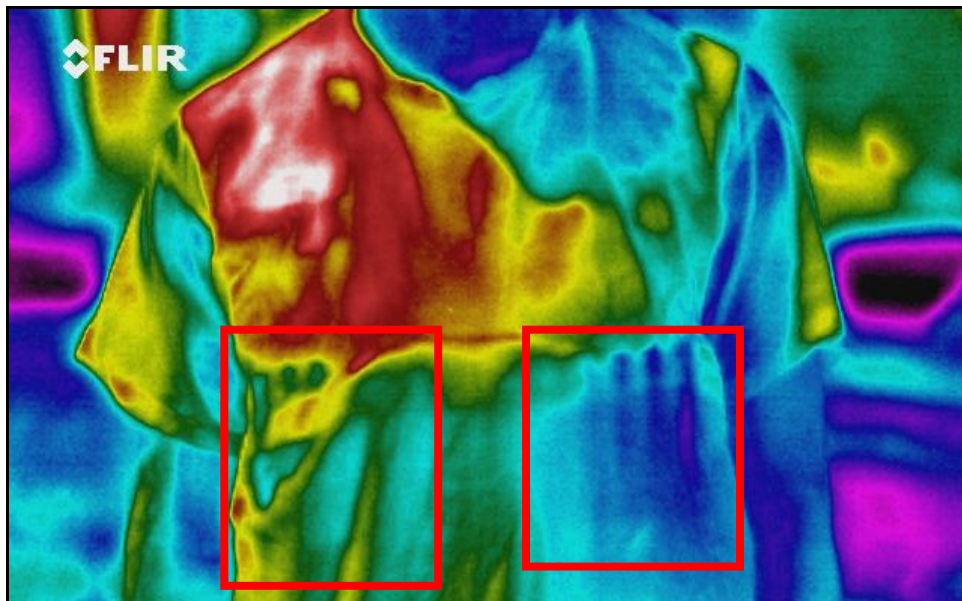


*Figure 138—Metal Bomb Package Shielded by 1 T-shirt at 6ft-
Automatic Temperature Range Setting*

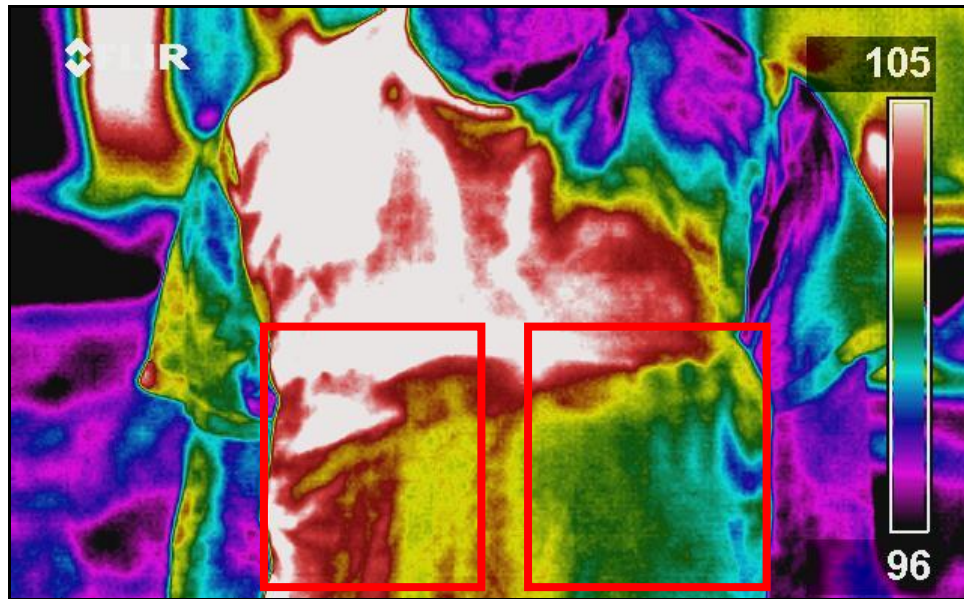


*Figure 139—Metal Bomb Package Shielded by 1 T-shirt at 6ft-
Manual Temperature Range Setting*

3.66 METERS (12 FT)

At 12 feet it is nearly impossible to make out individual parts of the bomb package, but the lower part of the vest and bomb package appear in the image at a slightly lower temp. Like when imaged at 6ft, the parts of the bomb that are noticeable are on the side away from the direct sunlight. The temperature difference across the shirt in places away from the bomb is larger than the temperature differences caused by the bomb.

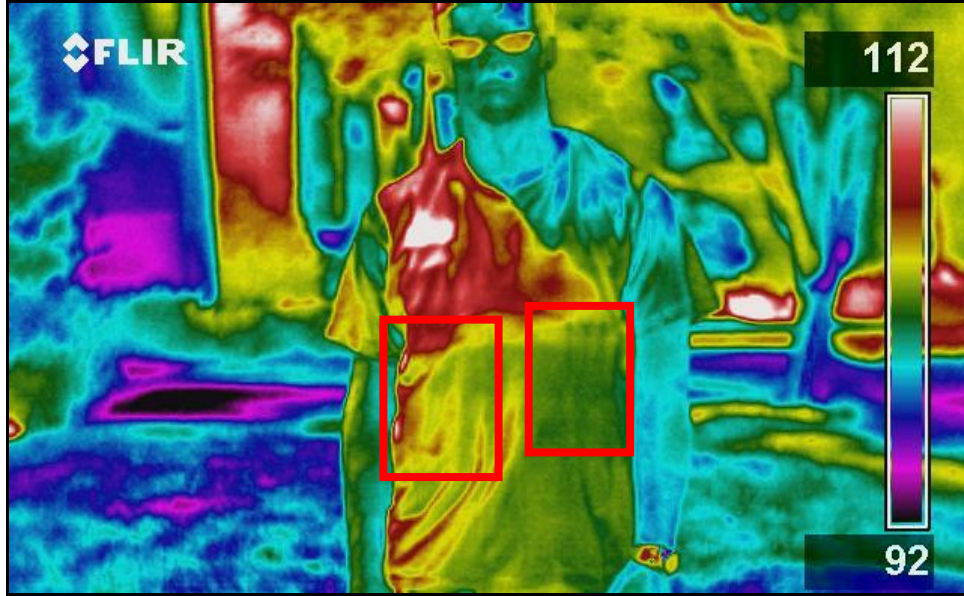


*Figure 140—Metal Bomb Package Shielded by 1 T-shirt at 12ft-
Automatic Temperature Range Setting*

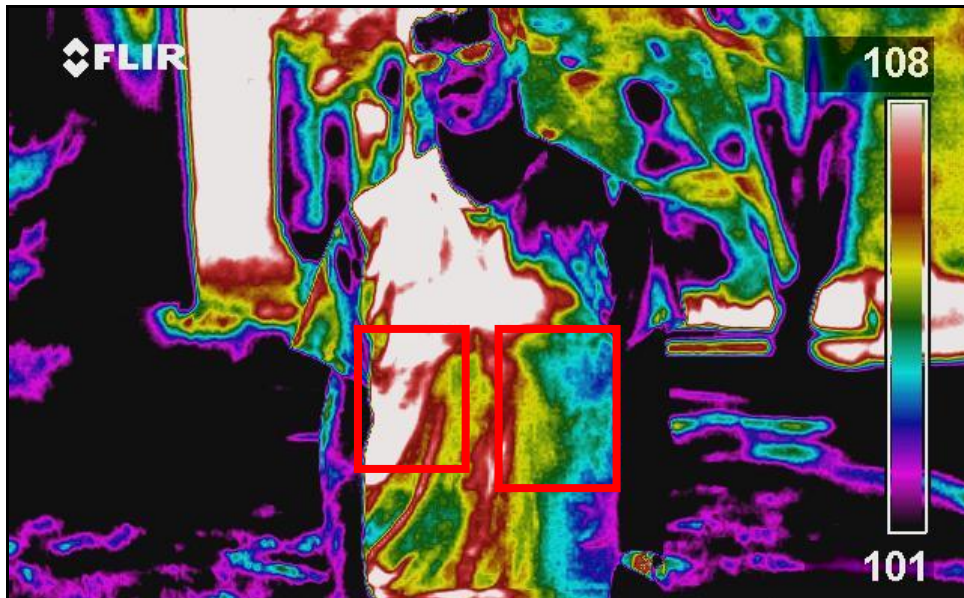


*Figure 141—Metal Bomb Package Shielded by 1 T-shirt at 12ft-
Manual Temperature Range Setting*

7.62 METERS (25 FEET)

The bomb components are very difficult to discern in both the automatically adjusted photos as well as the manual temperature range photos, but a slight temperature variation can be detected. The heat signature on the body images appears similar to that which appears in the images taken at 12 feet but the overall resolution of the bomb package is smaller. It is also harder to tell the specific temperature for a certain part of the body.

Because the images are zoomed out when imaging at a distance, more of the background is included in the image. This produces large temperature gradients in the image when the auto-adjust temperature range setting is used. The only zoom feature the camera has is an electronic zoom. The camera did not have an optical zoom feature. Because an electronic zoom feature “creates” resolution in an image that is not attainable by the camera, it was not used in this research.

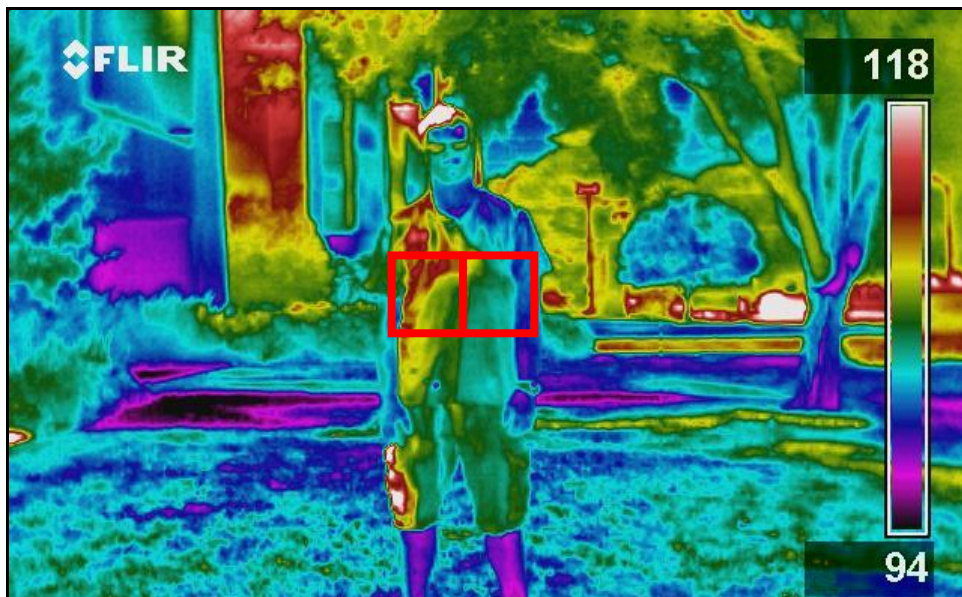


Figure 142—Metal Bomb Package Shielded by 1 T-shirt at 25ft- Automatic Temperature Range Setting

CHAPTER 7- DISCUSSION OF RESULTS

When looking at the results of the testing it can be seen that there are both possibilities for the IR technologies while at the same time there are limiting factors. Limits were found in the testing due to the nature of the technology, but there are also possibilities to improve on the research if it is conducted and analyzed in different ways.

MODEL COMPARISON

It was theorized at the beginning of the research that the IR image of a human borne threat would be substantially affected by the human's activity, clothing worn, and the environment. It was thought that the influence of the activity, clothing and environmental conditions could be accounted for in a model that would help predict how the IR image would look. Although this may be correct, that environmental conditions may have a much larger influence than previously thought. While this is advantageous to know, these environmental conditions are the hardest to model as they are constantly changing and are difficult to predict and control.

In multiple cases the average temperature of the clothing in the area covering the bomb seemed to correlate well with the LCM model. It is theorized that the LCM model performed the best because it was the only model that directly modeled the irradiation from the sun. As shown in Table 13 and Table 14, the sun has large effects on the temperature of the clothing. One problem with the LCM model is that it does not account for the thermal regulation controls of the body such as sweating. In some cases it is seen that the Temperature of the bomb area on the clothing would rise according to the LCM but then level off while the LCM continued to climb. It is theorized that the body began to sweat and in doing so introduce a factor that the LCM

model did not account for.

In observing the resistance model results, it can be predicted that the temperature of the clothing will be much closer to the environmental temperature than to the human body temperature. This supports other results that tend to indicate that the clothing temperature is much more dependent on the environmental temperature. Although this tends to indicate the effects of the environment, it does not account for the irradiation from the sun like the LCM model does.

The HTM model predicts an average temperature of the human skin. This model is not necessarily a good determination of the clothing temperature, but this model seemed to perform well when the human was not wearing a bomb and vest. In this case there was much less thermal resistance between the body and the exterior layer of clothing, so the effects of the human skin temperature had a much greater effect on the average temperature of the clothing.

ENVIRONMENTAL EFFECTS ON IMAGES

One major effect that was observed that would severely limit the possibly of modeling an operational scenario is the irradiation from the sun. As the exterior clothing on the body is irradiated from the sun there are dramatic changes in temperature. Tests were completed in order to specifically study the effects of the sun and the camera's orientation in relation to the sun. On one particular day when the sun was positioned behind the camera there was a 3.89°C to 4.44°C (7°F to 8°F) difference in average temperature of the clothing when comparing the subject between shaded and unshaded conditions. On the same day when the sun is positioned behind the subject being imaged, there is average difference of 1.67°C (3°F) when the subject moves from the shade into the sunlight.

In many cases the person's head may shade part of the clothing on their torso. If this

situation is encountered outside on a clear and sunny day, a difference in temperature of at least ten degrees due to the shadow can appear across the shirt. In this situation it is difficult to tell whether a temperature difference is due to a threat hidden beneath the clothing or if it is due to the effects of the sun. In this situation a human observing an image would only be able to base decisions on shape and position of thermal gradients. As a person moves around, this shadowing effect is continually changing. This makes it very difficult to model and predict temperatures that would appear in the IR image. It can be seen that shadows can cause drastic influences on an image. As a person moves in and out of buildings, under trees, through cloud-cover, and similar situations the temperature of the exterior clothing visible to the IR camera will continuously change. It is nearly impossible to predict the irradiation history of a subject before they are being observed by a camera, therefore making models of the thermal effects of the person becomes very difficult. If in an operational scenario the observation space was controlled there may be certain steps that might be taken to help control these problems. For instance, in a checkpoint scenario there may be sun shades set up to block all direct sunlight. Subjects may also be held in these conditions for a period of time in order to have better control of the conditions that are needed to be modeled.

Other indicators of the dramatic effects of the environmental conditions were observed when studying the effects of multiple layers of clothing. There was very little change in temperature on the exterior layer of the clothing. This would indicate that the temperature on the outside of the clothing is more related to the temperature of the external environment than to the heat from the human body and the thermal resistance due to the increased amount of clothing that it must pass through to change the temperature of the external layers of clothing. In tests where the temperature of the bomb package was taken, the temperature on the outside of the

bomb was always higher than the temperature on the inside of the bomb package. This would indicate that the temperature change of the bomb package is being influenced by the environmental factors more quickly than the human physiological factors. These were cases in which the bomb package started at a temperature lower than both the human body and the external environment. It could be seen that the outside of the package was increasing in temperature faster than the inside face that was closer to the body.

MANUAL VS. AUTOMATIC TEMPERATURE RANGE

The environment surrounding the subject of interest will dramatically affect the visible temperature difference. If the camera is set in automatic mode and there are large temperature variations in the image background, the camera will automatically adjust in order to scale the image color scale to these temperatures. If, for example, an image includes objects of 10°C (50°F) and 65.56°C (150°F) the camera will adjust the image color scale to cover this 55.56°C (100°F) range. In this case a 5.56°C (10°F) difference in temperature would appear much closer in temperature (image color) than a 5.56°C (10°F) difference in an image that's scale ranges from 10°C to 23.89°C (50°F to 75°F). It is much easier to detect a small temperature difference when the image color scale represents a smaller temperature range. This advantage led to experimentation with the camera's manual temperature scaling. It was found that when the camera was put into a manual mode in which the temperature range is specified that the operator is able to see the threat more distinctly.

When the manual temperature setting is used the temperature scale used in the image is specified by the operator. This allows the operator to concentrate the image on a particular temperature range even if the image scene contains temperature outside of this range. When the temperature is outside the desired temperature range it is assigned the color on the far end of the

manual temperature scale. When a small manual temperature range is used to display a scene with a large temperature range much of the scene is washed out in black or whites. The only colors that appear in the image are those that fall within the manually selected temperature range.

For example, if a scene has temperatures of 10°C to 55.56°C (50°F to 100°F) and the temperature scale was set from 18.33°C to 23.89°C (65°F to 75°F), all temperatures above 23.89°C (75°F) would appear white and all temperatures below 18.33°C (65°F) would appear black.

Although the manual temperature range images accentuate small temperature changes that humans can see, the average temperature data acquired from the images with our average temperature algorithm does not correspond with modeling data due to the treatment of temperatures outside the desired range. The algorithm that was used to calculate average temperature in this study does not work on manually scaled images due to the way associates temperature with color. For example, if the temperature scale is set from 18.33°C to 23.89°C (65°F to 75°F), all the temperatures under 18.33°C (65°F) appear black. The algorithm will treat that part of the image as if it is at 18.33°C (65°F) even though it may be 10°C (50°F). This skews the average generated by the algorithm away from the true average. This can be seen in tests where manual temperature range images were acquired as well as auto-adjusted images under the same conditions. In the outdoor case when the subject was walking the manual temperature range images were 12.22°C (22°F) above the auto-adjusted temperature at a distance of 0.9 miles. This is shown in Figure 90 and Figure 97.

While manually setting the temperature range helps the operator visualize the threat, one problem with using this feature in an operational scenario is the requirement that the operator must have prior knowledge of what the temperature range should be in order to image the threat

at all. If the temperature of the threat is within the temperature scale bounds then the image accentuates the threat, but if the temperature of the area around the threat is just outside the temperature scale the threat will now show up at all. So in order to use this manual mode, the operator must be able to predict the temperatures of threat area in the image correctly. Otherwise the operator will miss the threat completely.

SYSTEM OPERATION

The basic steps used in this research to identify concealed objects are shown in Figure 143. While these functions were performed manually in this research, they all have the potential to be automated in a computerized detection system.

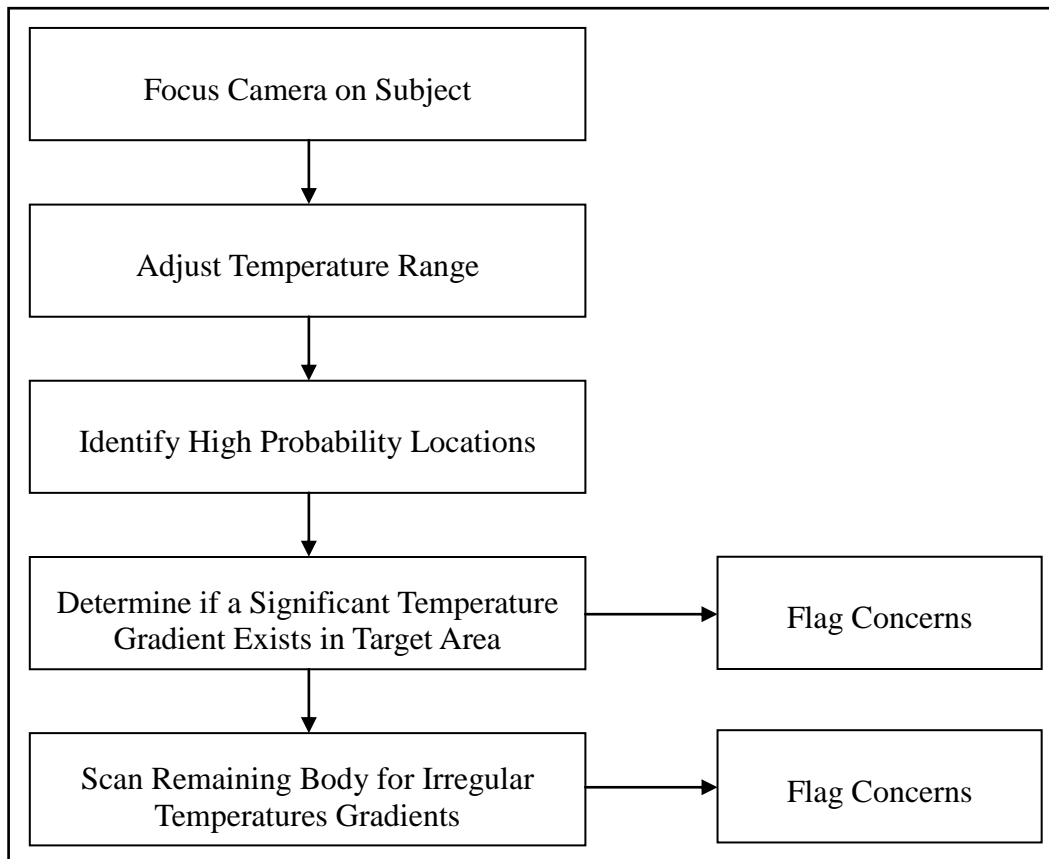


Figure 143—Guide to Find Bomb with Infrared Camera

Possible results from a detection system such as this are: correctly identifying a threat, correctly detecting no threat, misidentify a non-threat as a threat, and misidentify a threat as a non-threat. The first and second situations are the desired outcomes of a detection system. The third possible result, misidentifying a non-threat as a threat, is usually a necessary condition but undesirable. The fourth result, misidentifying a threat as a non-threat is unacceptable in the use of a detection system.

While detection is one problem, reaction to a threat is a completely different one. In (Kress, Moshe, 2005) it was numerically shown that casualty rates for suicide bombings are dependent on the crowd density as well as the blast location size. It was found that crowd blocking can have a significant effect on the number of casualties, and that by dispersing a crowded area due to an alarm will tend to increase the number of casualties. While most suicide bombs are detonated in areas with large crowds, this study showed that the effectiveness of the explosion does not necessarily increase with the size of the crowd. When the crowd density is at or beyond a certain threshold, the number of casualties decreases due to the blocking of shrapnel by those in the crowd closest to the explosion.

How to respond to a threat once detected was beyond the scope of this research. This is a problem that may not be able to be solved by technology, as a solution may rely solely on human relation capabilities.

CHAPTER 8- CONCLUSIONS

Previous studies using infrared detectors for concealed weapon detection have tried to observe the image of the weapon. The research presented here determines the feasibility of modeling the heat signature produced by a suicide bomber using thermal models and comparing it to the images of the human subjects. This may lead to creating a detection system using these models as a comparator and signal for detection.

The first phase of experiments generally focused on the general capabilities of the camera and its application in an indoor situation. General conclusions from this phase of testing have been compiled in Table 16. The camera performed within the specification for the accuracy of the camera. The best performing camera settings for this research were fine tuned. It was confirmed that in a warm environment objects of lower emissivity can be seen at greater distances. It was also confirmed that larger objects can be seen at greater distances. Lastly, it was found that as more layers of clothing are worn, the temperatures on the exterior layers of clothing approach the ambient environmental temperature.

The second phase used an actual human in the indoor setting. These tests were a continuation of the phase one tests, but they had the added human element. General conclusions from this phase of testing have been compiled in

Table 17. In this phase of testing it was found that the material of the bomb can have a significant effect on the temperature measured by the camera. It was also found that convective cooling due to movements of the human body is an important modeling aspect that must be accurately modeled. Testing in this phase also confirmed the findings in Phase 1 that exterior layers of clothing approach environmental temperatures.

The third phase was completed in an uncontrolled outdoor environment with a human subject. This phase demonstrated the feasibility of using this technology for use in the field where the operator has no control of the environment. General conclusions from this phase of testing have been compiled in Table 18. Phase 3 results confirmed the findings in the first two phases. As the tests in this phase were conducted outside, it was found the clothing temperatures were very dependent on the irradiation levels. It was also found the certain clothing characteristics such as screen printing or embroidery may appear in infrared images and possibly distort the image of concealed objects. It was also discovered that the range that the camera was capable of clearly detecting the concealed object was 6-10 feet when in an outdoor situation, but it was still able to detect temperature changes on the body at distances up to 25 feet.

Table 16—General Conclusions from Phase 1 Testing

Phase	Testing Variable	Plots	Figures	Testing Conclusions
Phase 1	Effects of Size on Range	Figure 7	-	Larger objects are visible from longer distances.
	Effects of Emissivity on Range	Figure 8	-	When the background of an image is comprised of warm temperatures, materials of lower emissivity are visible at longer distances than materials of high emissivity.
	Shielding	Figure 10	Figure 11 - Figure 14	The temperature of the outer layers of clothing tends to approach the ambient environmental temperature.

Table 17—General Conclusions from Phase 2 Testing

Phase	Testing Variable	Plots/ Tables	Figures	Testing Conclusions
Phase 2	Material Testing	Table 10	Figure 33 - Figure 34	Materials with higher thermal conductivities will transfer heat to and from the human body at a quicker rate resulting in changing temperature of the outer layers of clothing. A difficulty arises in trying to model this due to the uncertainty of the bomb material.
	Transient Changes While Walking	Figure 51 - Figure 54 - Figure 57 - Figure 59	Figure 55 - Figure 56 - Figure 60 - Figure 61	Convective cooling due to movements of the human body is an important modeling aspect that must be accurately modeled. Demonstrated that background and foreground objects may enlarge the temperature scale, making visibility of the object difficult for humans.
	Shielding	Table 12	Figure 82 - Figure 89	As the number of clothing layers increases, the temperature measured by the camera of the clothing approaches the ambient environmental temperature. Modeling difficulties arise due to the uncertainty of the actual amount of clothing worn.

Table 18—General Conclusions from Phase 3 Testing

Phase	Testing Variable	Plots/ Tables	Figures	Testing Conclusions
Phase 3	Transient Changes While Walking	Figure 90 - Figure 92 Figure 97 - Figure 99 Figure 104 - Figure 106	Figure 93 - Figure 96 Figure 100 - Figure 103 Figure 107 - Figure 110	Over time the clothing temperature approaches the ambient environmental temperature. Convective cooling from human movement must be accounted for in thermal models. Temperature difference must be >7% of temperature scale for human to be relatively certain a hidden object exists.
	Vest vs. No Vest	Figure 111 - Figure 114	Figure 115 - Figure 118	When environmental temperatures are above the skin temperature the bomb vest and package resist the transfer of heat to the body leaving the exterior clothing at higher temperatures.
	Solar Irradiation	Table 13 - Table 15	Figure 119 - Figure 134	Temperature measurements in outdoor situations are very dependent on irradiation from the sun. Temperatures can vary under consistent irradiation levels due to orientation of the subject and the camera.
	Clothing Characteristics	-	Figure 135 - Figure 137	Characteristics such as screen printing may cause changes in the thermal signature that can mask other small temperature changes.
	Distances	-	Figure 138 - Figure 142	The camera was capable of picking up defined bomb package images at distances of 6-10 feet. The camera can detect changes in temperature on the body at distances up to 25 feet.

PROPOSED SOLUTIONS

DISTANCES

While it was possible to see a change in temperature on the shirt due to the vest and bomb at distances up to 25 feet, the equipment used in this research was not able to distinguish the temperature difference at longer distances. One possible way to increase this detection distance may be to experiment with other lenses available for the camera, such as a telephoto lens for longer distance viewing and a close-up lens for shorter distances. Experimenting with these lenses may lead to increased detection distances with this current infrared technology set-up.

FUSION

It is unreasonable to expect a single detector to be able to detect everything. One strategy in overcoming the disadvantages of certain types of sensors in concealed weapon detection systems is to pair them with other sensors that have different strengths. This act of fusing sensor information allows the information from one type of sensor to be supported by another type of sensor, and many times the second sensor will provide information that was not available from the first sensor. As mentioned previously, many times temperature differences appearing in the infrared images can be caused by various sources and the infrared detector is incapable of determining the difference between the sources. In this case other sensors would need to supplement the use of the infrared detector. If additional detectors must be used, interoperability of systems becomes very important as the use of one detector must not interfere with the use of another. The ideal sensor array is not only able to detect a threat, but also identify what it is and where it is located. This task is usually carried out by an array of sensors.

Work is being done in order to pair IR sensors with visual images. This combination not

only provides the thermal signature provided by the IR sensor, but it incorporates it into a full color image that is easy for the human eye to comprehend. This allows easier identification of individuals in a surveillance situation.

CONTROLLING CHECKPOINTS

In situations such as checkpoints it may be possible to create an area of controlled conditions that each human being observed must be subjected to before being imaged. The subjects may be held in a controlled temperature environment for a certain period of time. The checkpoint may also have shades set up to shield the subjects from direct sunlight. Controlling these conditions would allow for better modeling conditions. Controlling the conditions in this way is obviously not possible in all situations, but the infrared camera operator may position the camera in such a way that the natural surroundings provide certain controlling conditions. For example, the operator may choose to image people walking down a street that is fully shaded by buildings so as to limit the exposure to the intense irradiation from the sun.

CONFIDENCE INTERVALS

One important issue that needs consideration is the ability of the human eye to distinguish temperature, or color, differences in an IR image and relate that temperature difference to a possible threat. When there is a large temperature gradient the human eye has no problem distinguishing the threat location on a person's body, but this becomes harder to do as the temperature gradient decreases. In a computer operated system, a warning would be announced if a temperature difference greater than the threshold criteria were measured. If the IR system has a human operator monitoring the images then the human would also have a set of criteria that must be met in order to distinguish threats from non threats. Ideally these criteria would be the

same between operators, but most likely a subjective judgment would be made. It is assumed that with training the judgments between operators would be very similar.

If this technology were to be used, the criteria for a threat warning must be based on both the human and computer operations in the system. Most concealed weapon detection systems will first process the sensor information and quantify the possibility of a threat in a certain area. These systems will then usually feed this information to a human operator. The human will be provided with locations where potential threats may be, as well as a measure of the system's confidence (Chen, 2005). The human will then most likely make a decision based on the system's output. Basic operation of this type of system is diagrammed in Figure 144.

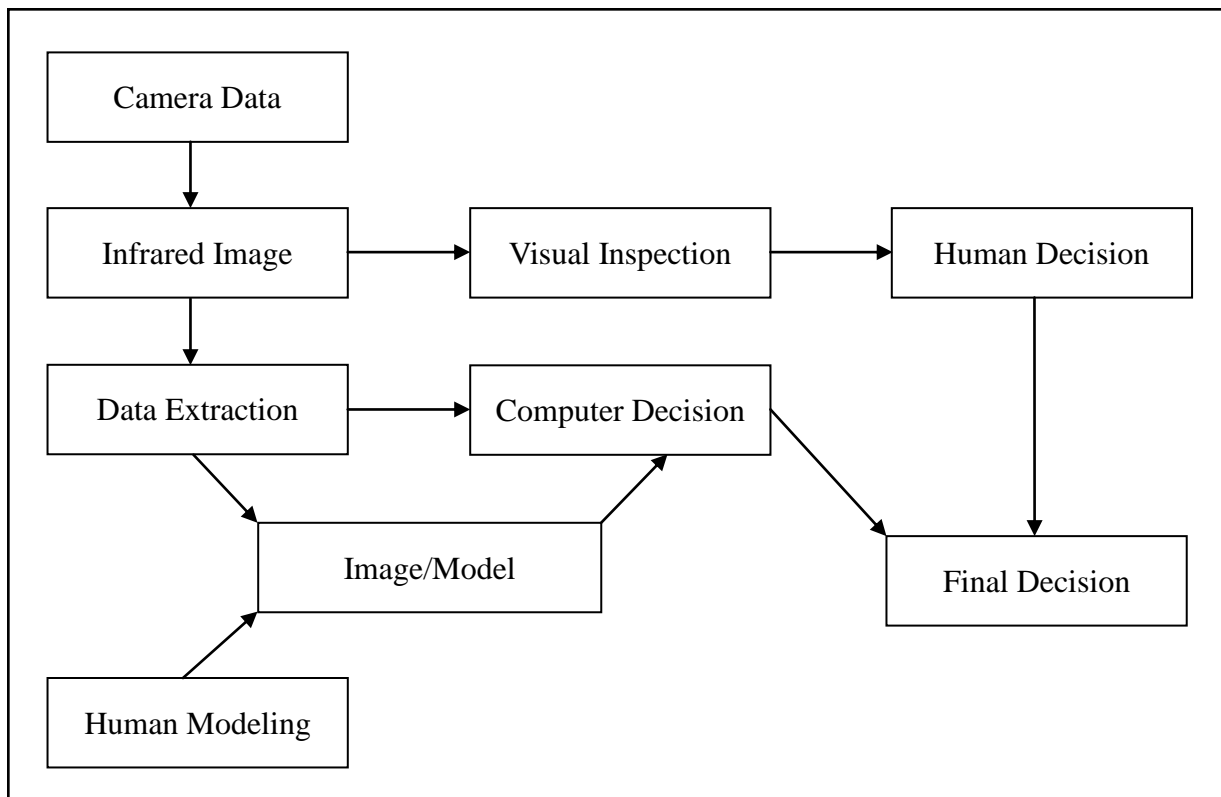


Figure 144—Possible Infrared Camera System Operation

Depending on the situation, this system may involve further scrutiny with other sensors or physical searches. Whereas the sensors give a response based on statistical measures, the human will tend to concentrate on faces and suspected threat area. Previous research has found that these differing approaches can give different results (Xue, 2002).

The images gathered in this testing were analyzed in order to determine a threshold for threat determination. In the tests that included a simulated bomb package, both the average temperature of the bomb area and the entire torso were calculated so they could be compared.

It was determined that over a scale of 45°F the average temperature of the area had to be at least 3°F different than the rest of the average torso temperature in order to be reasonably certain a foreign object was concealed underneath the person's clothing. This appears to indicate that, at a minimum, the temperature change should be at least 7% to 10% of the color scale. This threshold was determined by an operator with experience looking at IR images as well as having prior knowledge of where a threat may be.

This confidence interval used for determining the possibility of a threat has an important impact on the viability of using this technology in an operational scenario. This interval will determine the reliability of the system and how many false alarms are produced.

Concealed weapon detection systems are similar to biometric systems in terms of how they produce false alarms. In a biometric recognition system, a False Match occurs when someone who should not be able to pass the identification process is able to get past the system. A False Non-match occurs when a person that should be correctly identified by the system is denied access. The False Match Rate (FMR) and the False Non-match Rate (FNMR) are inversely correlated (Jain, 2004). In a concealed weapon detection system the same problem arises. When a lower threshold for threat determination is used, the chance that a non-threat will

be misclassified as a threat is greater. While this requires an increase of system resources, it is much better than having a threat get through the system.

A system that has a high threat detection capability can still have a high false alarm rate in which non-threats are classified as threats (Sherrah). Many times in a biometric system a higher FNMR is accepted because it is important not to miss a single threat even at the expense of increased resource use (Jain, 2004). The best system will not only be accurate in detecting threats, but will minimize the false alarm rate. If the false alarm rate is high enough, the detection system would most likely be unusable in practice due to the increase in needed resources for processing all the false alarms (Sherrah).

The range determined in this study, 7 to 10% of the temperature scale, which allows for human visual recognition of the bomb package, is a range that the operator would be relatively certain that an object was being concealed. This range may be lowered to 3 to 6% of the temperature range in order to increase the FNMR, but a much higher false alarm rate would have to be tolerated.

FINAL CONCLUSIONS

Though there are many shortcomings to infrared detectors, researchers continue to search for ways to use the technology's strengths for concealed weapon detection. While previous studies tested the use of infrared detectors to observe the image of the weapon, this research made steps toward using a thermal model to predict the appearance of the images produced by a suicide bomber. Temperature comparisons between the images acquired of the suspected bomber and the predicted temperatures from the thermal models at the same conditions would be used in a comparison system for concealed weapon detection. If a temperature difference meets certain criteria, the person being observed may be pulled aside to be searched further.

The models used in this research will not suffice for use in a detection system, but they point to the potential use in a computerized comparison system. A more precise model to predict the clothing temperature would need to be developed. The model would have to include the human thermal control mechanisms as well as precise environmental conditions such as solar irradiance, ambient temperature, and wind speed among others. The model would have to be adaptive on-the-fly to these environmental conditions in order to get accurate temperature predictions for the clothing temperatures. If a model such as this was used in a detection scenario, current reading of environmental factors would have to be continually supplied in order for the model to predict correct temperatures.

Others factors that would need to be assumed for the model would include the amount of clothing worn by the person, the material type, the person's activity level prior to being imaged. Some factors may be reasonably controlled in certain situations. For example, at a checkpoint it may be possible to hold the person in a controlled environment for a certain period of time. This capability would be limited, as it would be impossible to provide such control in other situations.

The ability to detect materials under various layers of clothing is probably the most important factor in implementing this technology in a real world application of stand-off bomb detection. Most likely this type of model comparison will not work well if the person goes to great lengths to conceal the weapon by covering their body with many layers of clothing. The camera was not capable of detecting weapons when covered by more than two layers of clothing. It is also difficult to predict the amount and type of clothing that a possible subject might be wearing.

This research also determined a temperature range over which a human operator viewing the infrared image of subjects may be relatively certain a foreign object is being carried underneath the subject's clothing. Two different temperatures were measured from the images gathered in this testing. The average temperature of the clothing at the site of the simulated bomb was taken as well as the average temperature of clothing over the entire torso. This allowed for a difference to be calculated between the two, and made it possible to find the limiting temperature difference perceptible to the human eye. This limit would determine the threshold for object detection by human sight.

It was determined that in order to be reasonably confident a foreign object is present, the average temperature of the suspected object's area had to be at least 7-10% of the temperature range shown in the image. This threshold was determined with experience looking at IR images as well as having a prior knowledge of where the hidden object may be. While it is possible to manually obtain images with smaller temperature ranges, the method used to calculate the average temperature of the bomb area will not work with these manually scaled images without raw data from the infrared sensor and proprietary algorithms from the manufacturer.

Lastly, the research determined those variables which influence the infrared image in

ways that help or hinder the use of the thermal models in predicting the clothing temperatures. It was determined that environmental factors have a large impact on the temperature of clothing that is imaged by the thermal camera. Specifically, the solar irradiation caused very large changes in temperatures on the exterior layer of clothing. This was not only shown with the thermal model but with the experimental results as well.

Factors that made using the models difficult included the addition of multiple layers of clothing to shield the simulated bomb package as well as attempting to acquire the images from beyond 25 feet.

In conclusion, it may be possible to use thermal models to help predict threats in a concealed weapon detection system. If these technologies were used they would most likely be in conjunction with multiple other types of sensors in a fused system that takes advantage of each sensor's strengths. By pairing human visual recognition experience with computer predictions infrared sensors may potentially be used as a tool for concealed weapon detection.

Works Cited

ASHRAE Handbook: Fundamentals. SI ed. American Society of Heating, Refrigerating and Air-Conditioning Engineers, Inc., 2005.

Berman, E., and D. Laitin. "Hard Targets: Theory and Evidence on Suicide Attacks." NBER Working Paper 11740 (2005).

Bloom, M. "Devising a Theory of Suicide Terror." Dying to Kill: The Global Phenomenon of Suicide Terror. Columbia University Press, 2004. Chapter 4.

Chen, H-M. Automatic Two-Stage IR and MMW Image Registration Algorithm for Concealed Weapons Detection. Vol. 148., 2001.

Chen, H-M. Imaging for Concealed Weapon Detection: A Tutorial Overview of Development in Imaging Sensors and Processing. Vol. 22., 2005.

Costianes, P. An Overview of Concealed Weapons Detection for Homeland Security., 2006.

Cronin, A. Terrorists and Suicide Attacks., 2003.
<<http://handle.dtic.mil/100.2/ADA445323>>.

FLIR. ThermaCAM S65 Operator's Manual. Vol. a62., 2004.

Haney, J. Personal Communication., 2006.

Incropera, F., and D. DeWitt. Introduction to Heat Transfer. 5th ed. John Wiley & Sons, 2002.

Jain, A. An Introduction to Biometric Recognition. Vol. 14. New York, NY: Institute of Electrical and Electronics Engineers, 2004.

Jones, B. W., and E. A. McCullough. "Computer Modeling for Estimation of Clothing Insulation." CLIMA 2000. August 25-30, 1985.

Jones, B. W., and Y. Ogawa. "Transient Interaction between the Human and the Thermal Environment." Ashrae Transactions Vol 98.Part 1 (1992).

Jones, B. F., and P. Plassmann. "Digital Infrared Thermal Imaging of Human Skin." IEEE engineering in medicine and biology magazine : the quarterly magazine of the Engineering in Medicine & Biology Society 21.6 (2002): 41-8.

Jones, B. W. "Capabilities and Limitations of Thermal Models for use in Thermal Comfort Standards." Energy and Buildings 34.6 (2002): 653-9.

Kakuta, N., S. Yokoyama, and K. Mabuchi. "Human Thermal Models for Evaluating Infrared Images." IEEE engineering in medicine and biology magazine : the quarterly magazine of the Engineering in Medicine & Biology Society 21.6 (2002): 65-72.

Kress, M. The Effect of Crowd Density on the Expected Number of Casualties in a Suicide Attack. Vol. 52., 2005.

Kribus, A. Systematic Errors in the Measurement of Emissivity Caused by Directional Effects. Vol. 42., 2003.

Liu, Z. Concealed Weapon Detection and Visualization in a Synthesized Image. Vol. 8., 2006.

McMakin, D. L., D. M. Sheen, and H. D. Collins. "Remote Concealed Weapons and Explosive Detection on People using Millimeter-Wave Holography." Security Technology, 1996.30th Annual 1996 International Carnahan Conference (1996): 19-25.

McMillan, R. W. Detection of Concealed Weapons using Far-Infrared Bolometer Arrays., 2000.

Nunn, S. "Thinking the Inevitable: Suicide Attacks in America and the Design of Effective Public Safety Policies." Journal of Homeland Security and Emergency Management 1.4 (2004).

Paulter, N. G. Guide to the Technologies of Concealed Weapon and Contraband Imaging and Detection. Vol. NCJ 184432. U.S. Department of Justice-Office of Justice Programs-National Institute of Justice, 2001.

Pavlidis, I., J. Levine, and P. Baukol. Thermal Imaging for Anxiety Detection., 2000.

Prokoski, F. Identification of Individuals by Means of Facial Thermography., 1992.

Ring, E. F. J. Quantitative Thermal Imaging. Vol. 11., 1990.

Sherrah, J. False Alarm Rate: A Critical Performance Measure for Face Recognition.

Shoji, Y. A Three-Dimensional, Clothed Human Thermal Model. Vol. 26., 1997.

Slamani, M.-A. Image Processing Tools for the Enhancement of Concealed Weapon Detection. Vol. 3., 1999.

Smith, J. and W. Thomas. The Terrorism Threat and US Government Response: Operational and Organizational Factors., 2001.

Socolinsky, D. A Comparative Analysis of Face Recognition Performance with Visible

and Thermal Infrared Imagery. Vol. 4., 2002.

Socolinsky, D and A. Selinger. Thermal Face Recognition in an Operational Scenario. Vol. 2., 2004.

Toet, A. Color Image Fusion for Concealed Weapon Detection. Vol. 5071., 2003.

Varshney, P. K. Registration and Fusion of Infrared and Millimeter Wave Images for Concealed Weapon Detection., 1999.

Wang, J.-G, E. Sung, and R. Venkateswarlu. Registration of Infrared and Visible-Spectrum Imagery for Face Recognition., 2004.

Xue, Z., and R. S. Blum. "Concealed Weapon Detection using Color Image Fusion." Proceedings of the 6th International Conference on Information Fusion (2003): 622–627.

Xue, Z. Fusion of Visual and IR Images for Concealed Weapon Detection., 2002

Appendix A

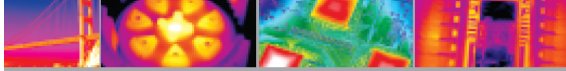
FLIR S65 Camera Specs



The Global Leader in Infrared Cameras

ThermaCAM® S65

INFRARED CAMERA



The ThermaCAM® S65 is a highly refined infrared research system. Its powerful new features and conveniences enable the professional thermographer to work with unprecedented efficiency and productivity. Working in concert with ThermaCAM Researcher reporting and database software, the S65 fully automates the process of collecting, reporting, and archiving infrared images and thermal data.



- > Bluetooth® Voice Recording Technology
- > Burst & AVI Recording
- > Radiometric FireWire®
- > Radiometric JPEG Image Storage
- > Auto-focus/Auto-hot-spot Tracker
- > Detachable Remote Control/LCD Handle
- > Built-in Ram/CompactFlash® Card
- > Built-in Laser LocatIR™ Target Pointer

Features both thermal and visual camera capabilities – at the touch of a button!

Extraordinary Thermal Sensitivity and Imaging Quality

Thermal sensitivity of 0.08C coupled with a 76,000pixel display provides extremely accurate, high-resolution 14-bit thermal images in real time. Plus, the state-of-the-art 320 x 240 uncooled microbolometer detector means the S65 is ready to go in seconds. The built-in external 4-inch LCD screen displays digital images of corresponding thermal images captured by the IR system.

Real-time Digital Storage and Analysis

Video rate imaging (60 Hz) allows you to inspect fast moving objects and scan while moving without image smear. Radiometric FireWire (IEEE 1394) output provides the bandwidth for fast downloading of calibrated thermal video of high-speed events.

Easy to Operate

Ergonomic, intuitive controls make operation seamless and efficient. A user-friendly joystick, familiar menus, and soft programmable buttons (allowing feature customization) on both the camera body and detachable handle provide for easy one-handed operation. The built-in Laser LocatIR™ provides point-and-shoot accuracy.

Flexible Image Storage

Images can be stored in Windows-friendly JPEG format, removable CompactFlash® memory card, or internal flash RAM. The camera may be set up to automatically capture images at preset intervals.

Rugged and Lightweight

The S65 was designed for use in harsh environments. It has an IP54 industrial shock rating and complete environmental encapsulation. At under 4.4 lbs., it is the lightest full-featured infrared camera available.

Flexible Viewing Options

The built-in color viewfinder is ideal for outdoor applications, while the detachable 4-inch color LCD on the camera's handle adjusts to any viewing angle, and may be used to operate the camera via redundant controls – for optimal use in hard-to-reach areas – indoors and out.

Burst and AVI Recording

Powerful burst recording captures moving targets for sequences up to 20 minutes long. Sequences may be played back on the camera or transferred to a PC for further analysis. Nonradiometric moving images may be optionally recorded in AVI file format for convenient report playback using industry-standard players.

Special Features Boost Your Efficiency

A brilliant LED target light automatically turns on when visual image mode is selected. Powerful auto-focus and auto-hot-spot features save time and effort. The S65 can automatically indicate the temperature and position of the hottest spot in the image and instantly calculate the difference between different measurement points. Sound and color alarms warn when targets exceed temperature maximums set by the user.

Voice Recording with Bluetooth Technology...and More

The S65 can record up to 30 seconds of voice comment with each image. A cordless Bluetooth earpiece eliminates all cable connections, increasing operator safety. In addition, text comments for each image can be entered manually or preloaded from a PC with optional ThermaCAM® Reporter software.

Store User Profiles

Personal camera settings may be stored on the S65, for several users, a time-saving feature.

Wide Range of Accessories

Optional optics include: microscopic, wide-angle and telescopic to address diverse application requirements. Infrared heads-up displays (IRHUD) are available, to augment situational awareness. Power options include lightweight, rechargeable, long-life Li-Ion batteries, and the ability to operate the S65 from external power sources.

Optional Software Does the Work for You!

ThermaCAM Researcher reporting and analysis software analyzes your data in real time. ThermaCAM Database software enables you to trend, archive, and organize inspection data and reports quickly and easily. ThermaCAM Image Builder knits multiple IR images together to create a single radiometric composite.

ThermaCAM® S65 Technical Specifications

Imaging Performance	
Thermal	
Field of view/min focus distance	24° x 18° / 0.3 m
Spatial resolution (IFOV)	1.3 mrad
Electronic zoom function	2, 4, 8, interpolating
Focus	Automatic or manual
Digital image enhancement	Normal and enhanced
Detector type	Focal plane array (FPA) uncooled microbolometer; 320 x 240 pixels
Spectral range	7.5 to 13 µm
Thermal sensitivity @ 50/60Hz	0.08° C at 30° C
Visual	
Built-in digital video	640 x 480 pixels, full color
Image Presentation	
Viewfinder	Built-in high-resolution color LCD (TFT)
Video output	4" LCD with integrated remote control RS 170 EIA/NTSC or CCIR/PAL
External display	Built-in high-resolution color LCD (TFT)
Measurement	
Temperature ranges	-40° C to +120° C (-40° F to +248° F), Range 1 0° C to +500° C (+32° F to +932° F), Range 2 +350° C to +1500° C (+662° F to +2732° F), Range 3 Up to +2000° C (+3632° F), optional
Accuracy (% of reading)	± 2° C or ± 2%
Measurement modes	Up to 10 movable spots. Automatic temperature difference (Δ) and placement and reading of maximum and minimum temperatures. Up to 5 movable circle areas or boxes. Up to 2 isotherms. Line profile.
Emissivity corrections	Variable from 0.1 to 1.0 or select from listings in pre-defined material list
Measurement features	Automatic corrections based on user input for reflected ambient temperature, distance, relative humidity, atmospheric transmission, and external optics
Optics transmission correction	Automatic, based on signals from internal sensors
Image Storage	
Type	Removable CompactFlash (256 MB) memory card; built-in Flash memory (100 images); built-in RAM memory for burst and AVI recording
File format - THERMAL	Standard JPEG; 14 bit thermal measurement data included
File format - VISUAL	Standard JPEG inked with corresponding thermal image
Voice annotation of images	Input via supplied Bluetooth® wireless headset up to 30 seconds of digital voice clip per image stored with image
Text annotation of images	Predefined by user and stored with image
System Status Indicator	
LCD display	Shows status of battery and storage media. Indication of power, communication and storage modes.
Power Source	
Battery type	Li-Ion, rechargeable, field-replaceable
Battery operating time	2 hours continuous operation
Charging system	In camera (AC adapter or 12V from car) or 2 bay intelligent charger
External power operation	AC adapter 110/220 VAC, 50/60Hz or 12V from car (cable with standard plug optional)
Power saving	Automatic shutdown and sleep mode (user-selectable)
Environmental	
Operating temperature range	-15° C to +50° C (5° F to 122° F)
Storage temperature range	-40° C to +70° C (-40° F to 158° F)
Humidity	Operating and storage 10% to 95%, non-condensing
Encapsulation	IP 54 IEC 529
Shock	Operational: 25G, IEC 68-2-29
Vibration	Operational: 2G, IEC 68-2-6
Physical Characteristics	
Weight	2.0 kg (4.4 lbs) w/battery and top handle (includes remote control, LCD, video camera and laser) 1.4 kg (3.1lbs) excluding battery and handle
Size	100mm x 120mm x 220 mm (3.9" x 4.7" x 8.7") camera only
Tripod mounting	1/4" - 20

ThermaCAM S65 System Includes:	
IR camera with visual camera, Laser LocatIR, remote with LCD display	
High-output multi-LED target light	
Bluetooth® wireless headset	
Carrying case, lens cap, shoulder strap, hand strap	
User manual (multilingual)	
Batteries (2)	
Power supply	
Battery charger	
FireWire® (IEEE 1394) cable	
Video cable with RCA plug	
USB cable	
S-video cable	
256 MB CompactFlash card	
ThermaCAM QuickView™ software	
Lenses (optional)	
Field of view/ minimum focus distance	3X Telescope (7° x 5.3°/4m) 2X Telescope (12° x 9°/1.2m) 0.5X Wide angle (45° x 34°/0.1m) 0.3X Wide angle (80° x 60°/0.1m) 200 µm Close-up (64mm x 48mm/150mm) 100 µm Close-up (34mm x 25mm/80mm) 50 µm Close-up (15mm x 11mm/19mm) Wearable Optics/Heads-up Display
Interfaces	
Firewire output (IEEE 1394)	Real-time digital transfer of radiometric thermal images or digital video (DV) out
USB / RS232	Image (thermal and visual), measurement data, voice and text transfer to PC
IrDA	Two-way data transfer from laptop, PDA
Remote control	Removable handle with redundant controls and LCD
Laser LocatIR	
Classification type	Class 2 Semiconductor AlGaInP Diode Laser: 1 mW/635 nm (red)



The Global Leader in Infrared Cameras

1 800 464 6372
www.flirthermography.com/S65data

Specifications subject to change. © Copyright 2005, FLIR Systems, Inc. All rights reserved. I061505PL

Appendix B

MATLAB® Temperature Averaging Code

```
function finalT = AverageTemperature()
% AVERAGE TEMPERATURE Summary of this function goes here
% Detailed explanation goes here
clc;

% Getting user input
[FileName, PathName] = uigetfile('*.jpg', 'Select the Image to Analyze');

% Opening File
imageS = imread([PathName, FileName]);
imshow(imageS);
load mask

% User input of the bounding box and temperature high lows
fprintf('Select the top left corner of the square you want to average\n');
topLeft = ginput(1);
topLeft = uint16(topLeft);
fprintf('Select the bottom right corner of the square you want to
average\n');
botRight = ginput(1);
botRight = uint16(botRight);
highTemp = input('\nWhat is the higher temperature? ');
lowTemp = input('\nWhat is the lower temperature? ');

% Loading the temperature scale
temperatureScale = zeros(4, 346-105+1);
for t = 105:346
    temperatureScale(1:3, t-104) = imageS(t, 590, 1:3);
    temperatureScale(4, t-104) = lowTemp + (highTemp-lowTemp)*(t-105)/(346-
105);
end

% Averaging pixel values
count = 0;
temp_total = 0;
othermask = zeros(size(imageS, 1), size(imageS, 2));
for x = topLeft(1):1:botRight(1)
    for y = topLeft(2):1:botRight(2)
        if (mask(y, x)) == 0
            count = count + 1;
            othermask(y, x) = 1;
            temp_total = temp_total +
findTemp(imageS(y, x, 1), imageS(y, x, 2), imageS(y, x, 3), temperatureScale);
        end
    end
end
finalT = temp_total/count;
```

```

%Applying mask to image
imageS(:,:,1) = imageS(:,:,1) .* uint8(othermask);
imageS(:,:,2) = imageS(:,:,2) .* uint8(othermask);
imageS(:,:,3) = imageS(:,:,3) .* uint8(othermask);
imshow(imageS);

%Saving the image of the pixels used
imwrite(imageS,['Z:\IDEAS Lab\Dickson Photo Temperature
Averager\Results\',FileName],'jpg');

end

%%

function temp = findTemp(r,g,b,Scale)
    distance = zeros(size(Scale,2),1);
    for t = 1:size(distance)
        distance(t) = sqrt((double(r)-Scale(1,t))^2+(double(g)-
Scale(2,t))^2+(double(b)-Scale(3,t))^2);
    end
    [C,I] = min(distance);
    temp = Scale(4,I);
end

```

Appendix C

LCM Method Computer Code

```
/* Conservation of energy requirement on the control volume, CV. */
Edotin - Edotout = Edotst
Edotin = As * ( + Gabs + q"a)
Edotout = As * ( + q"cv + E )
Edotst = rho * vol * cp * Der(T,t)

// Absorbed prescribed irradiation on CS
Gabs = alpha * G

// Emissive power of CS
E = eps * Eb
Eb = sigma * T^4
sigma = 5.67e-8 // Stefan-Boltzmann constant, W/m^2.K^4

//Convection heat flux for control surface CS
q"cv = h * ( T - Tinf )

/* The independent variables for this system */
As = // surface area, m^2
vol = // vol, m^3
rho = // density, kg/m^3
cp = // specific heat, J/kg.K

// Convection heat flux, CS
h = // convection coefficient, W/m^2.K
Tinf = // fluid temperature, K

// Emission, CS
eps = // emissivity

// Prescribed irradiation, CS
alpha = // absorptivity
G = // irradiation, W/m^2

// Applied heat source, CS
q"a = // applied heat flux, W/m^2
```

Appendix D

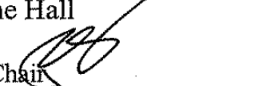
Research Compliance



University Research
Compliance Office
203 Fairchild Hall
Lower Mezzanine
Manhattan, KS 66506-1103
785-532-3224
Fax: 785-532-3278
<http://www.ksu.edu/research/comply>

TO: Akira Tokuhira
Mechanical Engineering
3032 Rathbone Hall

Proposal Number: 4193

FROM: Rick Scheidt, Chair 
Committee on Research Involving Human Subjects

DATE: March 29, 2007

RE: Approval of Proposal Entitled, "Concealed Weapons Detection Using Infrared Imaging (within the Urban Operations Environmental Laboratory Contract)."

The Committee on Research Involving Human Subjects has reviewed your proposal and has granted full approval. This proposal is **approved for one year from the date of this correspondence, pending "continuing review."**

APPROVAL DATE: March 29, 2007

EXPIRATION DATE: March 29, 2008

Several months prior to the expiration date listed, the IRB will solicit information from you for federally mandated "**continuing review**" of the research. Based on the review, the IRB may approve the activity for another year. **If continuing IRB approval is not granted, or the IRB fails to perform the continuing review before the expiration date noted above, the project will expire and the activity involving human subjects must be terminated on that date. Consequently, it is critical that you are responsive to the IRB request for information for continuing review if you want your project to continue.**

In giving its approval, the Committee has determined that:

- There is no more than minimal risk to the subjects.
 There is greater than minimal risk to the subjects.

This approval applies only to the proposal currently on file as written. Any change or modification affecting human subjects must be approved by the IRB prior to implementation. All approved proposals are subject to continuing review at least annually, which may include the examination of records connected with the project. Announced post-approval monitoring may be performed during the course of this approval period by URCO staff. Injuries, unanticipated problems or adverse events involving risk to subjects or to others must be reported immediately to the Chair of the IRB and / or the URCO.

Appendix E

Defense Presentation

Handheld Infrared Camera Use for Suicide Bomb Detection: Feasibility of Use for Thermal Model Comparison



Matthew R. Dickson
Dr. Akira Tokuhiko

Detection Problem-Objectives



- Determine a temperature range over which an operator can be relatively certain of a hidden foreign object being

- Determine variables that influence the IR image in ways that help or hinder the use of thermal models



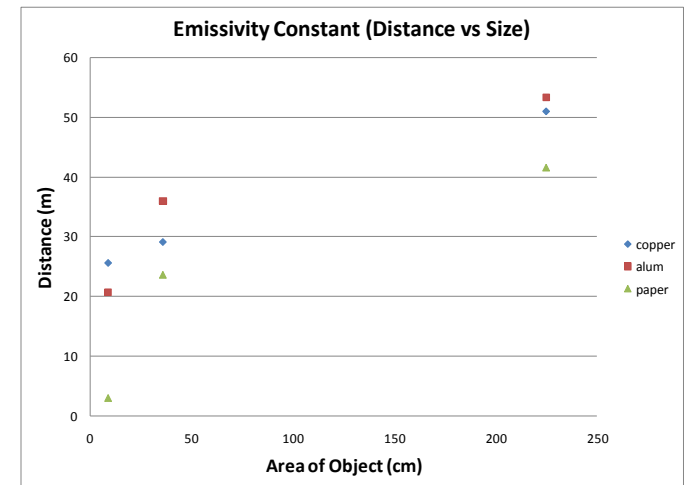
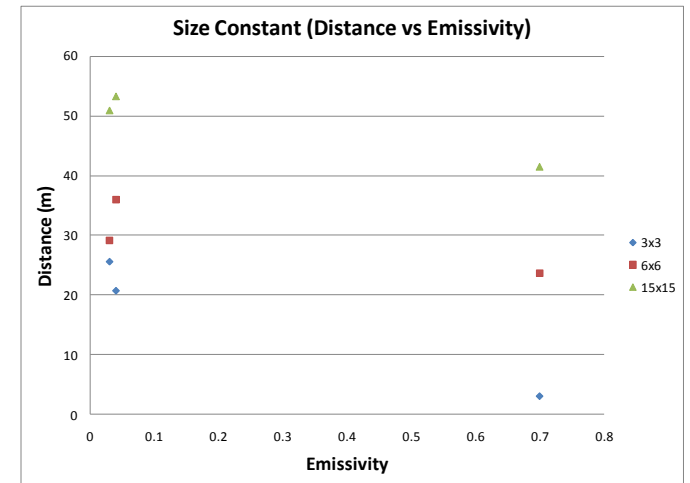
- Determine the feasibility of comparing the infrared images to thermal models that predict clothing temperatures

Camera Testing Phases

	Phase 1	Phase 2	Phase 3
Subject	Manikin	Human	Human
Environment	Indoors	Indoors	Outdoors
Temperature	Room Temperature	Warm/Hot	Warm/Hot
Phase Focus	Camera Settings/ Capabilities	Controlled Environment Capabilities	Uncontrolled Environment Capabilities

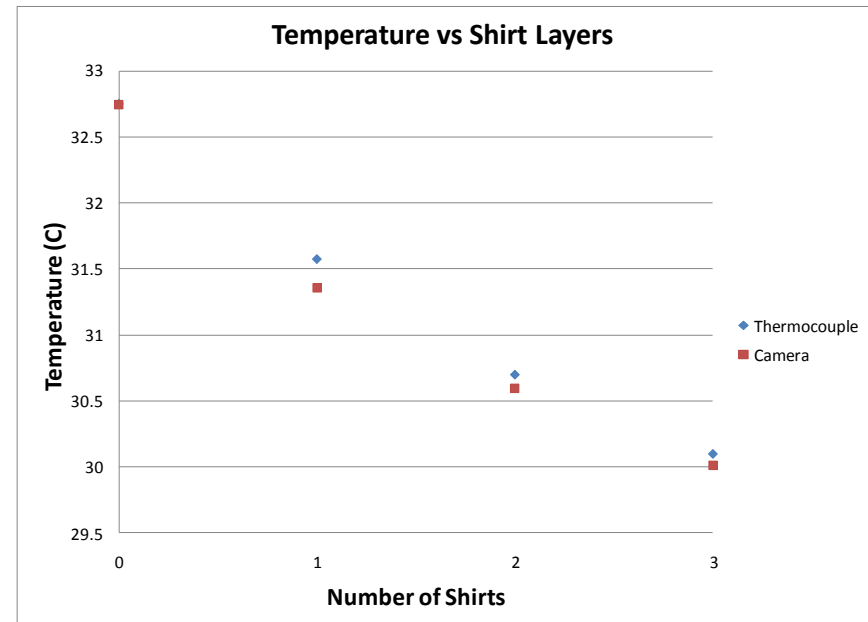
Effects of Coupon Area and Emissivity on Visible Distance

- Easier to discern larger object at greater distances
- Distance has minimal effect on temperature measurement
- Lower emissivity objects can be seen at greater distances(warm background)



External Clothing Temperature with Application of Clothing Layers

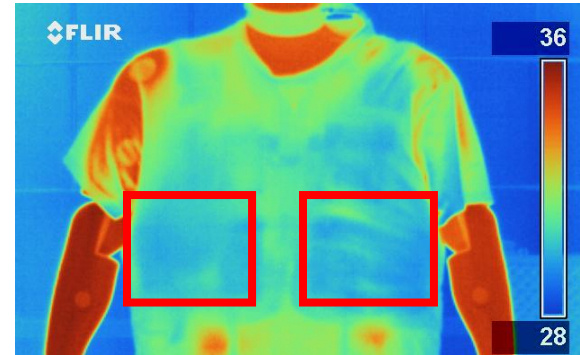
- Repeated at four distances with blue/yellow cotton t-shirts
- Effects of distance and t-shirt color were both negligible (temperatures were averaged for figure)
- Thermocouple and camera measurements within 0.25°C
- Exterior shirt temperature dropped as layers were added thermal resistance increased



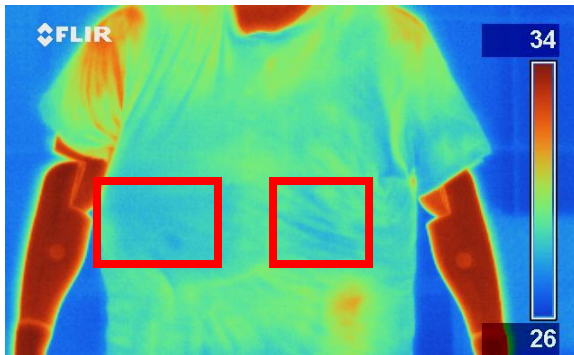
External Clothing Temperature with Application of Clothing Layers



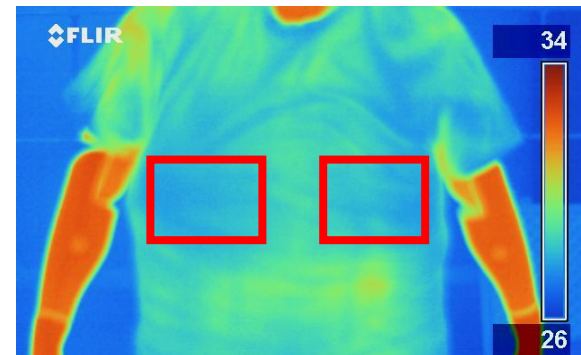
Clay Material Hidden in Vest Pocket



Clay Material Hidden in Vest Pocket
Shielded by 1 T-shirt



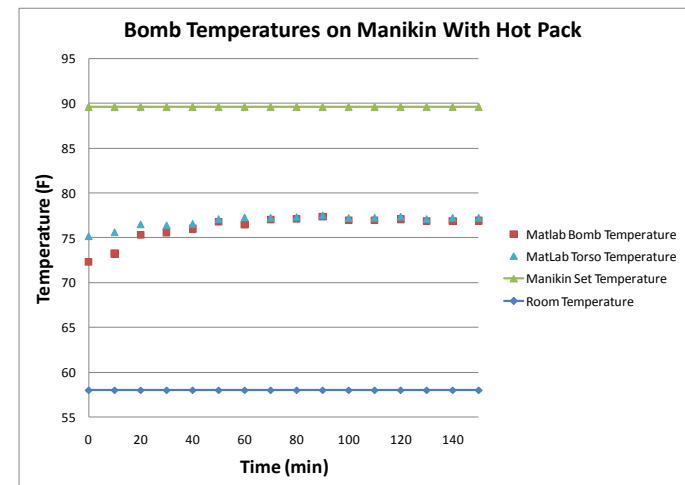
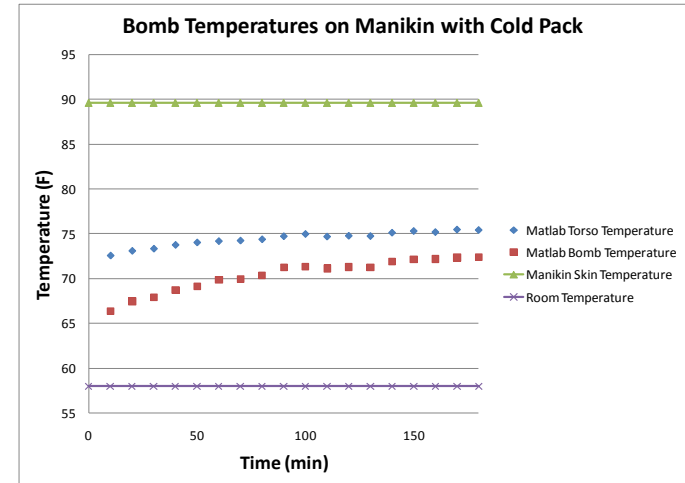
Clay Material Hidden in Vest Pocket
Shielded by 2 T-shirts



Clay Material Hidden in Vest Pocket
Shielded by 3 T-shirts

Bomb Temperatures on Manikin with Cold Pack/Hot Pack

- Cold pack attached was still easily visible after 3 hours
- Cold pack difference is 1.67°C (3°F)
- 3°F difference is 15% of the overall temperature scale
- Hot pack made the bomb package reach a visible equilibrium within 20 minutes
- Hot pack difference was within 0.3°F of the average torso temperature
- 2% of the overall temperature scale



Bomb Temperatures on Manikin with Cold Pack/Hot Pack



Bomb with Hot Pack Attached to Manikin at 0 Minutes



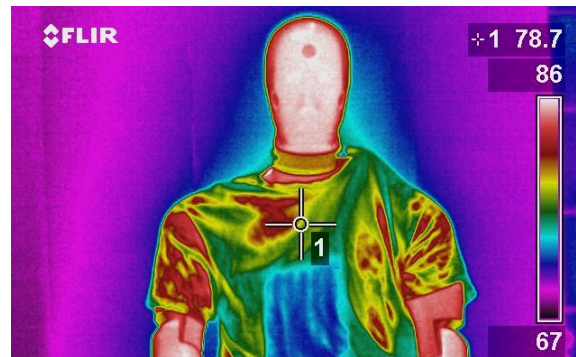
Bomb with Hot Pack Attached to Manikin at 90 Minutes



Bomb with Hot Pack Attached to Manikin at 150 Minutes



Bomb with Cold Pack Attached to Manikin at 0 Minutes



Bomb with Cold Pack Attached to Manikin at 140 Minutes



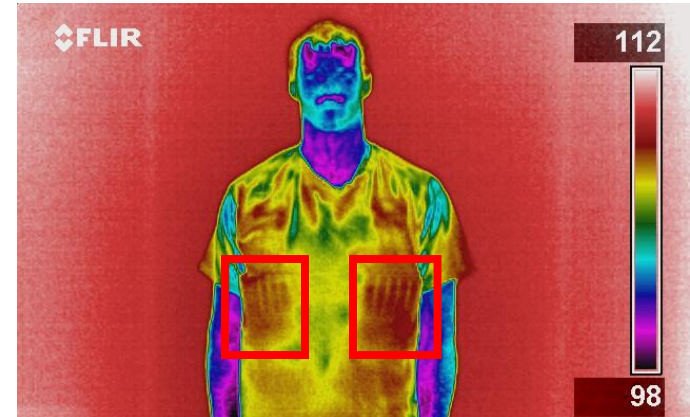
Bomb with Cold Pack Attached to Manikin at 180 Minutes

General Conclusions from Phase 1 Testing

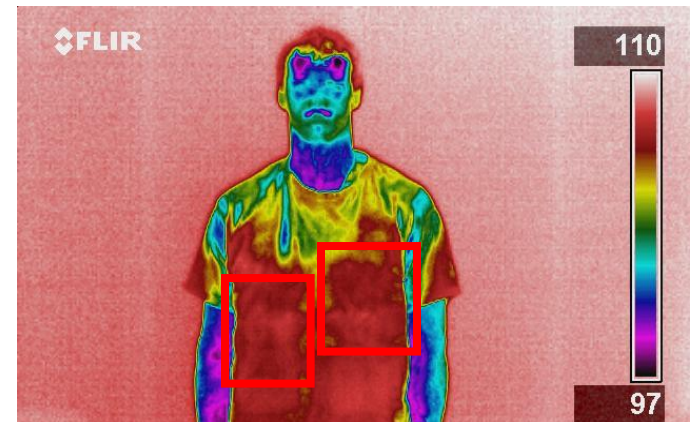
Phase	Testing Variable	Testing Conclusions
Phase 1	Effects of Size on Range	Larger objects are visible from longer distances.
	Effects of Emissivity on Range	When the background of an image is comprised of warm temperatures, materials of lower emissivity are visible at longer distances than materials of high emissivity.
	Shielding	The temperature of the outer layers of clothing tends to approach the ambient environmental temperature.

Bomb Package Material

- Metal more readily transfers the heat away from the clothing towards the body than plastic
- Metal packages can be seen when covered by one layer
- Metal package still had distinctive features visible when covered with two layers
- Glimpses of the metal package can be seen when covered by three shirts
- Plastic packages were barely discernable with only one t-shirt covering the package
- Almost impossible to see plastic package with multiple layers

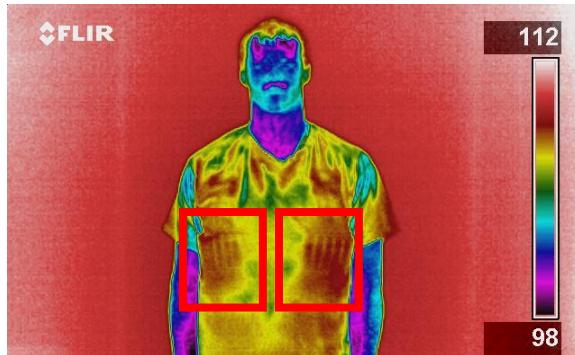


Metal Package Hidden in Vest
Shielded by 1 Tight T-Shirt

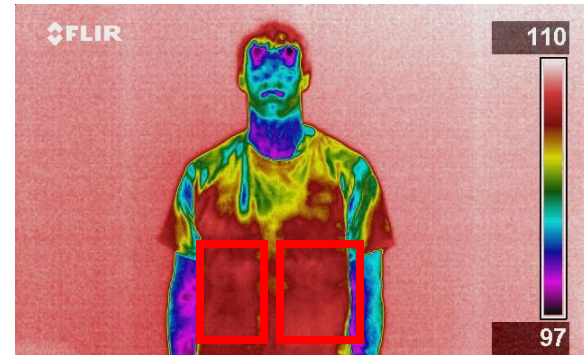


Plastic Package Hidden in Vest
Shielded by 1 Tight T-Shirt

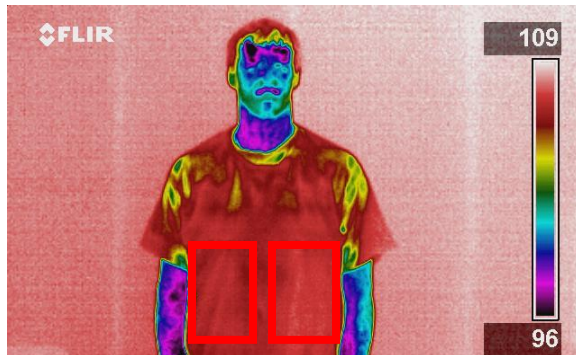
Varying Amounts of Shielding



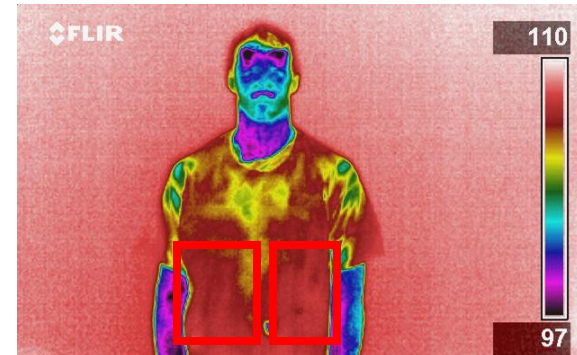
Metal Package Hidden in Vest
Shielded by 1 Tight T-Shirt
Automatic Temperature Range Setting



Plastic Package Hidden in Vest
Shielded by 1 Tight T-Shirt
Automatic Temperature Range Setting



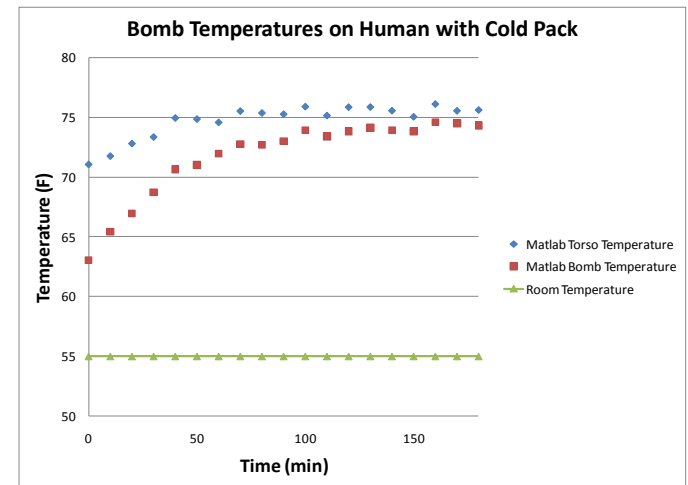
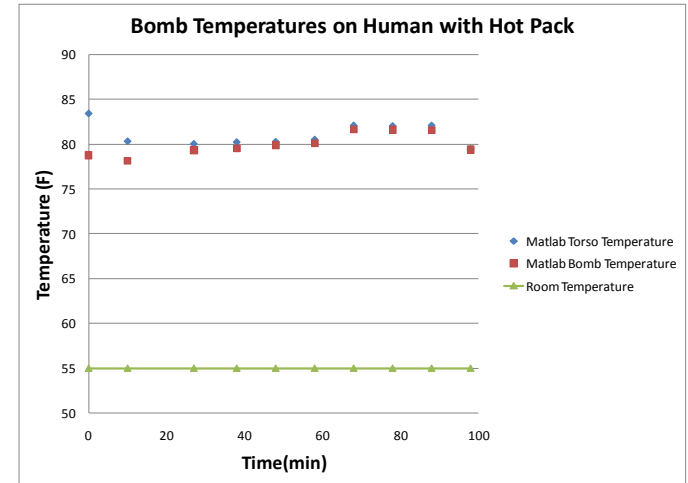
Metal Package Hidden in Vest
Shielded by 2 Loose T-Shirt
Automatic Temperature Range Setting



Plastic Package Hidden in Vest
Shielded by 2 Loose T-Shirts
Automatic Temperature Range Setting

Bomb Temperatures on Human with Hot Pack/Cold Pack

- Hot pack reached visible equilibrium within 20 minutes
- Cold package still visible after 3 hours
- Results match those using the Thermal Observation Manikin in Phase 1
- Human and bomb package have a greater effect on the external clothing temperature at lower environmental temperatures
- Human would have a better chance to visually see the bomb in a infrared image when the environmental temperature is lower than the body temperature



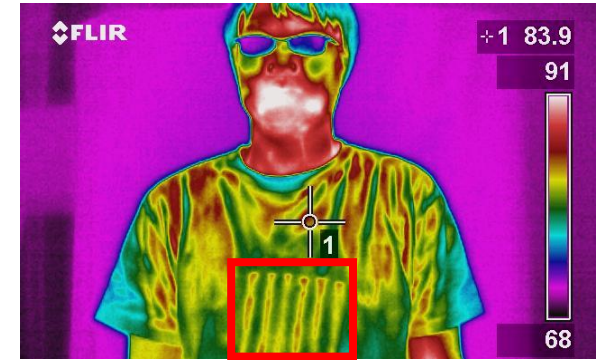
Bomb Temperatures on Human with Hot Pack/Cold Pack



Bomb with Hot Pack Attached to Human at 0 Minutes



Bomb with Hot Pack Attached to Human at 27 Minutes



Bomb with Hot Pack Attached to Human at 1 Hour 40 Minutes



Bomb with Cold Pack Attached to Human at 0 Minutes



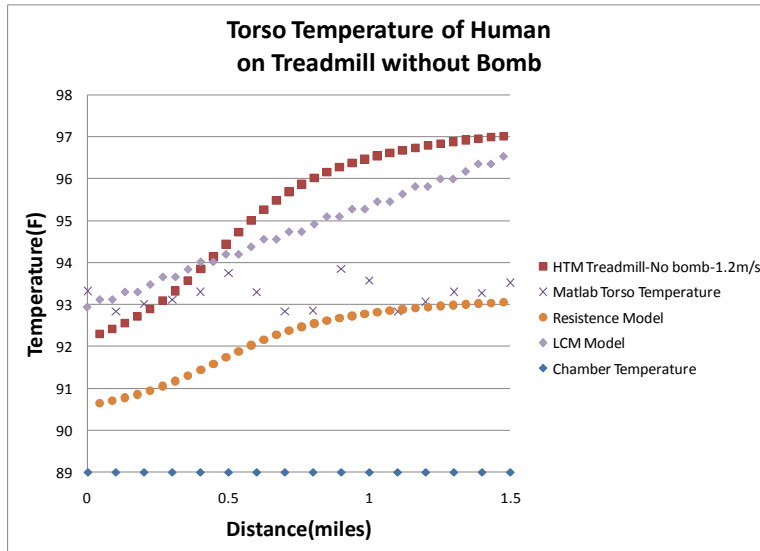
Bomb with Cold Pack Attached to Human at 1 Hour 30 Minutes



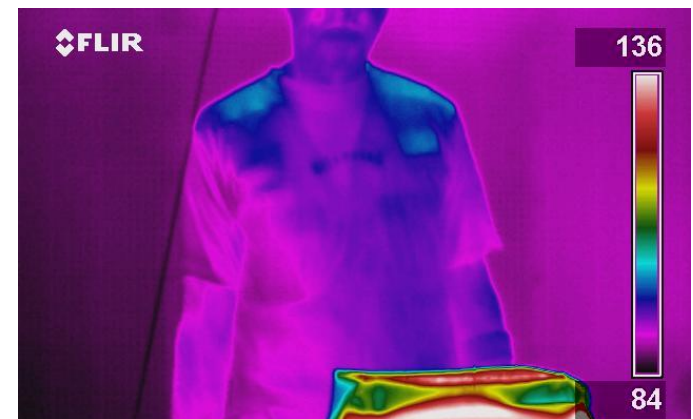
Bomb with Cold Pack Attached to Human at 3 Hours

Human on Treadmill without Bomb

- After 1.5 miles the resistance model approaches the measured temperature of the clothing
- LCM model predicts higher temperatures than those measured by the camera – irradiation not modeled
- Resistance model halfway between skin temperature and environmental temperature



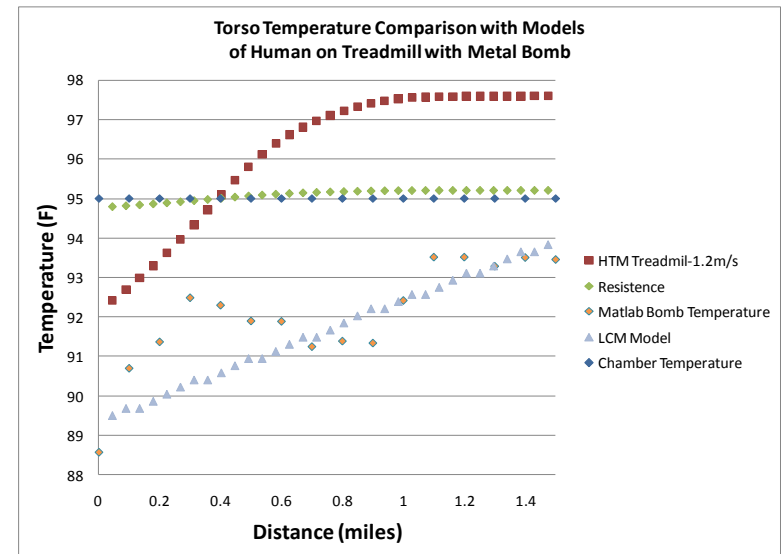
Walking on Treadmill Without Bomb 0.1 Miles



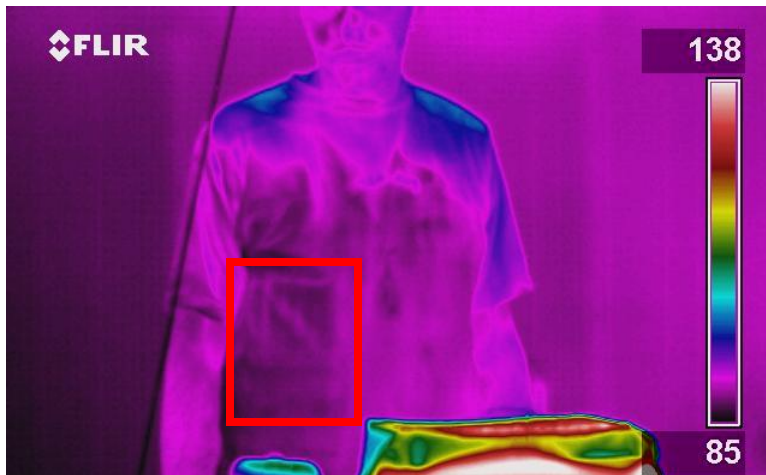
Walking on Treadmill Without Bomb 1.5 Miles

Human on Treadmill with Metal Bomb

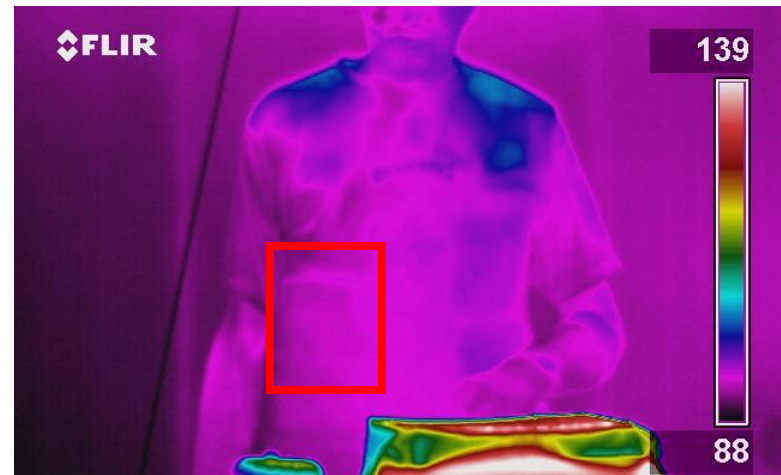
- Bomb area average temperature does not rise above the ambient temperature of 35°C (95°F)
- Difference between the temperature of the bomb area and the torso was approximately 1.5°F to 2°F
- Temperature difference is 3-4% of overall temperature scale
- Overall rise in temperature is consistent with the rise of the LCM model (irradiation and convection included)
- Resistance model shows higher results (does not consider convective cooling on outside of clothing or irradiation)
- Resistance model very close to environmental temperature
- Outside of the bomb is always at a higher temperature than the inside



Human on Treadmill with Metal Bomb



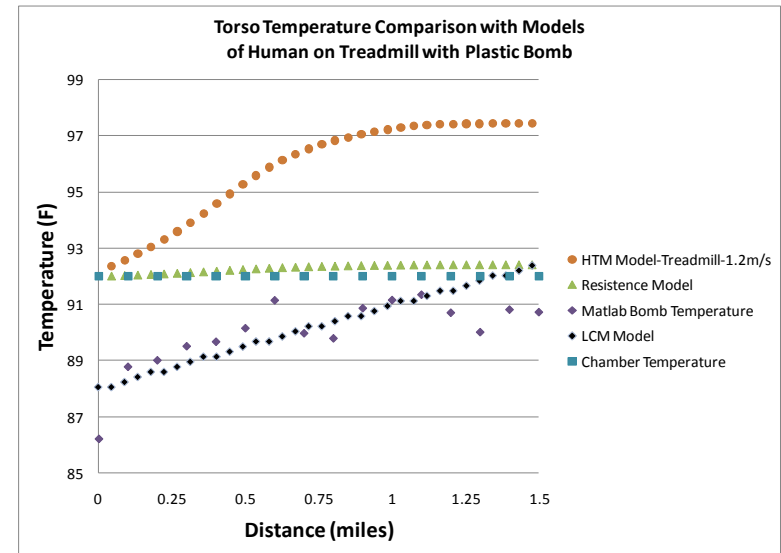
Walking on Treadmill with Metal Bomb 0 Miles



Walking on Treadmill with Metal Bomb 1.5 Miles

Human on Treadmill with Plastic Bomb

- Bomb area tended to be 2-4°F less than the average torso temperature
- less than 6% of the overall temperature scale
- Inside temperature of the bomb was higher than the outside until 0.5 miles
- Inside temperature of the bomb was lower than the outside after 0.75 miles
- When one compares this case to that of the metal bomb, one can see that it takes longer for the ambient air temperature to affect the temperature of the bomb (plastic bomb has lower thermal conductivity)
- The temperature was still climbing after 1.5 miles



Human on Treadmill with Plastic Bomb



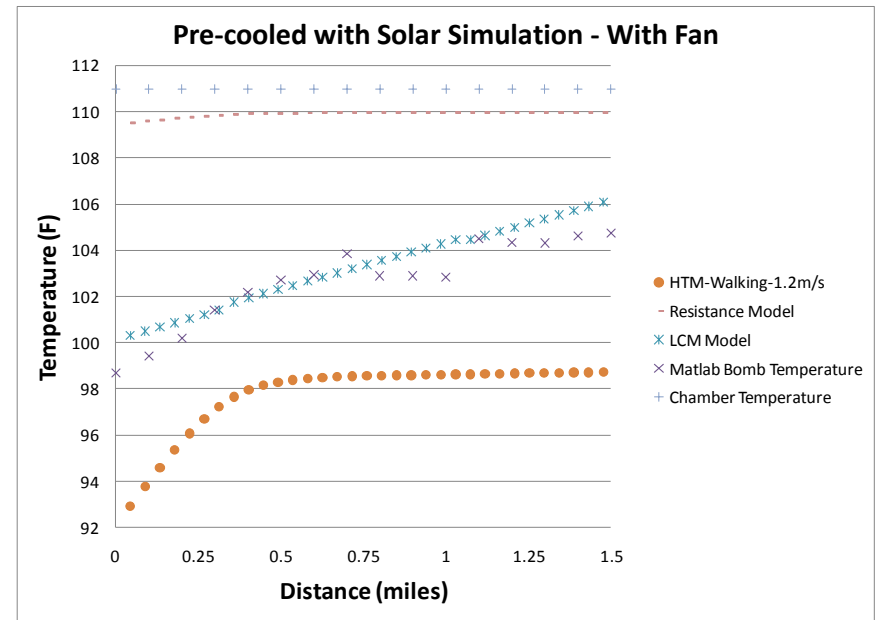
Walking on Treadmill with Plastic Bomb at 0 Miles



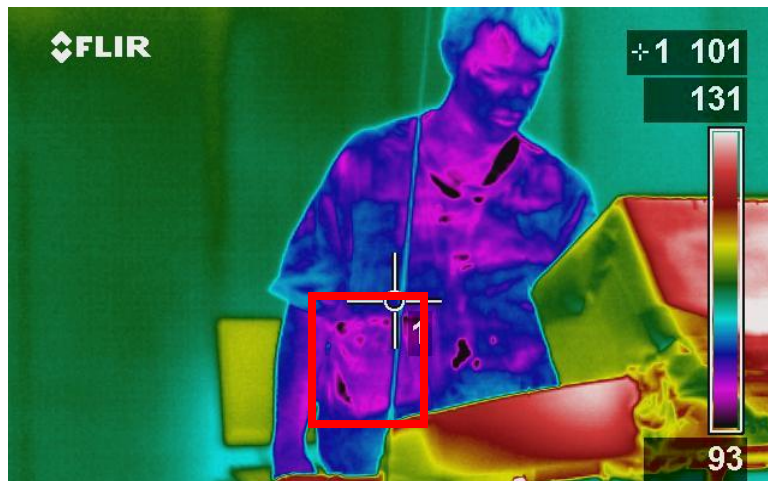
Walking on Treadmill with Plastic Bomb at 1.5 Miles

Human on Treadmill with Bomb Pre-cooled with Solar Simulation-With Fan

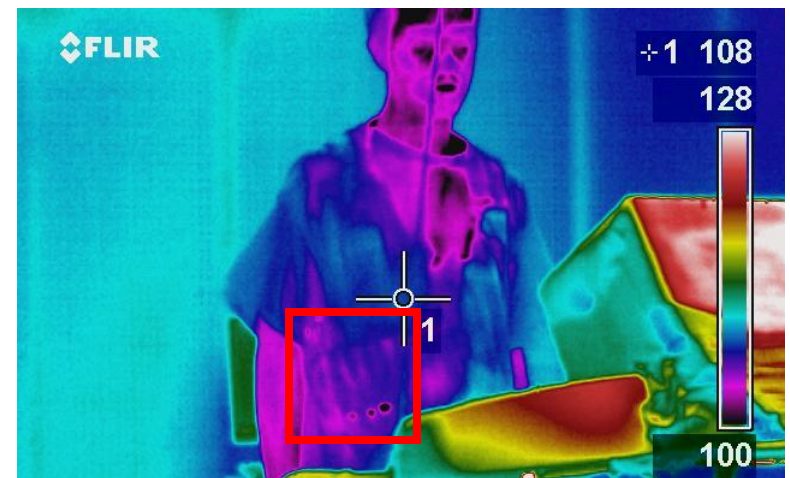
- Bomb area temperature followed the LCM model closely
- LCM model accounts for both simulated solar irradiation and convection due to the fan
- Bomb area is consistently 2°F to 3°F cooler than the entire torso area
- 2°F to 3°F difference is between 8% and 11% of the overall temperature scale
- The bomb package did not have sufficient time to come to a complete equilibrium



Human on Treadmill with Bomb Pre-cooled with Solar Simulation-With Fan



Walking on Treadmill with Cooled Bomb
Lights On- Fan On- 0 miles



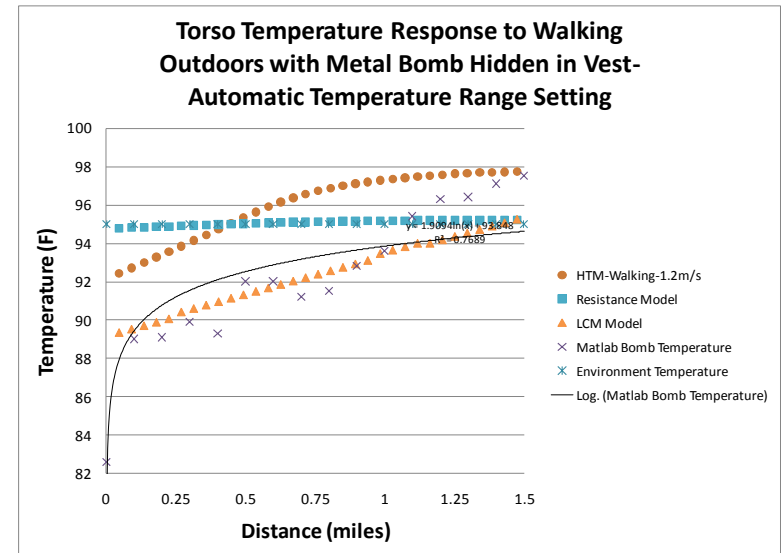
Walking on Treadmill with Cooled Bomb
Lights On- Fan On- 1.5 miles

General Conclusions from Phase 2 Testing

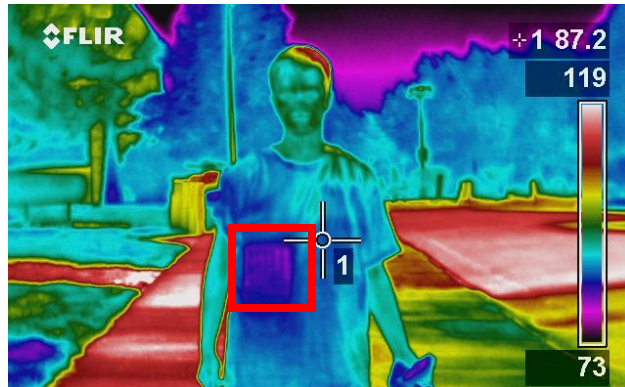
Phase	Testing Variable	Testing Conclusions
Phase 2	Material Testing	<p>Package material will determine the rate of heat transfer to and from the layers of clothing.</p> <p>Difficulties arise in modeling due to uncertainty of the bomb material.</p>
	Transient Changes While Walking	<p>Convective cooling due to movements of the human body is an important modeling aspect.</p> <p>Demonstrated that background and foreground objects may enlarge the temperature scale, making visibility of the object difficult for humans.</p>
	Shielding	<p>As the number of clothing layers increases, the temperature measured by the camera of the clothing approaches the ambient environmental temperature. Modeling difficulties arise due to the uncertainty of the actual amount of clothing worn.</p>

Walking Outdoors With Metal Bomb Hidden in Vest

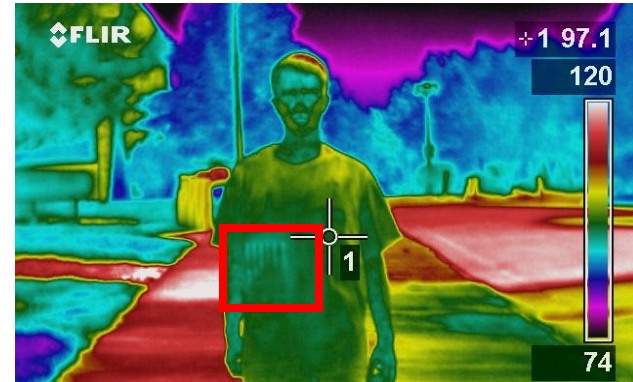
- Temperature increase of the bomb and torso follow the rise of the LCM model
- Resistance model predicts a much higher temperature due to not accounting for convective cooling on outside of clothing
- HTM program results, RTD measurements of the bomb, and temperatures acquired by the IR images all seem to converge at a walking distance of 1.5 miles
- Overall temperature scale in these images is 45°F to 46°F
- Temperature difference begins at 9% of the temperature scale and drops to 3% of the temperature scale



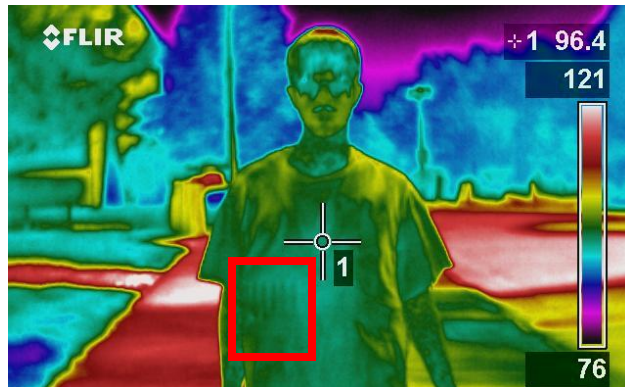
Walking Outdoors With Metal Bomb Hidden in Vest



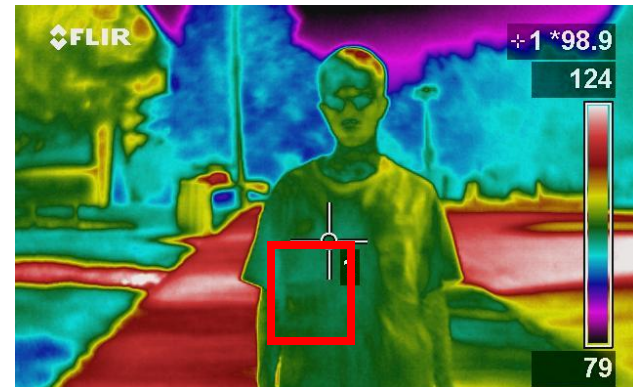
Walking Outside with Metal Bomb at 0 Miles
Automatic Temperature Scale Setting



Walking Outside with Metal Bomb at 0.5 Miles
Automatic Temperature Scale Setting



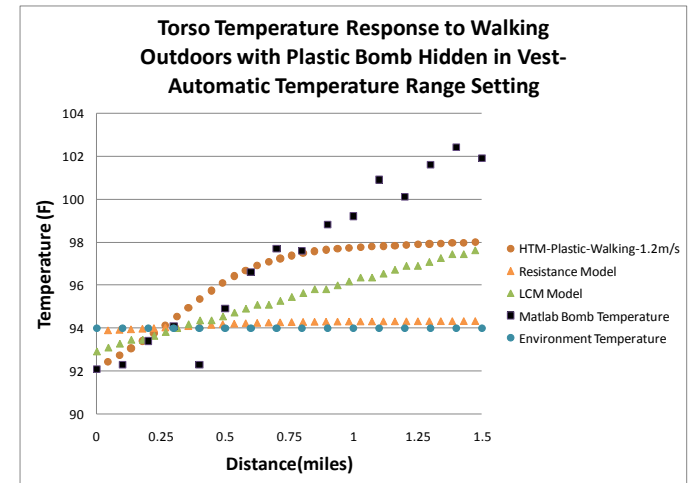
Walking Outside with Metal Bomb at 1 Mile
Automatic Temperature Scale Setting



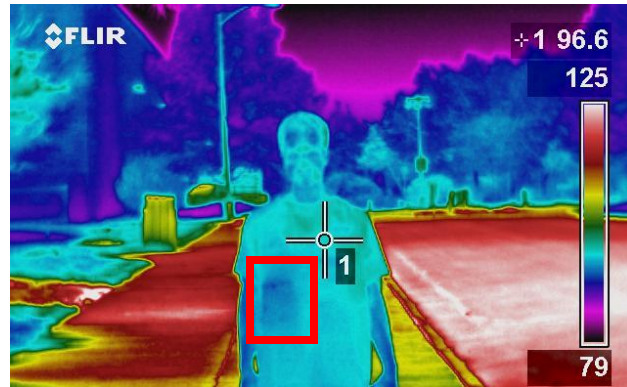
Walking Outside with Metal Bomb at 1.5 Miles
Automatic Temperature Scale Setting

Walking Outside with Plastic Bomb Package

- Plastic bomb area temperatures were usually two to three degrees higher than the RTD measurements of the bomb package, but they increased at the same rate
- Overall temperature range begins at 46°F and expands to 52°F
- Temperature differences represent only 1% to 3% of the temperature scale
- Larger convective cooling effect on the exterior of the bomb package due to the movement while walking
- Measurements continue to climb after the HTM levels out



Walking Outdoors with Plastic Bomb Package



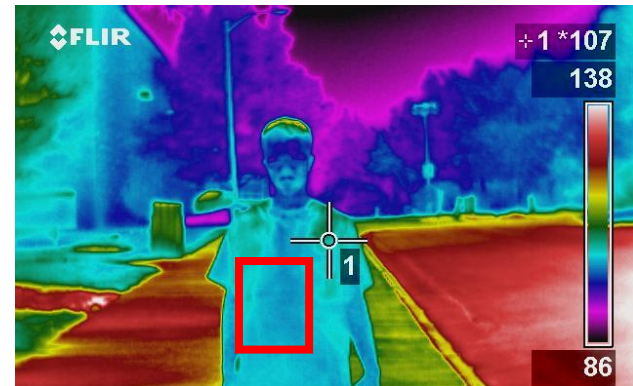
Walking Outside with Plastic Bomb at 0 Miles
Automatic Temperature Scale Setting



Walking Outside with Plastic Bomb at 0.5 Miles
Automatic Temperature Scale Setting



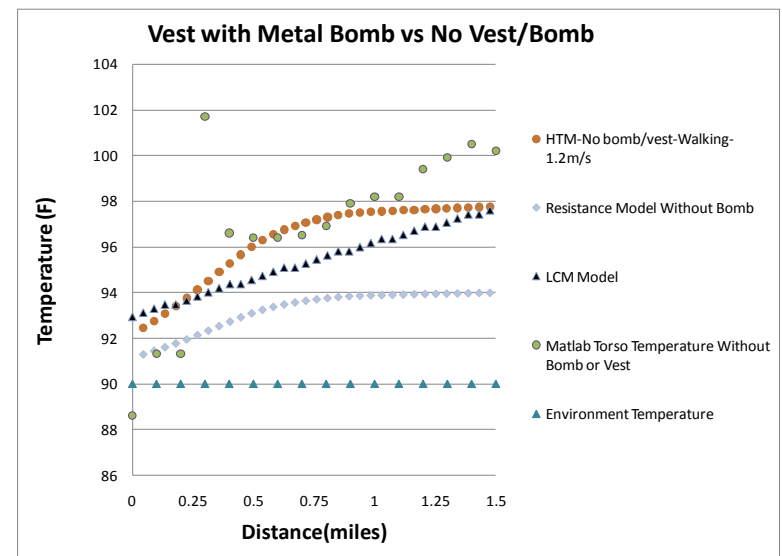
Walking Outside with Plastic Bomb at 1.0 Miles
Automatic Temperature Scale Setting



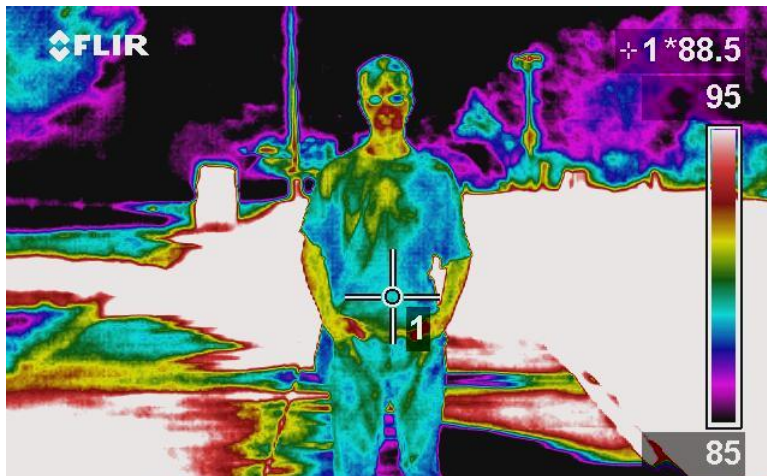
Walking Outside with Plastic Bomb at 1.5 Miles
Automatic Temperature Scale Setting

With Vest/Bomb vs without Vest/Bomb

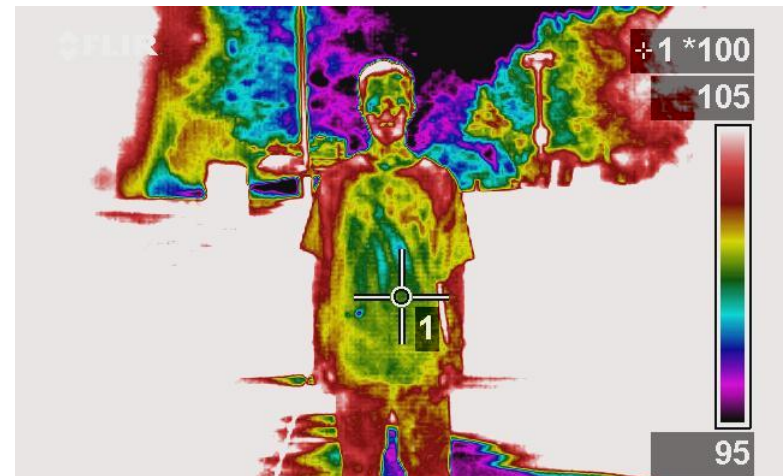
- Temperatures tend to follow the HTM model for the first mile
- Difference between the average torso temperature and the bomb area fluctuated around 1.11°C (2°F) for the length of the test
- Average torso temperature for the human with the bomb vest began the test 3.61°C (6.5°F) higher than human without the bomb vest and ended the test 7.61°C (13.7°F) higher
- Thermal resistance of the package slowed the transfer of heat from the solar irradiation from the shirt to the body



With Vest/Bomb vs without Vest/Bomb



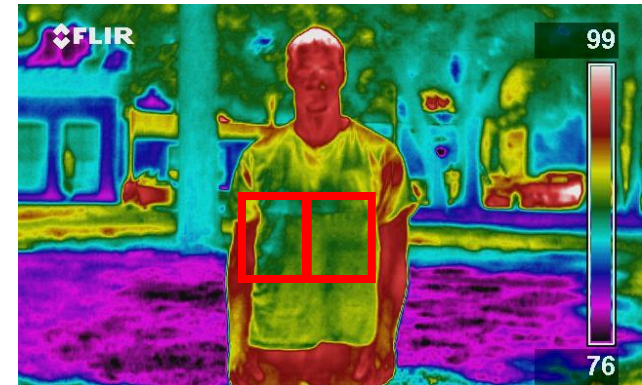
Walking Outside Without Bomb or Vest 0 Miles
Manual Temperature Range Setting



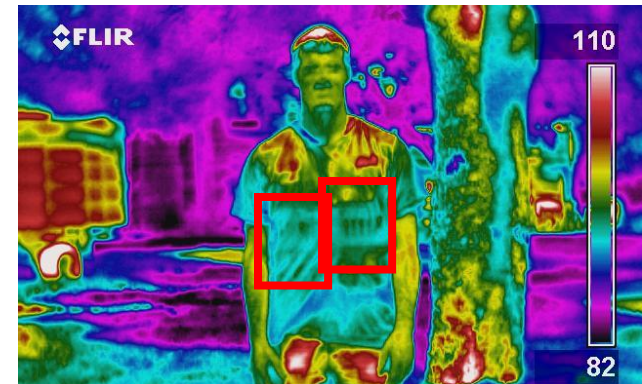
Walking Outside Without Bomb or Vest 1.5 Miles
Manual Temperature Range Setting

Effects of Solar Irradiation

- Highest temperatures were observed when the sun was behind the camera and the subject was unshaded
- Lowest temperatures were observed when the subject was in the shade and the sun was behind the camera
- In all of the images where the subject is shaded the clothing temperature is significantly lower than in the images where the subject is exposed to direct sunlight
- Having the camera in the shade and the subject in the sun has average external torso temperatures almost 5°C (9°F) higher than having both camera and subject in the shade
- Larger temperature differences when the subject is in the sun
- Larger temperature differences were also measured when the sun was positioned behind the camera



Sun Behind Subject with Metal Bomb Package



Sun Behind Camera with Metal Bomb Package

Effects of Solar Irradiation

Both Subject and Camera in Sun

<i>Average Bomb Package Temperatures with Exposure to Sun</i>		
	Sun behind subject	Sun behind camera
	<i>w/ Bomb Package</i>	<i>w/ Bomb Package</i>
both in sun	88.8	93.6
camera-sun subject-shade	86.6	87.5
camera-shade subject-sun	89.6	95.0
both in shade	87.2	86.1

<i>Average Torso Temperatures with Exposure to Sun</i>		
	Sun behind subject	Sun behind camera
	<i>w/ Bomb Package</i>	<i>w/ Bomb Package</i>
both in sun	89.3	94.5
camera-sun subject-shade	86.4	87.3
camera-shade subject-sun	89.9	95.6
both in shade	87.2	86.0

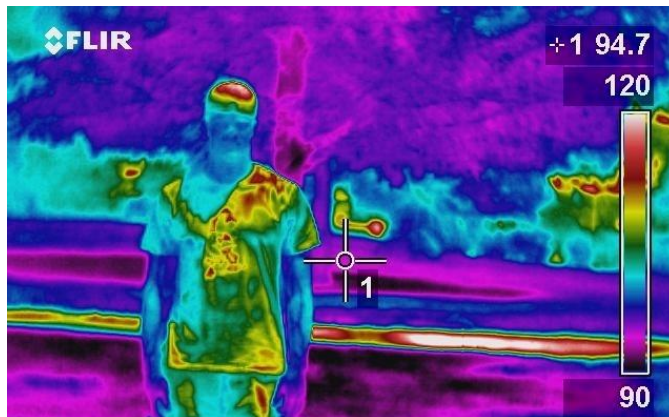
<i>Torso and Bomb Package Temperature Difference with Exposure to Sun</i>		
	Sun behind subject	Sun behind camera
	<i>w/ Bomb Package</i>	<i>w/ Bomb Package</i>
both in sun	.5	.9
camera-sun subject-shade	-.2	-.2
camera-shade subject-sun	.3	.6
both in shade	0	-.1

Clothing Characteristics

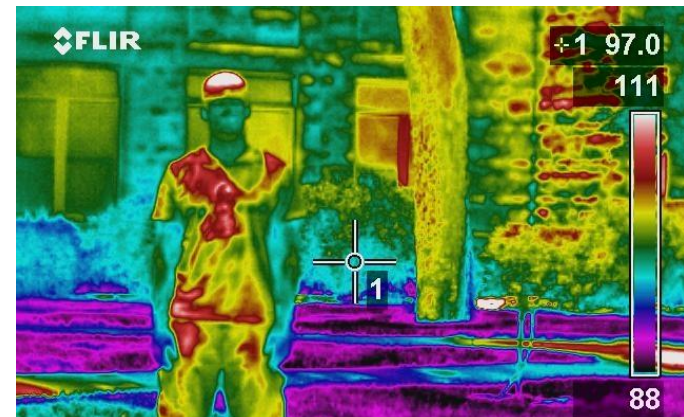
- Aesthetic details and logos may affect the appearance in the infrared image
- Using multiple different images and color palettes may aid in the detection of threats



Screenprinted T-Shirt with Grayscale Color Palette



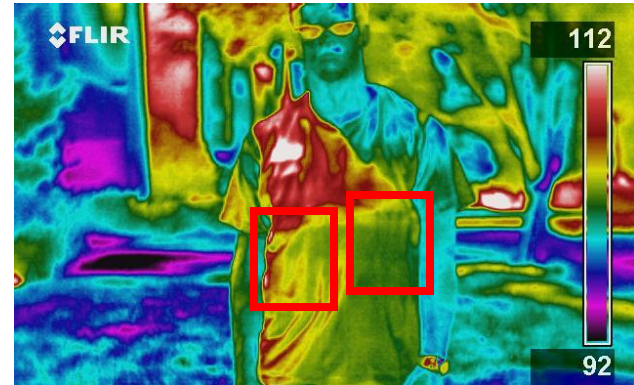
Screenprinted T-shirt with High Contrast Rainbow Color Palate Background #1



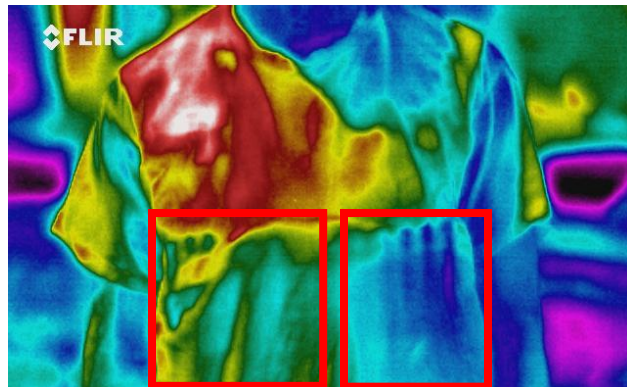
Screenprinted T-shirt with High Contrast Rainbow Color Palate-Background #2

Imaging at Various Distances

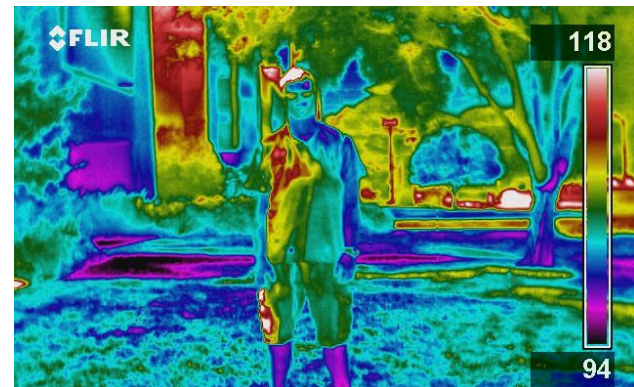
- Defined image of the bomb package if it is within 6-10 feet of the target
- At further distances it becomes hard to distinguish the bomb package's features
- Possible to see a change in temperature on the shirt due to the vest and bomb at distances up to 25 feet



Metal Bomb Package Shielded by 1 T-shirt at 12ft
Automatic Temperature Range Setting



Metal Bomb Package Shielded by 1 T-shirt at 6ft
Automatic Temperature Range Setting



Metal Bomb Package Shielded by 1 T-shirt at 25ft
Automatic Temperature Range Setting

General Conclusions from Phase 3 Testing

Phase	Testing Variable	Testing Conclusions
Phase 3	Transient Changes While Walking	Over time the clothing temperature approaches the ambient environmental temperature. Convective cooling from human movement must be accounted for in thermal models. Temperature difference must be >7% of temperature scale for human to be relatively certain a hidden object exists.
	Vest vs. No Vest	When environmental temperatures are above the skin temperature the bomb vest and package resist the transfer of heat to the body leaving the exterior clothing at higher temperatures.
	Solar Irradiation	Temperature measurements in outdoor situations are very dependent on irradiation from the sun. Temperatures can vary under consistent irradiation levels due to orientation of the subject and the camera.
	Clothing Characteristics	Characteristics such as screen printing may cause changes in the thermal signature that can mask other small temperature changes.
	Distances	The camera was capable of picking up defined bomb package images at distances of 6-10 feet. The camera can detect changes in temperature on the body at distances up to 25 feet.

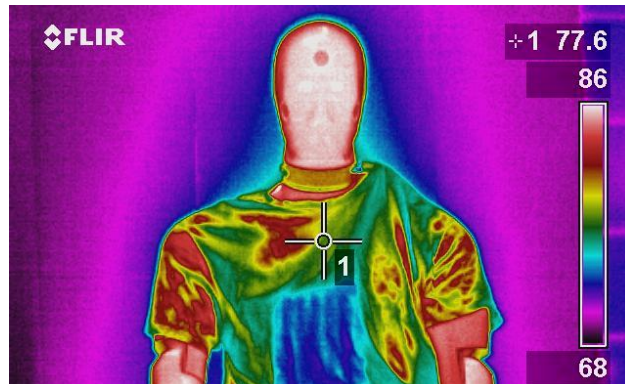
Overall Conclusions

Operator Confidence/Percentage of Temperature Scale

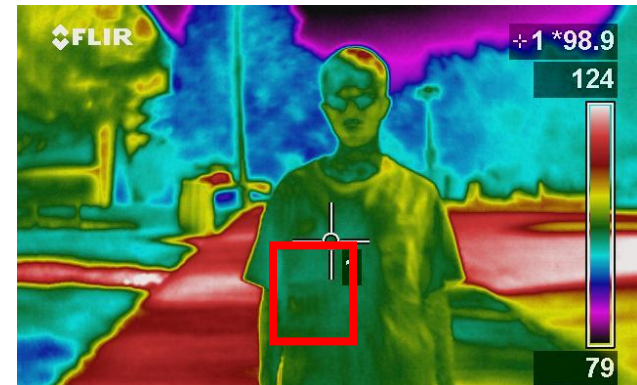
- For confident human observation, the average temperature of the suspected object's area needs to be at least 7-10% of the temperature range



~8% of overall scale



~15% of overall scale

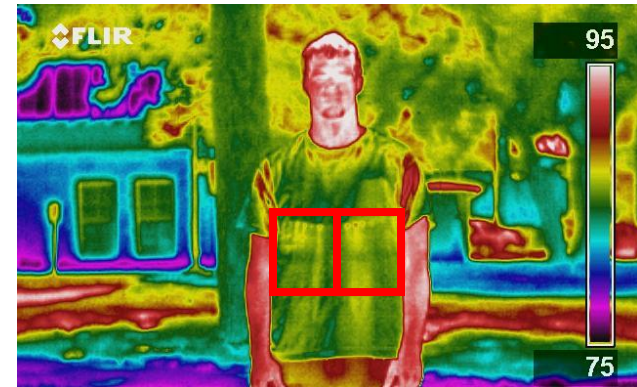


~3% of overall temperature scale

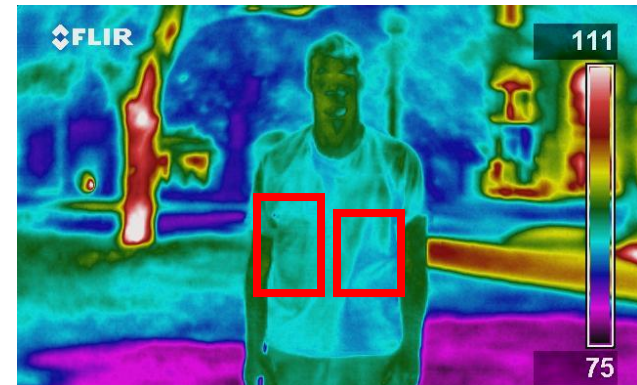
Overall Conclusions

Environmental/Solar Effects

- Environmental factors have a large impact on the temperature of clothing (esp. solar irradiation)
- Checkpoints may control shade, camera set-up/position, and possible hold period
- Camera set-up/placement is important in uncontrolled operations



Camera in Sun-Subject in Shade
Sun Behind Subject with Metal Bomb Package



Camera in Sun-Subject in Shade
Sun Behind Camera with Metal Bomb Package

Overall Conclusions Imaging at Distances

- Difficult to image for human observation beyond 25 feet
- Proposed Solution
 - Lens Attachments for optical zoom capabilities

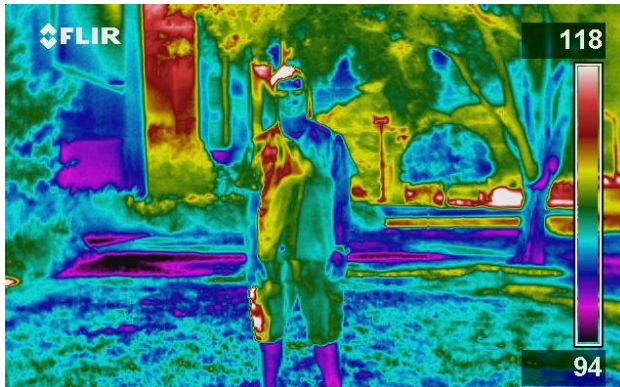


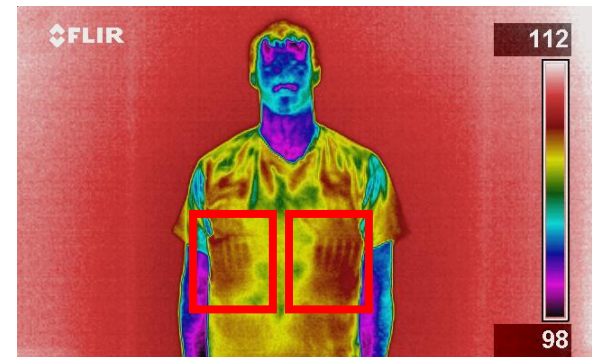
Image at 25 feet



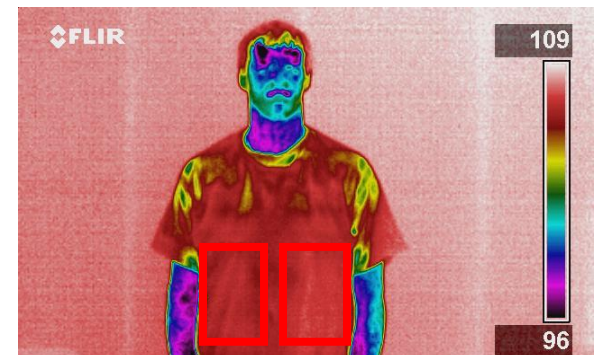
Overall Conclusions

Layers of Shielding

- Camera was not capable of producing image useful for human observation of weapons when covered by more than two layers of clothing
- Previous research has proposed fusion with millimeter wave and visual images



1 T-Shirt



2 T-Shirt

Overall Conclusions

Critical Modeling Factors

- Environmental conditions (esp. solar irradiation)
 - LCM model accounts for both simulated solar irradiation and convection due to the fan
 - When LCM model does not account radiation to and from clothing, the model predicts high
- Convective cooling due to human movement
 - Resistance model equilibrium temperature shows higher results than temperature readings (Relies on Human Thermal Model)
 - HTM accounts for increased body heat due to activity, but does not consider convective cooling due to the movement
- Package material
 - Resistance model equilibrium temperature shows clothing is much closer to the environmental temp with the plastic bomb

Final Conclusions

- Many operational limitations exist for infrared camera monitoring by humans
- Models used in this research would not suffice for use in a detection system, but they point to the potential use in a computerized comparison system and highlight necessary modeling factors
- Potential detection model must include:
 - Adaptive on-the-fly environmental conditions
 - solar irradiance
 - ambient temperature
 - wind speed
 - Human thermal control mechanisms
 - Human movement induced convection
 - Package Material

Questions/Discussion

Special Thanks

- Dr. Akira Tokuhiro
- Dr. Mo Hosni
- Committee members
- Research lab members

Color Palettes



Blue-Red



Grayscale



Iron



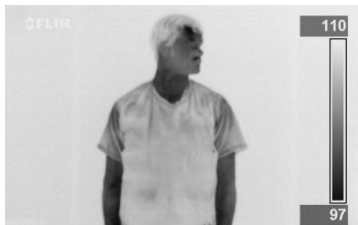
Rainbow



High Contrast Rainbow



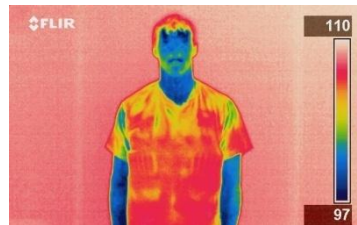
Inverted Blue-Red



Inverted Grayscale



Inverted Iron



Inverted Rainbow



Inverted High Contrast Rainbow

Exterior Clothing Temperatures for Torso and Bomb Package Areas with Various Layering and Package Material Combinations

		Metal Package			Plastic Package		
		1 Tight T-Shirt	1 Loose T-Shirt	2 T-Shirts	1 Tight T-Shirt	1 Loose T-Shirt	2 T-Shirts
MATLAB® Average Torso Temperature	Automatic Temperature Range	106.15	105.45	106.06	106.68	106.74	106.44
	Manual Temperature Range	106.47	107.08	107.86	107.08	107.12	107.17
MATLAB® Average Bomb Temperature	Automatic Temperature Range	106.39	105.93	105.81	107.29	107.15	106.57
	Manual Temperature Range	106.85	107.24	107.81	107.53	107.67	107.41

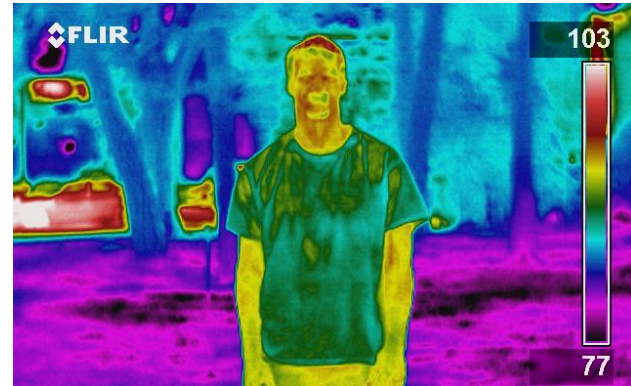
Temperatures Measured in Various Chamber Conditions While Walking on a Treadmill

Description	Speed	Time	Distance (miles)	inside	outside	Matlab Torso Temperature	Matlab Bomb Temperature
Ice-Lights-Fan	3.17mph	0 min	0	48	51	100.09	98.68
		9min 37 sec	0.5	81	82	105.35	102.71
		18min 56sec	1	86	89	105.84	102.83
		28min 20sec	1.5	91	94	105.68	104.76
Ice-Lights-No Fan	1.98mph	0 min	0	45	48	99.83	95.37
		15min 48sec	0.5	89	90	110.65	108.08
		30min 42sec	1	95	98	109.64	107.71
		45min 32sec	1.5	99	100	115.41	115.07
Warm-Lights-Fan	3.38mph	0min	0	104	106	100.12	101.1
		8min 53sec	0.5	101	104	107.04	106.84
		17min 46sec	1	101	104	107.9	109
		28min 37sec	1.5	102	105	106.88	106.98
Warm-Lights-No Fan	2.66mph	0min	0	103	105	102	101.92
		13min 43sec	0.5	103	106	108.14	109.01
		23min 47 sec	1	104	107	109.3	110.9
		33min 50sec	1.5	105	107	108.42	107.96

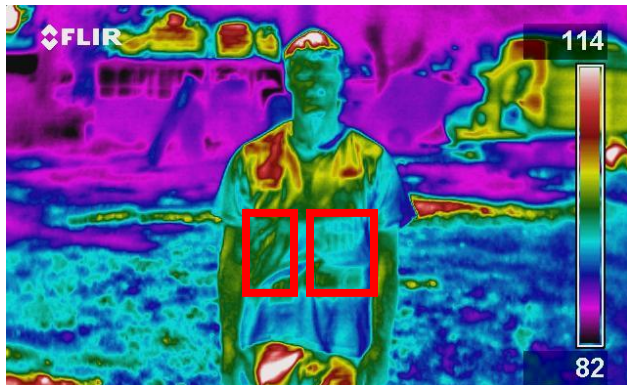
Camera in Shade-Subject in Sun



Sun Behind Subject with Metal Bomb Package



Sun Behind Subject with Only T-shirt

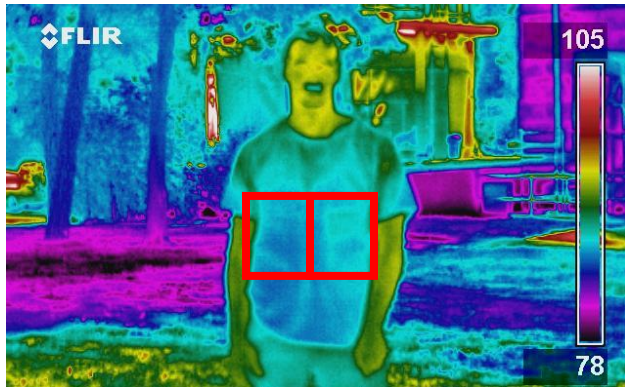


Sun Behind Camera with Metal Bomb Package

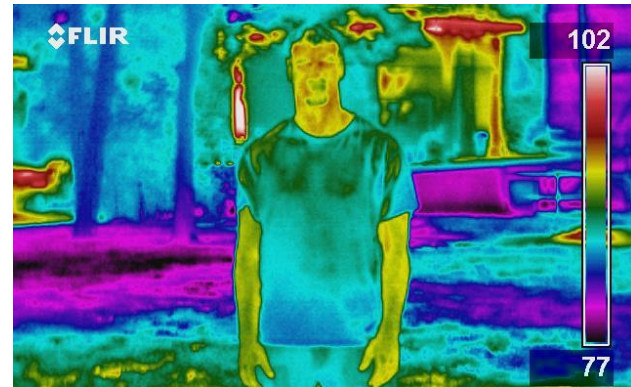


Sun Behind Camera with Only T-shirt

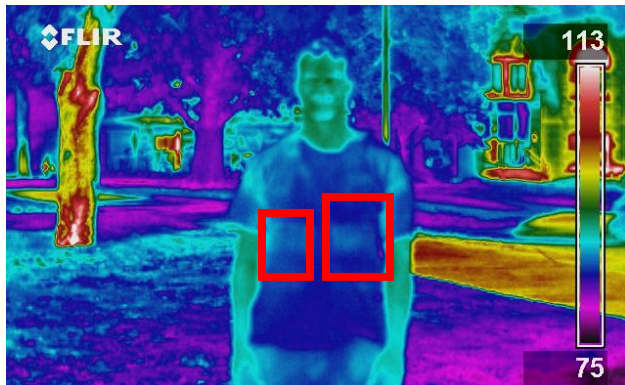
Both Camera and Subject in the Shade



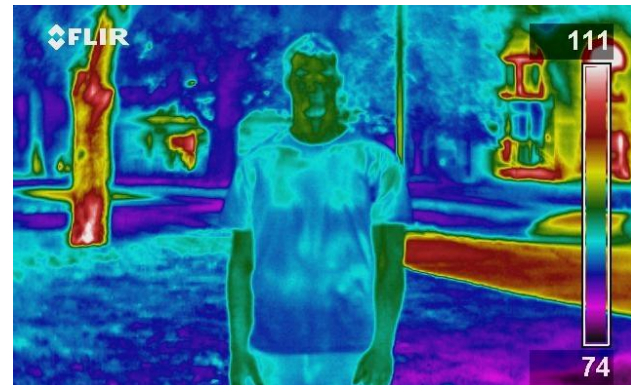
Sun Behind Subject with Metal Bomb Package



Sun Behind Subject with Only T-shirt

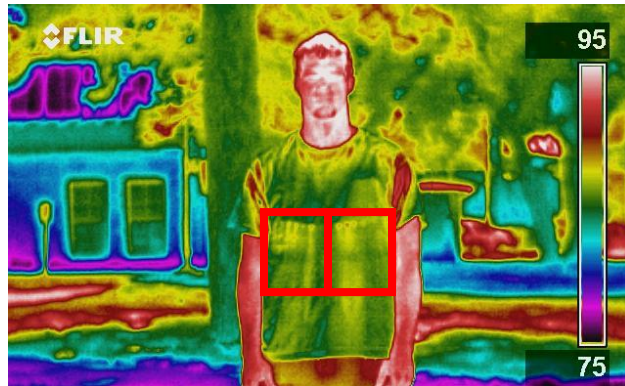


Sun Behind Camera with Metal Bomb Package

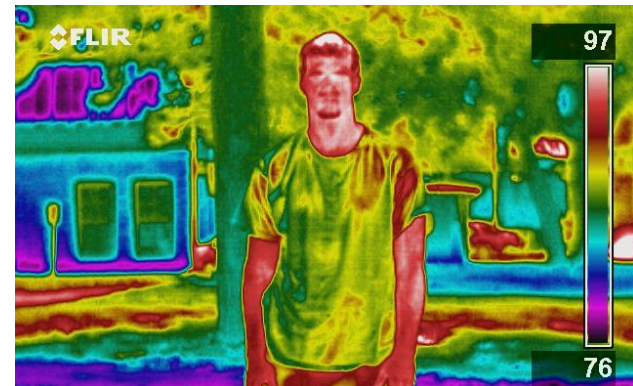


Sun Behind Camera with Only T-shirt

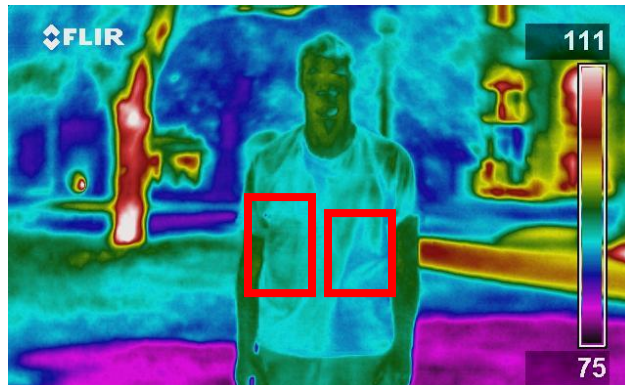
Camera in Sun-Subject in Shade



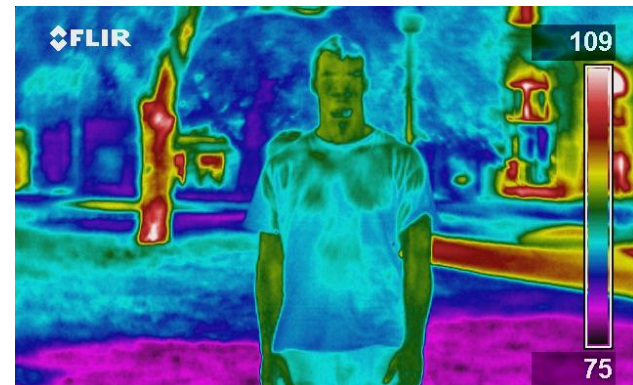
Sun Behind Subject with Metal Bomb Package



Sun Behind Subject with Only T-shirt



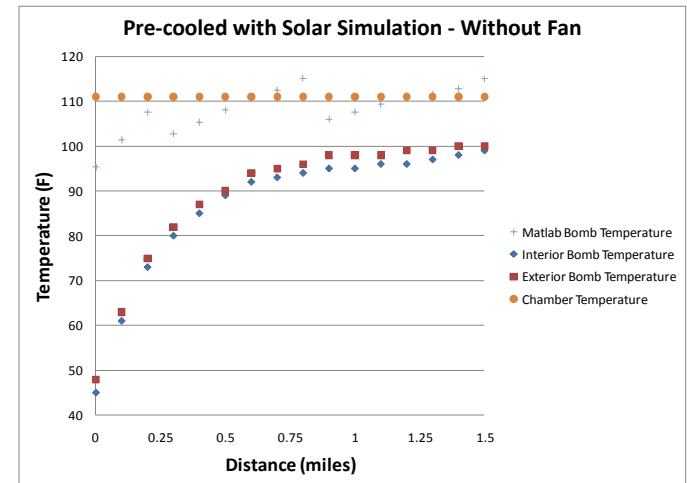
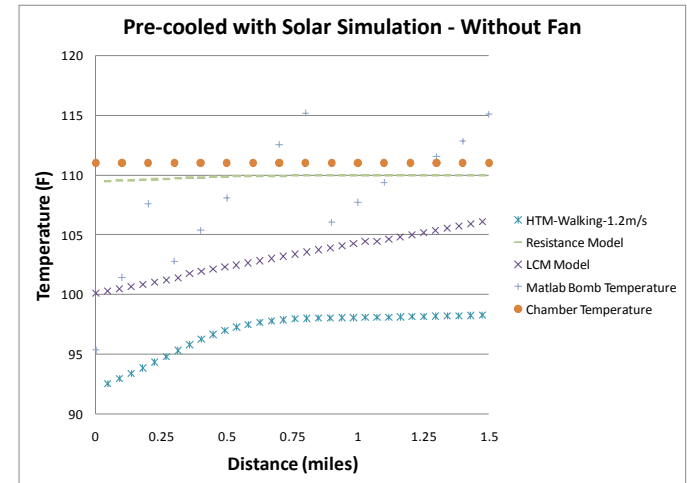
Sun Behind Camera with Metal Bomb Package



Sun Behind Camera with Only T-shirt

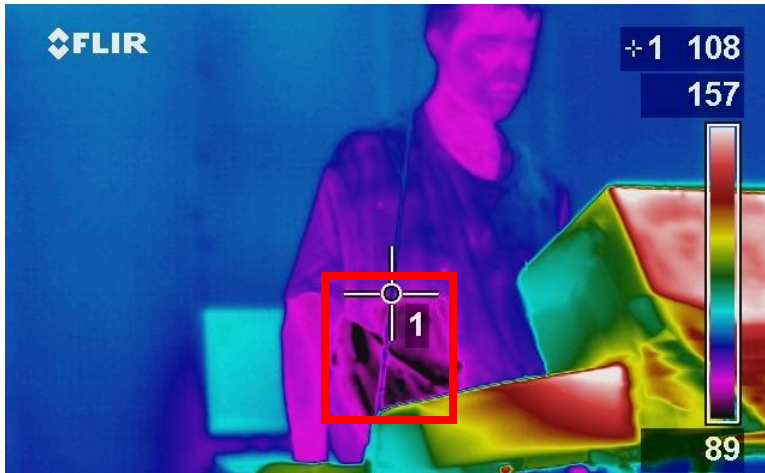
Human on Treadmill with Bomb Pre-cooled with Solar Simulation-Without Fan

- Similar to the test in which the fan was running, the bomb package did not have sufficient time to come to equilibrium
- Temperature of the bomb may be consistent, but there may still be spikes in the temperature measured on the external clothing layers
- Temperature difference between the bomb area temperature and the torso temperature begins at 7% of the temperature ranges and drops to 2% of the temperature range

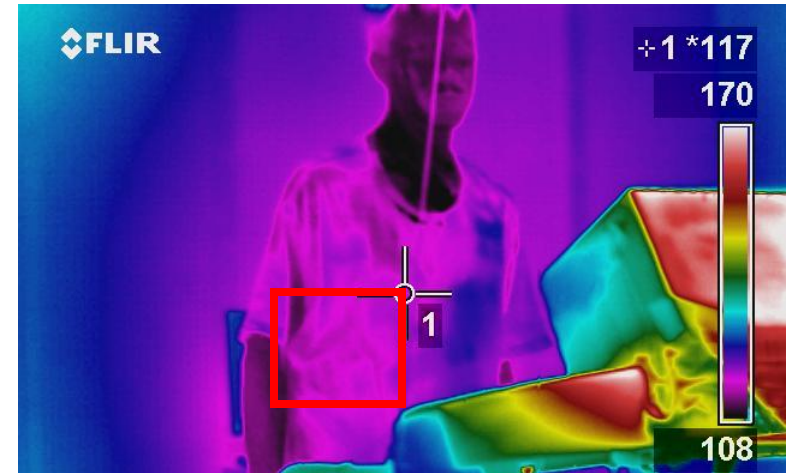


Human on Treadmill with Bomb

Pre-cooled with Solar Simulation-Without Fan



Walking on Treadmill with Iced Bomb
Lights On- Fan Off- 0 miles

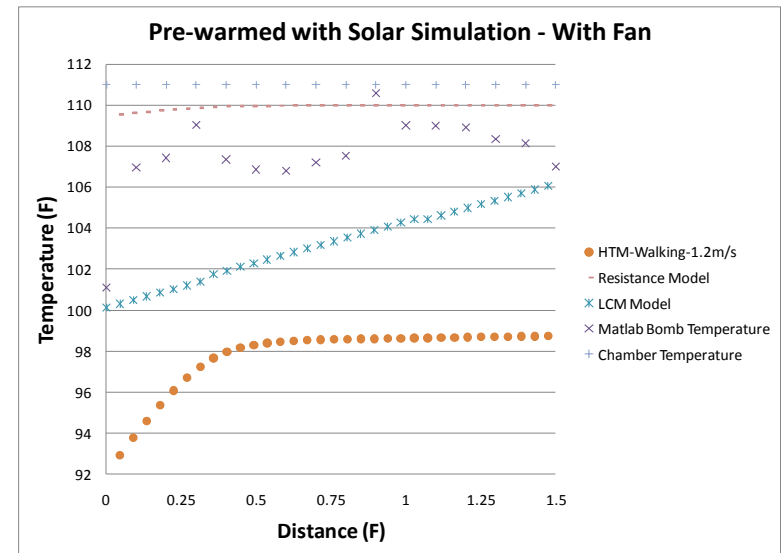


Walking on Treadmill with Iced Bomb
Lights On- Fan Off- 1.5 miles

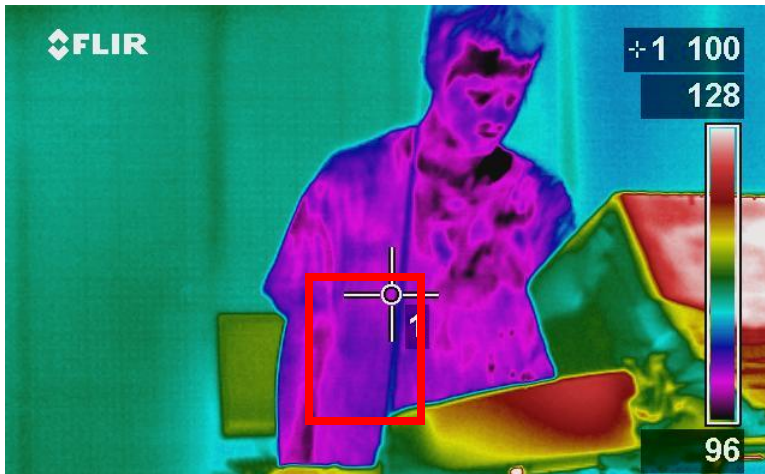
Human on Treadmill with Bomb

Pre-warmed with Solar Simulation-With Fan

- Temperature of the bomb area on the clothing quickly jumps to near the resistance model predicted temperature-fan modeled by walking speed
- Bomb area on the shirt remained midway between the bomb temperature and the environmental temperature throughout the test
- Large spikes in the bomb area temperature on the clothing are possible even when the bomb temperatures are consistent.
- Bomb area on the clothing is not always cooler than the average temperature over the entire torso



Human on Treadmill with Bomb Pre-warmed with Solar Simulation-With Fan



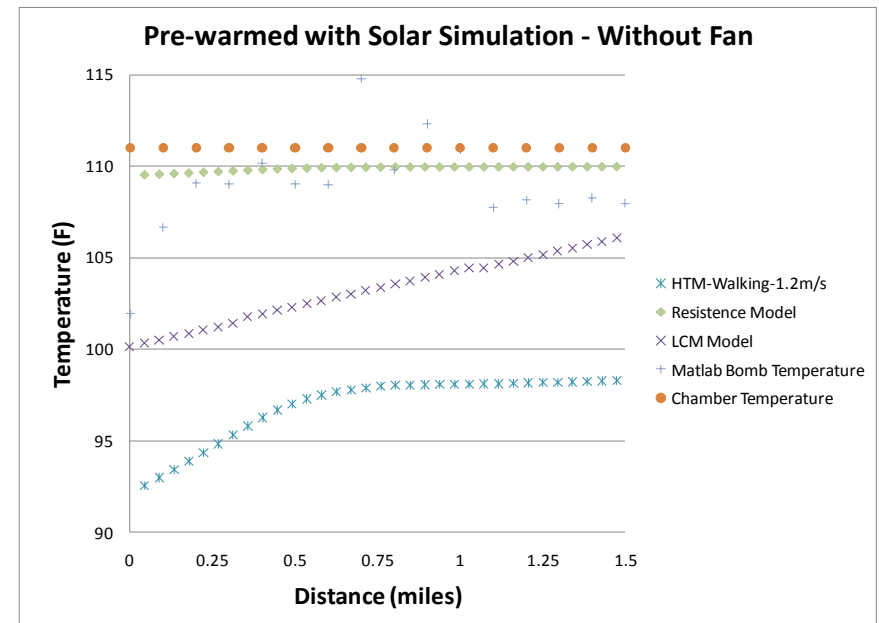
Walking on Treadmill with Warmed Bomb
Lights On- Fan On- 0 Miles



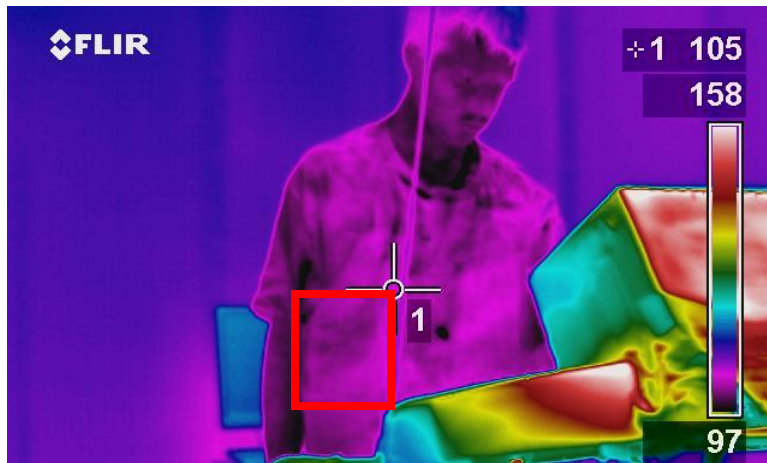
Walking on Treadmill with Warmed Bomb
Lights On- Fan On - 1.5 Miles

Human on Treadmill with Bomb Pre-Warmed with Solar Simulation-Without Fan

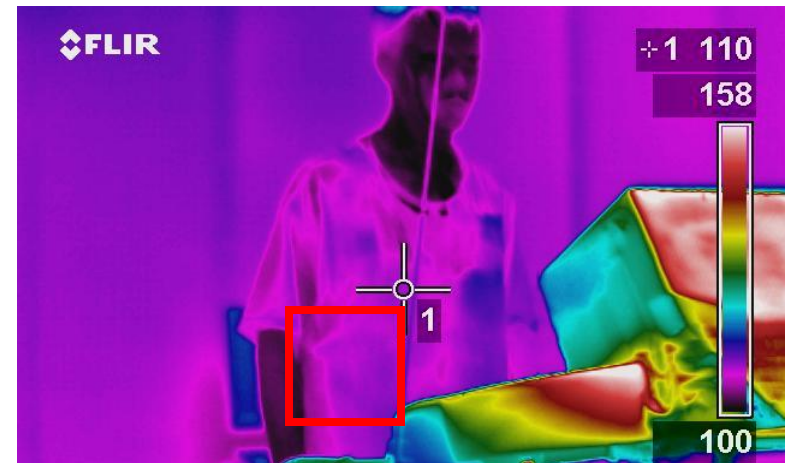
- Temperature of the bomb area on the clothing tends to fluctuate around the resistance model temperature
- Larger variations than seen in the other tests, but usually within 3°F to 5°F
- Large spikes in the bomb area temperature on the clothing are possible even when bomb temperatures are consistent
- Bomb area on the clothing is not always cooler than the average temperature over the entire torso, but these temperatures were usually within 1°F of each other



Human on Treadmill with Bomb Pre-Warmed with Solar Simulation-Without Fan



Walking on Treadmill with Warmed Bomb
Lights On- Fan Off - 0 Miles



Walking on Treadmill with Warmed Bomb
Lights On- Fan Off- 1.5 Miles